

**THE POSSIBLE LINKS BETWEEN
COPD AND LUNG CANCER:
CELLULAR AND MITOCHONDRIAL FUNCTION
IN AIRWAY EPITHELIAL CELLS**

Weerawon Thangboonjit

**National Heart and Lung Institute
Faculty of Medicine
Imperial College London**

A thesis submitted for the degree of Doctor of Philosophy

Declaration of Originality

I, Weerawon Thangboonjit declare that this thesis and the experiments presented here, except where appropriately referenced, are my own investigation and that all the support received in preparing this thesis and sources have been acknowledged.

Copyright Declaration

The copyright of this thesis rests with the author and is made available under a Creative Commons Attribution Non-Commercial No Derivatives licence. Researchers are free to copy, distribute or transmit the thesis on the condition that they attribute it, that they do not use it for commercial purposes and that they do not alter, transform or build upon it. For any reuse or redistribution, researchers must make clear to others the license terms of this work.

Abstract

Cigarette smoke (CS) is a major risk factor for both COPD and lung cancer and many lung cancer patients have COPD. CS-derived oxidant exposure in airway epithelial cells leads to abnormal function. Persistent inflammation in COPD together with mutations and dysregulated cell cycle contributes to lung cancer development. Mitochondria are the hub of bioenergetics, reactive oxygen species (ROS) production and intracellular signalling pathways. The role of mitochondria in the development of lung cancer in COPD is not widely investigated. We hypothesised that mitochondrial dysfunction causes some COPD patients to develop lung cancer.

Treatment of bronchial epithelial cell line (BEAS-2B) with hydrogen peroxide (H_2O_2) caused mitochondrial function alteration and apoptosis. Interleukin (IL)-1 β -induced proliferation and inflammation was greater when co-treated with H_2O_2 . N-acetyl cysteine had a greater protective effect than mitochondrial-targeted antioxidants. The effects of mitochondrial-directed antioxidants were also investigated in BEAS-2B, normal primary bronchial epithelial cells (NHBE) and the lung cancer cell line (A549). At baseline, A549 showed lower mitochondrial membrane potential and higher mitochondrial superoxide and respiration spare capacity. Mitochondrial protection by antioxidants in these cell types was unclear as H_2O_2 minimally affected the mitochondrial parameters and cell functions.

Gene Set Variation Analysis (GSVA) revealed that oxidative phosphorylation (OXPHOS) and glycolysis pathway signatures in lung cancer patients were related to smoking status. Matched normal-tumour pairs showed significantly higher glycolytic gene expression in tumour whereas higher mitochondrial protein (NDUFA9) expression was detected in background tissue from smokers compared with tumour tissue in COPD patients suggesting an early OXPHOS compensatory mechanism in background tissue and glycolytic switching in the tumour. Background and tumour tissues suggested defects in mitochondrial structure in COPD.

This study provides an initial insight into how changes in mitochondria and metabolic pathways could link COPD and lung cancer and has clinical implications for carcinogenesis prevention by treating COPD patients.

Acknowledgement

I would like to express my deep gratitude to Professor Ian Adcock for his patient guidance, valuable suggestions, encouragement and support throughout my study; Dr Andrew Durham, my former second supervisor, for his experimental advice and guidance; and Dr Sharon Mumby, my later second supervisor, for her fruitful suggestions in thesis writing with great help and advice.

I would also like to thank Professor Peter Barnes for giving me an opportunity to study in the Airway disease section, National Heart and Lung Institute. I wish to thank various people in Imperial College London for their contribution to my work; Dr Michaeloudes Charalambos for suggestions and reagents used whenever needed; Dr Francois Kwong for the lung tissue scoring assessment; Dr Stelios Pavlidis from Data Science Institute for running the GSVA and Elen Jazrawi for the basic laboratory skills training. My grateful thanks are also extended to Eleanor Tucker and Tony Umelo for their help finding the best option for me to get through the study course, and everyone at the Airway disease section, especially Tankut Guney, my dear friend for his moral support. I would also like to thank staff at the Centre for Cell Signalling and Inflammation, Department of Medicine, Hammersmith Campus, for giving me access to the Seahorse XF Analyser facility with the training.

I would also like to give thanks to the technicians and staff at Respiratory Biomedical Research Unit, Royal Brompton Hospital for invaluable lung tissue samples, immunohistochemistry works and transmission electron microscopy facilities.

I wish to acknowledge the financial support provided by the Faculty of Medicine Siriraj Hospital, Mahidol University, and also extend thanks to my senior colleagues at the Department of Pharmacology for placing their trust and confidence in my abilities to complete the study.

Last but not least, I am thankful to my family and friends particularly my mom and dad as well as my brother for unconditional love and support while being away from them.

Above all, nothing can happen without God. Thank You for your plan in my life with endless love, giving me strength to complete my work and being the light throughout my life.

Table of Contents

Declaration of Originality	2
Abstract	3
Acknowledgement	4
Abbreviations	15
Chapter 1 Introduction	22
1.1 Chronic Obstructive Pulmonary Disease (COPD): an oxidative stress and inflammation associated disease	23
1.1.1 Definition	23
1.1.2 Diagnosis	23
1.1.3 Assessment.....	24
1.1.4 Risk factor and prevalence.....	25
1.1.5 Pathophysiology.....	26
1.1.6 Treatments	28
1.1.7 Cell types in the lung and their roles in COPD	29
1.2 Lung cancer	39
1.2.1 Prevalence and risk factors	39
1.2.2 Lung cancer cell types.....	40
1.2.3 Lung cancer staging	43
1.2.4 Importance of epithelial cells in lung cancer.....	45
1.2.5 Current treatment of lung cancer.....	47
1.3 Possible links between COPD and lung cancer	53
1.3.1 Chronic inflammation.....	53
1.3.2 Apoptosis and cell proliferation.....	55
1.3.3 Genetic and epigenetic modulation.....	56
1.3.4 Reactive oxygen species (ROS) production and mitochondria involvement....	58
1.4 Mitochondria.....	59
1.4.1 History and evolution.....	59
1.4.2 Structure, compartments and bioenergetics	59
1.4.3 Mitochondrial morphological regulation	72
1.4.4 Mitochondrial biogenesis and mitophagy	73
1.4.5 Mitochondrial dysfunction.....	75

1.5 Reactive oxygen species (ROS).....	84
1.5.1 Exogenous ROS.....	85
1.5.2 Endogenous ROS	85
1.5.3 ROS elimination (Antioxidant systems)	90
1.5.4 Roles of oxidative stress in COPD	96
1.5.5 Roles of oxidative stress in lung cancer	98
1.6 Hypothesis	99
1.7 Aims	100
Chapter 2 Materials and Methods	101
2.1 Materials.....	102
2.2 Methods	108
2.2.1 Lung tissue clinical samples.....	108
2.2.2 Cell lines and cell culture.....	109
2.2.3 Cell viability	111
2.2.4 Apoptosis assay	112
2.2.5 Proliferation assay.....	113
2.2.6 RNA extraction	114
2.2.7 Reverse transcription	115
2.2.8 Real time quantitative polymerase chain reaction (PCR)	115
2.2.9 Bradford protein assay	116
2.2.10 Enzyme-linked immunosorbant assay (ELISA) for CXCL8.....	117
2.2.11 Immunohistochemistry (IHC).....	118
2.2.12 Transmission electron microscopy (TEM)	120
2.2.13 Fluorescence intensity measurement of mitochondrial function parameters	121
2.2.14 Extracellular flux analysis (MitoStress test)	123
2.2.15 Isolation of mitochondria from lung tissue	126
2.2.16 Detection of mitochondrial membrane potential and mitochondrial ROS in isolated mitochondria	127
2.2.17 Gene set variation analysis (GSVA).....	128
2.2.18 Statistical analysis	128

Chapter 3 Effect of H₂O₂ and pro-inflammatory cytokine (IL-1β) on mitochondrial function and cell inflammation, proliferation and apoptosis in a bronchial epithelial cell line	130
3.1 Introduction	131
3.2 Hypothesis	135
3.3 Aims	135
3.4 Results	136
3.4.1 Cell viability (Mitochondrial activity) in H ₂ O ₂ treated BEAS-2B cells.....	136
3.4.2 Effect of H ₂ O ₂ on mitochondrial superoxide levels in BEAS-2B cells.....	137
3.4.3 Effect of H ₂ O ₂ on intracellular reactive oxygen species in BEAS-2B cells	141
3.4.4 Effect of H ₂ O ₂ on mitochondrial membrane potential ($\Delta\Psi_m$) in BEAS-2B cells....	145
3.4.5 Effect of H ₂ O ₂ stimulation on BEAS-2B cell apoptosis	148
3.4.6 H ₂ O ₂ and IL-1 β stimulated inflammatory cytokine secretion (CXCL8) in BEAS-2B cells.....	152
3.4.7 Effect of H ₂ O ₂ and IL-1 β stimulation on BEAS-2B cell proliferation.....	154
3.4.8 Optimisation of antioxidant concentrations used in BEAS-2B cells	156
3.4.9 Effect of antioxidants on H ₂ O ₂ stimulated mitochondrial superoxide production in BEAS-2B cells	161
3.4.10 Effect of antioxidants on the H ₂ O ₂ stimulated decrease in mitochondrial membrane potential in BEAS-2B cells.....	163
3.4.11 Effect of antioxidants on H ₂ O ₂ stimulated BEAS-2B cell apoptosis	165
3.4.12 Effect of antioxidants on H ₂ O ₂ and IL-1 β induced inflammation	168
3.4.13 Effect of antioxidants on BEAS-2B cell proliferation	172
3.4.14 Effect of antioxidants pre-treatment on IL-1 β induced BEAS-2B cell proliferation	174
3.5 Discussion	176
Chapter 4 Differences in cellular function among lung epithelial cell types (BEAS-2B, NHBE, and A549)	188
4.1 Introduction	189
4.2 Hypothesis	191
4.3 Aims	191
4.4 Results	192

4.4.1 Mitochondrial superoxide, intracellular ROS and mitochondrial membrane potential ($\Delta\Psi_m$), in BEAS-2B, NHBE and A549 cells (baseline and after H ₂ O ₂ exposure)	192
4.4.2 Characteristics of mitochondrial respiration in BEAS-2B, NHBE and A549 cells using Extracellular Flux Analyser (Seahorse technology)	195
4.4.3 Changes in gene expression in response to H ₂ O ₂ and pro-inflammatory cytokine exposure in BEAS-2B, NHBE and A549 cells	204
4.4.4 Change in CXCL8 release in response to H ₂ O ₂ and pro-inflammatory cytokine exposure in BEAS-2B, NHBE and A549 cells	206
4.4.5 Effect of antioxidants on mitochondrial respiration parameters in H ₂ O ₂ stimulated BEAS-2B, NHBE and A549 cells	209
4.5 Discussion	214
Chapter 5 Investigation of mitochondrial function, gene expression and morphology in lung tissue of lung cancer patients	227
5.1 Introduction	228
5.2 Hypothesis	230
5.3 Aims	230
5.4 Results	231
5.4.1 Enrichment scores in metabolic pathway signatures by gene set variation analysis (GSVA).....	231
5.4.2 Comparison of mitochondrial function and metabolic gene expression between tumour and matched non-tumour tissue in lung cancer patients	239
5.4.3 Mitochondrial protein expression in lung tissue from lung cancer patients....	246
5.4.4 Mitochondrial morphology in cells from lung tissue of lung cancer patients ..	258
5.5 Discussion	262
Chapter 6 General Discussion and Future Directions	275
6.1 General Discussion	276
6.1.1 Roles of oxidative stress in COPD and lung cancer involving mitochondria..	276
6.1.2 Protective effect of antioxidants on cellular functions	282
6.1.3 Comparison of mitochondrial and cellular functions between airway epithelial cell types	284
6.1.4 Importance of genomic and proteomic approaches in genes and pathway identification	287
6.1.5 Sources of ROS and cell culture models in <i>in vitro</i> studies for airway epithelial cells	289

6.1.6 Differences in mitochondrial function and metabolic gene expression in matched normal-tumour pairs	290
6.1.7 Mitochondrial morphological studies and their biogenesis in COPD and lung cancer.....	292
6.2 Future plans	296
References	298

List of figures

Figure 1.1 Updated ABCD assessment tools diagram (from Global Initiative for Chronic Obstructive Lung Diseases).....	25
Figure 1.2 Pathophysiological changes in the COPD lung.....	27
Figure 1.3 Airway epithelial cell type composition in the lungs.....	30
Figure 1.4 Alveolar cell types in alveoli and their functions	33
Figure 1.5 Classification of lung cancer.....	41
Figure 1.6 Types of lung cancer.....	42
Figure 1.7 TNM Staging of lung cancer.....	44
Figure 1.8 Schematic presenting the site of different airway epithelial cell types and other cells along the respiratory tract	45
Figure 1.9 Summary flowchart of non-small cell lung cancer treatment	48
Figure 1.10 Summary flowchart of small cell lung cancer treatment	52
Figure 1.11 Schematic diagram of mitochondria	60
Figure 1.12 Schematic diagram of glycolysis pathway	62
Figure 1.13 Schematic presentation of tricarboxylic acid (TCA) cycle.....	67
Figure 1.14 Schematic diagram of mitochondrial electron transport chain (mtETC)	69
Figure 1.15 Schematic representation of the difference in metabolism between differentiated cells and tumour cells	81
Figure 1.16 Schematic presentation of mitochondrial ROS (mROS) generation sites and its effects	87
Figure 1.17 Antioxidant mechanism of mitoTEMPO.....	93
Figure 1.18 Antioxidant mechanism of AP39	94
Figure 1.19 Antioxidant mechanism of SS31	95
Figure 3.1 Effect of H ₂ O ₂ on BEAS-2B cell viability (mitochondrial activity)	136
Figure 3.2 Gating strategy used for measuring mitochondrial superoxide in BEAS-2B cells.....	138
Figure 3.3 Overlay histogram of MitoSOX™ fluorescence intensity	139
Figure 3.4 Effect of H ₂ O ₂ on mitochondrial superoxide production in BEAS-2B cells	140

Figure 3.5 Gating strategy for the detection of intracellular ROS in BEAS-2B cells	142
Figure 3.6 Overlay histogram of the effect of H ₂ O ₂ on DCFH-DA fluorescence intensity	143
Figure 3.7 Effect of H ₂ O ₂ on intracellular ROS levels in BEAS-2B cells	144
Figure 3.8 Gating strategy for BEAS-2B cells for measuring mitochondrial membrane potential	146
Figure 3.9 Effect of H ₂ O ₂ on mitochondrial membrane potential of BEAS-2B cells	147
Figure 3.10 Gating strategy for detection of apoptosis in BEAS-2B cells	149
Figure 3.11 Gating strategy for detection of apoptosis in BEAS-2B cells using a high H ₂ O ₂ concentration	150
Figure 3.12 Effect of 400µM H ₂ O ₂ on apoptosis in BEAS-2B cells	151
Figure 3.13 CXCL8 release and cell viability from BEAS-2B stimulated with H ₂ O ₂ or IL-1β	153
Figure 3.14 Effect of H ₂ O ₂ and IL-1β on proliferation in BEAS-2B	154
Figure 3.15 Effect of H ₂ O ₂ and IL-1β stimulation on BEAS-2B cell proliferation	155
Figure 3.16 Cell viability in NAC, mitoTEMPO, SS31, AP39 and AP219 treated BEAS-2B cells	158
Figure 3.17 Cell viability of antioxidant treated BEAS-2B cells using propidium iodide (PI) assay	160
Figure 3.18 Effect of antioxidants on H ₂ O ₂ stimulated mitochondrial superoxide production in BEAS-2B cells	162
Figure 3.19 Effect of antioxidant pre-treatment on mitochondrial membrane potential (ΔΨ _m) of H ₂ O ₂ induced BEAS-2B	164
Figure 3.20 Effect of antioxidants on apoptosis in H ₂ O ₂ induced BEAS-2B	167
Figure 3.21 Effect of antioxidants on H ₂ O ₂ and IL-1β stimulated IL8 mRNA expression in BEAS-2B cells	169
Figure 3.22 Effect of antioxidants on H ₂ O ₂ and IL-1β stimulated CXCL8 release in BEAS-2B cells	171
Figure 3.23 Effect of antioxidants on BEAS-2B cell proliferation	173
Figure 3.24 Effect of antioxidants on IL-1β induced BEAS-2B cell proliferation	175
Figure 4.1 Mitochondrial function of BEAS-2B, NHBE and A549 cells at baseline and after H ₂ O ₂ exposure	194

Figure 4.2 Cell density optimisation for mitochondrial respiration analysis in BEAS-2B, NHBE and A549 cells.....	197
Figure 4.3 Mitochondrial respiration profiles of BEAS-2B, NHBE and A549 cells ..	199
Figure 4.4 Comparison of mitochondrial respiration parameters of BEAS-2B, NHBE and A549 cells.....	201
Figure 4.5 Proliferation of BEAS-2B, NHBE and A549 cells in basal state and after H ₂ O ₂ exposure	203
Figure 4.6 Gene expression in response to H ₂ O ₂ and pro-inflammatory cytokine exposure in BEAS-2B, NHBE and A549 cells	206
Figure 4.7 CXCL8 release in response to H ₂ O ₂ and pro-inflammatory cytokine exposure in BEAS-2B, NHBE and A549 cells	207
Figure 4.8 Effect of antioxidants on basal respiration of BEAS-2B, NHBE and A549	210
Figure 4.9 Effect of antioxidants on ATP production of BEAS-2B, NHBE and A549	211
Figure 4.10 Effect of antioxidants on mitochondrial reserve capacity of BEAS-2B, NHBE and A549.....	212
Figure 4.11 Effect of antioxidants on proton leak of BEAS-2B, NHBE and A549 ...	213
Figure 5.1 Enrichment scores (ES) of the OXPHOS signature in squamous cell tumour of both current smokers and ex-smokers (GSE12428)	233
Figure 5.2 Higher enrichment scores (ES) of glycolysis signatures in squamous cell tumour of both current smokers and ex-smokers (GSE12428)	234
Figure 5.3 Enrichment scores (ES) of the OXPHOS signature in squamous cell tumour of both non-COPD and COPD patients (GSE12472).....	235
Figure 5.4 Higher enrichment scores (ES) of glycolysis signatures in squamous cell tumour of both non-COPD and COPD patients (GSE12472).....	237
Figure 5.5 Enrichment scores (ES) of OXPHOS and glycolysis signatures in bronchial epithelial cells of smokers with or without lung cancer (GSE19027).....	238
Figure 5.6 Comparison of $\Delta\Psi_m$ and mitochondrial superoxide levels between tumour and matched non-tumour tissue from lung cancer patients.....	242
Figure 5.7 EGFR and KRAS gene expression levels of tumour and matched non-tumour tissue from lung cancer patients.....	243
Figure 5.8 Metabolic related gene expression levels in tumour and matched non-tumour tissue from lung cancer patients	245
Figure 5.9 Positive control for immunohistochemistry assessment of NDUFA9.....	250

Figure 5.10 Negative control for NDUFA9 in lung tissue slides.....	251
Figure 5.11 NDUFA9 expressions in alveolar macrophages and bronchial epithelium from background lung tissue of patients.....	252
Figure 5.12 NDUFA9 expressions in tumour epithelium from lung tumour tissue of patients.....	253
Figure 5.13 NDUFA9 average staining score of alveolar macrophage and normal bronchial epithelium in lung tissue of lung cancer patients.....	255
Figure 5.14 NDUFA9 average staining score compared among non-smokers, smokers and COPD groups	257
Figure 5.15 Mitochondrial morphology in alveolar macrophage of non-smoker, smoker and COPD patients with lung cancer.....	259
Figure 5.16 Mitochondrial morphology in normal bronchial epithelium of smoker and COPD patients with lung cancer	260
Figure 5.17 Differences in mitochondrial morphology between alveolar type II epithelium (A2I2) and adenocarcinoma cell in non-smoker, smoker and COPD.....	261
Figure 6.1 Diagram summarising main results from BEAS-2B cells with H ₂ O ₂ exposure and mitochondrial parameters between BEAS-2B, NHBE and A549 cells	287
Figure 6.2 Summary of proposed mechanism involving in some metabolic pathways, relationship between COPD and lung cancer.....	295

List of tables

Table 2.1 Cell Culture Reagents	102
Table 2.2 Laboratory Reagents.....	103
Table 2.3 Assay Kits.....	104
Table 2.4 Reagents and kits used for immunohistochemistry	104
Table 2.5 PCR primers and annealing temperatures	104
Table 2.6 TaqMan® Gene Expression assays for real-time RT-PCR (Applied Biosystems®, Invitrogen, UK)	105
Table 2.7 QuantiTect Primer assays for SYBR® Green-based expression analysis (Qiagen) for real-time RT-PCR.....	105
Table 2.8 Compounds	105
Table 2.9 Antioxidants and their actions.....	106
Table 2.10 Equipment	107
Table 2.11 Characteristic comparison between BEAS-2B, NHBE and A549	110
Table 2.12 SYBR® Green RT-qPCR master mix components for each PCR tube	116
Table 2.13 TaqMan® Green RT-qPCR master mix components for each well in PCR microplate.....	116
Table 2.14 Reagents used in CXCL8 ELISA.....	118
Table 2.15 Details of mitochondrial protein antibody used in IHC	119
Table 2.16 Fluorescence dye concentrations.....	123
Table 2.17 Compound concentration for loading sensor cartridge ports of XFe96.	126
Table 2.18 Mitochondrial respiration parameter equations.....	126
Table 5.1 Gene sets representing specific processes and cell signature	232
Table 5.2 Individual characteristics and demographic data of lung cancer patients	241
Table 5.3 RNA expression ratio and PRECOG Z-score of candidate genes.....	247
Table 5.4 Level of protein expression (IHC) of candidate genes in lung cancer tissue and normal lung tissue	248
Table 5.5 Demographic data, histopathology characteristics and cancer stage of non-smoker, smoker and COPD groups of patients	249

Abbreviations

$\Delta\Psi_m$	Mitochondrial membrane potential
$\cdot\text{OH}$	Hydroxyl radical
2DG	2-deoxy-D-glucose
5-FU	Fluorouracil
5-oxo-ETE	5-oxo-eicosatetraenoic acid
A549	Human lung adenocarcinoma cell line
ADC	Adenocarcinoma
ADT	Anethole dithiolethione
AEC	Alveolar epithelial cell
AIDS	Acquired immune deficiency syndrome
<i>AKT1</i>	Protein kinase B
ALD	Advanced Lung disease
ALK	Anaplastic lymphoma kinase
<i>ALK</i>	Anaplastic lymphoma kinase (receptor tyrosine kinase)
AM	Alveolar macrophage
AMPK	AMP-activated protein kinase
ANOVA	Analysis of variance
Anti-BrdU-POD	Anti-bromodeoxyuridine-peroxidase
AP219	(9-carboxynonyl) triphenyl-phosphonium bromide
AP39	(10-oxo-10-(4-(3-thioxo-3H-1,2-dithiol-5yl)phenoxy)decyl) triphenyl-phosphonium bromide
Apaf-1	Apoptotic protease activating factor-1
<i>APC</i>	Adenomatous polyposis coli
ASM	Human airway smooth cells
ASMC	Airway smooth muscle cell
ATI	Alveolar epithelial type I
ATII	Alveolar epithelial type II
ATP	Adenosine triphosphate
BAC	Bronchioalveolar carcinoma
BADJ	Bronchoalveolar duct junction
BAL	Bronchoalveolar lavage fluid
BASC	Bronchoalveolar stem cell
BCL-2	B-cell lymphoma-2
BEAS-2B	Transformed human bronchial epithelial cell line
BEC	Bronchial epithelial cell
BEGM	Bronchial epithelial cell growth medium
BOLD	Burden of obstructive lung disease
BPE	Bovine pituitary extract
<i>BRAF</i>	B-raf proto-oncogene
<i>BRCA1</i>	Breast cancer 1

BrdU	5-bromo-2'-deoxyuridine
BRU	Respiratory Biomedical Research Unit
BSA	Bovine serum albumin
CAT	COPD Assessment Test
<i>CDKN2</i>	Cyclin-dependent kinase inhibitor 2
cDNA	Complementary DNA
CMT	Chemotherapy
<i>C-MYC</i>	Avian myelocytomatosis viral oncogene homolog
CO	Carbon monoxide
COI	Cytochrome c oxidase subunit 1
COPD	Chronic obstructive pulmonary disease
CoQ	Ubiquinol
CS	Cigarette smoke
CSE	Cigarette smoke extract
C _t	Cycle threshold
CTCs	Circulating tumour cells
CTL	Cytotoxic T lymphocyte
CTLA-4	Cytotoxic T-lymphocyte-associated antigen 4
CXCL8	C-X-C motif chemokine ligand 8
CYP450	Cytochrome P450
Cyt c	Cytochrome c
DAB	3,3'-diaminobenzidine tetrahydrochloride
DCA	Dichloroacetate
DCFH-DA	2',7'-dichlorodihydrofluorescein diacetate
DMEM	Dulbecco's modified Eagle's medium
DMSO	Dimethylsulphoxide
DNA	Deoxyribonucleic acid
Drp1	Dynamain-related protein 1
EASE	Expression Analysis Systematic Explorer
EBC	Exhaled breath condensate
ECAR	Extracellular acidification rate
ECM	Extracellular matrix
ED	Extensive disease
EGFR	Epidermal growth factor receptor
ELISA	Enzyme-linked immunosorbent assay
EMA	European Medicines Evaluation Agency
EMT	Epithelial-mesenchymal transition
ER	Endoplasmic reticulum
ERR	Estrogen related receptor
ES	Enrichment scores
ETC	Electron transport chain

FADH ₂	Reduced flavin adenine dinucleotide
FBP	Fructose-1,6-bisphosphate
FBS	Fetal bovine serum
FCCP	Carbonyl cyanide-4-(trifluoromethoxyphenylhydrazine)
FDG	¹⁸ F-labeled 2-fluoro-deoxy-glucose
FEV ₁	Forced expiratory volume in 1 second
FGF-10	Fibroblast growth factor 10
FH	Fumarate hydratase
FITC	Fluorescein isothiocyanate
FoxO3A	Forkhead transcription factor class O 3A
FSC	Forward scatter
FVC	Forced vital capacity
G6P	Glucose-6-phosphate
GHRH	Growth hormone-releasing hormone
GLUTs	Glucose transporters
GM-CSF	Granulocyte colony-stimulating factor
GOLD	Global initiative for obstructive lung disease
GOx	Glucose oxidase
GRXa	Glutaredoxins
GSE	Gene series
GSH	Reduced glutathione
GSSH	Oxidised glutathione
GSVA	Gene set variation analysis
GTP	Guanosine triphosphate
H ₂ O ₂	Hydrogen peroxide
H ₂ S	Hydrogen sulfide
HBE1	Immortalised human bronchial epithelial cell line
HBSS	Hank's balanced salt solution
HDAC2	Histone deacetylase 2
hEGF	Human epidermal growth factor
HepG2	Hepatoma G2 cell line
<i>HER2</i>	Human epidermal growth factor receptor 2
HIF	Hypoxia-inducible factor
HIV	Human immunodeficiency virus
HKs	Hexokinases
HOCl	Hypochlorous acid
HUVEC	Human umbilical vein endothelial cell
IBD	Inflammatory bowel disease
ICS	Inhaled corticosteroid
IDH	Isocitrate dehydrogenase
IFN-γ	Interferon gamma

IHC	Immunohistochemistry
IL-1 α	Interleukin 1 alpha
IL-1 β	Interleukin 1 beta
IL-6	Interleukin 6
IL-8	Interleukin 8
IMM	Mitochondrial inner membrane
IMS	Intermembrane space
IMS	Industrial methylated spirit
irAEs	Immune-related adverse events
JC-1	J-aggregate-forming cationic dye
Keap1	Kelch-like ECH-associated protein 1
KEGG	Kyoto Encyclopaedia of Genes and Genomes
KRAS	v-Ki-ras2 Kristen rat sarcoma viral oncogene homolog
KRT5	Keratin 5
LABA	Long-acting beta-adrenoceptor agonist
LAMA	Long-acting muscarinic receptor antagonist
LD	Limited disease
LDH	Lactate dehydrogenase
LNCaP	Prostate cancer cell line
LPS	Lipopolysaccharide
LTB4	Leukotriene B4
M059K	Glioblastoma cell line
MAPK	Mitogen-activated protein kinase
MCF-7	Michigan Cancer Foundation-7 (breast cancer cell line)
MDA	Malondialdehyde
<i>MDM2</i>	Murine double minute 2
MEK	Mitogen-activated kinase kinase
MFI	Mean fluorescence intensity
Mfn, MFN	Mitofusin
MitoTEMPO	2-(2,2,6,6-Tetramethylpiperidin-1-oxyl-4-ylamino)-2-oxoethyl) triphenylphosphonium chloride
MLE12	Mouse SV40 transformed alveolar epithelial cell line
MMP	Matrix metalloproteinase
mMRC	Modified British Medical Research Council
MOM	Mitochondrial outer membrane
MPC	Mitochondrial pyruvate carrier
mRNA	Messenger RNA
mROS	Mitochondrial ROS
mtDNA	Mitochondrial DNA
mTOR	Mammalian target of rapamycin
MTT	Methylthiazolyldiphenyl-tetrazolium bromide

NAC	N-acetyl cysteine
NADH	Reduced nicotinamide adenine dinucleotide
NADPH	Nicotinamide adenine dinucleotide phosphate
NaN ₃	Sodium azide
nDNA	Nuclear DNA
NDUFA9	NADH:ubiquinone oxidoreductase subunit A9
NEB	Neuroepithelial bodies
NF-κB	Nuclear factor kappa-light-chain-enhancer of activated B cells
NHBE	Human normal bronchial epithelium
NICE	National Institute for Health and Care Excellence
NK	Natural killer cell
NLRP3	Nucleotide-binding domain, leucine-rich repeat-containing protein 3
NO ₂	Nitrogen dioxide
NRF	Nuclear respiratory factor
Nrf2	Nuclear respiratory factor 2
NRK	Normal rat kidney epithelial cell line
NSCLC	Non-small cell lung cancer
O ₂ ⁻	Superoxide anion radical
O ₃	Ozone
OCR	Oxygen consumption rate
OD	Optical density
Opa1	Optic atrophy 1
OS	Overall survival
OXPPOS	Oxidative phosphorylation
<i>PARK2</i>	Parkin RBR E3 ubiquitin protein ligase
PBMC	Peripheral blood mononuclear cell
PCR	Polymerase chain reaction
PD-1	Programmed death protein 1
PDE-4	Phosphodiesterase 4
PDH	Pyruvate dehydrogenase
PDK	Pyruvate dehydrogenase kinase
PDP	Pyruvate dehydrogenase phosphatase
PE	Phycoerythrin
PEP	Phosphoenolpyruvate
PET	Positron emission tomography
<i>PGC1b</i>	PPAR-gamma co-activator 1-beta
<i>PGC-1α, PGC1a</i>	PPAR-gamma co-activator 1-alpha
PGZ	Pioglitazone

PI	Propidium iodine
<i>PIK3CA</i>	Phosphatidylinositol-4,5-bisphosphate 3-kinase
PINK1	PTEN (phosphatase and tensin homologue)-induced putative kinase 1
PKL	Liver pyruvate kinase
PKM	Muscle pyruvate kinase
PKR	Red cell pyruvate kinase
PKs	Pyruvate kinases
PM	Particulate matter
PMSC	Pulmonary smooth muscle cell
PPAR	Peroxisome-proliferator activator receptor
PPP	Pentose phosphate pathway
PRC	PGC-related co-activator
PRECOG	Prediction of Clinical Outcomes from Genomic Profiles
PRXs	Peroxiredoxins
PS	Phosphatidylserine
PTEN	Phosphatase and tensin homologue
Rb	Retinoblastoma
rEGF	Recombinant epithelial growth factor
RM one-way ANOVA	Repeated measures one-way ANOVA
RFU	Relative fluorescence unit
RIPA	Radioimmunoprecipitation assay
ROOH	Lipid peroxides
ROS	Reactive oxygen species
RPE	Retinal pigment epithelium
SAEC	Small airway epithelial cells
SCLC	Small cell lung cancer
SD	Standard deviation
SEM	Standard error of mean
SO ₂	Sulphur dioxide
SOD	Superoxide dismutase
SP	Surfactant protein
SP-A	Surfactant protein A
SQCC	Squamous cell carcinoma
SS	Szeto-Schiller
SS31	D-Arg-2',6'-dimethyltyrosine-Lys-Phe-NH ₂
SSC	Side scatter
STAT	Signal transducer and activator of transcription
<i>t</i> BHP	<i>t</i> -butylhydroperoxide
TCA	Tricarboxylic acid
TCR	T-cell receptor

TEM	Transmission electron microscopy
TGFB1	Transforming growth factor beta 1
TGF β	Transforming growth factor beta
TiO ₂ -NP	Titanium dioxide nanoparticle
TKI	Tyrosine kinase inhibitor
TMRM	Tetramethyl rhodamine methyl ester
TNFR1	Tumour necrosis receptor factor 1
TNF- α	Tumour necrosis factor alpha
TPP ⁺	Triphenylphosphonium
TRXs	Thioredoxins
VEGF	Vascular endothelial growth factor
WHO	World Health Organisation
WNT	Wingless-related integration site
XF	Extracellular flux
β -ME	Beta-mercaptoethanol

Chapter 1 Introduction

1.1 Chronic Obstructive Pulmonary Disease (COPD): an oxidative stress and inflammation associated disease

1.1.1 Definition

The Global Initiative for Obstructive Lung Disease (GOLD) committee gives the definition of COPD as a common, preventable and treatable disease which is characterised by persistent respiratory symptoms and limited airflow caused by abnormal respiratory tract and/or alveoli markedly exposed to noxious particles or gases (GOLD, 2017). This highlights the global incidence of COPD and its impact on society with the understanding that our goal should be disease prevention i.e. stopping exposure to cigarette smoke and pollution and that understanding the underlying pathophysiology of the disease should result in novel effective therapies. COPD is one of the four leading causes of death along with ischemic heart disease, cerebrovascular disease and HIV/AIDS and it is expected to become the third leading cause of death by 2030 (Mathers & Loncar, 2006). It is also, not surprisingly therefore, recognised as one of the top five respiratory diseases that causes morbidity and mortality worldwide (GOLD, 2017).

1.1.2 Diagnosis

The diagnosis of COPD is made by considering the symptoms (shortness of breath, chronic cough and chronic sputum production) together with the history of risk factor exposure e.g. smoking, environmental exposure and clinically confirmed persistent airflow limitation by spirometry (a post-bronchodilator $FEV_1/FVC < 0.7$) (GOLD, 2017).

1.1.3 Assessment

By determining the level of disease severity and the future risks such as exacerbation and hospitalisation frequency, an effective treatment plan can be devised that maintains as healthy a life as possible. The overall assessment consists of the classification of the severity of airflow limitation (GOLD 1-4), symptom assessment using the modified British Medical Research Council (mMRC) questionnaire or the COPD Assessment Test (CAT) and exacerbation history. Using this assessment, COPD patients are grouped into A, B, C or D. Each group requires different options for treatments in both pharmacological and non-pharmacological aspects. A refined ABCD assessment plan is shown in Figure 1.1. For example, group A patients should receive a bronchodilator with interval evaluation of efficiency. Group D patients with severe symptoms and assessment should step up therapy with the combination of long-acting β -agonist (LABA) and long-acting muscarinic antagonist (LAMA) with/without an inhaled corticosteroid (ICS). For non-pharmacological treatment, smoking cessation is essential for all patient groups but lung rehabilitation is needed for group B and D patients (GOLD, 2017). However, recent evidence highlights the need for lung function measurement to inform and predict mortality (Papi et al., 2018).

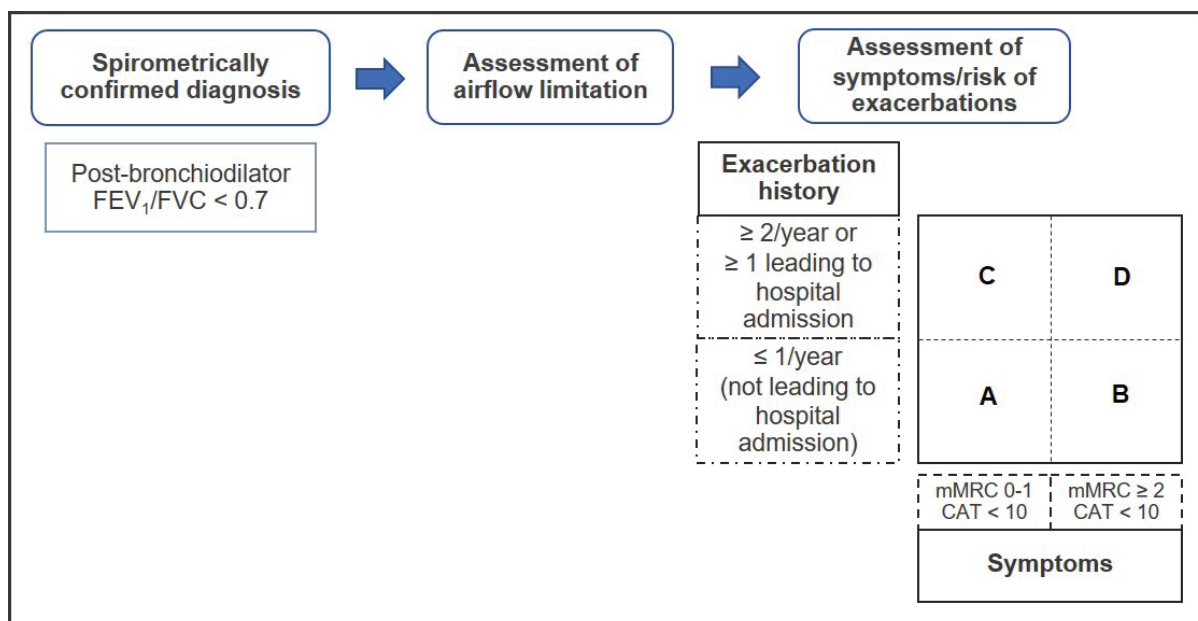


Figure 1.1 Updated ABCD assessment tools diagram (from Global Initiative for Chronic Obstructive Lung Diseases)

Diagram shows the steps of COPD assessment for patient categorisation. First, COPD diagnosis is confirmed using spirometry. The severity of airflow limitation (% FEV₁) is then assessed. COPD patients are grouped into A-D by the assessment of symptoms (mMRC or CAT questionnaires) with the history of exacerbation.

1.1.4 Risk factor and prevalence

The main risk factor for COPD was originally believed to be cigarette smoking but the importance of exposure to particulates and organic volatiles from the combustion of biomass fuels in cooking and from air pollution derived from farming, industry, and transportation has become increasingly more recognised globally (Forum of International Respiratory Societies, 2013). The Burden of Obstructive Lung Disease (BOLD) program (Burney et al., 2014) has been assessing the prevalence and risk factors for COPD in people aged over 40 globally using standardised methods. BOLD recently revealed a greater reduction in lung function than previous studies with 10.1% of the global population having COPD grade 2 or higher with the incidence in men being higher (11.8%) than that in females (8.5%) (GOLD, 2017). Even though smoking prevalence has decreased since 1980

(41.2% to 31.1% for males and 10.6% to 6.2% for females in 2012) (Ng et al., 2014), the prevalence of COPD is postulated to increase over the next 30 years and it is predicted that over 4.5 million people will die of COPD and related conditions annually by 2030 (GOLD, 2017; Lopez et al., 2006).

1.1.5 Pathophysiology

Chronic bronchitis, obstructive bronchiolitis and emphysema are the main disease pathologies of COPD (Barnes et al., 2015). As shown in Figure 1.2, chronic exposure of the airways to smoke can lead to pathological changes, also known as airway remodelling. Changes in the lungs include increased numbers of inflammatory cells: neutrophils, macrophages and lymphocytes, loss of mucociliary clearance by ciliated cells and mucous hypersecretion due to increasing number of goblet cells and enlarged submucosal glands in bronchioles resulting in excess mucous blocking the larger airways. The narrowing of airways also results from the thickening of airway smooth muscle cells and fibrosis (Barnes et al., 2015). In addition, the loss of alveolar cells leading to the reduction of alveolar surface in lung parenchyma, the ineffective elastic recoil and pulmonary gas exchange - emphysema (Bozinovski et al., 2016). Many cell types have been implicated in the pathophysiology of COPD and section 1.1.7 summarises some of these. For a full in-depth discussion of the role of all implicated cells in COPD the reader is directed towards several excellent reviews (Barnes, 2017; Barnes et al., 2015; Gao et al., 2015; Guillot et al., 2013; Tetley, 2005).

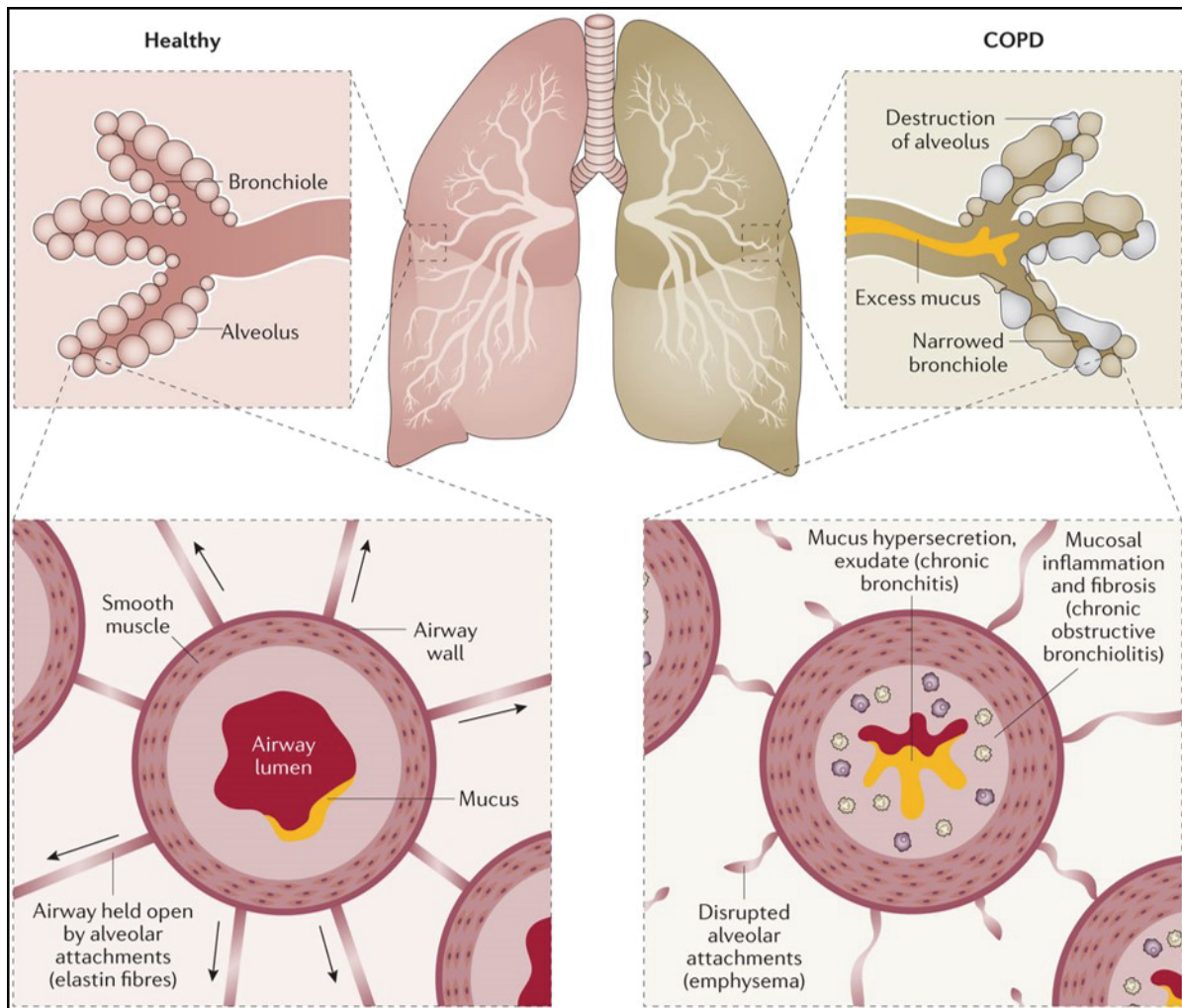


Figure 1.2 Pathophysiological changes in the COPD lung

In healthy lungs, the airway is maintained using the cooperation of various cells e.g. airway epithelium, alveolar epithelium, smooth muscle cells and alveolar macrophages to sustain normal lung function, mucous secretion and gas exchange. In COPD lungs, airflow limitation occurs as narrowing of lumen due to mucous hypersecretion, malfunction of mucociliary clearance and smooth muscle cell thickening with fibrosis. Abnormal gas exchange results from decreasing elastic recoil and surface area in destructive alveoli.

Reprinted from Nature Reviews Diseases Primers, Vol 1, Barnes et al., Chronic obstructive pulmonary disease, 1-21, ©2015, with permission of Nature Publishing Group.

1.1.6 Treatments

The multi-component and progressive disease COPD has management goals including; relieving symptoms, treating and preventing exacerbations and slowing down disease progression (Welte, 2009).

To maintain a stable disease (non-exacerbation), core management of COPD is a combination of pharmacological and non-pharmacological treatment (Barnes et al., 2015). Non-pharmacological management is recommended, as it helps improve symptoms and quality of life, including smoking cessation, immunisation against influenza, pulmonary rehabilitation, oxygen therapy and surgery (Safka & McIvor, 2015). Bronchodilators and inhaled corticosteroids (ICS) are the main medications used but other treatments such as phosphodiesterase-4 (PDE-4) inhibitors, antibiotics, mucolytics and antioxidants are used to prevent exacerbations (Barnes et al., 2015). Long-acting bronchodilators are recommended for COPD and are classified into long acting β_2 -agonists (LABA) such as salmeterol and indacaterol and long acting antimuscarinics (LAMA) such as tiotropium and glycopyrrolate (Beeh, 2016). The combination of LABA and LAMA improves lung function and reduces symptoms compared to the individual drugs (van der Molen & Cazzola, 2012).

Methylxanthines, non-selective PDE inhibitors such as theophylline and the selective PDE-4 inhibitor roflumilast are also used as anti-inflammatory drugs for symptomatic treatment (Cazzola & Matera, 2014). GOLD 2017 suggests using ICS in combination with LABA/LAMA in patients with frequent exacerbations or with moderate to severe COPD as this improves lung function and decreases

exacerbations. Recent studies comparing individual components against triple therapy (LABA, LAMA and ICS) have emphasised the value of this approach in COPD (Agusti, 2018; Papi et al., 2018; Lipson et al., 2018).

Corticosteroids suppress inflammation by a variety of mechanisms including reducing inflammatory gene expression and protein secretion by attenuating nuclear factor kappa B (NF- κ B)-driven gene activation or by degrading inflammatory gene messenger RNA (mRNA) (Barnes, 2010). Antioxidants such as N-acetylcysteine and carbocysteine are currently used as mucolytics in COPD although they have potential as anti-inflammatory agents (GOLD, 2017). The effect of other antioxidants as potential COPD therapies has been investigated both *in vitro* and *in vivo* (Rahman, 2008). A review of antioxidants and their possible roles in COPD is provided in section 1.5.3.

1.1.7 Cell types in the lung and their roles in COPD

Over 40 cell types have been identified in the lung including epithelial, connective tissue, vascular, immune system and mesothelial cells (Franks et al., 2008). Lung cells are grouped by their site and structure for example bronchial epithelial cells (BEC), alveolar epithelial cells, endothelial cells, airway smooth muscle cells, fibroblasts, and both resident and infiltrating immune cells (Franks et al., 2008). I have provided an overview of some of the key cell types involved in COPD, but a more extensive review is provided elsewhere (Bhat, Panzica, Kalathil, & Thanavala, 2015; Caramori et al., 2016).

1.1.7.1 Bronchial epithelial cells (BEC)

Groups of BEC form a pseudostratified layer as shown in Figure 1.3 and provide a defensive barrier against foreign particles and microorganisms coming from the external environment (Camelo, Dunmore, Sleeman, & Clarke, 2014; Chung, 2005). BEC can be grouped into three main types based on their morphology, function and biochemical characteristics, namely basal, ciliated and secretory cells (Gao et al., 2015). The composition of BEC varies depending on the airway level. The epithelial cells in the upper airway and bronchioles consist of basal cells, ciliated cells, secretory cells (goblet and club cells) whilst neuroendocrine cells reside at the bronchioalveolar junction (Succony & Janes, 2014).

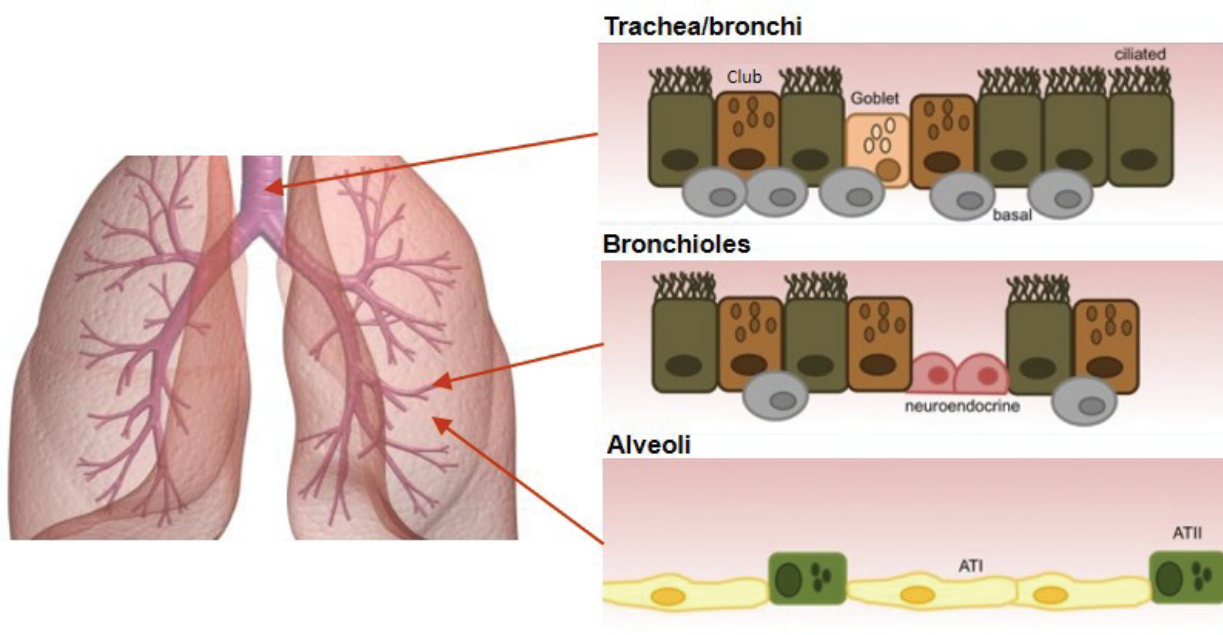


Figure 1.3 Airway epithelial cell type composition in the lungs

The upper airway (trachea and bronchi) consists of basal cells (grey), ciliated columnar cells (green), goblet cells (beige), and club cells (brown). The cell types in the smaller airway are similar with the addition of neuroendocrine cells (red). The alveoli are formed of alveolar epithelium type I (yellow) and II (light green). Adapted from: Camelo et al, 2014.

Basal cells underneath the airway mucosa not only have an important role in cell adhesion but also act as progenitor cells for epithelial renewal and restoration (Hong, Reynolds, Watkins, Fuchs, & Stripp, 2004). *TGFB1* (transforming growth factor β 1), a COPD risk gene encoding TGF- β , is upregulated in airway basal cells of smokers and is involved in squamous metaplasia (Ryan et al., 2014). Ciliated epithelial cells, the major type of BEC are responsible for clearing mucus using directional cilia beating (Gao et al., 2015). Loss of the pseudostratified epithelial lining pattern along with increased squamous cell metaplasia has been shown in patients with COPD GOLD 1 and 2 compared to smokers and non-smokers (Ryan et al., 2014). Goblet cells, also called mucus cells, produce mucus to capture foreign bodies and to moisten the airways. Club cells, are non-ciliated columnar cells, identified by a unique secretory protein, produce surfactants and anti-proteases that enables BEC integrity and regulation of airway immune responses (Gao et al., 2015). Goblet cell hyperplasia is found in chronic bronchitis and is increased in the lung periphery of patients with COPD (Ryan et al., 2014).

Apart from structural changes in response to cigarette smoke in COPD, BEC can express and release a host of inflammatory mediators including cytokines, lipid mediators, growth factors, proteases and reactive oxygen species (ROS) (Gao et al., 2015). For example, BEC treated with cigarette smoke extract (CSE) show increased expression of the pro-inflammatory cytokines interleukin (IL)-1 β , IL-8 (CXCL8), tissue necrosis factor- α (TNF- α) and granulocyte colony-stimulating factor (GM-CSF) via activation of mitogen activated protein kinase (MAPK) and NF- κ B pathways (Hellermann, Nagy, Kong, Lockey, & Mohapatra, 2002; Mio et al., 1997).

The production of CXCL8, a chemoattractant for neutrophils, was higher in BEC from patients with COPD than those from smokers (Heijink et al., 2011).

1.1.7.2 Alveolar epithelial cells (AEC)

Alveolar epithelial cells (AEC) forming the lung alveoli, consist of alveolar epithelial type I (ATI) and type II (ATII) cells (Figure 1.4). ATI, account for 96% of all AEC, they form a thin line on the alveolar surface whereas the rest are ATII. The ATII are large cuboidal cells with apical microvilli, they produce and release surfactant which is collected in their lamellar bodies (Guillot et al., 2013).

At the bronchoalveolar junction, bronchoalveolar stem cells (BASC) can differentiate into club cells to form terminal bronchioles or into AEC to form alveoli (Guillot et al., 2013). Differentiation of BASC into AEC is regulated by the fibroblast growth factor (FGF)-10 signalling, the WNT/ β -Catenin complex, Notch pathway and transforming growth factor (TGF)- β (Domyan & Sun, 2011).

Moreover, lung progenitor cells potentially differentiate into alveolar type II (ATII) cells which, in turn, can trans-differentiate into ATI cells for regeneration by re-entering cell cycle and starting cell division (Fehrenbach, 2001; Guillot et al., 2013). Lung repair associated with increased ATII proliferation was found in damaged lungs (Fujino et al., 2011).

Both ATI and ATII work together to enable efficient gas exchange, form barrier against microorganisms and other harmful substances, and along with alveolar macrophages play an important role in surfactant homeostasis, immunomodulation and inflammatory responses (Guillot et al., 2013).

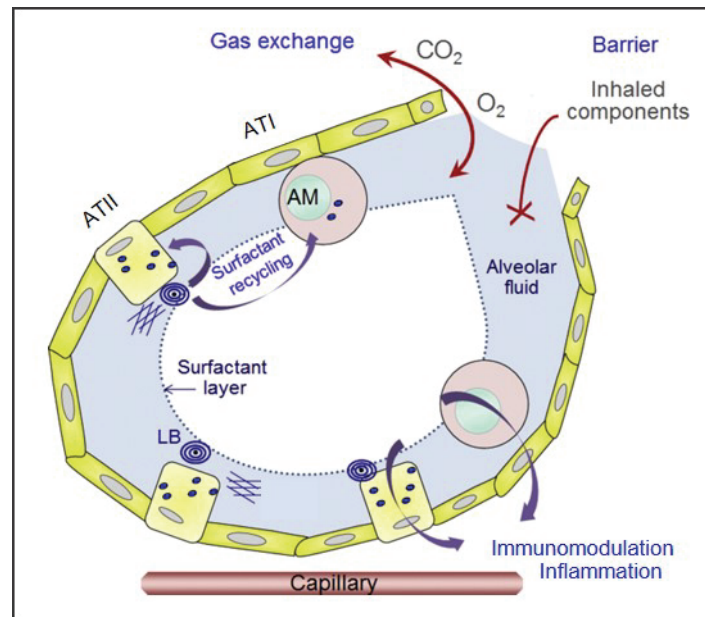


Figure 1.4 Alveolar cell types in alveoli and their functions

Structural cells in alveoli consist of alveolar epithelium type I (ATI) forming an alveolar sac along with alveolar epithelium type II (ATII) which produce surfactant provided in lamellar bodies (LB). ATI, ATII and alveolar macrophage together maintain the normal function of gas exchange, barrier against foreign bodies and immunomodulation and inflammatory response. Adapted from: Guillot et al. 2013.

ATI cells lining the alveoli are in contact with both the airspace and the blood capillaries whereas ATII cells produce surfactant proteins (SP) to decrease the surface tension of the alveoli (Guillot et al., 2013). Short-term cigarette smoking *in vivo* affects AEC by limiting repair and decreasing SP production by ATII cells (Agarwal, Yin, & Cadenas, 2014). In contrast, smokers with COPD have an increased number of ATII cells and alveolar macrophages compared to those without COPD. In addition, the percentage of SP-A positive cells in these two cell types was increased and SP-A expression was negatively correlated with the severity of obstruction (Agarwal et al., 2014). CSE also induces ROS production and stimulates inflammatory cytokine (CXCL8 and IL-6) release in isolated human ATII cells from smokers as well as inducing ATII cell injury and apoptosis in mice (Messier et al., 2013).

1.1.7.3 Airway smooth muscle cells (ASMCs)

Airway smooth muscle cells (ASMCs) form a functional banded structure beneath the airway epithelial layer in both large and small airways which regulates airflow by constriction and dilatation in response to various stimuli (Amrani & Panettieri, 2003). In COPD, changes in ASMCs, hyperplasia and hypertrophy, were found in the small airway (<2 mm in inner diameter) (Chung, 2005) and increased areas of larger ASMCs were reported in the large airways (Pini et al., 2014). The increased muscle area when normalised to the internal perimeter was found to negatively correlate with %FEV₁ in smokers (Saetta et al., 1998). The volume of smooth muscle expressed per unit of basement membrane surface area was increased 1.5-fold in patients with COPD GOLD stage 3 and 4 compared to patients with lower disease stage (Hogg et al., 2004). Besides controlling contraction, ASMCs can express and release inflammatory cytokines, growth factors e.g. TGF- β and proteases which are involved in inflammation and airway remodelling (Chung, 2005). In a feed-forward manner, these pro-inflammatory cytokines (IL-1 β and TNF- α) and growth factors (TGF) can further promote ASMCs proliferation *in vivo* and *in vitro* (Stamatiou, Paraskeva, Gourgoulianis, Molyvdas, & Hatziefthimiou, 2012). Alterations in the metabolic profile and energy balance also occurs in COPD ASMCs and are associated with hyperproliferation (Michaeloudes et al., 2017). Limited studies have examined the effect of CSE on ASMC function but CSE induced the proliferation and reduced the contractility of isolated bovine ASMCs (Pera et al., 2010).

1.1.7.4 Fibroblasts

Lung fibroblasts are located in the interstitium and are responsible for producing extracellular matrix (ECM) e.g. fibrous proteins, glycoproteins, and proteoglycans for the basement membrane and interstitial space, and in shaping ECM responses during the repair of injured lung tissue, which helps maintain the structure of lung tissue (Basma et al., 2014; White, 2015). Small airway remodelling occurs in the COPD lung and includes abnormal production and degradation of ECM in the alveoli and excessive formation and deposition of ECM and fibrosis within the bronchi and bronchioles (Hallgren et al., 2010). TGF- β 1-stimulated fibroblasts from COPD patients have enhanced proteoglycan production compared to fibroblasts from healthy controls (Hallgren et al., 2010). In addition, the repair function of lung fibroblasts is impaired in cells from COPD patients compared to healthy controls (Togo et al., 2008). In addition, CSE enhanced cell cycle progression from S phase towards G1/G2/M and activated pro-inflammatory signalling pathways and elevated IL-8 release from HFL-1 fibroblasts. CSE also increased p21 and p53 expression which overall suggests that cells enter a senescence-like state with a reduced capacity to undertake repair processes. Importantly, ERK1/2 activation and the number of cells in G1 compared to G2 cell cycle were increased in primary lung fibroblasts from current smokers compared to those from former smokers suggesting that cigarette smoke induces a senescence-like pro-inflammatory status (D'Anna et al., 2015).

In patients with emphysema, lung fibroblasts show a decreased proliferation rate and they express markers of senescence which inhibit insulin-like growth factor *in vitro* (Holz et al., 2004; Müller et al., 2006). Moreover, in response to lung injury,

lung fibroblasts can be activated by inflammatory mediators as occurs in COPD (Basma et al., 2014). Lung fibroblasts also communicate with other cell types in response to inflammation in COPD. Fibroblasts from patients with COPD released increased *IL-8/CXCL8* in co-culture with primary airway epithelial cells, and medium from COPD-derived airway epithelial cells exposed to CSE induced *IL-1 α* expression in foetal fibroblasts (Osei et al., 2016).

1.1.7.5 Inflammatory cells

1.1.7.5.1 Macrophages

Macrophages are differentiated from monocytes in the lung parenchyma (Barnes, 2004). There are two main types of macrophages in the lung, alveolar macrophages (AM) and macrophages in lung tissue (Vlahos & Bozinovski, 2014). Alveolar macrophages are located in the alveolar spaces where air and lung tissue interconnect, they have an important role in defending against microorganisms and clearing inhaled foreign bodies using phagocytosis (Barnes, 2004). This is in contrast to dendritic cells, another group of antigens presenting cells which predominantly initiate the innate and adaptive immune responses. Moreover, macrophages have the capability of inflammatory and anti-inflammatory mediator production and secretion in response to stimuli such as cigarette smoke and pro-inflammatory cytokines (Barnes, 2004). In patients with COPD, there is increased numbers of macrophages in the lungs and in bronchoalveolar lavage fluid (BAL) and sputum (Traves, Culpitt, Russell, Barnes, & Donnelly, 2002). *IL-1 β* and CSE were found to induce greater release of *CXCL8* in macrophages from BAL of patients with COPD compared with smokers (Culpitt et al., 2003). Although the number of BAL macrophages is increased in COPD they are defective

with respect to phagocytosis of bacteria such as *S. pneumoniae*, *H. influenzae*, and *P. aeruginosa* (Bewley et al., 2018). Macrophages also play a role in lung destruction in COPD as T-lymphocytes stimulate alveolar macrophages to produce matrix metalloproteinase (MMP)-12 which degrades elastin which in turn stimulates monocyte differentiation (Grumelli et al., 2004).

1.1.7.5.2 Neutrophils

Neutrophils are granulocytes that defend against microorganisms by phagocytosing and subsequent digestion of bacteria using a combination of ROS and proteases such as neutrophil elastase and cathepsins (Hoenderdos & Condliffe, 2013). Neutrophils can migrate into tissue to the site of inflammation by adhering to endothelial cells via E-selectin which is known to be upregulated in COPD (Barnes, 2017). Neutrophil chemotactic factors including CXCL1, -5 and -8 and LTB₄ induce migration into the lungs and all have increased expression in the fluidic part of the sputum in COPD patients. However, although the levels were increased, their chemotactic activity was impaired (Yoshikawa et al., 2007). CSE decreased neutrophil clearance after bacterial infection *in vivo* and impaired phagocytosis in an *in vitro* study (Drannik et al., 2004; Stringer, Tobias, O'Neill, & Franklin, 2007). Neutrophilia has been described as a characteristic of COPD inflammation because of the increased number of activated neutrophils found in sputum and BAL fluid in patients with COPD which is related to disease severity (Barnes, 2017). Neutrophil myeloperoxidase (MPO) which induces oxidative stress in inflammatory conditions, its activity was found to be increased in peripheral blood neutrophils of smokers (Bridges, Fu, & Rehm, 1985).

1.1.7.5.3 Lymphocytes

Lymphocytes are white blood cells broadly divided into T, B and natural killer (NK) cells by their phenotypes and functions (LaRosa & Orange, 2008). Lymphocytes originate from the bone marrow and generate their specificity and diversity through the T-cell receptor and B-cell receptor in the thymus gland and lymphoid tissues (LaRosa & Orange, 2008). T-cell and B-cell lymphocytes, the effectors of the adaptive immune system, play a role in inflammatory processes in COPD and in the tumour microenvironment of lung cancer (Banat et al., 2015; Barnes, 2017). In patients with COPD there is association between decreased lung function and increased percentage of CD4⁺ and CD8⁺ T lymphocytes (Grumelli et al., 2004). CD8⁺ T lymphocytes are a central regulator of inflammation in COPD. An *in vivo* study showed the loss of emphysema progression in CD8⁺ T cell-deficient mice in response to cigarette smoke. Furthermore interferon- γ (IFN- γ) and IFN- γ -inducible protein-10 produced from CD8⁺ T lymphocytes can induce MMP-12 production which activates macrophages causing lung destruction (Maeno et al., 2007). Moreover, CD8⁺ T lymphocytes in sputum from smokers with COPD have higher cytotoxic activity and greater perforin expression compared to non-COPD smokers (Chrysofakis et al., 2004). Reduced numbers of regulatory T cells are reported in COPD which may affect the immune responses seen in these patients (Bhat et al., 2015). This is covered in greater detail by Bhat and colleagues (Bhat et al., 2015).

B lymphocytes which mediate the humoral immune response also reside in the lungs; these include plasma cells and memory B cells. Plasma cells located in the submucosal airway synthesise immunoglobulin (Ig) A and IgM into

the mucosal layer. In an *in vitro* study of COPD lung, bronchial epithelial cells increased IgA synthesis when co-cultured with B lymphocytes suggesting a crosstalk between them in regulating immunity (Ladjemi et al., 2015). Memory B lymphocytes originated from peribronchial lymphoid follicles are activated in response to lung infection and are promptly activated in response to reinfection (Onodera et al., 2012). As well as other immune cells, the percentage of airways with B lymphocytes present was associated with COPD progression (Hogg et al., 2004). B lymphocytes also activate macrophages to release MMPs which cause loss of alveolar surface leading to COPD (Polverino, Seys, Bracke, & Owen, 2016).

1.2 Lung cancer

1.2.1 Prevalence and risk factors

Lung cancer is the most commonly diagnosed cancer and is the most common cause of death from cancers in the world representing 12.7% of the total cancer deaths (Ferlay et al., 2010). This reflects the paucity of treatments and the late stage at which lung cancer is usually detected. In 2016 the National Lung Cancer Audit reported that of cancers in the UK 88% of patients had non-small cell type (NSCLC), 11% was small cell lung cancer (SCLC) and the rest was other tumours (Royal College of Physicians, 2016). Over 80% of patients who develop lung cancer in the UK do so as a result of cigarette smoking including exposure to second hand smoking (Cancer Research UK, 2015). Other risk factors include a family history of lung cancer, exposure to radon gas, a history of other lung diseases like tuberculosis and reduced immune function (FIRS, 2013). Lung cancer commonly occurs in elderly people and in patients with COPD or emphysema. Similar to COPD, prolonged exposure to air pollution is also

a risk factor for lung cancer initiation. Lung cancer can develop along the respiratory tract and in the lung parenchyma. Formation of lung tumours can either originate from an abnormal cell in the lung itself (a primary lung cancer) or metastasise from other parts of the body (secondary lung cancer).

1.2.2 Lung cancer cell types

In 2015 the World Health Organisation (WHO) published an updated classification of Tumours of the Lung, Pleura, Thymus, and Heart. Lung cancer classification has been changed to include both immunohistochemistry and genetic analysis (Travis et al., 2015). The new classified groups of lung cancer predominantly consist of epithelial tumours (adenocarcinoma and squamous cell carcinoma), neuroendocrine tumours (small cell lung cancer (SCLC) and large cell carcinoma) and other cancer types as shown in Figure 1.5.

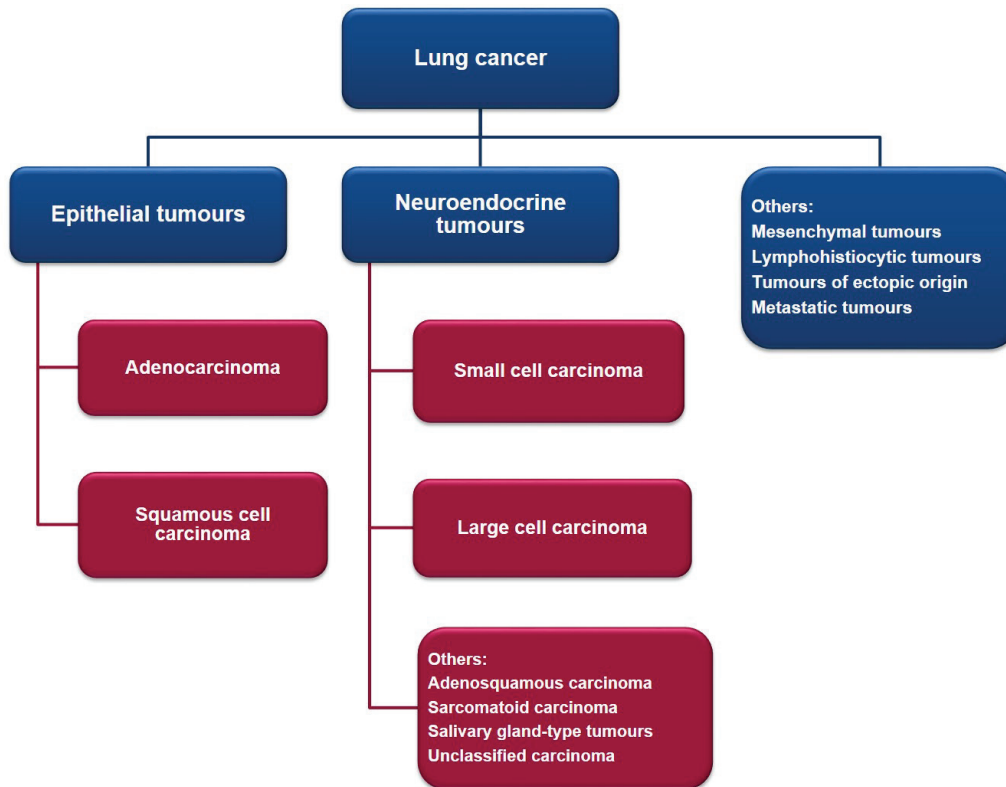


Figure 1.5 Classification of lung cancer

The 2015 classification of lung cancer. Lung cancer types are classified using morphology and immunohistochemistry, and re-categorised into epithelial tumours, neuroendocrine tumours and other types. From Travis et al., 2015.

Despite the new classification, the therapeutic approach for lung cancer still uses the previous classification which categorised lung cancer into small cell lung cancer (SCLC) and non-small cell lung cancer (NSCLC) (Assi, Kamphorst, Moukalled, & Ramalingam, 2017; Forde & Ettinger, 2013; Langer, 2015; Mehta, Dobersch, Romero-Olmedo, & Barreto, 2015; Zhao, Ren, & Tang, 2014). NSCLC can be subcategorised into squamous cell carcinoma (SQCC), adenocarcinoma, and large cell carcinoma (Petersen, 2011). The histological morphology of SCLC and NSCLC are shown in Figure 1.6 (Travis, 2011). The identification of SQCC includes squamous differentiation, keratinisation and intercellular bridges. Adenocarcinoma is characterised by mucus formation with abnormal cell growth like glandular pattern, papillary growth. Even though most adenocarcinoma cell types are invasive,

cancer cells of a subtype called bronchioalveolar carcinoma (BAC) grow along alveolar septa and bronchioles with non-invasive pattern (Travis, 2011). Large cell carcinoma is a poorly differentiated tumour which cannot be classified into SQCC or adenocarcinoma, and also has poor prognosis (Petersen, 2011). SCLC is another poorly differentiated lung cancer as shown by its histological appearance. Additionally, SCLC tumour cells are small tumour cells no more than 3-lymphocytes in size with a scant cytoplasm (Travis, 2011). Also SCLC tumour cells display differentiated neuroendocrine activity (Petersen, 2011).

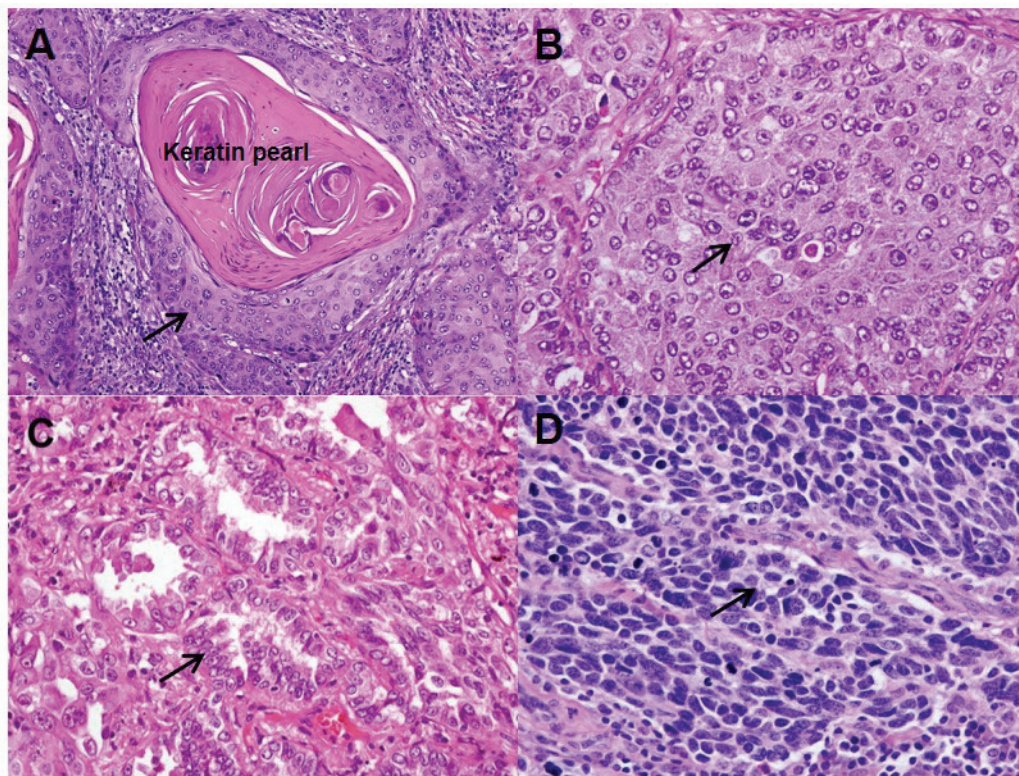


Figure 1.6 Types of lung cancer

Types of lung cancer are mainly categorised by histological findings into non-small cell lung cancer and small cell lung cancer. Non-small cell type is subcategorised into squamous cell carcinoma which has stratified squamous cell (arrow) surrounding keratin pearl (H&E, x200) (A), large cell carcinoma (H&E, x400) (B) and adenocarcinoma (H&E, x400) (C). Small cell lung cancer (H&E, x400) (D). Arrows in each picture show the typical cell in each cancer type.

Rearranged and reprinted from *Clinics in Chest Medicine*, Vol 32, Issue 4, Travis WD, *Pathology of Lung Cancer*, 669-92, ©2011, with permission of Elsevier.

1.2.3 Lung cancer staging

Staging of lung cancer is assessed by considering the size of the tumour, adjacent lymph node involvement and metastasis and is useful for planning treatment management and for predicting prognosis. The TNM staging system is used to classify different stages of lung cancer. This system defines the characteristics of the primary tumour (T) based on size, the regional lymph node involvement (N) and the tumour metastasis (M) as illustrated in Figure 1.7 (Lababede, Meziane, & Rice, 2011).

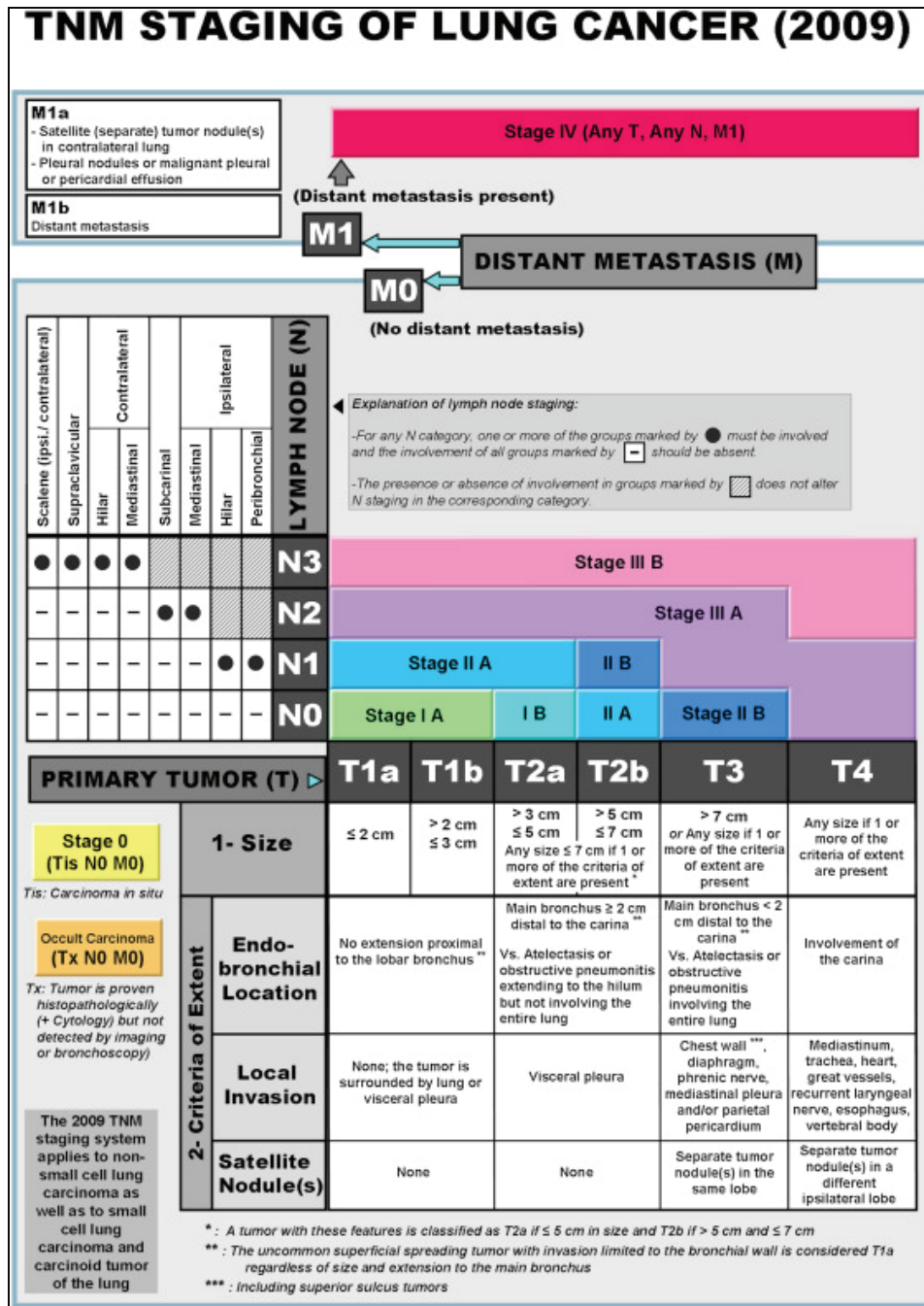


Figure 1.7 TNM Staging of lung cancer

Reprinted from Chest, Vol 139, Lababede O, Meziane M, Rice T, Seventh Edition of the Cancer Staging Manual and Stage Grouping of Lung Cancer Quick Reference Chart and Diagrams, 183-9, ©2011, with permission of Elsevier.

1.2.4 Importance of epithelial cells in lung cancer

The epithelium of the airway is different in terms of type, role and location which together maintain the integrity of the airway structure. Airway stem cells, with the ability of self-renew and high proliferation, play an important role in differentiation to produce daughter cells with various functions (Succony & Janes, 2014). In the lungs, the locations of groups of stem cells (niche) were identified as the possible sites of lung cancer development. Mouse injury models have been used to damage specified cell populations and then study the repair response. This injury model has identified areas of stem cell niches localised to the (i) submucosal gland area in the upper airway, (ii) neuroepithelial bodies (NEB) and (iii) the bronchoalveolar duct junction (BADJ) (Singh & Chellappan, 2014) (Figure 1.8).

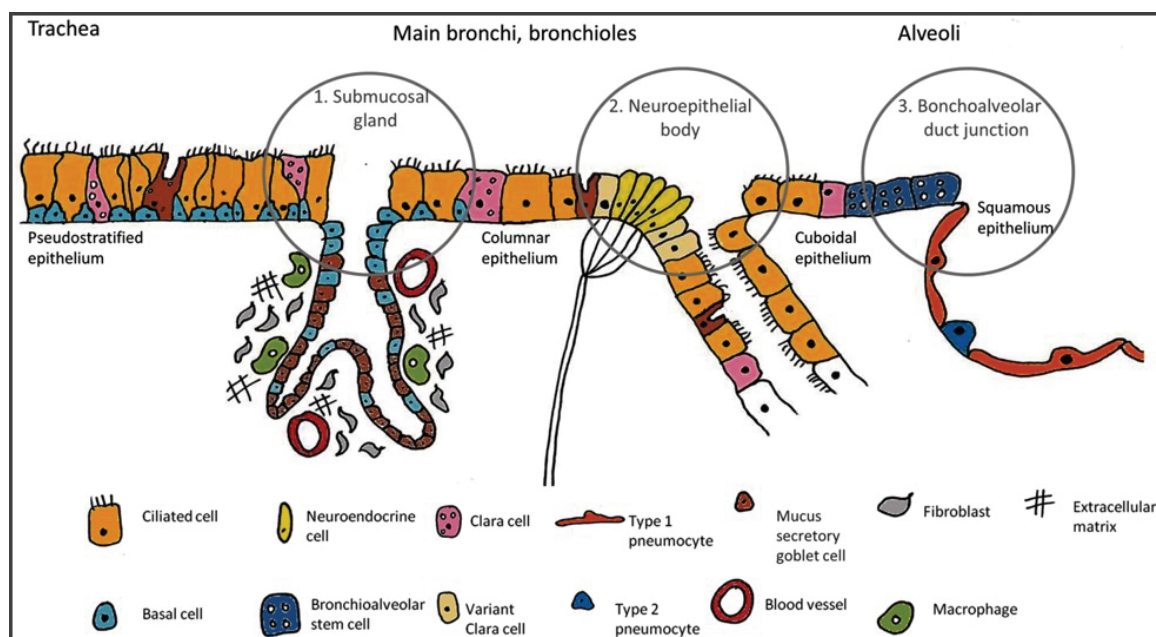


Figure 1.8 Schematic presenting the site of different airway epithelial cell types and other cells along the respiratory tract

Three possible areas which develop lung cancer are presented in the circles which comprise submucosal gland area, neuroepithelial body and bronchioalveolar duct junction. Basal cells from these areas are believed to become squamous cell carcinoma, small cell carcinoma and adenocarcinoma, respectively.

Reprinted from QJM: An International Journal of Medicine, Vol 107, Succony & Janes, Airway stem cells and lung cancer, 607-12, ©2014, with permission of Oxford University Press.

Keratin 5 (KRT5)-labelled basal cells were tracked and found in club cells and ciliated cells in the submucosal gland area and were increased in damaged airway *in vivo* (Rock et al., 2009). The stem cell niche in NEB was identified in mice exposed to naphthalene and was specific to club cell damage. A higher activity and repair capability was found in the resistant variant club cells (secretory protein positive) under these conditions (Reynolds, Giangreco, Power, & Stripp, 2000). Bronchoalveolar stem cells at BADJ were also found to be resistant in the naphthalene-induced mouse injury model and were highly proliferative (Reynolds et al., 2000). As well as the impairment of cell repair and regeneration in COPD, these three stem cell niches are the origins of various types of lung cancer due to genetic mutations in stem cells - also known as cancer stem cells (Succony & Janes, 2014). Squamous cell carcinoma retains the characteristics of basal cells with KRT5 expression. They are mostly found in the upper airway including in the submucosal gland area where the basal cells are mostly located (Barth et al., 2000). The expression of neuroendocrine markers such as calcitonin gene-related protein was found in SCLC suggesting that NEB could be the site of SCLC origin (Succony & Janes, 2014). BADJ is a possible area for the development of adenocarcinoma since markers of club cell secretory protein and surfactant protein C, which are derived from club cells and ATII cells respectively, were found in this cancer cell type (Giangreco, Reynolds, & Stripp, 2002).

In addition to cancer stem cells, epithelial-mesenchymal transition (EMT) in COPD was found to play an important role in cancer formation and progression (De Craene & Berx, 2013). *TGF β 1* mRNA expression was upregulated in airway basal cells isolated from smokers and was associated with squamous metaplasia in COPD

(Ryan et al., 2014) as mentioned previously (section 1.1.7.1). This is consistent with a study that demonstrated that increased numbers of TGF β -positive epithelial and sub-mucosal cells within the bronchial mucosa of patients with chronic bronchitis was correlated with the increased overall thickness of the basement membrane (Vignola et al., 1997). The expression of EMT biomarkers (S100A4, vimentin and N-cadherin) in tumour samples was significantly higher in the leading-edge peripheral area than in the central area. There was a positive correlation between EMT biomarker expression in the peripheral area of the tumour and poor prognosis suggesting that it may be a useful tool for clinical assessment (Mahmood, Ward, Muller, Sohal, & Walters, 2017).

1.2.5 Current treatment of lung cancer

The National Institute for Health and Care Excellence (NICE) recommends multimodality therapy for lung cancer treatment to improve survival, control disease and maintain quality of life (National Institute for Health and Care Excellence, 2017).

NSCLC and SCLC have separate treatment approaches. Therapy for NSCLC depends on clinical staging and patient health status. The modalities of treatment for NSCLC mainly consist of surgery, chemotherapy (CMT) and radiotherapy as shown in Figure 1.9, and other additional treatments e.g. photodynamic therapy and percutaneous radiofrequency ablation for specific indications (NICE, 2017).

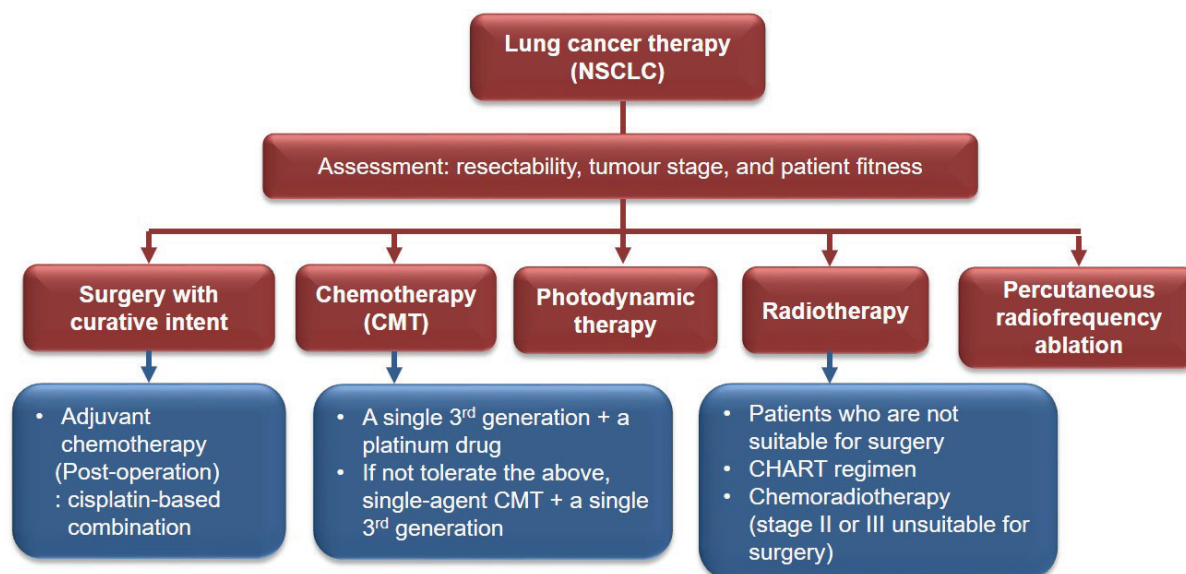


Figure 1.9 Summary flowchart of non-small cell lung cancer treatment

Consideration for multimodality treatment for lung cancer depends on resectability, stage of tumour and patient health status. Platinum drugs: carboplatin and cisplatin. Third generation drugs: docetaxel, gemcitabine, paclitaxel and vinorelbine. Single-agent chemotherapy e.g. gefitinib (1st line treatment of NSCLC), CHART = Continuous hyperfractionated accelerated radiotherapy. Adapted from an interactive flow chart from NICE (National Institute for Health and Care Excellence), website, accessed 18 Dec 2017.

Surgery is considered in patients with NSCLC stage I and II who are generally asymptomatic and can maintain daily activity (Lang-Lazdunski, 2013). In addition to surgical treatment, adjuvant CMT is recommended to decrease the risk of the cancer recurrence.

According to NICE guidelines (NICE clinical guideline 121 'Lung cancer') (NICE, 2011), a chemotherapy regimen using a combination of platinum-based treatments with a single 3rd generation CMT agent such as docetaxel, paclitaxel, gemcitabine and vinorelbine, can be used as adjuvant CMT in previously untreated patients with stage III or IV NSCLC. Platinum based agents including cisplatin and carboplatin can interfere with DNA repair leading to cancer cell apoptosis (Dasari & Bernard Tchounwou, 2014). Docetaxel and paclitaxel are mitotic inhibitors which disrupt microtubules and inhibit cancer cell proliferation (Joshi, Liu, & Belani, 2014) whereas

gemcitabine is a nucleoside analogue of deoxycytidine cytotoxic drug and vinorelbine is a semisynthetic vinca alkaloid inhibiting mitosis (Go et al., 2014).

For patients with NSCLC stage III or IV who cannot tolerate the side effects of platinum agents, single-agent CMT with 3rd generation CMT is an option (NICE, 2017). Examples of single-agent CMT are gefitinib and pemetrexed. Gefitinib (an epidermal growth factor receptor, EGFR, tyrosine kinase inhibitor - TKI) is used as the 1st line treatment for NSCLC with EGFR mutation positive (Liu, Jin, Wang, & Wang, 2017). Pemetrexed, an antifolate agent, is recommended as the 1st line treatment combined with cisplatin for patients with adenocarcinoma or large cell carcinoma (NICE, 2017; Tomasini, Barlesi, Mascoux, & Greillier, 2016).

Besides adjuvant CMT, oral agents such as fluorouracil (5-FU) and EGFR-targeted drugs: gefitinib and erlotinib are in clinical trials as targeted therapy (Wakelee, Kelly, & Edelman, 2014). The discovery of mutations in EGFR, vascular endothelial growth factor (VEGF) and anaplastic lymphoma kinase (ALK) in NSCLC has hastened the development of drugs targeting these pathways. EGFR TKI such as gefitinib inhibits EGFR transduction by binding the TK region of EGFR. Clinical studies have reported efficacy and outcome of a monoclonal antibody specific to VEGF for advanced NSCLC (Forde & Ettinger, 2013). Other novel molecular therapeutic approaches including immunotherapy and epigenetic therapy have been extensively investigated particularly in mutation-negative tumours (Forde & Ettinger, 2013).

Cancer cells have many tactics to escape being recognised and destroyed by immune cells such as impaired antigen presentation, immunosuppressive cytokine secretion, NK cell down regulation and T-cell inactivation through immune checkpoint pathway modulation (Langer, 2015). Cytotoxic T lymphocytes (CTLs) are the main immune cells responsible for attacking cancer cells (Aerts & Hegmans, 2013); however, CTLs activity is suppressed in NSCLC microenvironment. Co-inhibitory molecules which suppress CTLs activity, including cytotoxic T-lymphocyte-associated antigen 4 (CTLA-4) and programmed death protein 1 (PD-1) appear to be overexpressed in NSCLC (Salvi et al., 2012; Zhang, Huang, Gong, Qin, & Shen, 2010). Therefore, these molecules are the main targets for the development of a novel class of drugs called checkpoint inhibitors (Langer, 2015).

Ipilimumab (CTLA-4 antibody) and nivolumab (PD-1 antibody) have been approved for use in patients with NSCLC. Clinical trials demonstrated an improvement in efficacy with immune checkpoint inhibitors compared to CMT in NSCLC (Assi et al., 2017). However, immune-related adverse events (irAEs) of the checkpoint inhibitors have been reported with development of autoimmune symptoms in up to 90% and 70% of patients treated with a CTLA-4 antibody and a PD-1 antibody, respectively (Michot et al., 2016).

Epigenetic changes are associated with phenotypic changes in the absence of changes in gene sequences and is exemplified by modulation of DNA methylation, which is a major characteristic of cancer cells, histone modification and nucleosome remodelling (Mehta et al., 2015). Since epigenetic changes can be reversed by

drugs that inhibit epigenetic enzymes, these drugs may represent an alternative treatment approach for NSCLC (Liu, Fabbri, Gitlitz, & Laird-Offringa, 2013). Current epigenetic drugs approved by the European Medicines Evaluation Agency (EMA) target DNA methyl transferases and histone deacetylases (Mehta et al., 2015).

For small cell lung cancer (SCLC) the therapeutic approaches depend on the extent of the disease. SCLC is the most aggressive type of lung cancer with median of 12 months overall survival (OS) period and the possibility of long term survival is very low (Stupp, Monnerat, Turrisi, Perry, & Leyvraz, 2004). The classification of SCLC can be divided into limited disease (LD) and extensive disease (ED) (Carter, Glisson, Truong, & Erasmus, 2014) as shown in Figure 1.10.

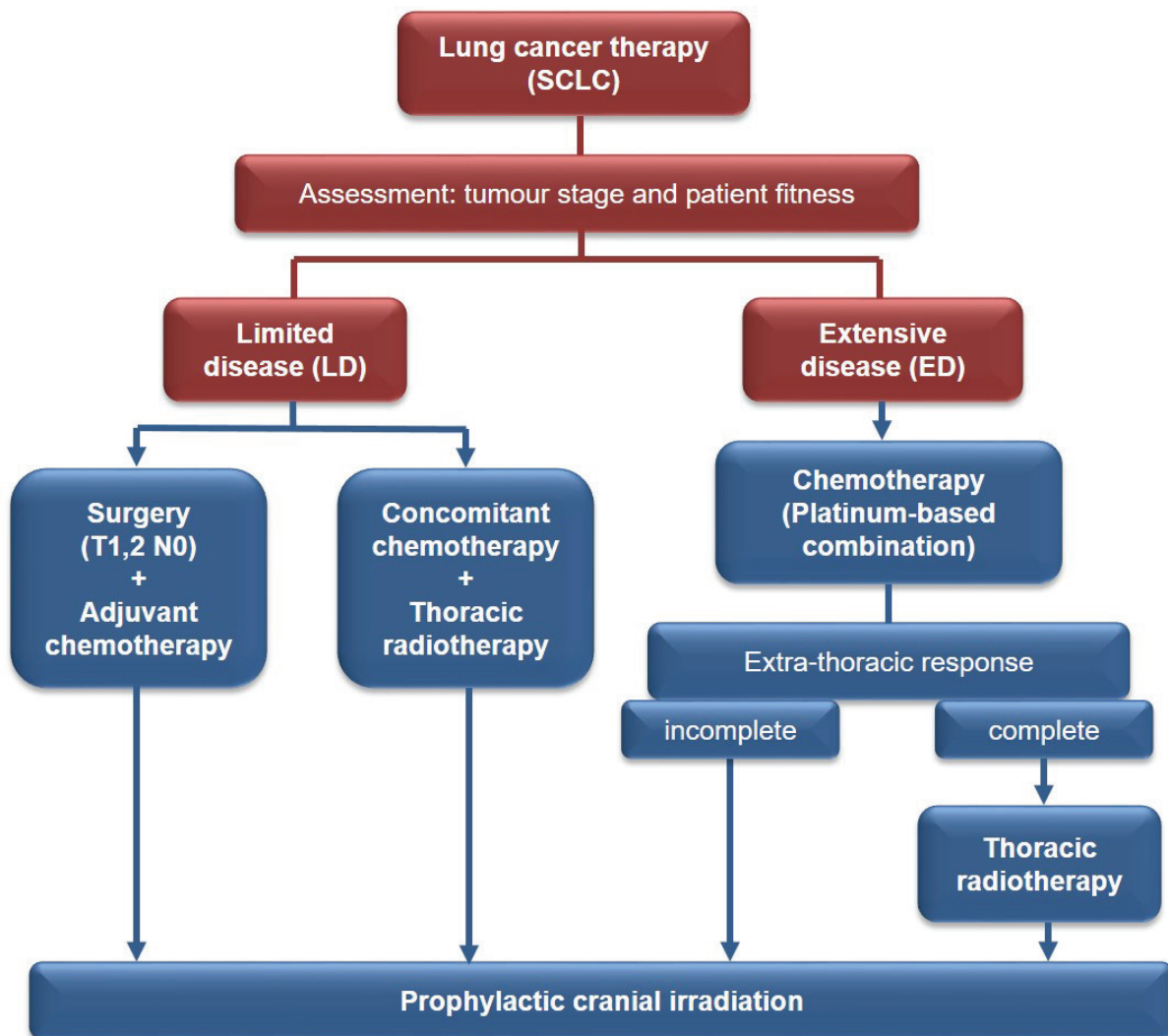


Figure 1.10 Summary flowchart of small cell lung cancer treatment

Consideration for small cell lung cancer treatment depends on the stage of disease divided into limited and extensive conditions which require different treatment approaches. Adapted from Morabito et al., 2014.

For patients with limited disease (LD)-SCLC which is restricted to one hemithorax with/without regional lymph node involvement with no distant metastasis (Stupp et al., 2004), the standard treatment requires concomitant CMT (cisplatin and etoposide) combined with thoracic radiotherapy followed by prophylactic cranial irradiation. Curative-intent surgery can be considered in patients with SCLC stage I and is followed by adjuvant CMT (Low & Ben-Or, 2018). In patients with extensive disease (ED-SCLC), CMT is the standard treatment (platinum-based combination for

4-6 cycles); subsequently thoracic radiotherapy for extra-thoracic tumours responding to the CMT should be considered (Morabito et al., 2014). Prophylactic cranial irradiation is also suggested for CMT responders to reduce the incidence of brain metastasis and improve OS (Zhang et al., 2014).

Similar to NSCLC, targeted therapy has been evaluated in SCLC. Ipilimumab was used in combination with CMT in a clinical phase II study of ED-SCLC and showed some improvement in OS compared to CMT with placebo (12.9 VS 9.9 months, $p=0.13$) (Reck et al., 2013). However, a clinical phase III randomised study (NCT01450761) evaluating ipilimumab in combination with CMT compared and CMT alone in 1,414 patients with ED-SCLC showed that the addition of ipilimumab did not improve OS (10.22 VS 9.95 months, $p=0.57$) (Reck et al., 2016).

1.3 Possible links between COPD and lung cancer

1.3.1 Chronic inflammation

Chronic inflammation is a key characteristic in both diseases and may cause a repetitive epithelial injury and increase cell turnover which may lead to errors in DNA transcription and translation leading to genetic mutation (Raviv, Hawkins, DeCamp, & Kalhan, 2011). Long-term inflammatory responses in disease can promote cancer initiation in other organs such as in patients with ulcerative colitis which is an autoimmune disease and chronic viral hepatitis B who develop colon cancer and liver cancer, respectively.

The inflammatory cell types seen in COPD and lung cancer are similar and include macrophages, neutrophils, helper-T cells and cytotoxic-T-cells. In COPD, the increase in alveolar macrophages can damage the lung matrix. An *in vivo*

murine study showed that lymphocytes infiltrating the CS-induced emphysematous lung can produce interferon- γ (IFN- γ), which induces the release of cytokines from cytotoxic T-cells (Maeno et al., 2007). The inflammatory-stimulated alveolar macrophages and lung epithelial cells also release IL-8/CXCL8 resulting in the infiltration of neutrophils into COPD lung (Mio et al., 1997). Cigarette smoke can also induce the release of IL-8/CXCL8 and IL-1 β from an airway epithelial cell line (HBE-14o) through inflammasome activation (Mortaz et al., 2011). Interestingly, a randomised, double-blind, placebo-controlled trial of the anti-IL-1 β mAb canakinumab in >10000 patients with atherosclerosis who had had a myocardial infarction but with no evidence of cancer showed that anti-IL-1 β therapy significantly reduced the incidence and mortality of lung cancer. This was associated with a reduction in the blood inflammatory biomarkers CRP and IL-6 (Ridker et al., 2017).

Besides inflammatory cell stimulation, chronic inflammation from repetitive smoking exposure causes squamous cell metaplasia which has the potential to develop into cancer (Adcock, Caramori, & Barnes, 2011). This, together with the persistent irritation and inflammation of the airway that occurs with prolonged exposure to cigarette smoke may promote lung cancer development (Rakoff-Nahoum, 2006).

Inflammation is one of the key pathological changes observed in neoplastic tissue and infiltration of immune/inflammatory cells into this microenvironment may induce carcinogenesis (Sekine, Hata, Koh, & Hiroshima, 2014). The mechanisms and pathways involved in this interaction between inflammation and cancer are multi-factorial and complex but include cytokines, oxidative stress and interactions between the transcription factors NF- κ B and the signal transducer and activator of

transcription (STAT)3 in lung epithelial cells (Grivennikov & Karin, 2010; Potnis, Mitkus, Elnabawi, Squibb, & Powell, 2013). An in-depth review of the regulation of the communication between cancer cells and their microenvironment is provided in some recent excellent reviews (Binnewies et al., 2018; Brücher & Jamall, 2014; Wang et al., 2017).

1.3.2 Apoptosis and cell proliferation

Oxidative stress is well-established as a major cause of both lung destruction in COPD and abnormal cellular proliferation in lung cancer (Lawless, O'Byrne, & Gray, 2009). Apoptosis plays an important role in cellular homeostasis and eliminates unwanted cells by triggering programmed cell death. Cigarette smoke is the major source of the oxidants that drive the induction of apoptosis in COPD. Abnormal apoptosis is present in the lungs and airways of COPD patients and plays an important role in its pathogenesis. Increased numbers of apoptotic airway epithelial cells and T-lymphocytes are observed in COPD patients compared to healthy volunteers (Hodge, Hodge, Holmes, & Reynolds, 2005). Moreover, the phagocytic ability of COPD alveolar macrophages is decreased resulting in a reduced ability to eradicate apoptotic epithelial cells (Hodge, Hodge, Scicchitano, Reynolds, & Holmes, 2003). The presence of excessive numbers of apoptotic cells and their decreased clearance can promote inflammation and increase lung destruction (Henson, Cosgrove, & Vandivier, 2006). An *in vivo* rat study showed that increased alveolar septal cell apoptosis and airspace enlargement was associated with increased expression of markers of oxidative stress (Kasahara et al., 2001). Apoptosis can be triggered via the death receptor pathway or the mitochondrial

pathway (caspase pathway). The alteration of the mitochondrial-driven apoptotic pathway was found to be involved in lung cancer and is reviewed in section 1.4.5.2.

In COPD, airway epithelial hyperplasia and metaplasia are adaptive responses to persistent cigarette smoke exposure (Herfs et al., 2012) and are associated with higher incidence of bronchogenic carcinoma (Vine, Schoembach, Hulka, Koch, & Samsa, 1990). Key events regulating cellular proliferation in response to oxidant stress include cancer-related gene mutations or post translational modification of proteins by free radicals or from by-products of lipid peroxidation (Kaushik, Kaushik, Khanduja, Pathak, & Khanduja, 2008). Low concentrations of CSE (0.1µg/ml) promote proliferation of the lung cancer cell line (A549) whereas high concentrations of CSE (50µg/ml) induced apoptosis and ROS production suggesting that mild oxidative stress induces the proliferative effect seen in lung cancer (Kaushik et al., 2008). In addition, EGFR phosphorylation was increased by hydrogen peroxide (H₂O₂) and by CSE in A549 cells and in a human bronchial epithelial cell line (HBE1) (Khan, Lanir, Danielson, & Goldkorn, 2008). These data suggest that oxidant exposure may have differential effects on cell apoptosis and proliferation depending upon cell type which may result in differential effects in COPD and lung cancer.

1.3.3 Genetic and epigenetic modulation

In smokers who develop lung cancer 48% develop SQCC and 44% adenocarcinoma (Poullis et al., 2013). The genetic mutations observed in these two cancer cell types are different. In adenocarcinoma, *EGFR* and *KRAS* oncogene mutations are more common than in SQCC (<5%) (Gou, Niu, Wu, & Zhong, 2015) whereas *p53* and *CDKN2A* are the more common genetic alterations in SQCC (Sabari & Paik, 2017).

In patients with NSCLC, *EGFR* and *ALK* mutation prevalence was lower in patients who also had COPD compared to those without COPD (Lim et al., 2015). However, *KRAS* mutation was not associated with COPD status in NSCLC patients (Saber et al., 2016).

In addition to genetic mutations, epigenetic changes can also cause lung cancer. Various epigenetic changes exist including DNA methylation, histone modifications and remodelling of the nucleosome (Durham & Adcock, 2015). In many lung cancers DNA methylation modifies the expression of tumour suppressor genes including *APC*, *BRCA1*, *CDKN2*, *MDM2* and *Rb* leading to hyper-proliferation of cells (Liloglou, Bediaga, Brown, Field, & Davies, 2014; Sato, Shames, Gazdar, & Minna, 2007). Histone modifications such as acetylation modify DNA:protein interactions and thereby modulate gene expression transcription. Cigarette smoke can enhance histone modifications along with DNA methylation through an oxidative stress-mediated process (Barnes, 2017; Liu et al., 2010). For example, gene expression and protein levels of HDAC2 (histone deacetylase 2), an enzyme which removes acetyl groups from histones leading to silencing of gene expression, is decreased in lung biopsies and alveolar macrophages of smokers and subjects with COPD and could be mimicked *in vitro* by cigarette smoke and oxidative stress (Ito et al., 2001; Ito et al., 2005). These changes in HDAC2 activity altered promoter-specific histone acetylation and inflammatory gene expression in a cell-dependent manner. In addition, activation of HDAC2 or inhibition of IL17A, or both, prevented airway remodelling by repressing inflammation and regulating fibroblast activation in COPD (Lai et al., 2017). TGF β -induced airway stromal cell proliferation is regulated by histone acetylation status (Perry, Durham, Austin,

Adcock, & Chung, 2015) and an HDAC inhibitor in combination with a MEK (mitogen-activated kinase kinase) inhibitor resulted in a greater effect on inhibition of tumour formation in NSCLC (Yamada et al., 2017).

1.3.4 Reactive oxygen species (ROS) production and mitochondria involvement

From the above sections it is highly likely that oxidative stress plays a critical role in the enhanced inflammation and epigenetic changes seen in the airway of COPD patients and those with lung cancer. The greatest cellular source of oxidative stress are mitochondria that provides even more ROS than cigarette smoke (Perry et al., 2015). The studies of COPD and lung cancer that involve ROS and mitochondrial function are reviewed in sections 1.4.5, 1.5.4 and 1.5.5.

1.4 Mitochondria

1.4.1 History and evolution

In 1890 the existence of mitochondria within the cell and their importance to cell function was first recognised (Ernster & Schatz, 1981), resulting in them being known as the power-house organelle of the cell. An historical review (Ernster & Schatz, 1981) highlighted the key discoveries in mitochondrial function. These included Warburg's report in 1913 which demonstrated that "grana" from guinea-pig liver had a role in cellular respiration; the study of cytochrome oxidase function (Keilin & Hartree, 1939) and the formulation of tricarboxylic acid (TCA) cycle for the metabolism of α -ketoglutarate in 1939 (Krebs & Cohen, 1939) and the first demonstration by Kagawa and Racker in 1966 showing that the whole mitochondrial ATPase complex, rather than the ATPase alone, was sensitive to oligomycin (an ATP synthase inhibitor) (Kagawa & Racker, 1966). Later, self-regeneration of mitochondria or biogenesis was observed in experimental studies in sea urchin eggs and in mouse renal tubules (Ernster & Schatz, 1981). In 1958 it was discovered that rat muscle and liver mitochondria had the ability to synthesise protein (McLean, Cohn, Brandt, & Simpson, 1958). Finally, using mitochondrial DNA (mtDNA) sequencing, the discovery of the mitochondria genome has proved that the genomic profiles of mitochondria are evolved from endosymbiotic bacteria (Roger, Muñoz-Gómez, & Kamikawa, 2017).

1.4.2 Structure, compartments and bioenergetics

The mitochondrion is a double-layer membrane organelle which can be divided into four compartments; mitochondrial outer membrane (MOM), mitochondrial inner membrane (IMM), intermembrane space (IMS) and matrix (Palade, 1953)

as illustrated in Figure 1.11. The crucial role of the mitochondria is ATP production, serving cellular metabolism known as bioenergetics (Vyas, Zaganjor, & Haigis, 2016). Besides this role, mitochondria also have roles in ROS production, balancing redox processes, maintaining substrates required for biosynthesis and regulating cell signalling and cell death pathways (Vyas et al., 2016).

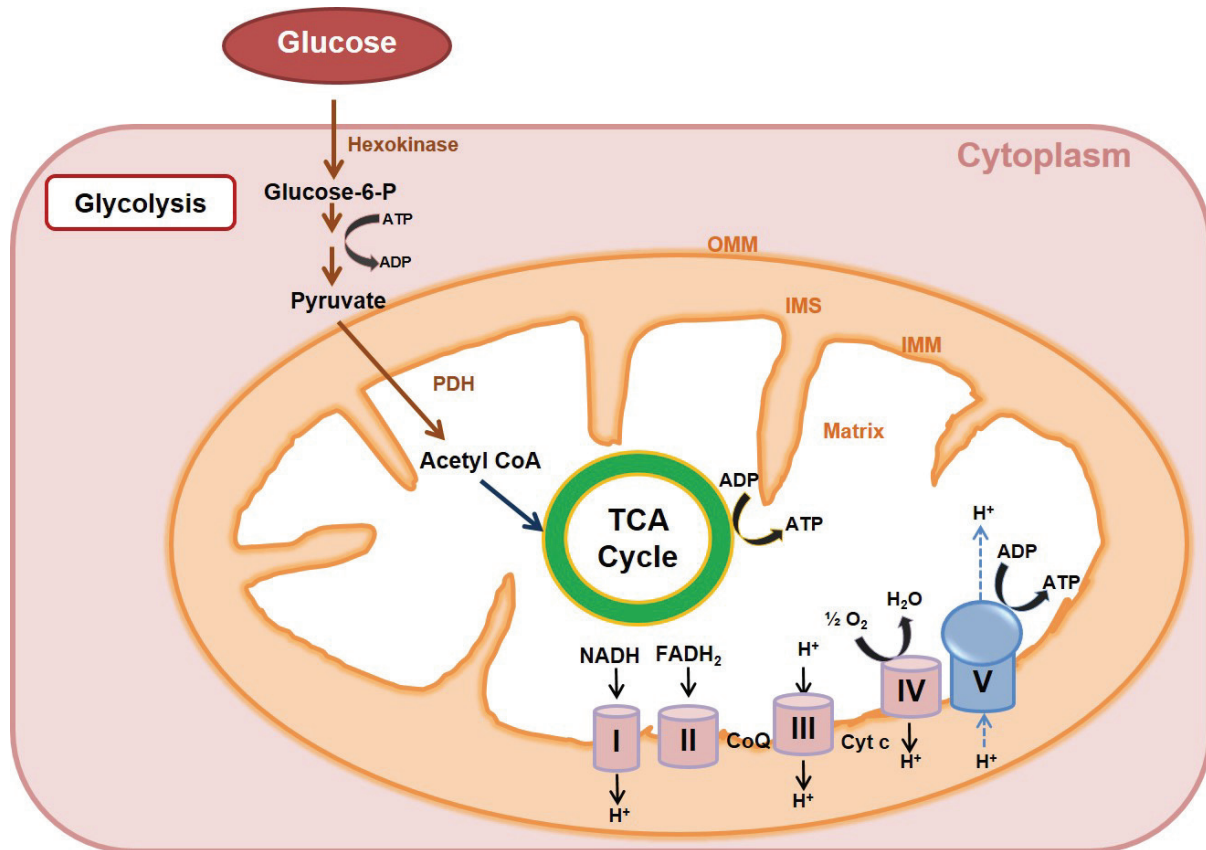


Figure 1.11 Schematic diagram of mitochondria

Compartments of mitochondria are divided by double-layer membrane into outer mitochondrial membrane (OMM), inner mitochondrial membrane (IMM), intermembrane space (IMS) and matrix. Normally, energy production, adenosine triphosphate (ATP), occurs via glycolysis and transforms pyruvate into acetyl CoA by pyruvate dehydrogenase (PDH) in the matrix prior to entering TCA cycle where ATP is generated. Reduced nicotinamide adenine dinucleotide (NADH) and reduced flavin adenine dinucleotide ($FADH_2$) from TCA cycle are oxidized providing the electrons to transfer along complex I-V of electron transport chain located in IMM which generate H^+ gradient between matrix and IMS. At complex V (ATP synthase complex), protons are forced back to the matrix causing the induction of ATP synthase subunits to produce ATP.

1.4.2.1 Cellular bioenergetics

1.4.2.1.1 Glycolysis

Glycolysis, the first step in glucose metabolism occurs in the cytoplasm and converts glucose, (a substrate to produce energy for the cell), into pyruvate which can then enter the mitochondria (Gray, Tompkins, & Taylor, 2014; Li, Gu, & Zhou, 2015) as shown in Figure 1.12. In normoxia, glucose is taken up by glucose transporters (GLUTs) in the cell membrane, once in the cytoplasm it is transformed along the glycolytic pathway to generate 2 molecules of pyruvate and 2 molecules of reduced NADH (Ngo, Ververis, Tortorella, & Karagiannis, 2015). There are several points in the pathway which have a role as gate keepers to control further steps. The following sections focus on the roles of some of these which are relevant to this thesis, glucose transporters (GLUTs), hexokinases (HKs) and pyruvate kinases (PKs) in physiological conditions and in relation to disease.

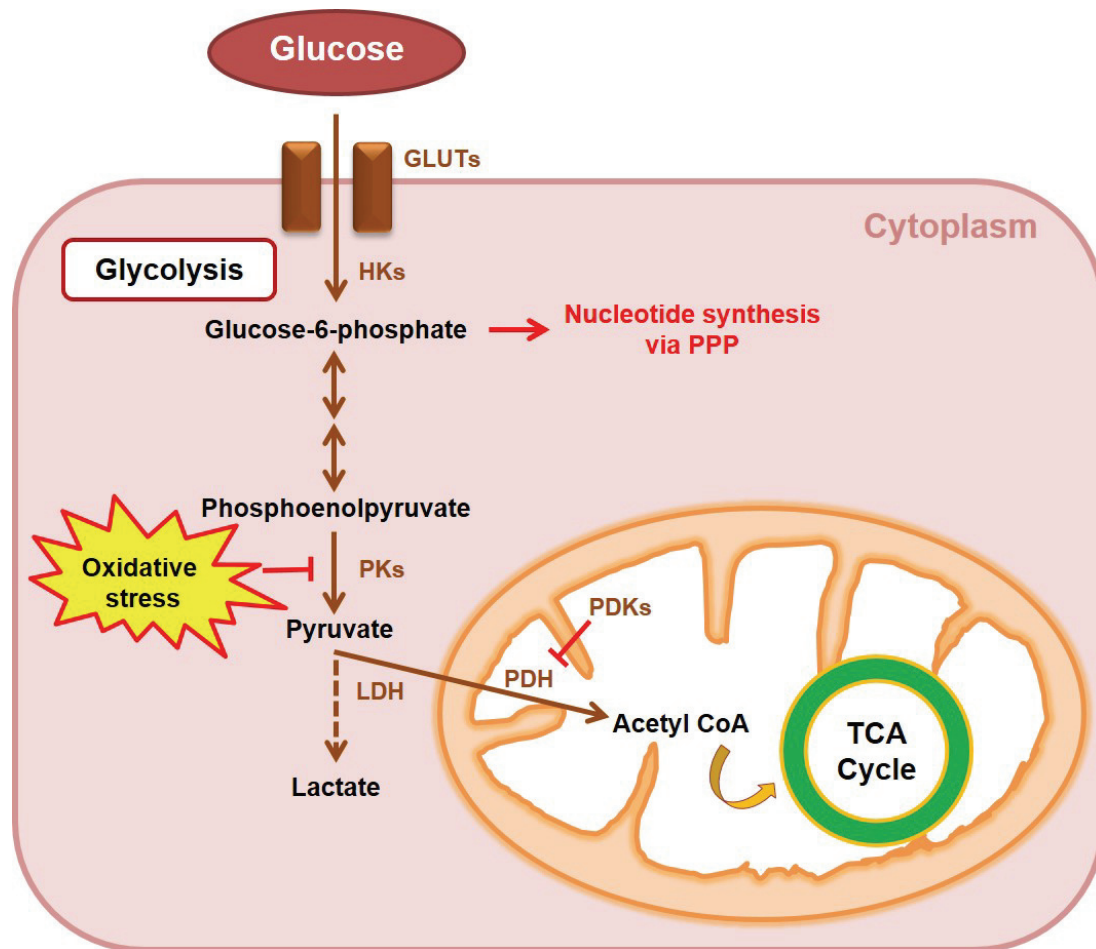


Figure 1.12 Schematic diagram of glycolysis pathway

Glucose enters the cytoplasm via glucose transporters (GLUTs) and becomes phosphorylated to glucose-6-phosphate (G6P) by hexokinases (HKs). Subsequently, with multiple steps, pyruvate is the final product of the glycolysis pathway which is phosphorylated from phosphoenolpyruvate using pyruvate kinases (PKs). In this step, oxidative stress can impair PK activity leading to less production of pyruvate. Under normoxia, most of the pyruvate enters the mitochondria and is transformed into acetyl CoA, the substantial substrate for TCA cycle, using pyruvate dehydrogenase (PDH), which can be inhibited by pyruvate dehydrogenase kinases (PDKs) to control the flow of pyruvate whereas a smaller amount of pyruvate is converted to lactate using lactate dehydrogenase (LDH).

Glucose transporters (GLUTs)

Glucose enters the cytoplasm facilitated by glucose transporter proteins (GLUTs) as the first rate-limiting step of the pathway (Macheda, Rogers, & Best, 2005). GLUTs are a family of membrane transporter proteins having 14 isoforms, divided into 3 classes depending on the similarity of amino acid sequences (Palmieri et al., 2009). GLUTs affinity for glucose varies depending on type of tissue and conditions (Adekola, Rosen, & Shanmugam, 2012). In cancer tissue, higher glucose uptake

was observed using ^{18}F -labeled 2-fluoro-deoxy-glucose (FDG) detected using positron emission tomography (PET) scan compared to normal surrounding tissue which indicates increased metabolism related to the aggressive tumour (Macheda et al., 2005). GLUT1, the isoform in class I (which also includes GLUT2-4 and 14), has been widely studied since its first purification from human red blood cells (Kasahara & Hinkle, 1977). GLUT1 protein is encoded by *SLC2A1* gene and is present in various tissues including red blood cells, brain endothelial cells (Koranyi et al., 1991), and placental tissue (Illsley, 2000) with high affinity for glucose uptake in basal conditions but it can be altered by growth factors and by stress (Adekola et al., 2012; Macheda et al., 2005). Overexpression of GLUT1 is observed in many types of cancers including liver, prostate and lung cancer (Amann et al., 2009; Jans et al., 2010; Minami, Saito, Imamura, & Okamura, 2002) and was associated with tumour progression and mortality.

Hexokinases (HKs)

Once inside the cell the first step of glucose metabolism is the phosphorylation of glucose into glucose-6-phosphate (G6P) by hexokinases (HKs). The feedback inhibition of HKs activity is controlled by G6P production (Wilson, 2003). Since G6P is the substrate at the start of several metabolic pathways such as glycolysis, glycogenesis and the pentose phosphate pathway (PPP), HKs play an important role in metabolic and biosynthetic processes (Calmettes et al., 2015). Moreover, HKs bound to the outer mitochondrial membrane facilitate the connection between glycolysis and oxidative phosphorylation (OXPHOS) regarding mitochondrial ATP production (Roberts & Miyamoto, 2015). There are 4 HK isoforms (I-IV) depending on molecular weight and these are located in different tissues: HK-I is mainly

expressed in the brain and HK-II is mainly present in skeletal muscle, heart and adipose tissue (Heikkinen et al., 2000). The glucose affinity of HK-I, II and III is superior to that of HK-IV (Roberts & Miyamoto, 2015). The importance of the regulation of HKs in disease was established when upregulation of HK-II in cancer cells was found to enhance aerobic glycolysis (Warburg effect, discussed later in Section 1.4.5.3) (Roberts & Miyamoto, 2015). Further studies demonstrated an association between the upregulation of HK-II and the poor prognosis of breast cancer with brain metastasis and between the increased HK-II expression and mortality in liver cancer (Kwee, Hernandez, Chan, & Wong, 2012; Palmieri et al., 2009).

Pyruvate kinases (PKs)

Pyruvate kinase (PK) is a key glycolytic enzyme which dephosphorylates phosphoenolpyruvate (PEP) into pyruvate, the rate-limiting step of glycolysis (Eigenbrodt & Glossmann, 1980). There are 4 isoforms including PKM1, PKM2, PKR and PKL. In normal tissue PKM1 is the main isoform that exists as an active tetramer, whereas PKM2 is expressed in proliferating cells e.g. embryonic stem cells and in cancer cells indicating a shift in PK isoform expression from PKM1 (Lee, Kim, Han, & Kim, 2008; Warner, Carpenter, & Bearss, 2014). The activation of PKM2 is regulated by an allosteric activator, fructose-1,6-bisphosphate (FBP) to form tetrameric enzyme complex (Warner et al., 2014). However, PKM2 can release FBP and become less active when interacting with phosphotyrosine residues in other proteins. This results in the diversion of glycolysis into the anabolic pathway (Anastasiou et al., 2012) and the PPP to increase biosynthesis and enable cell proliferation which is important for cancer cell growth (Anastasiou et al., 2011).

Moreover, PKM2 is the key enzyme involved in regulating the balance between cellular ROS accumulation and detoxification in the A549 lung cancer cell line (Anastasiou et al., 2011). Inhibition of PKM2 activity by ROS contributed to glucose being catalysed through the PPP producing nicotinamide adenine dinucleotide phosphate (NADPH), a coenzyme, required for glutathione (GSH) production (Anastasiou et al., 2011). Besides its metabolic function, PKM2 is a transcriptional coactivator which can activate hypoxia-inducible factor (HIF) 1- α and alter glucose catabolism in cancer cells (Luo et al., 2011).

1.4.2.2 Mitochondrial bioenergetics

Pyruvate is transported by the mitochondrial pyruvate carrier (MPC) into the mitochondrial matrix where it drives the TCA cycle to produce ATP and support OXPHOS. Pyruvate conversion into acetyl-CoA (Figure 1.12) also produces NADH and CO₂ in an irreversible reaction using the pyruvate dehydrogenase (PDH) complex (Gray et al., 2014). However, acetyl-CoA, ATP and NADH are feedback inhibitors of PDH (Harris, Bowker-Kinley, Huang, & Wu, 2002). The activity of PDH depends on the relative activities of pyruvate dehydrogenase kinase (PDK) and pyruvate dehydrogenase phosphatase (PDP). PDK phosphorylates PDH leading to its inactivation resulting in the shift of pyruvate to other metabolic pathways e.g. gluconeogenesis in the fasting state (Gray et al., 2014). Under hypoxic conditions, PDK1 can inhibit PDH leading to a decrease in acetyl-CoA followed by a reduction in mitochondrial oxygen consumption (Kim, Tchernyshyov, Semenza, & Dang, 2006; Papandreou, Cairns, Fontana, Lim, & Denko, 2006). In cancer cells, PDK1 can be upregulated by HIF-1 and the c-Myc oncogene (Kim, Gao, Liu, Semenza, & Dang, 2007; Papandreou et al., 2006) and inhibited by dichloroacetate allowing PDH to become active resulting in a shift in metabolism towards OXPHOS and reduced growth of tumour (Bonnet et al., 2007).

1.4.2.2.1 Tricarboxylic acid (TCA) cycle

Inside the mitochondria, the TCA cycle (Figure 1.13) operates in the matrix providing electron donors consisting of reduced nicotinamide adenine dinucleotide (NADH) and reduced flavin adenine dinucleotide (FADH₂) to drive the reactions of the electron transport chain (ETC) located along the IMM to finally produce energy, ATP (Ernster & Schatz, 1981).

In addition to glucose metabolism, the cycle participates in several metabolic pathways such as metabolism of amino acids, lipid biosynthesis and initiation of heme synthesis (Raimundo, Baysal, & Shadel, 2011).

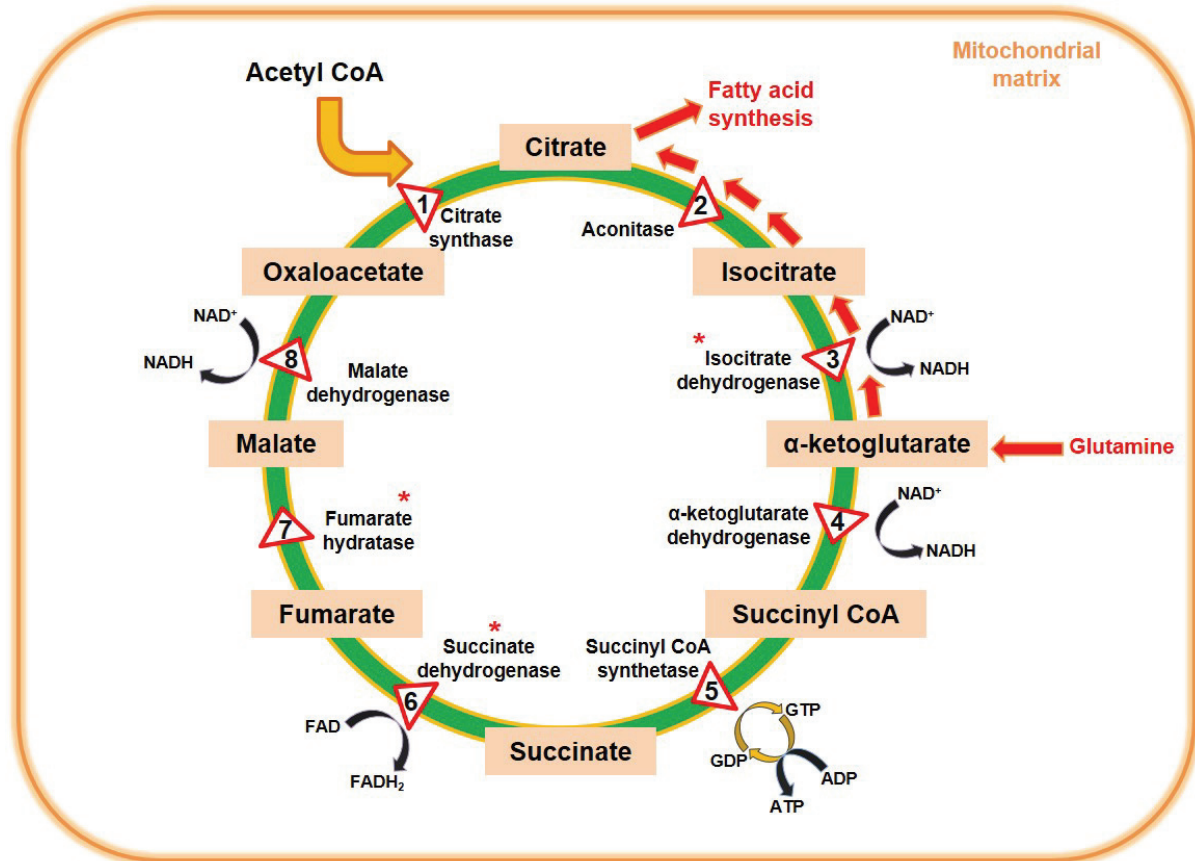


Figure 1.13 Schematic presentation of tricarboxylic acid (TCA) cycle

In mitochondrial matrix, the TCA cycle begins with (1) the condensation of acetyl CoA to oxaloacetate to form citrate by citrate synthase. (2) Citrate is converted to isocitrate using aconitase. (3) Isocitrate is oxidative decarboxylated by isocitrate dehydrogenase into α -ketoglutarate then (4) it is catalysed to form succinyl CoA using α -ketoglutarate dehydrogenase. Both (3) and (4) generate NADH to serve electrons (e^-) to complex I of ETC. (5) The succinyl CoA is catalysed by succinyl CoA synthetase which provides guanosine triphosphate (GTP) to generate ATP. (6) Succinate is oxidised to fumarate by succinate dehydrogenase that gives e^- to ETC via $FADH_2$. (7) Fumarate hydratase catalyses the hydration of fumarate to form malate. (8) The cycle is completed by the formation of oxaloacetate from malate catalysed using malate dehydrogenase which also gives NADH. The enzymes related to mitochondrial dysfunction and tumourigenesis are marked with asterisks. To serve fatty acid oxidation (lipid synthesis) for proliferation, the TCA cycle in some cancer cells alter the flux and increase citrate export. In addition, glutamine is utilised as a substrate to be converted into α -ketoglutarate followed by a backwards flow through the TCA cycle to generate citrate which occurs due to mutated enzymes in TCA cycle. (red arrows) adapted from Kishton & Rathmell, 2015.

Genetic abnormality of three metabolic enzymes in the TCA cycle related to mitochondrial dysfunction, isocitrate dehydrogenase (IDH), succinate dehydrogenase (SDH) and fumarate hydratase (FH), can lead to tumourigenesis (Raimundo et al., 2011). Mutations in IDH1 and IDH2 subunits, which causes less α -ketoglutarate production, are found in brain cancers and knockdown of IDH1 in glioma cancer cells *in vitro* resulted in decreased cell proliferation (Ward et al., 2010; Yan et al., 2009). Increased IDH1 protein expression found using a proteomic screen in NSCLC was negatively correlated with survival (Tan et al., 2012). SDH drives mitochondrial oxidation of succinate into fumarate (Mills et al., 2016). A clinical study showed that mutation of SDH subunits (A-D) led to a lack of SDH and the possible development of a neuroendocrine tumour: pheochromocytoma (Richter et al., 2014). FH is responsible for converting fumarate into malate. Mutation of FH results in the intracellular accumulation of fumarate and the upregulation of HIF in renal tumour cells (Isaacs et al., 2005). The FH mutation has been reported in many cancers including breast cancer, leiomyosarcoma and ovarian cancer (Raimundo et al., 2011). The alteration of FH expression was also discovered in a bioinformatics analysis of lung cancer: FH down-regulation was evident in lung cancer cell lines and lower FH protein expression was seen in lung cancer tissue compared to normal lung tissue (Ming et al., 2014).

1.4.2.2.2 Electron transport chain

The ETC is responsible for transferring electrons, carried by NADH and FADH₂ from the TCA cycle, to oxygen. There are five complexes which are embedded along IMM together with ubiquinol (CoQ) and cytochrome c (Cyt c) (Garcia-Heredia & Carnero, 2015). As electrons are transferred from complex I to IV, protons are also pumped out from the matrix into the IMS which creates an electrochemical gradient called mitochondrial membrane potential ($\Delta\Psi_m$) (Michaeloudes, Bhavsar, Mumby, Chung, & Adcock, 2017). Protons can re-enter the matrix, influenced by $\Delta\Psi_m$, as well as the phosphorylation of ADP to ATP, via a proton channel in complex V (mitochondrial ATP synthase) (Weinberg & Chandel, 2015) as illustrated in Figure 1.14.

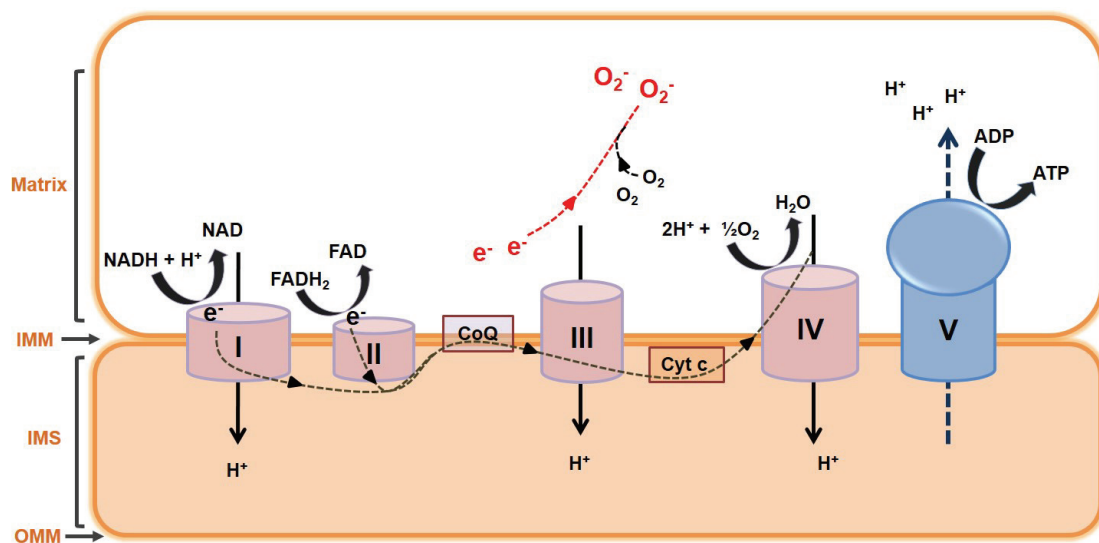


Figure 1.14 Schematic diagram of mitochondrial electron transport chain (mtETC)

The synthesis of ATP via mtETC requires electron (e⁻) transfer and proton (H⁺) translocation through complex I-IV and phosphorylation of ADP at complex V, called oxidative phosphorylation (OXPHOS). First, complex I (NADH dehydrogenase) and complex II (succinate dehydrogenase) remove e⁻ from NADH and FADH₂ respectively. Next, the flow of e⁻ is supported by complex III (ubiquinol-cytochrome c oxidoreductase) together with ubiquinol (CoQ) and cytochrome C (Cyt c). Complex IV (cytochrome c oxidase) is the last complex that these flowing e⁻ are used to reduce O₂ into H₂O. These biochemical reactions from complex I, III and IV allow H⁺ to translocate from the matrix to IMS which creates H⁺ gradient called mitochondrial membrane potential ($\Delta\Psi_m$). Finally, complex V (ATP synthase) allows H⁺ to flow back to the matrix facilitating the ATP generation from ADP. However, free radicals such as superoxide anion (O₂⁻) are produced due to the reduction of O₂ by some e⁻ leakage at complex III. Adapted from Garcia-Heredia & Carnero, 2015.

Complex I, known as NADH dehydrogenase, oxidises NADH and transfers electrons to reduce CoQ. There are three different modules within complex I; an N-module (NADH dehydrogenase), a Q-module (ubiquinone reduction) and a P-module (proton translocation) which have a role in the binding and oxidation of NADH and proton pumping, respectively (Garcia-Heredia & Carnero, 2015). There are 14 central polypeptide subunits responsible for bioenergetic functions. The first seven hydrophobic subunits are encoded by mitochondrial DNA (mtDNA) and comprise mtDN1-6 and mtND4L which are all Q-module proteins whereas the latter seven hydrophilic subunits are encoded by nuclear DNA (nDNA). These are NDUFV1, 2 and NDUFS1 (the N-module proteins) and NDUFS2, 3, 7, and 8 (the Q-module proteins) (Mimaki, Wang, McKenzie, Thorburn, & Ryan, 2012). A nuclear encoded protein, NDUFA9 (NADH:Ubiquinone Oxidoreductase Subunit A9), is a component of the Q-module (ubiquinone reduction), one of the three functional modules of complex I (Baertling et al., 2018). The roles of NDUFA9 in complex I include structural assembly and stability (Stroud, Formosa, Wijeyeratne, Nguyen, & Ryan, 2013). There is no published study specific to NDUFA9 related to cancer. However, complex I has been investigated as a target site for cancer therapy. Inhibition of complex I activity and of cellular respiration by metformin, an anti-diabetic drug, was demonstrated in colon cancer cells resulting in decreased cellular proliferation and increased cell death in glucose-deprived conditions (Wheaton et al., 2014). In a liver cancer cell line (HepG2) and an *in vivo* mouse study, another anti-diabetic drug, pioglitazone (PGZ), a peroxisome-proliferator activator receptor (PPAR) γ agonist decreased the activity of complex I by binding to NDUFA9, NDUF6 and NDUFA6 subunits and causing complex disassembly.

However, the gene expression of these subunits was increased suggesting a compensatory response (García-Ruiz, Solís-Muñoz, Fernández-Moreira, Muñoz-Yagüe, & Solís-Herruzo, 2013). An active metabolite of isoflavone derivatives (ME-344) caused degradation of NDUFA9 resulting in complex I disassembly and subsequently disrupted mitochondrial metabolism of cancer cells *in vitro* in an osteosarcoma cell line (143B) without affecting mitochondrial metabolism in primary human skin fibroblasts (Lim, Carey, & McKenzie, 2015). This further suggests that NDUFA9 could be a target for anti-cancer drugs.

Complex II (succinate dehydrogenase) receives electrons from the TCA cycle and transfers them to CoQ regardless of proton pumping (Garcia-Heredia & Carnero, 2015). There are 4 subunits including SDHA, B, C, and D which are encoded from nDNA (Garcia-Heredia & Carnero, 2015).

Complex III (ubiquinol-cytochrome c oxidoreductase) is involved in the oxidation of Cyt c by transferring electrons from CoQ (Garcia-Heredia & Carnero, 2015). The complex contains 11 subunits of which only one subunit, cytochrome b, is encoded by mtDNA (Garcia-Heredia & Carnero, 2015). In the ETC, about 1-2% of oxygen used for respiration is reduced to superoxide (O_2^-) and other ROS (Turrens, 2003). Complex III is the main site of O_2^- production due to electron leakage which accounts for its great capacity to drive ROS-mediated signalling (Orr et al., 2015). Deletion of the conserved tyrosine³⁰² residue in cytochrome b in *Rhodobactor capsulatus*, a model for mitochondria, decreased complex III activity and increased ROS production suggesting that this subunit controls most ROS production (Lee et al., 2011).

Complex IV (cytochrome c oxidase, COI) passes electrons to O₂ which, combined with protons, forms water whilst pumping out protons (Garcia-Heredia & Carnero, 2015). The complex consists of 13 subunits, three of which are encoded from mtDNA (MTCO1, 2, and 3). A rare mutation in the *COI* gene in prostate cancer tissue was associated with increased ROS production and reduced cytochrome oxidation in mitochondria isolated from lymphocytes. In addition, this mutation caused increased proliferation of tumour xenografts in nude mice indicating that mutations in complex IV genes induces ROS production and may be involved in carcinogenesis (Arnold et al., 2013).

Finally, complex V (mitochondrial ATP synthase) is divided into two subunits, the F₀ subunit embedded in IMM and the F₁ subunit anchored in the matrix (Garcia-Heredia & Carnero, 2015). F₁ subunit proteins are encoded by nDNA whereas only two F₀ subunit proteins (mtATP6 and 8) are encoded by mtDNA (Jonckheere, Smeitink, & Rodenburg, 2012).

1.4.3 Mitochondrial morphological regulation

Mitochondrial morphological changes are dynamic; they can switch from a reticulated pattern formed because of fusion to fragmented and smaller pieces due to fission. Mitochondrial fusion is controlled by three main proteins, mitofusin (Mfn) 1 and 2 at the OMM, and optic atrophy 1 (Opa1) at the IMM whereas mitochondrial fission is mainly regulated by dynamin-related protein 1 (Drp1) (Boland, Chourasia, & Macleod, 2013). Mitochondrial fusion can be induced by stress e.g. ultraviolet (UV) light which promotes ATP production via OXPHOS (Tondera et al., 2009) and prevents apoptosis (Rambold, Kostecky, Elia, & Lippincott-Schwartz, 2011). The lack of Mfn1 and 2 in mouse embryonic fibroblasts

caused a loss of fusion ability and a defect in cell growth (Chen, Chomyn, & Chan, 2005). Increased mitochondrial fragmentation is also present in human genetic diseases such as autosomal dominant optic atrophy (Boland et al., 2013). In contrast, the process of mitochondrial fission plays an important role in mitosis by controlling the distribution of mitochondria in daughter cells (Kashatus et al., 2011). However, high glucose (30mM) can induce mitochondrial fission leading to apoptosis as demonstrated in a renal tubular cell line (Lee, Chiu, Chen, Chen, & Chang, 2016). The alteration of mitochondrial dynamics from fusion to fission in acute cortical injury induced the expression of inflammatory mediators from astrocytes which was triggered by phosphorylated Drp1 and decreased respiratory capacity (Motori et al., 2013). Mitochondrial dynamics are also involved in cancer growth; the Ras oncogene enhanced mitochondria fragmentation whereas Drp1 knockdown inhibited tumour growth in kidney, cervical and pancreatic cancer cell lines (Kashatus et al., 2015).

1.4.4 Mitochondrial biogenesis and mitophagy

Changing mitochondrial mass in cells is under the control of mitochondrial biogenesis (reproduction) and mitophagy. Similar to cell division, mitochondria replicate the mitochondrial genome in coordination with induction of mtDNA- and nDNA-encoded mitochondrial proteins (Boland et al., 2013). Mitochondrial biogenesis is regulated by a number of nuclear transcription factors such as PPAR α , PPAR γ , nuclear respiratory factor 1 (NRF1), NRF2 and estrogen related receptor (ERR) (Boland et al., 2013). NRFs are groups of anti-oxidant genes which modulate the expression of the Cyt c and Cyt c oxidase subunits. PPARs and ERRs families regulate the expression of genes related to mitochondrial bioenergetics, lipid

metabolism and fatty acid oxidation (Scarpulla, Vega, & Kelly, 2012). A transcription coactivator, PPAR- γ co-activator 1- α (PGC-1 α) regulates the activity of these transcription factors in response to fasting induced stress along with PGC-1 β and PGC-related co-activator (PRC) (Dominy, Lee, Gerhart-Hines, & Puigserver, 2010). Therefore, PGC-1 could be a central regulator of mitochondrial biogenesis, cell metabolism and antioxidant response (Boland et al., 2013). Indeed, PGC-1 α has been shown to have an important role in mitochondrial biogenesis in cancer (Vyas et al., 2016). Overexpression of PGC-1 α in cancer can support both tumour growth or act as a tumour suppressor depending on PGC-1 α -related signalling pathways and cancer cell types (Tan et al., 2016; Vyas et al., 2016). For example, as a supporter of tumour cell growth, the inhibition of the ERR-PGC-1 α signalling pathway reduced mitochondrial function and blocked mammosphere formation by breast cancer cells (De Luca et al., 2015); PGC-1 α may promote tumour metastasis since silencing PGC-1 α in circulating tumour cells (CTCs) originated from breast cancer decreased CTCs and metastasis (LeBleu et al., 2014). On the other hand, overexpressed PGC-1 α prevented colon cancer formation in murine intestinal epithelium and PGC-1 α induced mitophagy in breast cancer by stabilising mitostatin, a tumour suppressor gene (D'Errico et al., 2011; Neill et al., 2014).

Mitophagy is a process of mitochondrial degradation to remove dysfunctional mitochondria (Boland et al., 2013). Dysfunctional mitochondria undergo mitophagy through the PTEN (phosphatase and tensin homologue)-induced putative kinase 1 (PINK1)/Parkin pathway triggered by mitochondrial membrane depolarisation (Vyas et al., 2016). PINK1 phosphorylates Mfn2 at the OMM leading to recruitment of

Parkin from the cytoplasm to PINK1 on damaged mitochondria which subsequently signals to the cell to remove them using lysosomes (Boland et al., 2013).

Mitophagy can suppress tumourigenesis as shown by the decreased proliferation of a Parkin-deficient breast cancer cell line following ectopic Parkin expression (Tay et al., 2010). Decreased Parkin activity correlates with tumorigenesis in various cancer cell types (Bernardini, Lazarou, & Dewson, 2017). For example, genetic deletion of *PARK2*, a gene encoding Parkin, increased cancer progression which suggests that *PARK2* can be a tumour suppressor gene (Veeriah et al., 2010). *PARK2* mutations have been reported in brain cancer and in glioblastoma multiforme and was associated with increased tumour development resulting from the failure to transcribe the p53 tumour suppressor gene (Viotti et al., 2014). Impaired mitochondrial and autophagic function leads to apoptosis resistance in a lung cancer cell line (A549). Comparing to a non-tumourigenic normal bronchial epithelial cell line (NL20), A549 cells showed lower Drp1 expression and no recruitment of Drp1 to mitochondria and had reduced levels of lysosome degradation which correlated with the degree of mitophagy (Thomas & Jacobson, 2012).

1.4.5 Mitochondrial dysfunction

ATP production via OXPHOS is the most important function of the mitochondria. Mitochondria also fulfil other roles such as ROS production and elimination, mitochondrial biogenesis, partial regulation of cellular apoptosis, control of calcium transport between cytoplasm and mitochondrial matrix, production of metabolites and intra- and inter-cellular localisation (Brand & Nicholls, 2011).

Mitochondrial dysfunction has been implicated in the pathogenesis of many diseases. In neurodegenerative diseases such as Alzheimer's disease, β -amyloid deposits cause loss of OXPHOS activity leading to a decrease in $\Delta\Psi_m$ and apoptosis via activation of the caspase pathway (Hroudová, Singh, & Fišar, 2014). Mitochondrial dysfunction in the intestinal epithelium is thought to be involved in inflammatory processes in inflammatory bowel disease (IBD), since abnormal mitochondria shape, increased ROS and decreased ATP levels together with inflammatory conditions have been reported in IBD patients (Novak & Mollen, 2015). Mitochondrial dysfunction leading to an imbalance in energy homeostasis also affects individual tissues including pancreatic β -cells, liver, skeletal muscle and adipose tissue in diabetes mellitus (Patti & Corvera, 2010).

1.4.5.1 Mitochondrial dysfunction in COPD

Mitochondrial dysfunction has been reported in skeletal and respiratory muscle dysfunction in patients with COPD (Nam, Izumchenko, Dasgupta, & Hoque, 2017). Increased ROS production and Cyt c oxidase activity in skeletal muscle and respiratory muscle has been reported in mild-to-moderate COPD patients (Puente-Maestu et al., 2009). Other studies have reported a relationship between mitochondrial dysfunction and muscular dysfunction due to ineffective oxidative capacity and reduced mitochondrial mass (Gosker, Hesselink, Duimel, Ward, & Schols, 2007), and excessive mitochondrial ROS production (Picard et al., 2008). As shown in the previous section, PGC-1 α is important in mitochondrial biogenesis, and decreased expression of PGC-1 α and PPARs was linked to the reduction of oxidative capacity in skeletal muscle of patients with COPD (Remels et al., 2007).

Morphological changes in mitochondria have been shown in bronchial epithelial cells and airway smooth muscle cells of patients with COPD. Mitochondria in the airway epithelium from severe COPD subjects appeared to be swollen, with increased branching and elongation but with less cristae (Hoffmann et al., 2013). Bronchial epithelial (BEAS-2B) cells when exposed to long term cigarette smoke demonstrated increased expression of mitochondrial fusion and fission markers, OXPHOS related proteins and oxidative stress markers along with an increase in pro-inflammatory mediators (Hoffmann et al., 2013). Mitochondria in airway smooth muscle cells from COPD patients were found to be dysfunctional including decreased $\Delta\Psi_m$, ATP production and lower expression of complex proteins but increased mitochondrial ROS level (Wiegman et al., 2015). These findings were also demonstrated in an *in vivo* mouse model of oxidative stress induced by chronic inhalation of ozone. Prophylactic treatment with a mitochondrial-targeted antioxidant, MitoQ, attenuated the mitochondrial dysfunction (Wiegman et al., 2015). Thus, mitochondrial dysfunction could be important in the pathogenesis of COPD.

1.4.5.2 Mitochondrial dysfunction in lung cancer

Besides aerobic glycolysis, other alterations in mitochondrial function have been investigated in cancer cells. As stated above in the sections regarding the TCA cycle and ETC, mutations of both mtDNA and nDNA results in dysregulation of mitochondrial metabolic processes. Three alterations in mtDNA have been reported in lung carcinogenesis, including point mutations, deletions, and depletions. A collective cancer tissue study reported that 22% of lung cancer tissues contained mtDNA mutations of which 57% of the mutations were nucleotide repeats, deletions or multiple insertions and 22% were associated with decreased mtDNA copy number

(Lee et al., 2005). A significant increase in the mtDNA/nDNA ratio (which represents enhanced oxidative stress), has been reported in the exhaled breath condensate (EBC) of patients with COPD compared to healthy subjects (Carpagnano et al., 2016).

Chronic inflammation can initiate tumourigenesis directly or by ROS-activated signalling pathways (Rosanna & Salvatore, 2012). Increased ROS production results in mtDNA damage which affects mitochondrial function (Nam et al., 2017). Cigarette smoke-induced ROS production can cause mtDNA mutation; however, other pathways independent from smoking that induce mtDNA mutations in never smokers must exist. A higher frequency of mtDNA mutations has been reported in non-smokers compared to smokers, which correlated with *EGFR* mutation (Dasgupta et al., 2012). The complex I of ETC is the major site of mtDNA mutations. Mutation of the *ND5* gene, encoding the NADH:ubiquinone oxidoreductase core subunit 5 of complex I, promoted cell proliferation, invasion and ROS production in lung cancer cells *in vitro* (Dasgupta et al., 2012). This is consistent with a study in a murine lung cancer cell line derived from Lewis lung carcinoma which showed loss of function mutation of complex I leads to increased ROS production and enhanced metastatic capacity (Ishikawa et al., 2008).

Apoptotic resistance is a major characteristic of cancer cells (Hanahan & Weinberg, 2011). Caspase pathways are the main apoptotic pathways which are initiated by the intrinsic (mitochondrial-dependent) pathway and executed by the extrinsic pathway (Pore, Hiltermann, & Kruyt, 2013). The intrinsic pathway is triggered by disrupted mitochondria due to the induction of DNA damage, for example by apoptosome formation consisting of the apoptotic protease activating factor (Apaf)-1

and procaspase-9 leading to activation of caspase-9 (Pore et al., 2013). Interaction with B-cell lymphoma (BCL)-2 family proteins enables caspase-9 to trigger the release of Cyt c from mitochondria which induces further apoptosis (Pore et al., 2013). In lung cancer, apoptosis resistance affecting the sensitivity to chemotherapy may be associated with the expression of pathways involved in apoptotic regulation (Joseph et al., 2001). NSCLC cell lines express high levels of Apaf-1 and procaspase-3, but not procaspase-9, indicating that lung cancer cells have the ability to suppress apoptosome-initiated caspase activation (Křepela, Procházka, Liu, Fiala, & Kinkor, 2004).

Alterations in mitochondrial dynamics are involved in tumour proliferation, invasion and survival in lung cancer. Fragmented mitochondria are usually present in lung cancer cells compared to normal adjacent tissues with overexpression or increased activation of Drp1 and/or downregulation of Mfn2 (Senft & Ronai, 2016). In lung tissue from patients with lung adenocarcinoma, high nuclear Drp1 expression correlated with poor prognosis. Hypoxia can increase nuclear Drp1 expression and cisplatin resistance in lung cancer cell lines (Chiang et al., 2009). In contrast, inhibition of Drp1 or the overexpression of Mfn2 in A549 cells decreased proliferation and increased apoptosis (Rehman et al., 2012). Increased Opa1 expression has also been reported in tissue samples from patients with lung adenocarcinoma whereas Opa1 knockdown in lung adenocarcinoma cell lines was associated with decreased cisplatin resistance. Therefore, mitochondrial dynamics can play a role in lung cancer progression via drug resistance leading to poor prognosis (Fang et al., 2012).

The alteration of mitochondrial bioenergetics in lung cancer is briefly reviewed below.

1.4.5.3 Warburg effect (aerobic glycolysis)

In normoxic conditions, ATP is mainly produced via glycolysis through OXPHOS; however, in hypoxic states less ATP is produced via glycolysis. In a normoxic environment, tumour cells and some normal proliferating cells consume ATP rapidly via aerobic glycolysis via conversion of pyruvate to lactate to produce ATP (Figure 1.15) (Liberti & Locasale, 2016).

This phenomenon is known as the Warburg effect after its discovery by Otto Warburg in the 1920s (Koppenol, Bounds, & Dang, 2011; Warburg, Wind, & Negelein, 1927). The Warburg effect is an adaptive mechanism which aids cancer cell growth and survival (Liberti & Locasale, 2016). To meet the energy demands of the cell, in addition to ATP production, cancer cells also increase glucose uptake as the substrate for nucleic acid, amino acid and lipid synthesis to support cancer cell proliferation (Liberti & Locasale, 2016). In an endometrial cancer cell line high glucose increased glycolytic activity through protein kinases including AMPK and mechanistic target of rapamycin (mTOR), an intracellular signalling pathway regulating cell cycle (Han et al., 2015).

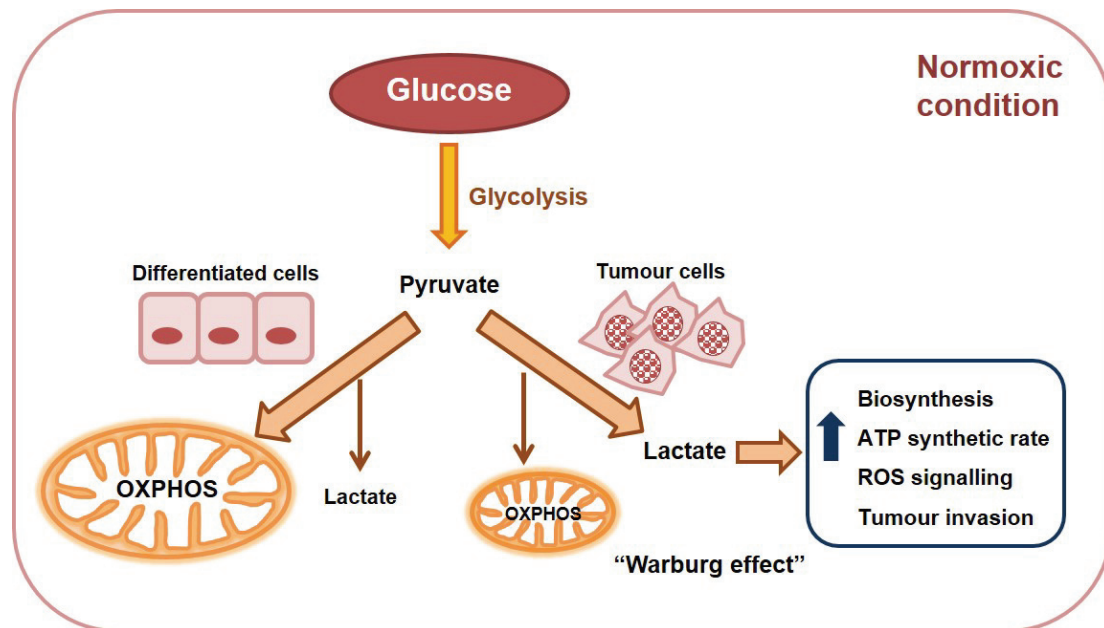


Figure 1.15 Schematic representation of the difference in metabolism between differentiated cells and tumour cells

In normoxic condition, normal differentiated cells convert glucose into pyruvate via glycolysis, which then enters mitochondria to get oxidised and produce ATP. Minimal amounts of pyruvate are converted into lactate. In contrast, tumour cells metabolise glucose via aerobic glycolysis (Warburg effect) which gives lactate rather than via OXPHOS. This effect also occurs in some normal proliferating cells. Warburg effect supports tumour cell growth by increasing glucose uptake to support biosynthesis and accelerate ATP production. The Warburg effect has a role in ROS generation and modulation of signalling in tumour cells and adjusting tumour microenvironment by increasing acidity with lactic acid allowing tumour cells to invade surrounding tissue.

Lactate or lactic acid from aerobic glycolysis decreases the pH in the tumour microenvironment enhancing cancer invasion of the normal surrounding tissue (Liberti & Locasale, 2016; Xu et al., 2015). Moreover, lactate signalling promotes glutamine uptake and metabolism in cervical cancer cells which leads to metabolic acidosis (Pérez-Escuredo et al., 2016). Lactic acid may play a key part in cancer proliferation, metastasis and survival prediction (Hirschhaeuser, Sattler, & Mueller-Klieser, 2011). Lactic acid produced from cancer cells suppresses the anti-cancer ability of human CD8⁺ T-cell and mouse tumour-infiltrating lymphocytes in terms of impaired cytokine secretion, reduced T-cell receptor (TCR) activation and decreased protein kinase activation in response to TCR activation (Calcinotto et al., 2012).

The rapid ATP production required to serve the energy demands of cancer cells depends on the activation of ATP-dependent pumps on the cell membrane. These include ion transporters which lead to increased glycolysis without altering OXPHOS (Epstein, Xu, Gillies, & Gatenby, 2014). However, the mtDNA and nDNA mutations which occur in cancer cells cause dysfunctional OXPHOS leading to a shift in the glucose metabolic pathway from OXPHOS to aerobic glycolysis, resulting in ROS overproduction (Zhang et al., 2015). Accelerated growth and proliferation of cancer cells causes greater imbalance between OXPHOS and glycolysis leading to a more hypoxic state with less apoptosis which drives carcinogenesis (Nelson et al., 2004). A549 cells exposed to hypoxia exhibit enlarged mitochondria due to increased Mfn-mediated mitochondrial fusion and enhanced resistance to staurosporine, a mitochondria-dependent pro-apoptotic agent (Chiche et al., 2009).

1.4.5.4 Mitochondrial dysfunction in COPD and lung cancer

Chronic inflammation occurs in both COPD and lung cancer. Chronic inflammation in COPD results in repetitive chronic lung injury which triggers cell repair and proliferation. While increasing the cell proliferation rate, external ROS e.g. cigarette smoke can also damage nDNA and mtDNA leading to carcinogenesis.

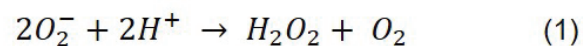
Decreasing airflow and air retention in COPD lungs leads to a decrease in gas exchange capacity causing hypoxia (Durham & Adcock, 2015). Hypoxia activates HIF1- α , the transcription factor which regulates genes for physiological adaptation in response to stresses. HIF1- α can modulate angiogenic factors to support hypoxic tissue, enhance glycolytic activity in O₂ starved conditions to produce energy; moreover, it was found to repress mitochondrial function by inducing PDK1 activity in cancer cell lines (Papandreou et al., 2006). *HIF-1* is

overexpressed in cancer under hypoxic conditions (Harris, 2002). In NSCLC upregulation of HIF-1 α in tumour tissue compared to adjacent non-tumour tissue is associated with tumour necrosis and survival. This positively correlated with *VEGF* and hexokinase 2 (*HK2*) expression and was associated with poor prognosis in lymph node-negative patients (Yohena et al., 2009). Another study in NSCLC also reported a positive association between HIF-1 α and tumour necrosis extension (Swinson et al., 2004). CSE induced HIF-1 α protein expression and activation which in turn induced COPD-related genes such as VEGF and increased ROS levels in A549 and BEAS-2B cells (Daijo et al., 2016). However, reduced HIF-1 α protein expression is seen in severe COPD suggesting that distinct mechanisms underlie severe COPD (Yasuo et al., 2011).

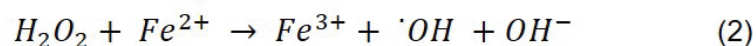
Gene expression signatures analysed using Expression Analysis Systematic Explorer (EASE) pathway analysis software, revealed relationships between COPD and SCLC; e.g. the KEGG-pathway for energy metabolism. Genes related to mitochondrial function and localisation were significantly overrepresented including a gene encoding NDUFA9 protein in complex I. There was a lower level of mitochondrial related genes in SCLC from non-COPD patients compared to SCLC from COPD patients (Boelens et al., 2011). This suggests that changes in genes which regulate mitochondrial function in COPD might also be involved in the development of cancer.

1.5 Reactive oxygen species (ROS)

ROS is a general term for a group of oxygen-containing molecules that can either accept or donate their electrons in a reaction which leads to them becoming less or more reactive molecules (Rosanna & Salvatore, 2012). There are many types of ROS generated in living systems including superoxide anion radical (O_2^-), hydroxyl radical ($\cdot OH$), hydrogen peroxide (H_2O_2), hypochlorous acid (HOCl), lipid peroxides (ROOH), and ozone (O_3) (Rosanna & Salvatore, 2012). The first step of ROS generation can be the reduction of O_2 by an electron leaking from mitochondrial respiratory chain to become O_2^- , a primary ROS which is moderately reactive (Venditti, Di Stefano, & Di Meo, 2013). The unstable O_2^- is subsequently catalysed by superoxide dismutase (SOD), producing H_2O_2 (equation 1).



H_2O_2 is then converted into $\cdot OH$, the highly reactive ROS, driven by catalytic metal ions e.g. Fe^{2+} or Cu^+ known as Fenton reaction (equation 2).



The catalysts for the Fenton reaction are in the mitochondrial matrix; therefore, excessive $\cdot OH$ may contribute to damage caused by cigarette smoke exposure as cigarettes contain metals and free radicals which may act as substrates in the Fenton reactions (Rosanna & Salvatore, 2012; Venditti et al., 2013).

Biological damage from ROS includes peroxidation of polyunsaturated fatty acids in cell membranes resulting in protein and enzyme dysfunction. ROS also damage

nucleic acids leading to abnormal DNA transcription and translation and further DNA strand breaks or base pair alteration (Kehrer, 1993).

1.5.1 Exogenous ROS

Exogenous ROS can be produced from substances in the environment which can generate or induce ROS in cells (Rosanna & Salvatore, 2012). The respiratory tract and the lungs are the main organs exposed to ROS generating substances. Pollution is one of the main sources of external ROS which our body receives on a daily basis. There are 6 major air pollutants including lead, carbon monoxide (CO), sulphur dioxide (SO₂), nitrogen dioxide (NO₂), ozone (O₃) and inhaled particle matter like cigarette smoke (Rosanna & Salvatore, 2012). Although non-cigarette smoke-derived ROS from traffic pollution plays an important role in the development of COPD, the focus of this discussion will be on cigarette smoke. A puff of cigarette smoke contains over 10¹⁴ free radicals and thousands of toxic chemicals which together represent a potent noxious insult to the lungs (Houghton, 2013). Studies show that cigarette smoke can generate ROS in airway epithelium (Pace et al., 2014) and activate signalling pathways such as NF-κB and MAPK (Mossman, Lounsbury, & Reddy, 2006; Rahman & Adcock, 2006) .

1.5.2 Endogenous ROS

Inside the cell, endogenous ROS can be generated mainly from the mitochondrial respiratory chain (reviewed in 1.5.2.1), metabolism of cytochrome P450 (CYP450), peroxisomes and activated inflammatory cells (Rosanna & Salvatore, 2012). Xanthine dehydrogenase, an enzyme involved in purine metabolism, is converted by proteases into xanthine oxidase which catalyses hypoxanthine to xanthine and

generates O_2^- and H_2O_2 (Harrison, 2002). O_2^- and H_2O_2 can be generated in the endoplasmic reticulum (ER) where CYP450 oxidizes exogenous ROS (Rosanna & Salvatore, 2012). In addition, CYP450 metabolises arachidonic acid which generates ROS as by-products (Rosanna & Salvatore, 2012). Intracellular NADPH is also a source of ROS production by reacting with O_2 using NADPH oxidases to become $NADP^+$ and O_2^- (Nauseef, 2014). This reaction typically occurs in inflammatory cells for phagosome activation in response to harmful particles, microorganism, and other inflammation (Rosanna & Salvatore, 2012).

Many cell types in the lung can produce ROS. Inflammatory cells (neutrophils, eosinophils) and alveolar macrophages are the main source for ROS production due to the presence of NADPH oxidases which can generate ROS to be used to kill infectious organisms (Tetley, 2005). Other cell types in the lung have been shown to produce ROS. For example, lung fibroblasts produced ROS after stimulation with TGF- β (Thannickal & Fanburg, 1995) and airway smooth muscle cells from COPD patients when stimulated with TNF- α showed increased expression of NOX-4 compared to cells from healthy controls (Hollins et al., 2016). Rodent ATII cells have an NADPH oxidase-like enzyme which generate O_2^- and H_2O_2 for bactericidal functions (van Klaveren, Roelant, Boogaerts, Demedts, & Nemery, 1997). Endothelial cells can also generate ROS through xanthine oxidoreductase under conditions of moderate hypoxia (10% O_2) (Kelley et al., 2006).

1.5.2.1 Mitochondrial ROS (mROS) production

Mitochondria are the major organelle for ROS production (Loschen & Flohé, 1971). Even though there are ROS derived from metabolic pathways occurring outside the mitochondria, the majority of ROS (90%) are from ETC in mitochondria

(Andreyev, Kushnareva, & Starkov, 2005). Complex I, II and III of ETC are the major sites of ROS production (Sabharwal & Schumacker, 2014) (Figure 1.16)

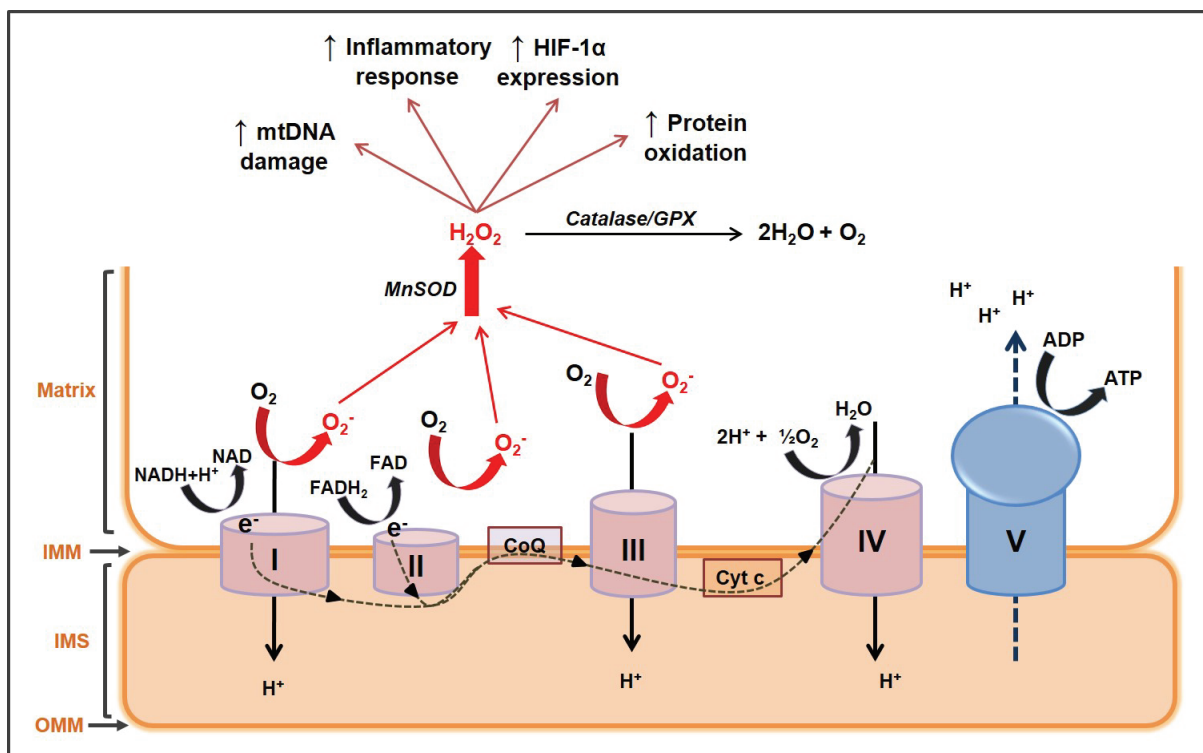


Figure 1.16 Schematic presentation of mitochondrial ROS (mROS) generation sites and its effects

Generation of mROS mostly occurs in complex I, II and III of ETC. The leaking electrons are transferred to O_2 resulting in O_2^- generation. The O_2^- can be converted to H_2O_2 mitochondrially catalysed by MnSOD. In physiological condition, H_2O_2 can be degraded to H_2O and O_2 using catalase or glutathione peroxidase (GPX). Overproduction of H_2O_2 can cause DNA damage, induce inflammatory pathways, HIF-1 α expression and protein oxidation possibly leading to tumorigenesis.

Complex I was the first site to be discovered where O_2^- production depends on NADH- and NADPH- reactions (Takeshige & Minakami, 1979). High levels of ROS are produced when complex I or III is blocked in rat skeletal muscle mitochondria using electrons derived from succinate which is oxidised by complex II or from reduced ubiquinone (Quinlan et al., 2012). Complex III is another site for ROS production which are formed by receiving electrons from an electron donor, ubisemiquinone ($Q\cdot$) (Turrens, Alexandre, & Lehninger, 1985). Eleven enzyme

complexes within complex I, II and III subunits which assist in the production of O_2^- and H_2O_2 . 2-oxoacid dehydrogenases contain a dihydrolipoamide dehydrogenase subunit, an FAD cofactor in complex I, which is a potent site of electron leak (Brand, 2016). The other ten sites involved in ROS production have been described in detail elsewhere (Brand, 2016). Due to complex IV (cytochrome c oxidase) having a high O_2 binding affinity, electrons and protons prefer reducing O_2 to H_2O rather than generating O_2^- (Sabharwal & Schumacker, 2014). Besides the electron leak, some mitochondrial proteins e.g. α -glycerophosphate dehydrogenase, α -ketoglutarate and pyruvate dehydrogenase have been found to play a role in ROS production (Andreyev et al., 2005).

1.5.2.1.1 Roles of mROS

mROS play important roles in the regulation of physiological systems in maintaining homeostasis and fluctuations in mROS levels can activate/deactivate signalling pathways, including those controlling inflammatory and hypoxic processes (Sena & Chandel, 2012).

Various cell types release inflammatory cytokines under the control of mROS. In endothelial cells, TNF- α -increased mROS levels cause the shedding of tumour necrosis receptor factor 1 (TNFR1) on the endothelial surface which protects the microvasculature against inflammation (Rowlands et al., 2011). Excessive mROS can act as signal transducers triggering inflammation by increasing the release of proinflammatory cytokines in many cell types (Singh & Costello, 2009). The involvement of mROS in the inflammatory response has also been demonstrated in microglia cells in the brain, whereby suppression of mROS by

a mitochondrial targeted antioxidant, mitoTEMPO, suppressed lipopolysaccharide (LPS)-induced TNF- α , IL-1 β and IL-6 levels. This suggests that mROS can modulate the production of pro-inflammatory cytokines independent of MAPK and NF- κ B inactivation (Park et al., 2015). In bone marrow-derived macrophages, IFN- γ induced OXPHOS and mROS production through PGC1 β /ERR α (Sonoda et al., 2007). Moreover, nucleotide-binding domain, leucine-rich repeat-containing protein 3 (NLRP3), a member of the inflammasome family, is induced by ROS which responds to cellular stress and is related to mitochondrial dysfunction (Zhou, Yazdi, Menu, & Tschopp, 2011). In primary mouse airway epithelial cells and in a murine model of allergic asthma Necro-X5, a mitochondrial ROS inhibitor, prevented NLRP3 activation and IL-1 β protein release which was associated with decreased mROS generation (Kim et al., 2014). An *in vivo* study in mice showed that ozone-induced airways are inflamed and hyperresponsive with decreased $\Delta\Psi_m$, increased mROS and decreased expression of complex I, III and V which can be reversed by a mitochondrial targeted antioxidant, MitoQ (Wiegman et al., 2015). MitoQ decreased inflammation (CXCL8 release) in TNF- α treated human airway smooth muscle cells from patients with COPD (Wiegman et al., 2015).

mROS also have a role in the cells response to hypoxia acting via the HIF family of transcription factors (Sena & Chandel, 2012). Stabilised HIF-1 α initiates gene transcription by binding to HIF-response elements at low O₂ (5% O₂) leading to angiogenesis and increasing glycolytic enzymes to maintain ATP production (Sena & Chandel, 2012). HIF-1 α expression is regulated differentially depending on cellular conditions. For example, an experimentally-based computational model showed that cancer cells can maintain intracellular H₂O₂ levels as well as increased HIF-1 α

expression in hypoxic conditions, which over time leads to cell survival which is believed to contribute to cancer cells being more aggressive and resistant to chemotherapy (Qutub & Popel, 2008).

A study of lung cancer and bone cancer cell lines found that a defect in the cytochrome b subunit in complex III resulted in increased mROS, which was required for HIF-1 α stabilisation and the cell's adaptation to hypoxia (Bell et al., 2007). In human NSCLC cell lines HIF-1 α is upregulated by nicotine but decreased when incubated with rotenone, a complex I inhibitor (Guo et al., 2012). In chronic hypoxia, an increase in mROS levels stabilises HIF-1 α ; however, HIF-1 α itself controls the mROS level to prevent further cellular damage as a study in murine embryonic fibroblasts showed that HIF-1 α targets *NDUFA4L2*, a gene in complex I which downregulates OXPHOS and limits ROS production under hypoxic conditions (Tello et al., 2011).

1.5.3 ROS elimination (Antioxidant systems)

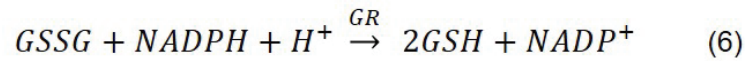
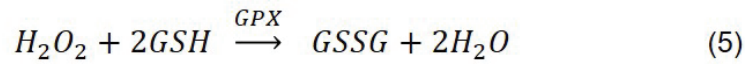
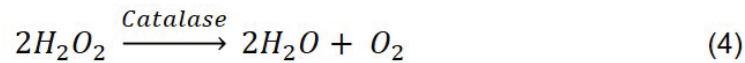
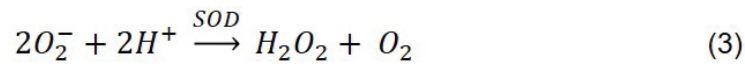
ROS formation is counterbalanced by ROS elimination by various antioxidant systems controlling redox homeostasis of the cell. (Espinosa-Diez et al., 2015). Protein antioxidants can be divided according to their subcellular location and chemical reactions and include glutathione, superoxide dismutase (SOD), catalase, peroxiredoxins (PRXs), thioredoxins (TRXs) and glutaredoxins (GRXs) (Finkel, 2011). O_2^- and H_2O_2 require different removal systems. O_2^- is converted into H_2O_2 by SOD whereas H_2O_2 is catalysed by catalase and PRXs (Finkel, 2011). In mitochondria, MnSOD catalyses O_2^- to H_2O_2 whereas cytoplasmic O_2^- is catalysed using CuZnSOD (Sabharwal & Schumacker, 2014). Families of TRXs and GRXs

have a role in redox homeostasis by catalysing the reduction of disulfide bridges in oxidised proteins (Finkel, 2011). Excessive ROS can overwhelm the elimination processes resulting in an imbalance between ROS generation and ROS elimination leading to the triggering of cell signalling responses (Aravamudan, Thompson, Pabelick, & Prakash, 2013).

1.5.3.1 Antioxidant defence system

Antioxidants are substances which react with ROS (oxidants) by transferring and removing electrons from oxidants resulting in redox balance control and lowering of cellular oxidative damage (Oyewole & Birch-Machin, 2015). Antioxidant defence systems can be grouped into endogenous and exogenous types.

Endogenous antioxidants consist of enzymatic antioxidants: SOD, catalase and glutathione peroxidase (GPX), and non-enzymatic antioxidants such as α -tocopherol (vitamin E), GSH, and bilirubin (Oyewole & Birch-Machin, 2015). As shown in section 1.5, O_2^- is converted into H_2O_2 by SOD (equation 3). H_2O_2 is subsequently converted into H_2O and O_2 by catalase (equation 4). H_2O_2 can be scavenged using the glutathione system (GSH) and GSH is the largest component of endogenous antioxidants. In humans, GSH concentrations range between 1 and 10mM (Hwang, Sinskey, & Lodish, 1992). The major ROS eliminated by GSH using GPX is H_2O_2 . GSH is converted into oxidised glutathione (GSSG) as shown in (equation 5). GPX can be found in both cellular and mitochondrial compartments (Espinosa-Diez et al., 2015) and the capacity for H_2O_2 removal depends upon both GPX activity and GSH concentration. GSSG is reduced back to GSH by glutathione reductase (GR) in the presence of NADPH (equation 6) (Espinosa-Diez et al., 2015).



Exogenous antioxidants are derived from natural sources e.g. carotenoids (lycopene and lutein), flavonoids (anthocyanine) and vitamins (A and C) or synthetic processes such as AP39, a synthetic mitochondrial targeted hydrogen sulfide donor (Oyewole & Birch-Machin, 2015). The addition of exogenous antioxidants is important in disease states as the cellular and particularly mitochondrial levels of endogenous antioxidants are low and may not be effective in eliminating ROS.

1.5.3.2 Mitochondrial targeted antioxidants

In order to improve the ability of ROS scavenging, especially of mROS, various mitochondrial targeted antioxidants have been developed and evaluated by their effects on the alteration or improvement in diseases.

Triphenylphosphonium cation (TPP⁺) is a lipophilic cell- and mitochondrial-membrane penetrating peptide that is conjugated with antioxidant molecules. Due to its positive charge (cation) it accumulates in the mitochondria via uptake through the electrochemical gradient (Oyewole & Birch-Machin, 2015). TPP⁺- conjugated antioxidants include mitoQuinone, mitoVitE, and mitoTEMPO. Other mitochondrial permeable antioxidants are SS (Szeto-Schiller) peptides e.g. SS31 and SS20 which contain an aromatic-cationic sequence which aids delivery into the mitochondria (Jin et al., 2014).

Mitochondrial targeted antioxidants used for experiments in this thesis include mitoTEMPO, AP39 and SS31.

MitoTEMPO(2-(2,2,6,6-tetramethylpiperidin-1-oxyl-4-ylamino)-2-oxoethyl) triphenyl phosphonium chloride) has a dynamic hydroxylamine group creating a catalytic cycle to scavenge O_2^- which mimics SOD activity (Samuni, Krishna, Mitchell, Collins, & Russo, 1990; Trnka, Blaikie, Smith, & Murphy, 2008) (Figure 1.17).

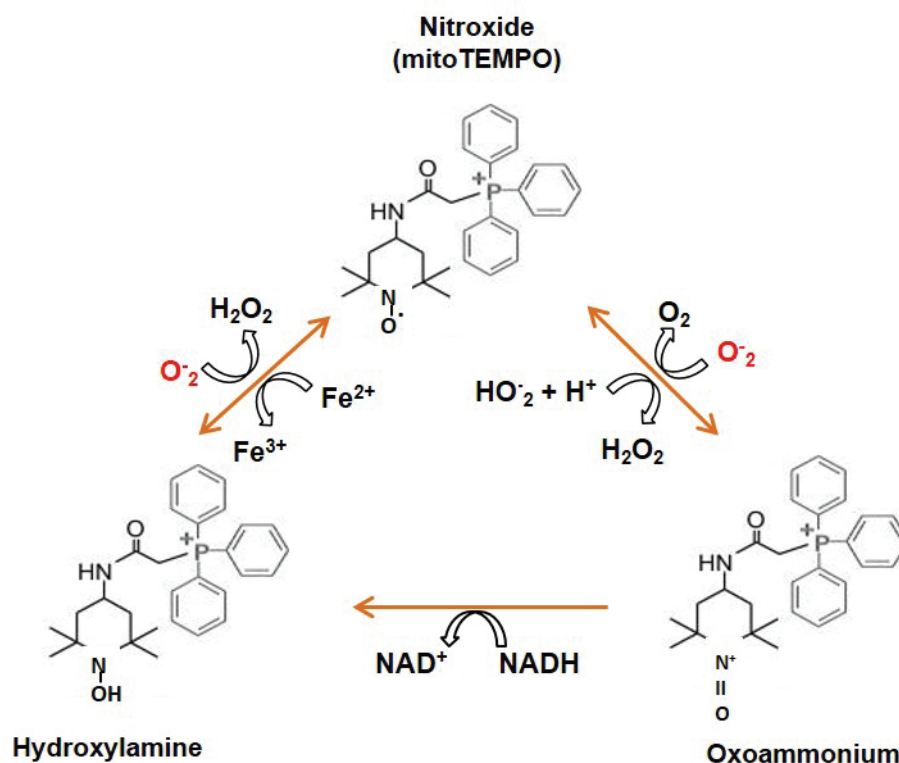


Figure 1.17 Antioxidant mechanism of mitoTEMPO

Once MitoTEMPO enter the mitochondria by TPP^+ , there is a cycle that catalyses O_2^- to H_2O_2 that mimics SOD. MitoTEMPO (nitroxide) is reduced to hydroxylamine or oxidised to oxoammonium by the conjugation of hydroperoxyl radical (HO_2) and H^+ . The oxoammonium can also oxidise O_2^- to regenerate nitroxide. Adapted from Trnka et al, 2008.

AP39 (10-oxo-10-(4-(3-thioxo-3H-1,2-dithiol-5yl)phenoxy)decyl triphenyl phosphonium bromide) has an ethole dithiolethione (ADT)-base providing a hydrogen sulfide (H_2S) donor portion which is a powerful reducing agent oxidised by O_2^- and H_2O_2 (Zhao, Biggs, & Xian, 2014) (Figure 1.18).

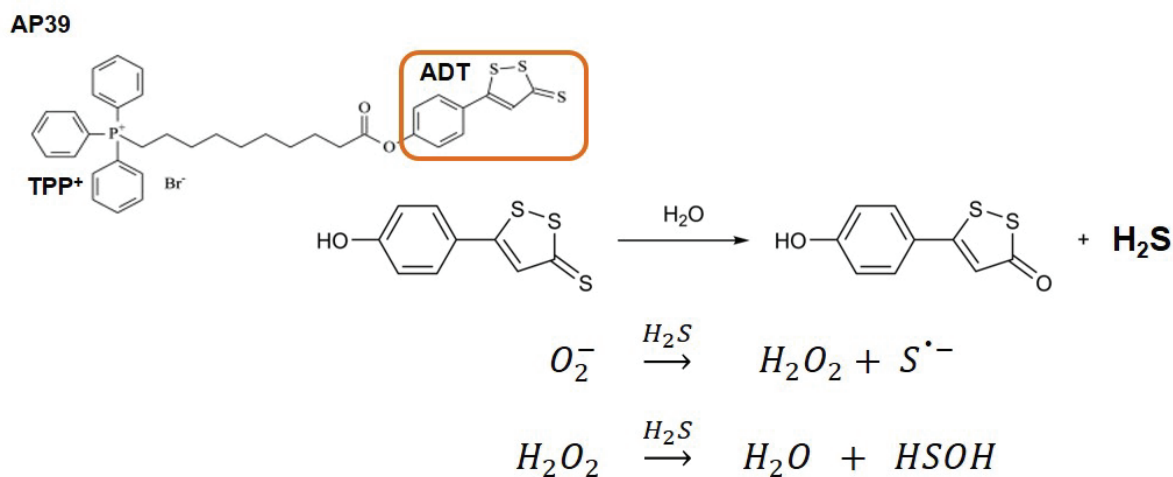


Figure 1.18 Antioxidant mechanism of AP39

Anethole dithiolethione (ADT) in AP39 molecule is the portion that produces hydrogen sulfide (H_2S) by the combination between hydrolysis and esterase enzyme. Superoxide is then oxidised by H_2S and converts into H_2O_2 . H_2S subsequently reduces H_2O_2 to H_2O . Adapted from Zhao, Biggs & Xian, 2014; Szabo, Papapetropoulos & Ohlstein, 2017.

SS31 known as bendavia or elamipretide is a cell-permeable tetrapeptide which has a phenol group in tyrosine residue which resides in the inner mitochondria membrane with 1000-5000 fold accumulation (Jin et al., 2014). Its phenol group is able to donate H^+ to unstable free radicals resulting in more stable molecules whereas the phenoxy-radical electron located in the phenol group can delocalise in the aromatic ring of SS31 (Craft, Kerrihard, Amarowicz, & Pegg, 2012) (Figure 1.19).

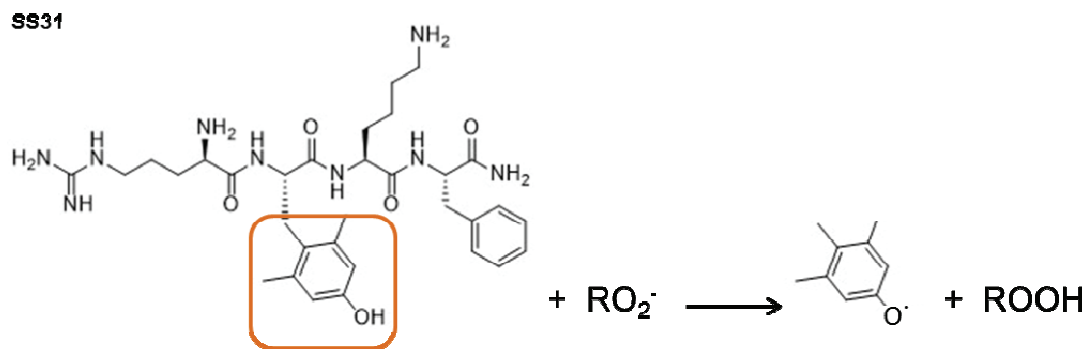


Figure 1.19 Antioxidant mechanism of SS31

SS31 scavenges free radicals by a phenol group on tyrosine which donates H^+ to an unstable free radical (RO_2^{\cdot}) and receives electron and then becomes phenoxy radical. However, the received electron can delocalised in the benzene ring which creates stabilisation.

1.5.4 Roles of oxidative stress in COPD

Oxidative stress is one of the main mechanisms in the pathogenesis of COPD. Besides the direct effect, oxidative stress can regulate or modulate other pathways e.g. inflammation, protease-anti-protease imbalance, and apoptosis (Rosanna & Salvatore, 2012).

Lipid peroxidation as a marker for oxidative stress and DNA damage was significantly increased in peripheral blood mononuclear cells (PBMC) of patients with COPD, especially those having a smoking history (Ceylan, Kocyigit, Gencer, Aksoy, & Selek, 2006). Lipid peroxidation products, including 4-hydroxynonenal and malondialdehyde, were increased in lung tissue from patients with COPD which had a negative correlation with lung function (Rahman et al., 2002). Plasma from patients with COPD and smokers was found to have lower catalase and SOD activity compared to non-smokers (Tavilani, Nadi, Karimi, & Goodarzi, 2012). Oxidative stress may disturb the imbalance between protease and anti-protease by impairing anti-protease function or enhancing protease activity. α 1-antitrypsin oxidised by oxidants from cigarette smoke or inflammatory cells was found to have decreased antiprotease activity in A549 cells, and also act as a proinflammatory inducer of IL-8 (Li et al., 2009). The connection between the protease pathway and oxidative stress was demonstrated in a severe COPD mouse (C57/BL6J- β ENaC-transgenic (Tg)) model treated with a serine protease inhibitor, ONO-3403 (Shuto et al., 2016). Pathway analysis in this study showed that ONO-3403 suppressed both protease and oxidative stress related pathways (Shuto et al., 2016). Oxidative stress also decreases the phagocytic activity of lung macrophages causing accumulation of apoptotic cells and subsequently persistent chronic inflammation in COPD (Hodge et

al., 2005). Lung macrophages from COPD patients show decreased phagocytic activity due to the oxidation of mannose binding lectin (Tran et al., 2014).

As described above, there is evidence for increased oxidant production in the airways, lungs, sputum and exhaled breath condensate (EBC) of smokers and COPD patients in stable disease and during natural (Dekhuijzen et al., 1996; Inonu et al., 2012) and viral-induced exacerbations (Footitt et al., 2016). Many clinical studies have investigated the effect of antioxidants on lung function improvement and the reduction in exacerbation rates in COPD patients. The small molecule thiol antioxidant, N-acetyl cysteine (NAC), a precursor of glutathione (GSH), has been used in several clinical trials due to its intracellular antioxidant properties (Rahman, 2012). The results have proved variable with some studies showing a reduction in EBC markers of oxidative stress such as H₂O₂, increased plasma GSH and decreased sputum IL-8 in COPD patients after 6-months treatment, (Bridgeman, Marsden, Selby, Morrison, & MacNee, 1994; Kasiel & Nowak, 2001; van Overveld, Demkow, Górecka, de Backer, & Zielinski, 2005). In the PANTHEON study, Patients with moderate-severe COPD (GOLD II-III) treated with 600mg NAC twice daily for 1 year were shown to decrease exacerbation rates and symptoms (Zheng et al., 2014) whilst other large studies such as the BRONCUS study in patients with frequent exacerbation (≥ 2 per year for 2 years) showed no difference of FEV₁ change between treated and placebo groups possibly due to the low dose of NAC (600mg/day) used despite 3 years of treatment (Decramer et al., 2005).

Other thiol antioxidants such as erdosteine that decreased peripheral blood ROS levels, the duration of exacerbation and reduced hospitalisation of COPD patients

(Dal Negro et al., 2017; Moretti et al., 2004; Negro, 2008) and carbocysteine which did not improve FEV₁, exacerbation and severity (Allegra, Cordaro, & Grassi, 1996; Yasuda et al., 2006) highlight the variable response in COPD clinical trials. These thiol antioxidants may have failed to achieve their goals of ROS scavenging and subsequent treatment efficacy in COPD due to their poor bioavailability, the formation of cysteine radicals as well as their non-specific cellular site of action (Rahman, 2012). Mitochondria are the major sites of free radical production in the cell and regulate redox homeostasis (Brand, 2016). Antioxidants targeting mitochondria have been found to be effective in many disease models and in clinical studies (Carter et al., 2011; Gane et al., 2010; Jin et al., 2014; Wang et al., 2014). Therefore, mitochondrial targeted antioxidants could be potential therapeutic candidates in COPD.

1.5.5 Roles of oxidative stress in lung cancer

Oxidative stress also plays an important role in carcinogenesis either by direct exposure i.e. oxidation of nDNA, RNA, and lipids or as a mediator in signalling pathways (Rosanna & Salvatore, 2012). Direct effects on DNA mutation include DNA strand breaks, point mutations, aberrant DNA cross-linking and oncogene and tumour suppressor gene mutations (Rosanna & Salvatore, 2012). Several key mutations associated with lung cancer have been identified including oncogenes: *EGFR*, *KRAS*, *ALK*, *HER2*, *BRAF*, *PIK3CA*, and *AKT1*, and a *MAPK* gene: *MAP2K1* (Pao & Girard, 2011). Nuclear factor erythroid 2-like 2 (*Nfe2l2* also known as *Nrf2*) encodes a transcription factor which regulates the adaptive response to oxidative stress and is overexpressed in premalignant cells which helps them survive in the tumour microenvironment (Kensler & Wakabayashi, 2010).

A loss-of-function mutation in *Nrf2* is associated with a higher risk of NSCLC (Hu et al., 2012). Besides cancer cell survival, *Nrf2* also mediates NSCLC proliferation following cooperation between EGFR signalling and the Nrf2 repressor protein Keap1 (Kelch-like ECH-associated protein 1) (Yamadori et al., 2012). A glycolytic inhibitor, 2-deoxy-D-glucose (2DG) causes A549 and H358 lung cancer cell lines to produce ROS and induces p53 tumour suppressor protein activation which protects cancer cells by increasing OXPHOS and inducing the antioxidant enzyme, SOD. It may indicate that induction of oxidative stress might kill cancer cells in the absence of p53 (Sinthupibulyakit, Ittarat, St Clair, & St Clair, 2010).

1.6 Hypothesis

Oxidative stress is a key component of both COPD and lung cancer pathogenesis that induces chronic inflammation and alters cellular and redox homeostasis. Mitochondria are important organelles for redox control of ROS production and elimination. Abnormal mitochondrial function not only impairs ROS production and elimination but also affects mitochondrial bioenergetics which may be a causative factor in why some COPD patients develop lung cancer. Therefore, the hypothesis of the study is that oxidative stress leads to the cellular and mitochondrial dysfunction which is exaggerated in COPD to drive a phenotype more conducive to the development of lung cancer.

1.7 Aims

- To investigate the effect of hydrogen peroxide and IL-1 β on mitochondrial function in the bronchial epithelial cell line (BEAS-2B)
- To investigate functional differences between airway epithelial cell types including BEAS-2B cells, normal human bronchial epithelial cells (NHBE) and lung adenocarcinoma cells (A549)
- To investigate the effect of cellular- and mitochondrial-targeted antioxidants on mitochondrial and cellular function in BEAS-2B, NHBE and A549 cells
- To establish a mitochondrial function monitoring protocol for extracellular flux analysis (Seahorse Technology)
- To investigate the expression of mitochondrial and metabolic genes in tumour and matched non-tumour lung tissue from lung cancer patients

Chapter 2 Materials and Methods

2.1 Materials

Table 2.1 Cell Culture Reagents

REAGENT	SUPPLIER
A549 (ATCC [®] CCL-185 [™]) (human lung adenocarcinoma cell line)	LGC Standards, Teddington, UK
Airway Epithelial Cell Basal Medium	PromoCell GmbH, Heidelberg, Germany
Airway Epithelial Cell Basal Medium Supplement Pack (Bovine Pituitary Extract [BPE], human Epidermal Growth Factor [hEGF], Recombinant human insulin, Hydrocortisone, Epinephrine, Triiodo-L-thyronine, Transferrin [holo,human], Retinoic Acid)	PromoCell GmbH, Heidelberg, Germany
BEAS-2B (ATCC [®] CRL-9609 [™]) (SV-40 transformed human bronchial epithelial cell line)	LGC Standards, Teddington, UK
BEGM [™] Bronchial Epithelial Cell Growth Medium	Lonza, Basel, Switzerland
BEGM [™] SingleQuots [™] Kit (BPE, Hydrocortisone, hEGF, Epinephrine, Transferrin, Insulin, Retinoic Acid, Triiodothyronine, and Gentamicin/Amphotericin B)	Lonza, Basel, Switzerland
Bovine Collagen Solution, Type I (3mg/ml) (PureCol [®])	Cell Systems, Troisdorf, Germany
Bovine Pituitary Extract (BPE) (Gibco [™])	Fisher Scientific, Loughborough, UK
Dulbecco's Modified Eagle's Medium (DMEM) - high glucose (without glutamine)	Sigma-Aldrich, Poole, Dorset, UK
Epidermal Growth Factor (EGF), Human Recombinant (Gibco [™])	Fisher Scientific, Loughborough, UK
Hank's Balanced Salt Solution	Sigma-Aldrich, Poole, Dorset, UK
Hank's Balanced Salt Solution with calcium and magnesium	Fisher Scientific, Loughborough, UK
Heat-inactivated, foetal bovine serum (FBS)	Sigma-Aldrich, Poole, Dorset, UK
Hepes Buffer Saline Solution	PromoCell GmbH, Heidelberg, Germany
Keratinocyte-SFM(1x) (Gibco [™])	Fisher Scientific, Loughborough, UK
L-Glutamine	Sigma-Aldrich, Poole, Dorset, UK
NHBE (human normal bronchial epithelial cell)	Lonza, Basel, Switzerland
Trypan blue	Sigma-Aldrich, Poole, Dorset, UK
Trypsin Neutralising solution	PromoCell GmbH, Heidelberg, Germany
Trypsin/EDTA	PromoCell GmbH, Heidelberg, Germany

Table 2.2 Laboratory Reagents

REAGENT	SUPPLIER/MANUFACTURER
2', 7'-dichlorodihydrofluorescein diacetate (DCF-DA) (Molecular Probes™)	Life Technologies, Paisley, UK
Anti-NDUFA9 antibody, mouse monoclonal [20C11B11B11]	Abcam, Cambridge, UK
Bovine serum albumin (BSA)	Sigma-Aldrich, Poole, Dorset, UK
Bradford Solution	Bio-Rad Laboratories, Watford, UK
Buffer RLT	Qiagen, Manchester, UK
D-(+)-Glucose	Sigma-Aldrich, Poole, Dorset, UK
Dimethylsulphoxide (DMSO)	Sigma-Aldrich, Poole, Dorset, UK
Ethanol (absolute)	Sigma-Aldrich, Poole, Dorset, UK
Hank's Balanced Saline Solution with calcium and magnesium, no phenol red	Life Technologies, Paisley, UK
LIVE/DEAD Fixable Aqua Dead Cell Stain Kit (Molecular Probes™)	Life Technologies, Paisley, UK
Methylthiazolyldiphenyl-tetrazolium bromide (MTT)	Sigma-Aldrich, Poole, Dorset, UK
MitoSOX™ Red (Molecular Probes™)	Life Technologies, Paisley, UK
Phosphate buffered saline with Tween® 20 (dry powder)	Sigma-Aldrich, Poole, Dorset, UK
Phosphate-buffer saline tablets	Sigma-Aldrich, Poole, Dorset, UK
Protease inhibitors (EDTA free) tablets	Roche diagnostics Ltd. Burgess Hill, West Sussex, UK
RIPA lysis buffer	Santa Cruz Biotechnology, Inc. Heidelberg, Germany
RNAlater®	Sigma-Aldrich, Poole, Dorset, UK
RNase-free water	Sigma-Aldrich, Poole, Dorset, UK
Sodium azide (NaN ₃)	Sigma-Aldrich, Poole, Dorset, UK
Sodium chloride	Sigma-Aldrich, Poole, Dorset, UK
Sodium pyruvate solution (100mM)	Sigma-Aldrich, Poole, Dorset, UK
Sulfuric acid	Sigma-Aldrich, Poole, Dorset, UK
TMB Substrate Reagent Set (BD OptEIA™)	BD Bioscience, Reading, UK
Trizma® base (Tris base)	Sigma-Aldrich, Poole, Dorset, UK
Tween® 20	Sigma-Aldrich, Poole, Dorset, UK
XF Assay media	Agilent Technologies, Cheadle, UK
XF Calibrant	Agilent Technologies, Cheadle, UK
β-mercaptoethanol	Sigma-Aldrich, Poole, Dorset, UK

Table 2.3 Assay Kits

KIT	SUPPLIER/MANUFACTURER
Cell Proliferation ELISA, BrdU (chemiluminescent)	Roche diagnostics Ltd. Burgess Hill, West Sussex, UK
FITC Annexin V/Dead Cell Apoptosis Kit with FITC annexin V and PI, for Flow Cytometry (Molecular Probes™)	Life Technologies, Paisley, UK
High Capacity cDNA Reverse Transcription Kit (Applied Biosystems™)	Fisher Scientific, Loughborough, UK
Human CXCL8/IL8 Duoset ELISA kit	Bio-Techne Ltd. Abingdon, UK
Mitochondria Isolation Kit for Tissue	Fisher Scientific, Loughborough, UK
MitoProbe™ JC-1 assay kit (Molecular Probes™)	Life Technologies, Paisley, UK
RNeasy® Mini Kit	Qiagen, Manchester, UK
Seahorse XF Cell Mito Stress Test Kit	Agilent Technologies, Cheshire, UK

Table 2.4 Reagents and kits used for immunohistochemistry

REAGENTS	SUPPLIER/MANUFACTURER
EZ-Prep Solution (paraffin removal solution)	Ventana Medical Systems, Inc. Salisbury, UK
Ventana Optiview Peroxidase Inhibitor (3%)	
Ventana Optiview DAB detection Kit	
Hematoxylin II	
Ventana Bluing Reagent	
Reaction Buffer	

Table 2.5 PCR primers and annealing temperatures

GENE	OLIGO SEQUENCE	ANNEALING TEMPERATURE (°C)	SUPPLIER
<i>18S</i> forward	5'-CTTAGAGGGACAAGTGGCG-3'	60	Life Technologies, Paisley, UK
<i>18S</i> reverse	5'-ACGCTGAGCCAGTCAGTGTA-3'		
<i>IL8</i> forward	5'-TTTTGCCAAGGAGTGCTAAAG-3'		
<i>IL8</i> reverse	5'-TTTCTGTGTTGGCGCAGTGTGG-3'		
<i>PDK1</i> forward	5'-GTCGCCACTCTCCATGAAG-3'	55	Eurofins Genomics, Wolverhampton, UK
<i>PDK1</i> reverse	5'-TGGGGTCCTGAGAAGATTATC-3'		

Table 2.6 TaqMan® Gene Expression assays for real-time RT-PCR (Applied Biosystems®, Invitrogen, UK)

GENE	PRODUCT CODE	DETECTION CHANNEL
<i>18S</i>	4310893E	VIC™TAMRA™
<i>AMPK (PRKAA1)</i>	Hs01562315_m1	FAM
<i>HIF1A</i>	Hs00153153_m1	FAM
<i>IL8</i>	Hs00174103_m1	FAM

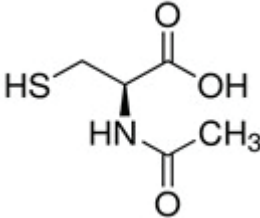
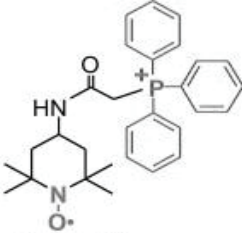
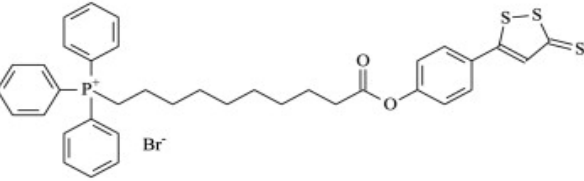
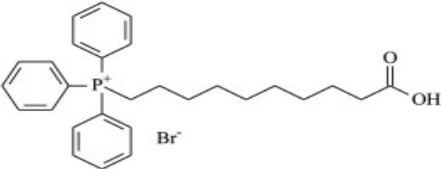
Table 2.7 QuantiTect Primer assays for SYBR® Green-based expression analysis (Qiagen) for real-time RT-PCR

GENE SYMBOL	ASSAY NAME	CATALOGUE #
<i>EGFR</i>	Hs_EGFR_1_SG	QT00085701
<i>GLUT1</i>	Hs_SLC2A1_1_SG	QT00068957
<i>HK2</i>	Hs_HK2_1_SG	QT00013209
<i>KRAS</i>	Hs_KRAS_1_SG	QT00083622
<i>PGC1A</i>	Hs_PPARGC1A_1_SG	QT00095578
<i>PGC1B</i>	Hs_PPARGC1B_1_SG	QT00081365

Table 2.8 Compounds

COMPOUND	SUPPLIER/MANUFACTURER
(10-oxo-10-(4-(3-thioxo-3H-1,2-dithiol-5yl) phenoxy) decyl) triphenyl-phosphonium bromide (AP39)	University of Exeter Medical School, Exeter, UK
(9-carboxynonyl) triphenyl-phosphonium bromide (AP219)	University of Exeter Medical School, Exeter, UK
2-(2,2,6,6-Tetramethylpiperidin-1-oxyl-4-ylamino)-2-oxoethyl) triphenylphosphonium chloride (MitoTEMPO)	Sigma-Aldrich, Poole, Dorset, UK
D-Arg-2',6'-dimethyltyrosine-Lys-Phe-NH ₂ (SS31)	ChinaPeptides, HangZhou, China
Hydrogen peroxide solution (H ₂ O ₂) 30% (w/w) in H ₂ O, contain stabilizer	Sigma-Aldrich, Poole, Dorset, UK
N-Acetyl-L-cysteine (NAC)	Sigma-Aldrich, Poole, Dorset, UK
Recombinant Human IL-1β/IL-1F2	Bio-Techne Ltd. Abingdon, UK

Table 2.9 Antioxidants and their actions

ANTIOXIDANTS	ACTIONS
<p>N-acetyl cysteine (NAC)</p> 	<p>Sulfhydryl containing compound. A precursor of L-cysteine and reduced glutathione which scavenges free radicals in cells (Matera, Calzetta, & Cazzola, 2016).</p>
<p>MitoTEMPO</p> 	<p>A Dynamic hydroxylamine group mimics the action of superoxide dismutase to scavenge O_2^- (Samuni et al., 1990; Trnka et al., 2008).</p>
<p>AP39</p> 	<p>Triphenylphosphonium (TPP⁺) of AP39 helps accumulate in the mitochondria whereas anethol dithiolethione (ADT) based donor provides H₂S portion to oxidise O_2^- and H₂O₂ resulting in support electron transport chain, ATP production and maintain mitochondrial integrity (Ahmad & Szabo, 2016; Craft et al., 2012).</p>
<p>AP219</p> 	<p>An AP39-like structure which does not have the H₂S donor group. It is a control compound of AP39.</p>

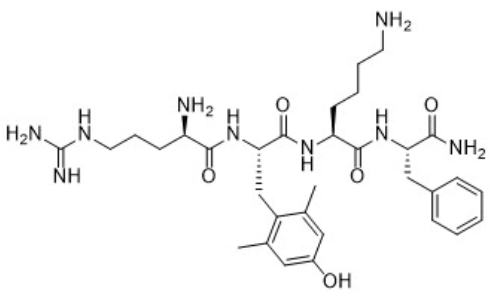
<p>SS31</p> 	<p>The molecule accumulates in the inner mitochondrial membrane. The phenolic group in tyrosine or dimethyltyrosine donates H⁺ to free radicals resulting in more stable molecule, and receives free-radical electron which is shared in the aromatic ring of SS31 (Craft et al., 2012).</p>
---	---

Table 2.10 Equipment

EQUIPMENT	SUPPLIER/MANUFACTURER
7500real-time PCR systems	Applied Biosystems, Invitrogen, UK
Analytical Balance HR-202i	A&D Company, Ltd. Tokyo, Japan
BD FACSCanto™ II flow cytometer	BD Bioscience, UK
Precellys® soft tissue homogenising CK14	VWR International, Lutterworth, UK
Biotek Instrument microplate reader	Biotek, Swindon, UK
Class II microbiological safety cabinet (BioMAT2)	Thermo Electron Corporation, UK
Corning® Black 96-well plates	Sigma-Aldrich, Poole, Dorset, UK
Corning® Clear bottom 96-well plates	Sigma-Aldrich, Poole, Dorset, UK
Coverslip	Fisher Scientific, Loughborough, UK
Galaxy S+ CO ₂ Incubator	RS Biotech Laboratory Equipment, Irvine, UK
Glass Tissue grinder	Kimble Chase Life Science, Rockwood, TN, USA
G-storm Thermocycler	LabTech International, Uckfield, East Sussex, UK
Heraeus Labofuge 400R	DJB Labcare, Newport Pagnell, Milton Keynes, UK
JEOL 2000 Transmission Electron Microscope	Joel UK, Welwyn Garden City, Herts, UK
Microcentrifuge Hettich Mikro 22R	DJB Labcare, Newport Pagnell, Milton Keynes, UK
Nanodrop™ Lite	LabTech International, Uckfield, East Sussex, UK
Optical microscope	Olympus Optical Company Ltd London, UK
Platform shaker (Titramax 1000)	Heidolph UK, Saffron Walden, Essex, UK
Precellys® 24 tissue homogenizer	Stretton Scientific Ltd. Stretton, Derbyshire, UK
QIAshredder homogenizer	Qiagen, Manchester, UK
RotorGene RG3000, RG6000	Qiagen, Manchester, UK

Seahorse XF Prepstation (Non-CO ₂ incubator)	Agilent Technologies, Cheadle, UK
Seahorse XF96 Calibrants	Agilent Technologies, Cheadle, UK
Seahorse XF96 Cell Culture Microplates	Agilent Technologies, Cheadle, UK
Seahorse XF96 sensor cartridges	Agilent Technologies, Cheadle, UK
Seahorse XFe96 Analyzer	Agilent Technologies, Cheadle, UK
SIGMA 4-16K Centrifuge	SciQuip Ltd, Newtown, Wem, Shropshire, UK
SkatWasher 400	Skatron, Sunnyvale, CA, USA
Superfrost Plus™ microscope slide	Fisher Scientific, Loughborough, UK
Ventana Benchmark Ultra Platform (Automated IHC/ISH slide staining system)	Ventana Medical Systems, Inc. Tuscon, AZ, USA
ZEISS Axiocam Microscope	Carl Zeiss Ltd. Cambridge, UK

2.2 Methods

2.2.1 Lung tissue clinical samples

Two sets of lung tissue samples were obtained for two different studies. The first study was to measure mitochondrial membrane potential and mitochondrial ROS from isolated mitochondria and to investigate metabolic gene expression. Tumour tissue and pathologically normal tissue was obtained from patients undergoing lung resection for lung cancer at the Royal Brompton Hospital. Fresh tissues were collected into basal DMEM for mitochondrial isolation or preserved in RNAlater for RNA extraction. This study was approved by the Respiratory Biomedical Research Unit (BRU) Heads of Consortia under the Ethical approval given to the BRU Advanced Lung disease (ALD) Biobank (NRES Reference 10/H0504/9).

The other study was to investigate the differential expression of the mitochondrial protein NDUFA9 by immunohistochemistry (IHC) in tumour and background tissue from lung tissue samples. Lung tissues were obtained from lung cancer patients, which were divided into non-smokers, smokers and COPD subgroups. This study

was approved by the Health Research Authority, South Central – Hampshire B Research Ethics Committee (REC Reference 15/SC/0569).

2.2.2 Cell lines and cell culture

BEAS-2B cells, a SV-40 transformed human bronchial epithelial cell line obtained from the American Type Culture Collection (LGC Standards, Teddington, UK) (Reddel et al., 1989), were maintained in keratinocyte serum-free media supplemented with 5ng/ml recombinant epithelial growth factor (rEGF) and 50µg/ml bovine pituitary extract (BPE) at 37°C and 5% CO₂ until 80% confluent. Cell used in experiments were between passages 4-12.

A549 cells, a human alveolar adenocarcinoma cell line (Cooper, 2012), were cultured in Dulbecco's modified eagle's media (DMEM) supplemented with 2mM glutamine and 10% foetal bovine serum.

NHBE cells, primary normal human bronchial epithelial cell, were cultured in bronchial epithelial cell growth medium (BEGM) supplemented with BEGM™ SingleQuots™ Kit. Cell used for experiments were between passages 2-4.

Cell number was determined using trypan blue (1:10 dilution) and haemocytometer. Before experiments, cells were synchronised by growing in basal media for 16-24h. The characteristics of BEAS-2B, NHBE and A549 cells are given in Table 2.11.

Table 2.11 Characteristic comparison between BEAS-2B, NHBE and A549

	BEAS-2B	NHBE	A549
Cell type	Virus transformed normal bronchial epithelial cells	Normal bronchial epithelial cells	Lung adenocarcinoma
Source	Epithelial lining of tracheobronchial part from non-cancerous individuals	Epithelial lining above basement membrane in conduction portion of the lungs before terminal bronchioles from non-cancerous individuals (Bhowmick & Gappa-Fahlenkamp, 2016)	Lung tumour explants of a 58-year-old Caucasian (Lieber, Todaro, Smith, Szakal, & Nelson-Rees, 1976), originated from the neoplastic transformation of ATII cell (Lieber et al., 1976)
Immortalisation	Adenovirus 12-SV40 (Reddel et al., 1989)	-	-
Morphology	Cuboidal shape in monolayer culture Possess both airway and bronchial epithelial cell properties	Cuboidal shape in monolayer culture Contain basal cells	Epithelial-like Possess ATII cell properties (lamellar bodies and microvilli) (Bhowmick & Gappa-Fahlenkamp, 2016)
Passages	2-8 (Khan, Kirkham, Barnes, & Adcock, 2014), 10-30 (Zhao & Klimecki, 2015)	2-4 (Thaikootathil et al., 2009)	>115 (Lieber et al., 1976)
Uses	Respiratory inflammation, cancer transformation, toxicology, wound repair, and infectious diseases studies (Garcia-Canton, Minet, Anadon, & Meredith, 2013; Hamada et al., 2016; Jagannathan et al., 2016; Khan et al., 2014; Ollikainen, Linnainmaa, Raivio, & Kinnula, 1998)	Respiratory infectious diseases, signalling pathway for pathogenesis, and drug development studies (Davis et al., 2015; Min, Rosania, & Shin, 2016; Thaikootathil et al., 2009)	Respiratory infectious diseases, chemotherapeutic drug testing, lung carcinogenesis studies (Fine-Coulson, Giguère, Quinn, & Reaves, 2015; Kwon et al., 2015; Yadong Wang et al., 2016)

2.2.3 Cell viability

2.2.3.1 MTT assay

Cell viability (Mitochondrial activity) was measured colourimetrically using the MTT assay. The MTT assay can be used to assess the mitochondrial activity as active mitochondrial dehydrogenase in a live cell changes the water-soluble MTT to an insoluble purple formazan. Briefly, after cell stimulation the supernatant was removed and replaced with fresh media containing MTT (5mg/ml). The cells were incubated at 37°C for 2h. The MTT reagent was removed and plates allowed to air dry before dissolving the resultant formazan crystals in DMSO. The optical density (OD) at 570nm was measured using spectrophotometer. The viability/activity was calculated by the subtraction of the absorbance of the blank wells, performed as above but with no cells present, from each sample absorbance.

2.2.3.2 Trypan blue assay

After completing experiments, the cells were washed once with Hank's Balanced Salt Solution (HBSS) and then trypsinised, followed by centrifugation at 1,500rpm for 5min. The cell pellet was resuspended in 500µl serum free media (SFM) in a microcentrifuge tube. 50µl of cell suspension was added to 50µl trypan blue (dilution 1:1) and mixed well. 10µl of cell dilution was pipetted into a space between haemocytometer grid and cover slip; the cells were then counted using light microscope. The evaluation is based on the fact that intact cell membranes in viable cells exclude trypan blue whereas dead cells do not. The average cell number was counted from cells located in 8 corner squares of the grid. Both stained and unstained cells were counted separately. The percentage of

cell viability was calculated by the average number of unstained cells (viable cells) divided by the average of total cell number and multiplied by 100.

2.2.3.3 Cell viability evaluation using flow cytometer

2.2.3.3.1 Red-fluorescent propidium iodine (PI) assay

PI is a nucleic acid binding dye which permeates dead cells and binds tightly to nucleic acids. Briefly, after treatment, supernatant from all samples were kept and the cells were trypsinized. The supernatant and trypsinized cells were then mixed together again in microtubes followed by centrifugation at 1,500rpm for 5min. The cell pellets were resuspended at concentration of 10^5 cells in 100 μ l 1x binding buffer. PI was then added to the cell suspension at a working concentration (100 μ g/ml) and incubated at room temperature for 15min. After incubation, 400 μ l of binding buffer was added and mixed well before analysis using flow cytometry. Untreated cells were used as negative control and cells killed by heating at 70°C for 5min were used as a positive control.

2.2.4 Apoptosis assay

Apoptosis was assessed using fluorescein isothiocyanate (FITC) Annexin V/Dead Cell Apoptosis Kit with FITC Annexin V and PI, for Flow Cytometry. In apoptotic cells, phosphatidylserine (PS) which is normally located in cytoplasm moves to the membrane surface which binds to FITC Annexin V. Dead cell population can be distinguished from apoptotic cell population by using PI. Dead cells are unable to maintain the cell membrane integrity; PI can pass through and bind directly to nucleic acids. Similar to PI assay, after treatment, supernatant from all samples were kept and the cells were trypsinized. The supernatant and trypsinized cells were then

mixed together again in microtubes followed by centrifugation at 1,500rpm for 5min. The cell pellets were resuspended at concentration of 10^5 cells in 100 μ l 1x binding buffer. 5 μ l FITC annexin V (green fluorescence) and 1 μ l of 100 μ g/ml of PI (red fluorescence) were added to cell suspensions. The samples were incubated at room temperature for 15min followed by adding 400 μ l of 1x annexin-binding buffer, mixed gently and kept on ice. Stained cells were analysed immediately using flow cytometer with the fluorescence excitation/emission 494/518nm for annexin V and 535/617nm for PI. In our experiments, cell populations were separated into live cells (annexin V⁻, PI⁻), apoptotic cells (annexin V⁺, PI⁻) and dead cells (annexin V⁺, PI⁺). Gate setting was carried out using a positive control of cells heated at 70°C for 5min and a non-treated stained sample was used as negative control.

2.2.5 Proliferation assay

Cell proliferation was measured by BrdU chemiluminescent immunoassay. 5-bromo-2'-deoxyuridine (BrdU), a synthesized pyrimidine analog, incorporates into the new DNA of proliferating cells. The incorporation of BrdU into the DNA is detected using an anti-BrdU antibody. Briefly, 2×10^3 cells/well were seeded in a black 96-well plate and treated with different concentrations of substances/stimulants/antioxidants in 100 μ l of final volume for 48h. BrdU labelling solution was added at a final concentration of 10 μ M 24h before the end of the experiment. Supernatant was removed, and wells allowed to dry. Cells were fixed with the manufacturer's Fix/Denat solution for 30min followed by incubation with anti-BrdU-POD working solution, which was allowed to bind to the incorporated DNA at room temperature for 1.5h, and then washed three times with 1X wash buffer. Substrate solution was then added 100 μ l/well and incubated for at least 3min at room temperature on

a platform shaker. Light emission of the antigen-antibody complexes was detected using spectrofluorometer. Fluorescence intensity was detected with excitation and emission wavelengths of 485/20nm and 528/20nm, respectively. The sensitivity of detection was set at 90%. Data were presented as the level of relative fluorescence unit (RFU).

2.2.6 RNA extraction

BEAS-2B, A549 and NHBE were seeded in 6-well plates and treated as described in the results sections. Total RNA was isolated using RNeasy[®] Mini Kit following the manufacturer's instructions. All steps were performed at room temperature. The cells were lysed with 350 μ l RLT buffer containing 1% β -mercaptoenol (β -ME). For lung tissues preserved in RNAlater solution, after thawing on ice, the tissue was disrupted by bead beating using a tissue homogeniser. Briefly, tissue with RLT buffer with 1% β -ME was placed in a tube containing 1.4mm ceramic (zirconium oxide) beads. The tube was shaken using tissue homogeniser for 10-15sec or until a cell lysate was obtained. Working temperature for lung tissues should be around 0°C to maintain high yield of total RNA.

Cell lysates were either passed through a 20G needle attached to a 1ml syringe 6 times or loaded onto a QIAshredder homogenizer and centrifuged for 3min at 10,000rpm. The homogenous lysates were mixed with an equal volume of 70% ethanol and transferred to RNeasy spin columns and centrifuged for 3min at 15,000rpm, and then washed with RW1 Buffer for 15sec at 10,000rpm. Spin columns were washed twice with RPE Buffer for 15sec at 10,000rpm. RNA was collected from spin columns by adding 50 μ l RNase free water and

centrifuged for 3min at 15,000rpm. Total RNA was kept at -80°C until use. RNA concentration (ng/μl) and purity were measured using a Nanodrop™ Lite. The RNA purity was determined with the ratio of absorbance at 260nm and 280nm (A260/A280). Acceptable ratio for RNA was between 1.8 and 2.0.

2.2.7 Reverse transcription

Single stranded complementary DNA (cDNA) was synthesized from 500ng of RNA in reverse transcription reaction mixture consisting of 1x RT Buffer, 1mM dNTP Mix, 1x RT Random Primers and Multiscribe Reverse Transcriptase and RNase free water in a final volume of 20μl. Samples were incubated at 37°C for 2h then the reactions were stopped at 85°C for 5min. 40μl of RNase free water was added to cDNA product which was stored at -20°C until use.

2.2.8 Real time quantitative polymerase chain reaction (PCR)

Levels of gene transcription were detected by real time qPCR using SYBR green incorporation. In this project, two approaches to RNA analysis were used: the SYBR® Green method was performed using a Rotor-Gene 3000/6000 and analysed using Rotor-Gene 6 software, and TaqMan® analysis was performed using the Applied Biosystems® 7500real Time PCR System. For the SYBR® Green analysis, the PCR was started with heating step to activate DNA polymerase at 95°C for 15min, and subsequently ran for 30-50 cycles of denaturation at 94°C for 15sec, annealing at 55-60°C for 30sec and extension at 72°C for 30sec. The component mixture is shown in Table 2.12.

For the TaqMan® method, pre-PCR preparation was set at 50°C for 2min followed by 95°C for 10min then thermal cycling of denaturation at 95°C for 15sec,

and combined annealing and extension was performed at 60°C for 1min. The component mixture for TaqMan® PCR is shown in Table 2.13. The list of PCR primers is shown in Table 2.5, 2.6 and 2.7.

Table 2.12 SYBR® Green RT-qPCR master mix components for each PCR tube

COMPONENT	VOLUME	FINAL CONCENTRATION
SYBR® Green Master Mix	10µl	50%
Forward primer	1µl	0.5µM
Reverse primer	1µl	0.5µM
RNase-free water	3µl	
Total Master Mix reaction volume	15µl	
cDNA product	5µl	
Total volume	20µl	

Table 2.13 TaqMan® Green RT-qPCR master mix components for each well in PCR microplate

COMPONENT	VOLUME
TaqMan® Master Mix	10µl
Gene expression assay probe	1µl
18S probe	1µl
RNase-free water	4µl
Total Master Mix reaction volume	16µl
cDNA product	4µl
Total volume	20µl

2.2.9 Bradford protein assay

Total protein concentration was determined in cell lysates obtained by addition of radioimmunoprecipitation assay (RIPA) buffer (20µl) to each well. The plate was left on ice for 20min, and subsequently cells were scraped. Supernatants were collected prior to assay. The Bradford assay solution was diluted with double distilled H₂O in 1:4 ratios. Standard dilutions from 2 to 0.0625mg/ml were prepared from 2mg/ml BSA solution. 2µl of each sample, standard dilutions and a no protein diluent were added in a clear 96-well plate in duplicates followed by 190µl diluted Bradford

assay solution. Optical density (OD) was measured using a microplate reader at 595/600nm after 5-10min of incubation at room temperature. The total protein concentration was determined based on the standard absorbance curve.

2.2.10 Enzyme-linked immunosorbant assay (ELISA) for CXCL8

CXCL8 release was measured using human CXCL8/IL8 Duoset (R&D Systems, Inc). Briefly, a 96-well microplate for ELSA was coated with 100µl per well of capture antibody (4µg/ml) in PBS and incubated overnight at room temperature. The plate was washed with Wash Buffer (Tween 20 and PBS) 400µl/well three times in an autowasher and blotted to discard any remaining Wash Buffer. Block buffer, (200µl/well, 1% BSA in PBS and 0.05% NaN₃) was added and incubated on a platform shaker at room temperature for 1h. Block buffer was removed and the plate was washed three times with Wash Buffer as described above. The plate was kept moistened. Recombinant human IL-8 was diluted in diluent in 2-fold serial dilutions to achieve concentrations from 2,000 to 31.25pg/ml including a zero (control) blank. Samples were diluted to obtain readings within the linear part of the concentration response curve. Standards were added in duplicate and diluted samples were added in triplicates (100µl/well). The plate was covered with adhesive strip and incubated at room temperature for 2h before washing three times with Wash Buffer. Detection Antibody, (biotinylated goat anti-human IL-8) was diluted in diluent to 20ng/ml and added to the microplate 100 µl/well and incubated for further 2h at room temperature. The microplate was washed three times and 100µl of the working solution of Streptavidin-HRP (1:40) was added to each well and further incubated for 20min in the dark at room temperature followed by three washes. Substrate solution prepared using 1:1 mixture of colour reagent A (H₂O₂) and B

(tetramethylbenzidine) from TMB Substrate Reagent Set was added (100µl/well) and incubated for 5-10min until a blue colour was detected in the wells containing the highest concentration of standard. Colour development was stopped by adding 50µl of stop solution (2N H₂SO₄), plate was gently tapped to mix all solution and the OD immediately determined using spectrophotometer at 540nm (correction mode). A standard curve was created using Microsoft Excel software. The concentrations of the samples were calculated from the standard curve. The actual concentrations of samples were finally corrected using a dilution factor. The reagents used in CXCL8 ELISA are shown in Table 2.14.

Table 2.14 Reagents used in CXCL8 ELISA

WASH BUFFER	BLOCK BUFFER	REAGENT DILUENT
PBS containing 0.05% Tween 20 [®]	1% BSA in PBS with 0.05% NaN ₃	0.1% BSA, 0.05% Tween 20 [®] in Tris-Buffered saline (20mM Tris base and 5M NaCl, pH 7.2-7.4)

2.2.11 Immunohistochemistry (IHC)

Lung tissues were fixed with 10% formalin solution for 24-48h and embedded in paraffin blocks using an automated tissue processor, then cut at 3µm thickness and mounted onto positively charged adhesion slides. Automated staining was performed by the Ventana Benchmark Ultra platform using an IHC slide staining system as follows; 3µm sections were deparaffinised for 8min at 60°C using EZ-Prep Solution. Then a pre-treatment step to allow antibody to access and bind a specific antigen in tissue sample, antigen retrieval, was performed using Cell Conditioning Solution (Ventana[®]) followed by incubation with the primary antibody (Table 2.15). Next endogenous peroxidase activity was blocked with

peroxidase Inhibitor (3%) for 8min. Antibody detection was performed using a detection kit (OptiView DAB IHC Detection Kit) which comprises a specific secondary antibody bound to an enzyme-labelled tertiary antibody. This antibody complex was visualized using H₂O₂ as a substrate and 3,3'-diaminobenzidine tetrahydrochloride (DAB) chromogen which produces a brown precipitate after adding copper sulphate (5g/l) and counterstained with Hematoxylin II for 8min and Bluing Reagent for 12min. All steps in the protocol were separated by rinsing with Reaction Buffer to remove unbound substance. Each slide was subsequently removed from the immunostainer and manually dehydrated through five solvent steps for 2min with gently shaking at each step as follows: 70% / 90% / 100% IMS (Industrial Methylated Spirit), and 100% / 100% xylene, and finally addition of a coverslip as indicated in the Manufacturer's standard protocol.

Table 2.15 Details of mitochondrial protein antibody used in IHC

ANTIBODY	NDUFA9
MANUFACTURER	Abcam, UK
SPECIES/CLONE/PRODUCT CODE	Rabbit/Monoclonal (20C11B11B11)/ab14713
ANTIGEN RETRIEVAL REAGENT	Ventana Cell Conditioning 1 with pH 8.5
DURATION OF ANTIGEN RETRIEVAL	64min at 100°C
ANTIBODY DILUTION FACTOR	1:30
PRIMARY ANTIBODY INCUBATION PERIOD	at 37°C for 72min

2.2.12 Transmission electron microscopy (TEM)

The standard TEM was used to visualise different cellular organelles in lung tissue samples especially mitochondria morphology. The tissue sample processing was performed by Andrew Rogers, a technician, and the TEM imaging was done at the histopathology service, Royal Brompton Hospital. The study was carried out with the approval of the Health Research Authority, South Central – Hampshire B Research Ethics Committee (REC Reference 15/SC/0569). Lung tissue samples consisted of tumour tissue and normal adjacent tissue collected during lung resection operations from a non-smoker, a healthy smoker and a COPD patient with lung adenocarcinoma (3 patients, 6 samples in total). Lung tissues were snap-frozen immediately to preserve organelle structures in cells. The snap-frozen tissue was fixed in 3% paraformaldehyde, 0.1M sucrose and 3% glutaraldehyde in 0.1M sodium cacodylate buffer at 5°C for at least 1h. The fixed tissue was completely dehydrated with 25, 50, 75 and 100% ethanol and embedded in Epoxy resin. Each sample block of embedded sample was cut into semi-thin sections (1-1.5µm thickness) and stained with 1% toluidine blue while the tissue slide was on a hot plate. The stain was allowed to remain on the tissue slide for a short time, but not to dry completely, and was then washed away with water. The semi-thin sections from the blocks were examined under light microscopy to select blocks containing mitochondria. The selected blocks were cut into ultra-thin sections (80-120nm thickness) and picked up on the TEM copper grids (300mesh). The sections were finally stained with uranyl acetate and lead citrate before visualisation. The sections were observed in a JEOL 2000 transmission electron microscope operated at an accelerating voltage of 200kV to increase contrast from

cell organelles. One block per sample was examined to look for mitochondria in alveolar macrophage, alveolar type II epithelium, bronchial epithelium and tumour epithelium. The images were captured using the AMT capture software.

2.2.13 Fluorescence intensity measurement of mitochondrial function parameters

Mitochondrial function parameters were measured using a fluorescence approach on a flow cytometer. BEAS-2B, A549 and NHBE cells were seeded at 0.25×10^6 cells/well in 24-well plates. The used solvent and concentrations of fluorescence dyes is shown in Table 2.16.

2.2.13.1 Mitochondrial membrane potential ($\Delta\Psi_m$) measurement

Mitochondrial membrane potential was assessed using the J-aggregate-forming cationic dye, JC-1. JC-1 monomers diffuse into the cytoplasm of cells and give a green fluorescence. When JC-1 monomers enter functional mitochondria they form aggregates which give a red fluorescent signal. Fluorescence intensity was detected with excitation wavelength of 514nm and emission wavelength of 529nm for green fluorescence and 590nm for red fluorescence.

After stimulation, cells were washed with HBSS, trypsinized and placed in microtubes and centrifugated at 1,200rpm for 3min. Cell pellets were resuspended in HBSS, and JC-1 added into each sample at a working concentration of 2 μ M and incubated at 37°C for 30min in the dark. Cells were then centrifuged at 2,000rpm for 5min, resuspended in HBSS and transferred to FACS tubes. The flow cytometer was set to collect at least 10,000 events/sample. An unstained, untreated control was gated using light scattered from the cells measured fluorescence emission by

side scatter (SSC) and forward scatter (FSC) and were plotted as a scatter plot to fix area of the most cells. The unstained untreated sample was used for gating a typical cell area and a stained untreated sample was used as a control. Fluorescence intensity was measured and analysed as the geometric mean in the phycoerythrin (PE) (red) and FITC (green) channels. $\Delta\Psi_m$ was derived from the ratio of red to green fluorescence.

2.2.13.2 Mitochondrial superoxide (mROS) detection

Mitochondrial ROS was assessed using MitoSOX™ Red (MitoSOX), a fluorogenic dye for highly selective detection of superoxide in the mitochondria. MitoSOX is able to permeate live cells. Owing to its cationic property, MitoSOX enters the mitochondria where it is oxidized specifically by mitochondrial superoxide. Oxidised MitoSOX produces a red fluorescence wavelength (~580nm) enabling detection of mitochondrial superoxide activity. Cells were incubated with MitoSOX at a working concentration of 2.5 μ M in HBSS with 140mg/L CaCl₂ and 100mg/L MgCl₂ (HBSS, Ca, Mg) at 37°C for 30min before stimulating the cells to allow the dye to enter the mitochondria of live cells.

Cells were washed with HBSS, trypsinized and centrifuged; the unstained untreated sample and a stained untreated sample were prepared for gating as mentioned previously in section 2.2.13.1. The flow cytometer was set to collect at least 10,000 events/sample. Fluorescence intensity was measured with 510nm for excitation wavelength and 580nm for emission wavelength and analysed as the geometric mean in the PE (red) channel. The geometric mean of fluorescence intensity was measured in each sample compared to control.

2.2.13.3 Intracellular reactive oxygen species (ROS) detection

Intracellular ROS was measured using 2',7'-dichlorodihydrofluorescein diacetate (DCFH-DA). DCFH-DA is converted to DCFH by a cellular esterase, which in turn reacts with ROS such as H₂O₂, resulting in a deacetylated, oxidized DCF molecule which is fluorescent with excitation wavelength of 492-495nm and emission wavelength of 517-527nm.

Cells were pre-incubated with DCFH-DA at a working concentration of 5µM for 30min before treatment. Then the cells were washed with HBSS, trypsinized and centrifuged; the unstained untreated sample and a stained untreated sample were prepared for gating as mentioned previously in section 2.2.13.1. Resuspended cells in HBSS were transferred to FACS tubes. The flow cytometer was set to collect at least 10,000 events/sample. The fluorescence intensity was measured using the FITC (green) channel. The geometric mean of fluorescence intensity was measured compared to control.

Table 2.16 Fluorescence dye concentrations

FLUORESCENCE DYES	SOLVENT /REQUIRED CONCENTRATION	STOCK CONCENTRATION	WORKING CONCENTRATION
JC-1	DMSO/ 200µM	-	2µM
MitoSOX	DMSO/ 5mM	50µM in HBSS with Ca ⁺⁺ and Mg ⁺⁺	2.5µM
DCF	DMSO/ 10mM	100µM in HBSS	5µM
Propidium Iodide	DMSO/ 1mg/ml	100µg/ml	40µg/ml

2.2.14 Extracellular flux analysis (MitoStress test)

Cell metabolism in live cells and real time can be assessed by monitoring oxygen consumption rate (OCR) using Seahorse extracellular flux (XF) analyser. Seahorse XF Cell Mito Stress Test Kit, a test to assess mitochondrial function, contains

pre-measured compounds which damage parts of the electron transport chain in mitochondria. The compounds comprise oligomycin (ATP synthase inhibitor), FCCP (carbonyl cyanide-4-(trifluoromethoxyphenylhydrazine)) (proton uncoupler), antimycin A (complex III inhibitor) and rotenone (complex I inhibitor). Protocol for OCR measurement by Seahorse XF analyser is shown below,

Day 1: Cell preparation

An XFe 96 cell culture microplate was coated with 30µg/ml collagen type I. BEAS-2B, NHBE and A549 cells were plated onto the microplate with supplemented Airway Epithelial Cell Medium 80µl/well and allowed to grow in a 37°C, 5%CO₂ incubator for 24h.

Day 2: Preparation of Sensor cartridge and cell starvation

An XFe96 sensor cartridge was hydrated overnight by submerging the sensors in an XF 96-well plate filled with XF calibrant solution at 37°C without CO₂. The cells were starved overnight by replacing the supplemented media with the Airway Epithelial Cell Basal Medium.

Day 3: Seahorse Analysis

Before starting the cell-treatment experiments, cell density was optimized to be able to detect oxygen consumption rate (OCR) and extracellular acidification rate (ECAR) sufficiently. Cell numbers were seeded as follows; BEAS-2B (2-6 x 10⁴/well), A549 and NHBE (1.5-4.5 x10⁴/well). Once the optimal cell density was selected, these were used for all subsequent basal and stimulated cell experiments.

Mitochondrial respiration was measured using the Seahorse XFe96 flux analyzer. On the day of experiment, cells were pre-treated with antioxidants (10mM NAC, 100µM mitoTEMPO, 500µM SS31, 10µM AP39 and 10µM AP219) for 1h, and

subsequently, treated with 100 μ M H₂O₂ for 4h. The treating media was removed but 20 μ l media was left in the well. The cells were then rinsed twice with 200 μ l XF assay medium supplemented with 10mM glucose, 1mM sodium pyruvate and 2mM L-glutamine. Next, the cells were incubated in 175 μ l XF assay medium in a non-CO₂ incubator (Seahorse XF96 Prepstation), for 45min - 1h before analysis. At the same time, compounds for loading in the sensor cartridge were prepared using a constant loading volume. Stock compounds of 100 μ M oligomycin, 100 μ M FCCP and 50 μ M rotenone/antimycin A were prepared in XF assay media. With a constant well volume of 175 μ l, 25 μ l of each stock compound was added into each injection port of the cartridge for each well to give final concentrations of 1 μ M oligomycin (Port A), 1.5 μ M FCCP (Port B) and 0.9 μ M rotenone/antimycin A (Port C). Compound concentration and volume preparation is shown in Table 2.17. The sensor cartridge was then calibrated for 15-30min on the instrument tray. After measurement of ECAR and OCR basal rates, oligomycin, FCCP, and rotenone/antimycin A were sequentially injected from the sensor cartridge ports at 14, 34 and 54min, respectively. Rates were normalized to protein content, quantified using the Bradford assay (Section 2.2.9). Mitochondrial respiration parameters including non-mitochondrial respiration, basal respiration, ATP production, maximal respiration, mitochondrial reserve capacity and proton leak are automatically calculated based on the normalised protein, followed rate measurement equations (Table 2.18) using Seahorse XF Cell Mito Stress Test Report Generator.

Table 2.17 Compound concentration for loading sensor cartridge ports of XFe96

CONSTANT VOLUME APPROACH			
Starting well volume: 175 µl assay medium			
Injection port	Stock concentration (µM)	Port concentration (µM)	Add to port volume (µl)
A (Oligomycin)	100	1	25
B (FCCP)	100	1.5	25
C (Rotenone/antimycin A)	50	0.9	25

Table 2.18 Mitochondrial respiration parameter equations

PARAMETER	RATE MEASUREMENT EQUATION
Non-Mitochondrial Respiration	Minimum rate measurement after Rotenone/antimycin A injection
Basal respiration	(Last rate measurement before 1 st injection)-(Non-Mitochondrial Respiration rate)
ATP production	(Last rate measurement before Oligomycin injection)-(Minimum rate measurement after Oligomycin injection)
Maximal Respiration	(Maximum rate measurement after FCCP injection)-(Non-Mitochondrial Respiration)
Mitochondrial Reserve Capacity	(Maximal Respiration)-(Basal Respiration)
Proton Leak	(Minimum rate measurement after Oligomycin injection)-(Non-Mitochondrial Respiration)

2.2.15 Isolation of mitochondria from lung tissue

Mitochondria were isolated using traditional dounce homogenisation for tissue disruption followed by using reagents from the mitochondrial isolation kit for tissue and centrifugation to pellet the purified mitochondria. Briefly, approximately 50mg lung tissue was diced into small pieces. Cells were disrupted using a rough dounce homogeniser, having a loose pestle “A”, in Reagent A Solution containing 4mg/ml BSA followed by homogenization in a fine dounce homogeniser, having a tight pestle “B”. The ruptured cells were transferred to a 2ml tube and

Reagent C Solution was added and the tube inverted several times. All steps were performed on ice. To obtain the mitochondrial fraction, the homogenised sample was centrifuged at 2,500rpm for 10min at 4°C. The supernatant was collected and transferred to another tube. Next, the supernatant was centrifuged at 10,500rpm for 5min at 4°C. The obtained pellet was kept as the mitochondrial fraction and the supernatant was discarded. The pellet was dissolved in 50-100µl HBSS, Ca, Mg solution and stored at -80°C until used.

2.2.16 Detection of mitochondrial membrane potential and mitochondrial ROS in isolated mitochondria

Protein concentration was measured in each sample using Bradford assay (section 2.2.9). Equal amounts of isolated mitochondrial proteins were used for comparisons between each sample. The total volume of saline solution and isolated mitochondria was standardised to 100µl. HBSS, Ca, Mg solution was added in a black 96-well plate for JC-1 and MitoSOX staining respectively. 30µg of isolated mitochondrial proteins were added to each well. JC-1 and MitoSOX dyes were added at 2 and 5µM final concentration, respectively. The plate was incubated in 5% CO₂ at 37°C for 30min before measuring fluorescence intensity using a microplate reader. Fluorescence intensity for JC-1 was measured with 2 sets of excitation wavelengths (530/25, 485/20nm) and emission wavelengths (590/35, 528/20nm) respectively with the 45% sensitivity of detection. For MitoSOX fluorescence intensity measurement, the excitation and emission wavelengths were set at 485/20 and 528/20nm respectively with the 45% sensitivity of detection.

2.2.17 Gene set variation analysis (GSVA)

Gene array data, from published datasets, were screened and selected in relation to COPD and lung cancer. A set of genes called a signature was used to analyse the gene array data from each sample. Enrichment scores (ES) were calculated using GSVA, regardless of group labels. Then I compared the ES of the gene signature among the groups. The details of the gene signatures used are shown in Chapter 5.

2.2.18 Statistical analysis

The data is presented as the mean \pm standard error of mean (SEM) for *in vitro* experiments ($n \geq 3$) and the mean \pm standard deviation (SD) for clinical samples. Statistical analysis was performed using GraphPad Prism[®]. Results from repeated experiments were analysed using repeated measure one-way analysis of variance (ANOVA) (parametric) and post hoc multiple comparisons tests to compare the means of treated groups with the mean of a control when data were normally distributed or Friedman test (non-parametric) and a Dunn's post-test to compare the mean rank of treated groups with the mean rank of a control when data were not normally distributed to compare data from different time points and different concentrations. Comparison of data from three different cell types was analysed using one-way ANOVA and a Tukey's multiple comparisons post-test when data were normally distributed or by using a Kruskal-Wallis test and a Dunn's multiple comparisons post-test when data were not normally distributed. Comparison of data from background tissue and tumour tissue samples was analysed using Wilcoxon matched-pairs signed rank test (non-parametric) for matched samples comparison and, Mann-Whitney U test (non-parametric) for average score comparison.

Comparison of data from non-smokers, smokers and patients with COPD groups using ANOVA, Kruskal-Wallis test (non-parametric) and Dunn's post-test. A statistically significant difference was considered when p value < 0.05 . In the GSVA analysis, one-way ANOVA was used to compare the ES differences among group means and Tukey's test was used for post-hoc analysis.

**Chapter 3 Effect of H₂O₂ and
pro-inflammatory cytokine (IL-1 β)
on mitochondrial function and
cell inflammation, proliferation and
apoptosis in a bronchial epithelial
cell line**

3.1 Introduction

The relationship between COPD and lung cancer was proposed after a 10-year follow-up study showed a higher rate of lung cancer in COPD patients compared to non-COPD patients (Skillrud, Offord, & Miller, 1986). Since then more studies have confirmed this higher incidence of lung cancer in patients with COPD which ranged from 0.64 to 16.7 cases per 1,000 person-years (Celli et al., 2009; De Torres et al., 2011; Smith, Smith, Hurria, Hortobagyi, & Buchholz, 2009). Overall, the data suggests that smokers who have impaired lung function are more at risk of developing lung cancer compared to those with normal lung function (Mannino, Aguayo, Petty, & Redd, 2003; Skillrud et al., 1986; van den Eeden & Friedman, 1992). The most common lung cancer type found in COPD patients is NSCLC which originates in the airway epithelium in areas highly exposed to cigarette smoke (Kadara, Scheet, Wistuba, & Spira, 2016; Mahmood et al., 2017; Sucony & Janes, 2014).

Exogenous reactive oxygen species (ROS) from long-term cigarette smoke exposure are a major driver of COPD pathology (Kirkham & Barnes, 2013). Increased ROS levels have also been reported in many cancers where they cause DNA mutations as well as mediate signalling pathways involved in carcinogenesis (Durham & Adcock, 2015; Goldkorn, Filosto, & Chung, 2014).

ROS impacts on chronic inflammation in COPD by increasing inflammatory gene expression and activating signal transduction pathways which can result in further inflammatory cell recruitment into the lungs (Domej, Oettl, & Renner, 2014). Airway epithelial cells exposed to exogenous ROS can enhance inflammatory gene expression such as *IL-8* in alveolar and bronchial epithelial cell lines (Lakshminarayanan, Drab-

Weiss, & Roebuck, 1998). In addition, cigarette smoke extract or H₂O₂ treatment, as models of oxidative stress, induce inflammatory mediator production such as IL-1 β , IL-6, CXCL-8 from airway epithelial cells (Hoffmann et al., 2013; Khan et al., 2014).

An imbalance between apoptosis and cell proliferation is observed in COPD. Studies have demonstrated that alveolar epithelial cells, endothelial cells, inflammatory cells and skeletal muscle cells in patients with COPD undergo excessive apoptosis (Agustí et al., 2002; Hodge et al., 2005; Kasahara et al., 2001; Yokohori, Aoshiba, & Nagai, 2004). Furthermore, the proliferation of primary bronchial epithelial cells and lung fibroblasts is decreased when exposed to cigarette smoke (Miglino et al., 2012; Perotin et al., 2014). In contrast, airway smooth muscle cells (ASM) from patients with COPD demonstrate increased proliferation when treated with TGF- β suggesting that inflammation promotes hypertrophy/hyperplasia in COPD (Perry, Baker, & Chung, 2011). Together this indicates that both ROS and chronic inflammation in COPD can affect cellular apoptosis and proliferation (Barnes, 2016).

Mitochondria are crucial for energy production in the cell. They also control the balance between oxidants and antioxidants, producing mitochondrial ROS (mROS), consisting of O₂⁻ and H₂O₂ (Sabharwal & Schumacker, 2014). mROS are known to regulate cell signalling and metabolic homeostasis (Sena & Chandel, 2012; Starkov, 2008). Measurements of mROS production are used to assess mitochondrial function as well as mitochondrial membrane potential ($\Delta\Psi_m$) and cell respiration dependent upon experimental setting and physiological interests (Brand & Nicholls, 2011).

Mitochondrial dysfunction plays an important role in the pathogenesis of many diseases such as cancers (Boland et al., 2013) and chronic lung disease such as COPD

(Aravamudan et al., 2013; Cloonan & Choi, 2016). Excessive ROS production in patients with COPD caused mitochondrial dysfunction in airway smooth muscle cells including decreased $\Delta\Psi$ and mROS accumulation which contributed to inflammatory mediator expression and increased cell proliferation (Wiegman et al., 2015).

The antioxidant response system protects cells from damage and is triggered by oxidants themselves (Espinosa-Diez et al., 2015). A reduction in antioxidant capacity has been reported in COPD patients and in people who smoke (Tavilani et al., 2012). Glutathione (GSH), a cellular antioxidant, highly expressed by the airway epithelium and its homeostasis may have a role in the maintenance of the airway epithelial barrier (Rahman, 2008). N-acetylcysteine (NAC), the precursor of GSH, has been used to treat COPD patients to enhance lung GSH levels which were found to be decreased during exacerbations (Drost et al., 2005). *In vitro* studies indicate that NAC prevents the release of inflammatory mediators such as CXCL8 by TNF- α - and IL-1 β -stimulated endothelial cells (EVC-304) and by bronchial epithelial cells (H292) (Radomska-Leśniewska et al., 2006) and inhibited IL-8 expression induced by particulate matter with a diameter $\leq 2.5\mu\text{m}$ (PM_{2.5}) in bronchial epithelial cells (BEAS-2B) and in the human macrophage-like cell line (THP-1) (Yan et al., 2016).

When mitochondria are dysfunctional, ROS elimination becomes inefficient leading to the accumulation of mROS. Mitochondrial targeted antioxidants have been investigated as a proposed novel approach in many diseases (Apostolova & Victor, 2015; Jin et al., 2014; Kezic, Spasojevic, Lezaic, & Bajcetic, 2016). Mitochondrial targeted antioxidants reduce oxidative stress-induced inflammation and mitochondrial dysfunction in human airway smooth muscle cells (ASM) and murine lungs and decrease TGF- β -induced ASM

proliferation (Wiegman et al., 2015). Decreased mROS production and lung fibrosis were demonstrated in mitoTEMPO pre-treated allergic 'asthmatic' mice and in human airway epithelial cells (Jaffer et al., 2015).

Previous studies have indicated an effect of ROS on mitochondrial function and inflammation in various cell types *in vivo*. The effect of ROS on mitochondrial function in bronchial epithelial cells needs investigation since these cells are likely drivers of remodelling in the context of COPD and COPD-lung cancer. The effect of mitochondrial-targeted antioxidants as a therapeutic strategy in this setting also needs to be explored. Mitochondrial-targeted antioxidants have shown therapeutic potential in preclinical and clinical settings in the fields of cardiovascular disease and neurological disorders (Apostolova & Victor, 2015; Jin et al., 2014). However, the effect of mitochondrial targeted antioxidants on mitochondrial dysfunction and inflammation found in COPD has not been examined.

In this chapter, a bronchial epithelial cell line is used to investigate the effect of oxidative stress (H_2O_2) and inflammation ($IL-1\beta$) on mitochondrial function and cell inflammation, proliferation and apoptosis. The effect of various antioxidants on these variables will also be investigated.

3.2 Hypothesis

Reactive oxygen species will alter mitochondrial function in BEAS-2B cells which will be restored by pre-treating with antioxidants. Antioxidants will also reduce IL-1 β -stimulated inflammation and proliferation in BEAS-2B cells and decrease apoptosis in H₂O₂-stimulated BEAS-2Bs

3.3 Aims

- To investigate the effects of H₂O₂ on mitochondrial function, cell inflammation, proliferation and apoptosis in a bronchial epithelial cell line (BEAS-2B)
- To investigate the effect of antioxidants on H₂O₂ induced mitochondrial changes in BEAS-2B cells
- To investigate the effect of antioxidants on H₂O₂ and IL-1 β stimulated inflammation, proliferation and apoptosis in BEAS-2B cells

3.4 Results

3.4.1 Cell viability (Mitochondrial activity) in H₂O₂ treated BEAS-2B cells

BEAS-2B cell viability was measured using MTT assay which can also be used to assess mitochondrial activity. BEAS-2B cells were treated with 100 and 200 μ M H₂O₂ for 0-24h. Cell viability at 1, 3 and 4h of 100 μ M H₂O₂ treated groups was significantly lower compared to their control ($p < 0.05$). The viability of cells following 0.5 and 2h of 200 μ M H₂O₂ treatment was also significantly reduced ($p < 0.05$). The viability of 0.5 and 24h H₂O₂ (200 μ M)-exposed cells were significantly lower than 100 μ M H₂O₂ exposed cells ($p < 0.05$) (Figure 3.1).

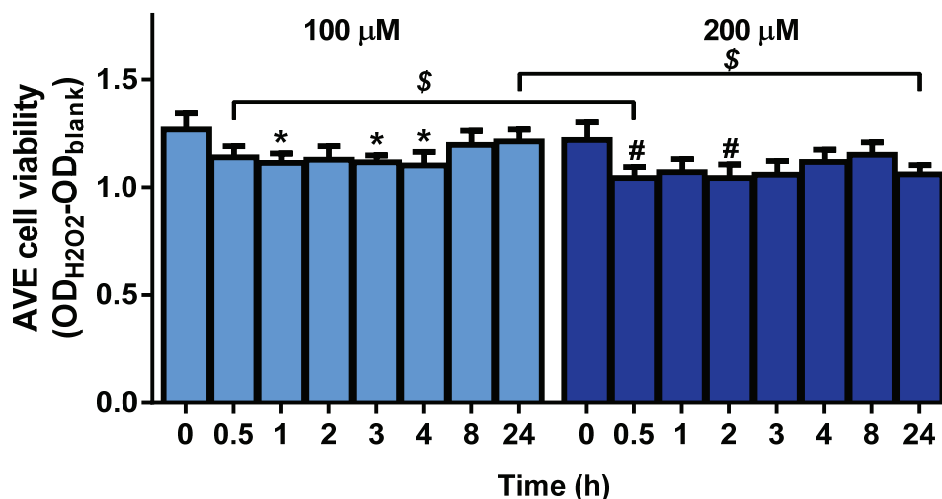


Figure 3.1 Effect of H₂O₂ on BEAS-2B cell viability (mitochondrial activity)

BEAS-2B cells (1.5×10^5 cells/well) were incubated with 100 or 200 μ M H₂O₂ for 0–24h. Cell viability (mitochondrial activity) was measured using MTT assay. Optical density (OD) was detected using spectrophotometer and cell viability (mitochondrial activity). Results are presented as the mean \pm S.E.M as average of OD_{H₂O₂} – OD_{blank} of four independent experiments. Statistical analysis was performed using repeated measures one-way ANOVA with a Bonferroni's multiple comparisons test to compare within the 100 μ M H₂O₂ group and 200 μ M H₂O₂ groups and using a paired t-test to compare results at each time point between these concentrations. * $p < 0.05$ vs control (0h-100 μ M H₂O₂ group), # $p < 0.05$ vs control (0h-200 μ M H₂O₂ group) and \$ $p < 0.05$.

Stimulation of BEAS-2B cells with 100 or 200 μ M H₂O₂ caused significant effect on cell viability at some timepoints. However, since the cell viability of all treated groups

was between 80-90% compared to control, these concentrations were therefore used for the remaining experiments.

3.4.2 Effect of H₂O₂ on mitochondrial superoxide levels in BEAS-2B cells

Mitochondrial superoxide production was measured using MitoSOX™ fluorescence staining. BEAS-2B cells were pre-incubated with 2.5µM MitoSOX™ at 37°C for 30min followed by treatment with different concentrations of H₂O₂ (50-400µM) for 2 and 4h.

In initial experiments a spectrofluorometer was used to measure the fluorescence but no differences in fluorescence intensity could be determined. Therefore, a flow cytometer was used as it is a more sensitive method.

The cell gating strategy using the flow cytometer was based on size and granularity (Figure 3.2A-F upper panels) and the subsequent histogram plots are based on red fluorescence (PE channel) (Figure 3.2A-F lower panels).

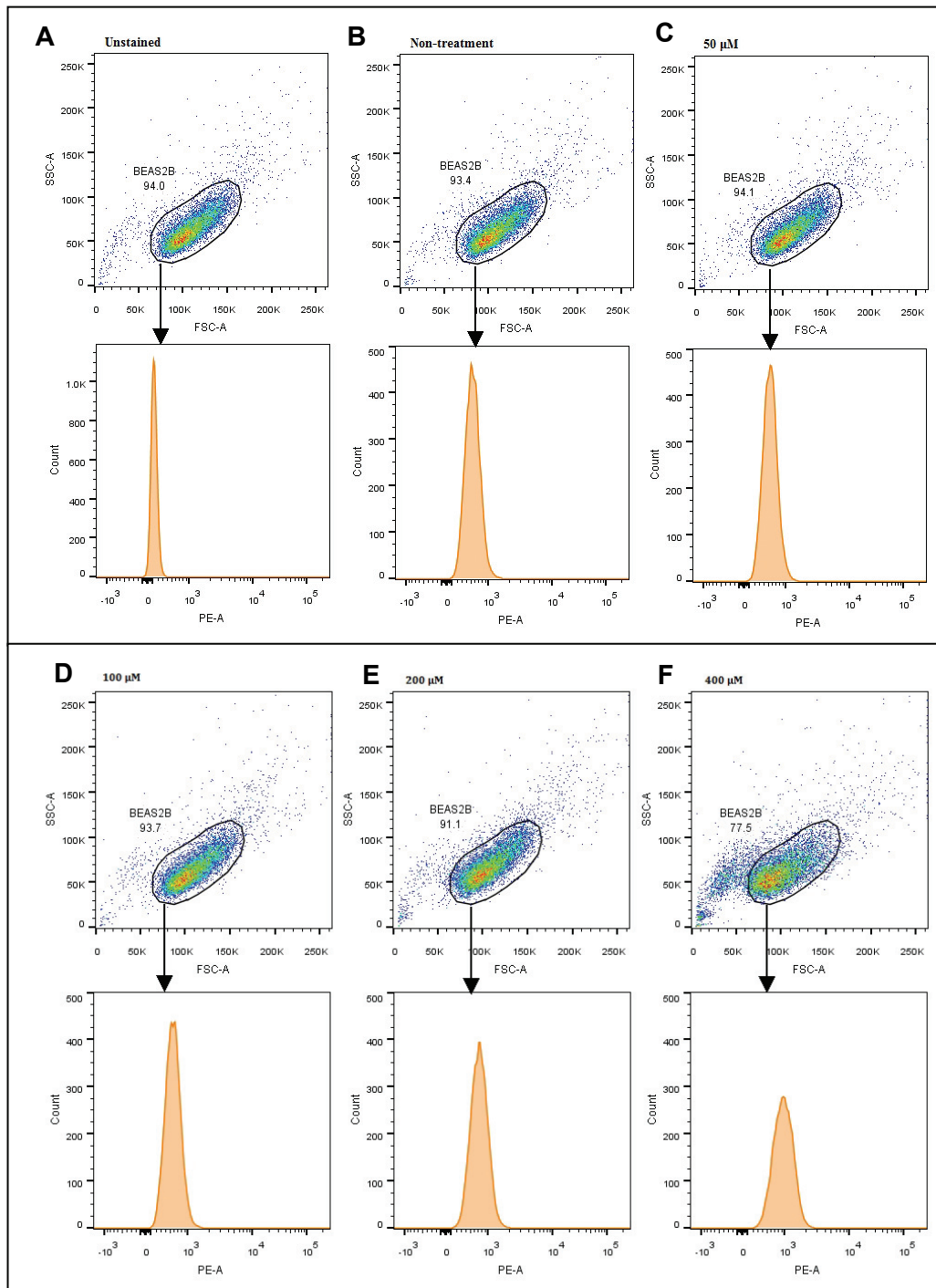


Figure 3.2 Gating strategy used for measuring mitochondrial superoxide in BEAS-2B cells
 An example of gated plot was from an experiment which BEAS-2B cells were treated with 0-400 μ M H₂O₂ for 2h (B-F). First, single normal cells were gated in unstained untreated sample based on forward scatter/ side scatter (FSC/SSC) (A), the gated area was fixed when running samples (circle, top panel). Normal sized cells in the gated area in each sample were then plotted as histograms based on MitoSOX™ PE: red (bottom panel). The geometric mean of red fluorescence intensity was used for comparison.

The mean fluorescence intensity (MFI) of each sample was analysed using histograms with an unstained sample used as a negative control (Figure 3.3).

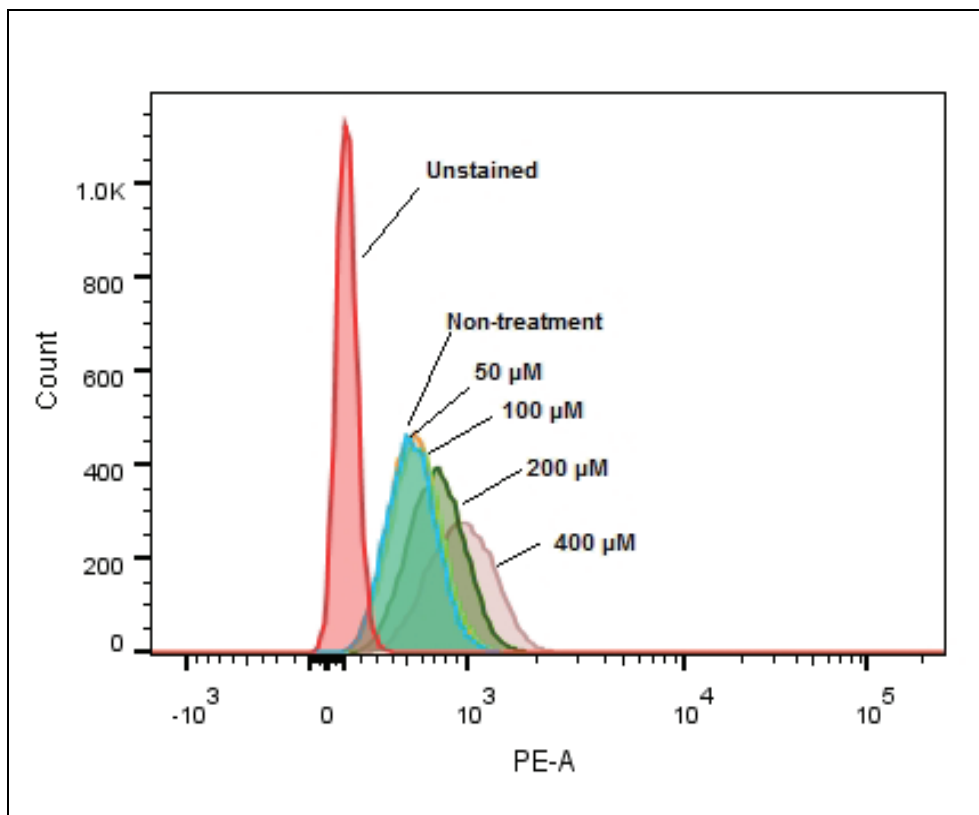


Figure 3.3 Overlay histogram of MitoSOX™ fluorescence intensity

An example of histograms from an experiment of 2-h H_2O_2 treated BEAS-2B in different concentrations. BEAS-2B cells were pre-incubated with MitoSOX™ (2.5 μ M) at 37°C for 30min prior to treatment with H_2O_2 . The histogram presents the number of gated cells (Y axis) and the fluorescence intensity (PE-A) (X axis). The mean fluorescence intensity (MFI) of H_2O_2 treated samples were compared with untreated sample. The higher fluorescence intensity was detected when the cells were treated with higher H_2O_2 concentration.

BEAS-2B cells were pre-incubated with a final concentration of 2.5 μ M MitoSOX™ for 30min before treatment with different concentrations of H_2O_2 (50-400 μ M) for 2 and 4h. The average of mean fluorescence intensity (MFI) of mitochondrial superoxide had a trend towards a decrease at 50 μ M H_2O_2 at 2h (Figure 3.4) which may be due to response of the mitochondria to compensate for oxidative stress stimulation. The average MFI was increased at 200 and 400 μ M H_2O_2 treatment at both 2 and 4h. The cells treated with 400 μ M H_2O_2 for 2h and 4h had a significantly higher MFI

compared to their controls ($p < 0.01$ and $p < 10^{-4}$, respectively). However, at $400 \mu\text{M}$ H_2O_2 , a lower percentage of gated cells (77.5%) (Figure 3.2F) was seen compared to those (>90%) at other H_2O_2 concentrations which may be due to cell death.

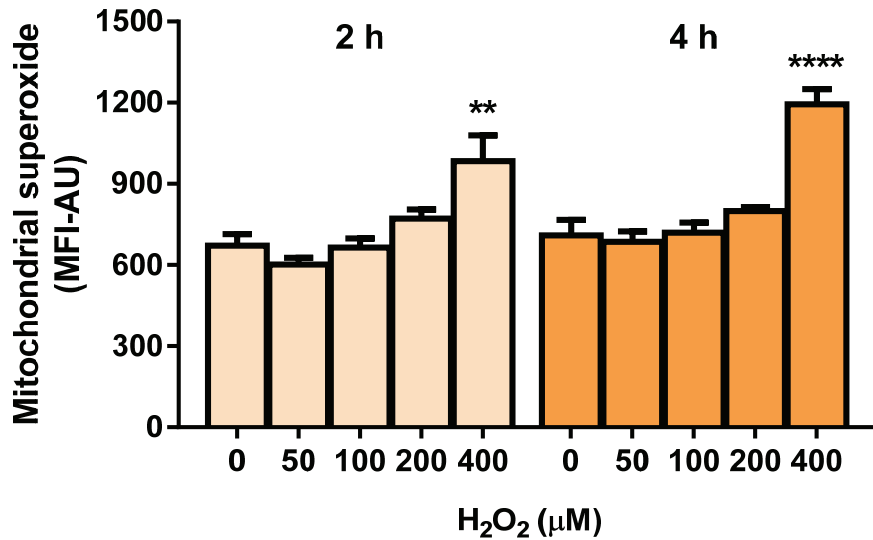


Figure 3.4 Effect of H_2O_2 on mitochondrial superoxide production in BEAS-2B cells

Cells were treated with 0-400 μM H_2O_2 for 2 and 4h after pre-incubation with MitoSOXTM dye (2.5 μM). Results are presented as the mean \pm S.E.M of the average of the mean fluorescence intensity-arbitrary unit (MFI-AU) of three independent experiments. Statistical analysis was performed using repeated measures one-way ANOVA with a Dunnett's multiple comparisons test to compare within the 2-h treated group and the 4-h treated group and using paired *t*-tests to compare each concentration at the two time points. ** $p < 0.01$ vs control (2-h treated group) and **** $p < 10^{-4}$ vs control (4-h treated group).

From these experiments, H_2O_2 at $200 \mu\text{M}$ increased mitochondrial superoxide production of BEAS-2Bs at 2h and 4h without killing the cells.

3.4.3 Effect of H₂O₂ on intracellular reactive oxygen species in BEAS-2B cells

To investigate whether H₂O₂ concentrations alter the production of intracellular reactive oxygen species (ROS), BEAS-2B cells were treated with different concentrations of H₂O₂ (50-400μM) for 2 and 4h. DCFH-DA was used for the detection of ROS.

Using the spectrofluorometer I was unable to differentiate the fluorescence intensity among different H₂O₂ concentrations, so I used the more sensitive flow cytometry method.

The cells were pre-incubated with 5μM DCFH-DA at 37°C for 30min followed by treatment with different concentrations of H₂O₂ for 2 and 4h. The cell gating strategy was based on size and granularity (Figure 3.5A-F upper panels) and the subsequent histogram plots are based on green fluorescence (Figure 3.5A-F, lower panels).

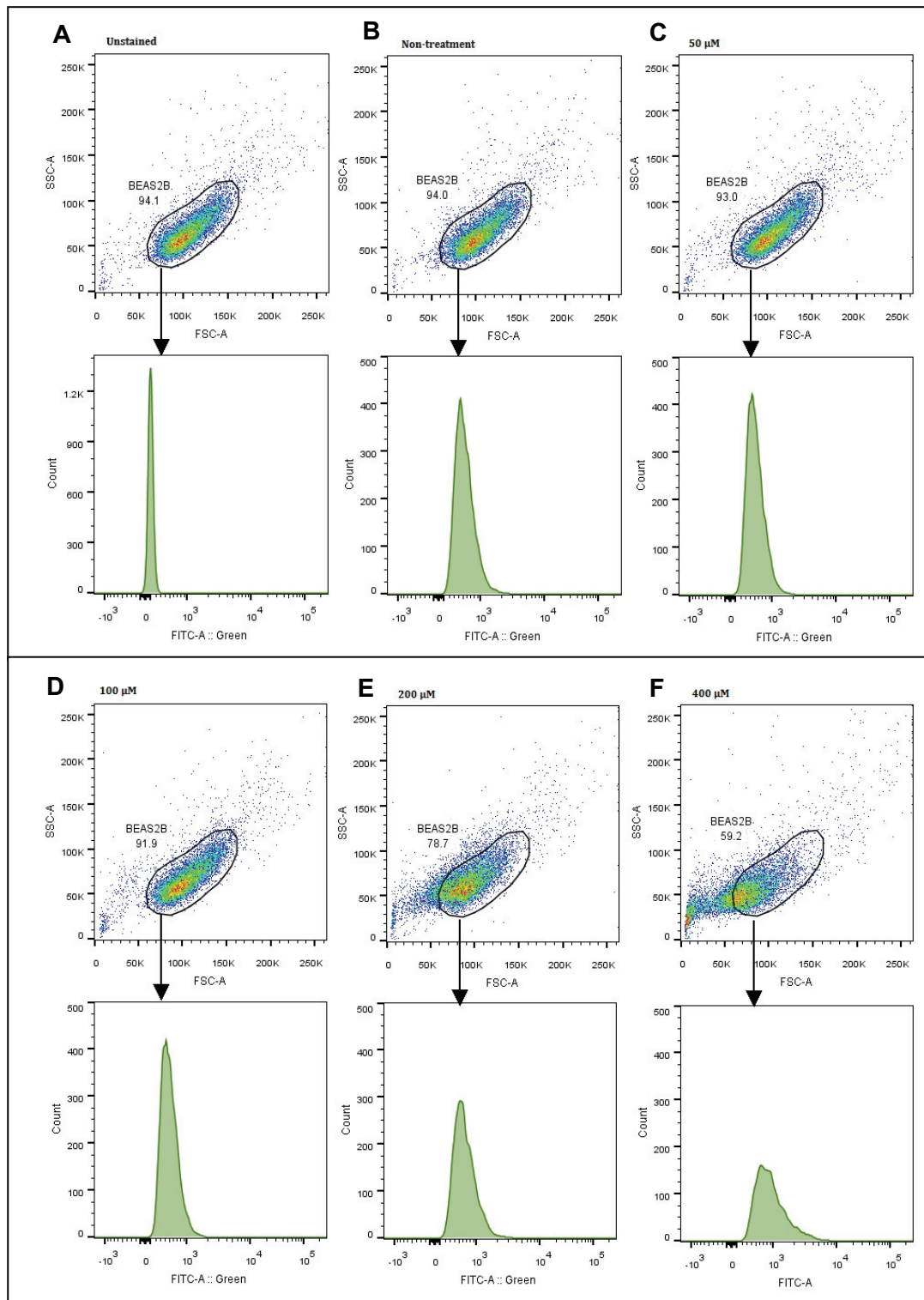


Figure 3.5 Gating strategy for the detection of intracellular ROS in BEAS-2B cells
 An example of gated plots was from an experiment which BEAS-2B cells were treated with 0-400 μ M H₂O₂ for 2h (B-F). Cells were gated on unstained untreated samples based on forward scatter/side scatter (FSC/SSC) (A) and the gated area fixed for comparison with treated samples (circle, top panel). Cells in the gated area in each sample were then plotted as histograms based on DCF FITC (green channel) (bottom panel). The geometric mean of green fluorescence intensity was used for comparison.

The MFI from histograms of green fluorescence intensity was used for sample comparisons (Figure 3.6).

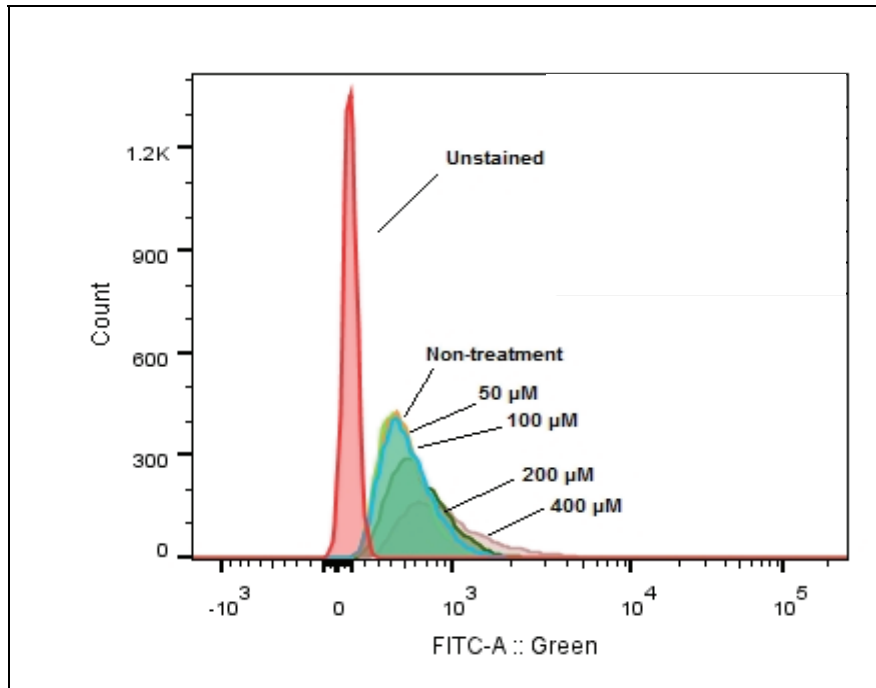


Figure 3.6 Overlay histogram of the effect of H_2O_2 on DCFH-DA fluorescence intensity

An example of histograms from an experiment of 2h H_2O_2 -treated BEAS-2B in different concentrations. BEAS-2B cells were pre-incubated with DCFH-DA at $37^\circ C$ for 30min. The histogram presents the number of gated cells (Y axis) and the fluorescence intensity (FITC-A) (X axis). The mean fluorescence intensity (MFI) of H_2O_2 treated samples were with untreated sample. The histogram of the group treated with higher H_2O_2 concentration was shifted to the right which represented higher fluorescence intensity (higher ROS) was detected.

There was a trend towards an increase in intracellular ROS production in BEAS-2B cells when treated with 400 μ M H₂O₂ for 2h or 200 and 400 μ M H₂O₂ for 4h (Figure 3.7). However, the percentage of gated cells in the high H₂O₂ samples was below 60% (example in Figure 3.5F) due to cell death, therefore, the 400 μ M H₂O₂ would not be used in further experiments.

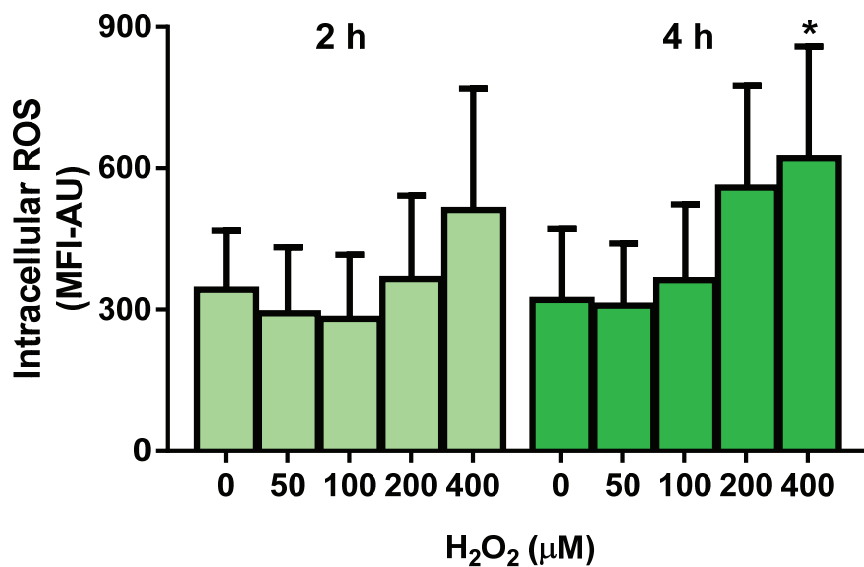


Figure 3.7 Effect of H₂O₂ on intracellular ROS levels in BEAS-2B cells

BEAS-2B cells were pre-incubated with DCFH-DA at 37°C for 30min followed by treatment with different concentrations of H₂O₂ for 2 and 4h. Green fluorescence intensity was measured using flow cytometer. Results are presented as the mean \pm S.E.M of the average mean fluorescence intensity-arbitrary units (MFI-AU) of three independent experiments. Statistical analysis was performed using Friedman's test with a Dunn's multiple comparisons post-test to compare within the 2-h treated group and 4-h treated groups and using the Wilcoxon's test to compare each concentration at the two time points. * p <0.05 vs control (4-h treated group).

These experiments show that 4h H₂O₂ at 200 μ M increased intracellular ROS production of BEAS-2Bs without killing cells.

3.4.4 Effect of H₂O₂ on mitochondrial membrane potential ($\Delta\Psi_m$) in BEAS-2B cells

BEAS-2B cells were exposed to different concentrations of H₂O₂ (50-400 μ M) for 2 and 4h. The measurement of $\Delta\Psi_m$ was performed initially using a spectrofluorometer. However, similar to the results for mROS and intracellular ROS, the measured fluorescence values did not vary among different conditions. Therefore, fluorescence detection using a flow cytometer was used for subsequent analysis.

The cell gating strategy was based on size and granularity and the subsequent plots based on red and green fluorescence (Figure 3.8 upper and lower panels respectively). An unstained untreated BEAS-2B cell sample (negative control) was used as a gating control which obtained more than 90% of the collected cell events. For the positive control, cells were treated with a mitochondrial membrane potential disruptor, CCCP (50 μ M final concentration), for 5-10min before staining. $\Delta\Psi_m$ was calculated from the ratio of red and green fluorescence and normalised by comparing fold change for each sample to the control.

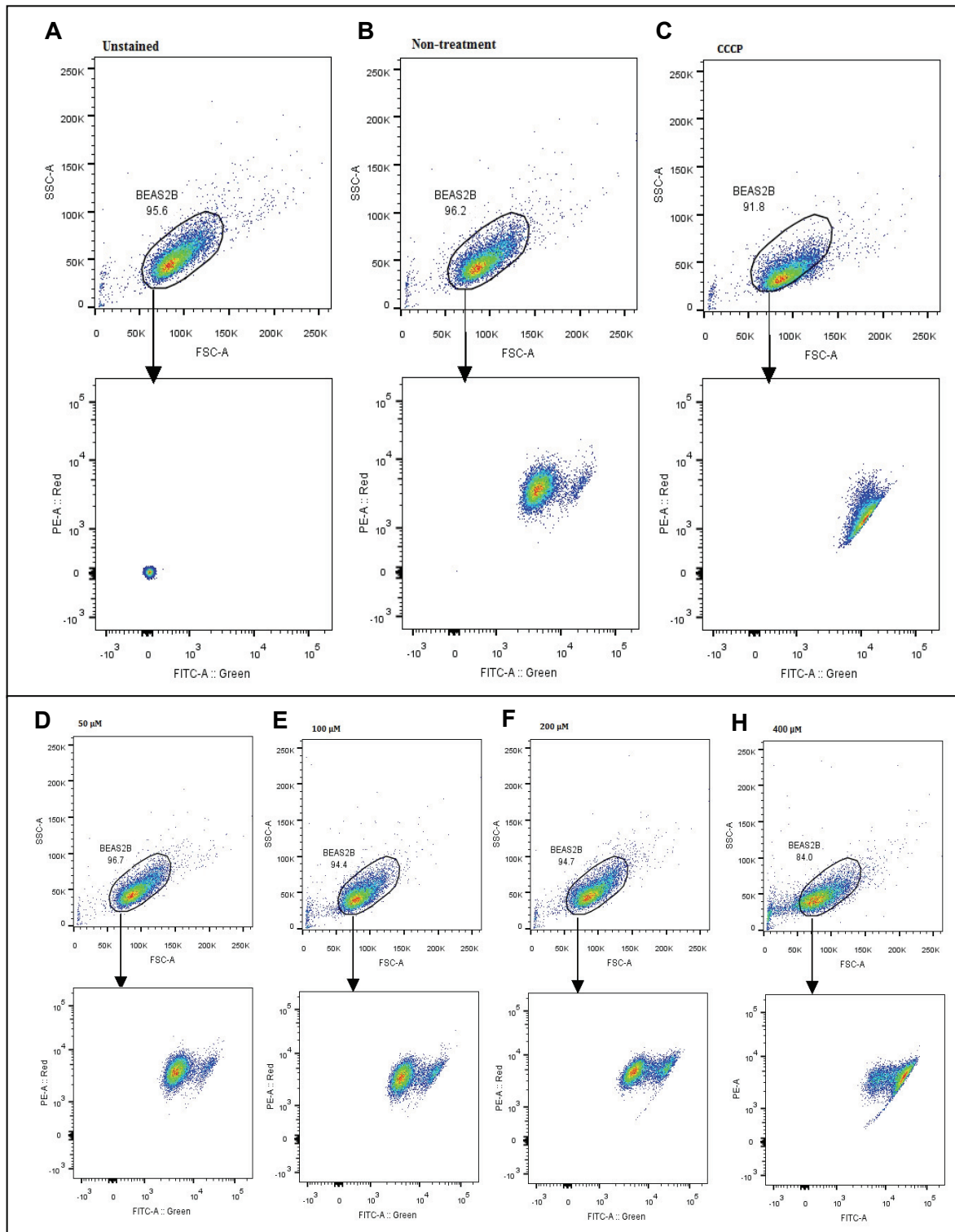


Figure 3.8 Gating strategy for BEAS-2B cells for measuring mitochondrial membrane potential
 An example of gated plots was from an experiment which BEAS-2B cells were treated with 0-400 μM H_2O_2 for 2h (B, D-H) and with 50 μM CCCP as positive control (C). Single normal cells were gated based on forward scatter/side scatter (FSC/SSC) of a negative control (unstained untreated sample (A)) and the gated area was fixed for running other samples (circle, top panel). Normal sized cells in the gated area were then plotted based on FITC green (JC-1 monomer)/PE red (JC-1 aggregates) (bottom panel). The geometric mean of green and red fluorescence intensity was used to calculate the red/green fluorescence ratio.

BEAS-2B cells treated with 50 and 100 μ M H₂O₂ for 2 or 4h showed very little change in $\Delta\Psi_m$. When cells were exposed to 200 μ M a trend towards a decrease in $\Delta\Psi_m$ was seen at 2h and 4h compared to the control which significantly decreased further with 400 μ M H₂O₂ at both 2h and 4h ($p < 10^{-3}$ and $p < 10^{-4}$, respectively) (Figure 3.9). This decrease in the $\Delta\Psi_m$ with 400 μ M H₂O₂ is probably due to cell death. The low $\Delta\Psi_m$ in CCCP treated cells (positive control) confirmed that the JC-1 used for the experiments was effective.

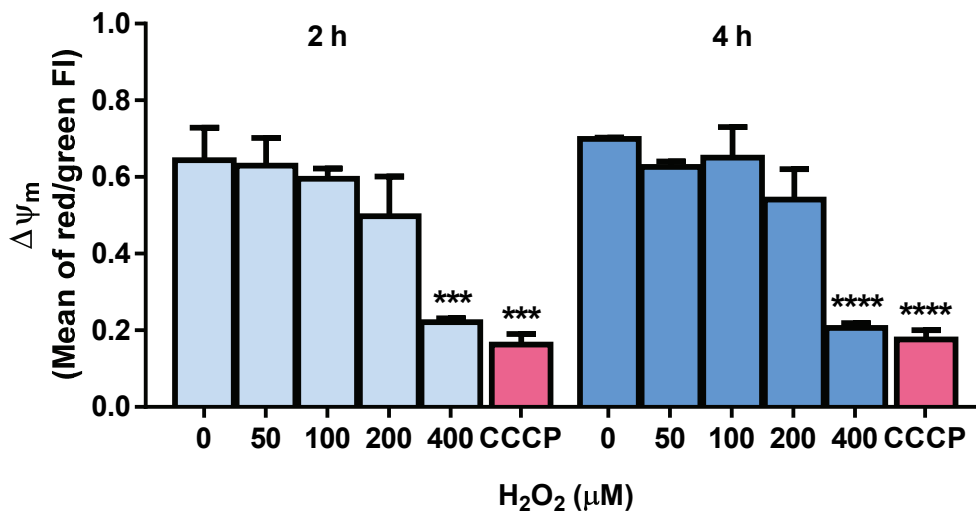


Figure 3.9 Effect of H₂O₂ on mitochondrial membrane potential of BEAS-2B cells

BEAS-2B cells were exposed to different H₂O₂ concentrations for 2 and 4h followed by JC-1 fluorescence staining and then trypsinised and prepared for measuring fluorescence intensity using flow cytometer. 50 μ M CCCP was used for the positive control (pink bar). $\Delta\Psi_m$ was calculated from means of the ratio of red and green fluorescence intensity. Results are presented as the mean \pm S.E.M of the average $\Delta\Psi_m$ from three independent experiments. Statistical analysis was performed using a repeated measures one-way ANOVA with a Dunnett's multiple comparisons test to compare within the 2-h and 4-h treated groups and using paired *t*-tests to compare each concentration at the two time points studied. *** $p < 10^{-3}$ vs control (2-h treated group) and **** $p < 10^{-4}$ vs control (4-h treated group).

From the experiments, 200 μ M H₂O₂ caused a small decrease (24 \pm 6% and 22 \pm 11% for 2h and 4h treatment respectively) in mitochondrial membrane potential of viable BEAS-2B compared to controls.

3.4.5 Effect of H₂O₂ stimulation on BEAS-2B cell apoptosis

It is well established that oxidative stress is one of the main drivers of cell death in COPD pathophysiology and that cigarette smoke exposure damages the lung epithelium and causes apoptosis (Baglolle et al., 2006; Demedts, Demoor, Bracke, Joos, & Brusselle, 2006; Goldkorn et al., 2014). In this section, experiments were performed to confirm that oxidative stress can cause apoptosis and to examine whether this was the cause of cell death observed with 400µM H₂O₂.

Apoptosis was determined by flow cytometry using an Annexin V and PI apoptosis kit, scatter plots were separated into four areas: live cells (Annexin-V⁻ PI⁻), early apoptotic cells (Annexin-V⁺ PI⁻), late apoptotic cells (Annexin-V⁺ PI⁺) and dead cells (Annexin-V⁻ PI⁺) as previously mentioned in section 2.2.4 (Figure 3.10). However, as PI stained positive in both late apoptotic and dead cells, they were counted as the same group. The scatter plots in Figure 3.10 are representatives of gate setting experiments. The live cell area was first set by selecting whole population of non-treated samples located in the left lower quadrant as shown in (Figure 3.10A). Next, the live cell area and dead cell areas were separated using an untreated sample and a heat-killed sample stained with PI alone. Most of the population of untreated samples (95.8%) (Figure 3.10B) were located in the same area as those in Figure 3.10A. Heating the samples for 5min at 70°C confirmed the efficacy of the method as 96.9% of heat-killed sample population was in left upper quadrant (Figure 3.10C).

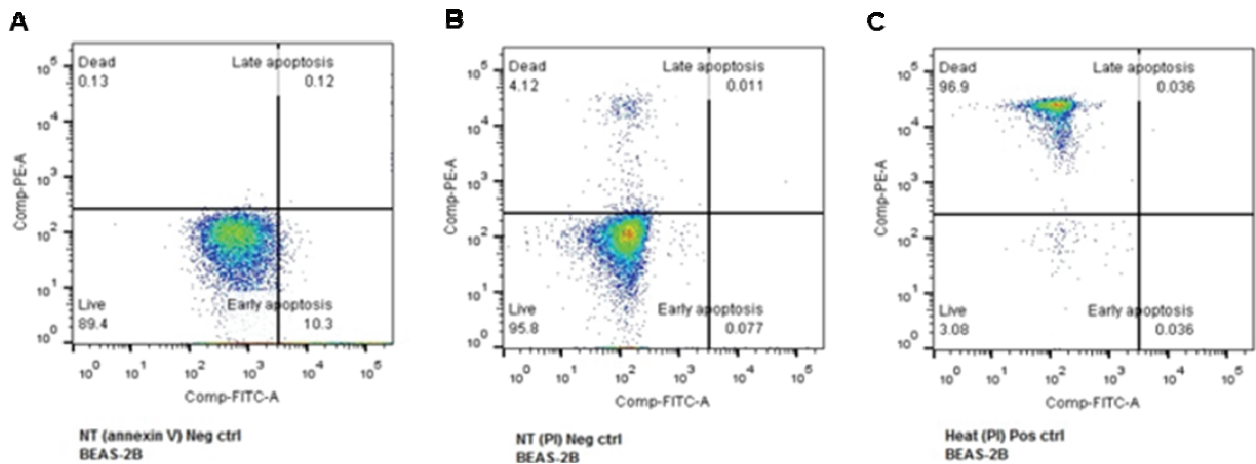


Figure 3.10 Gating strategy for detection of apoptosis in BEAS-2B cells.

To set the areas for live cells (left lower area), early apoptotic cells (right lower area), late apoptotic cells (right upper area) and dead cells (left upper area) in scatter plots, non-treated sample as negative control (A) was stained with Annexin V alone. An untreated sample as a negative control (B) and a heat-killed sample as a positive control (C) were stained with PI alone to separate live cells from dead cells. Treated samples were stained with both Annexin V and PI.

Previous studies have shown that H₂O₂ (250µM for 30min) can induce apoptosis in lung epithelial cells (BEAS-2B cell line) (Kazzaz et al., 1996) and increase DNA damage which resulted in apoptosis (Nanavaty et al., 2002). Therefore, I used a high concentration of H₂O₂ (400µM) for 30min to induce apoptosis in BEAS-2B as this concentration caused an increase in both mitochondrial superoxide and intracellular ROS and a decrease in mitochondrial membrane potential and this was associated with increased cell death.

BEAS-2B cells were gated by the population of untreated sample located in left lower area (Figure 3.11A). Approximately 62% of the gated population of 400µM H₂O₂-treated samples were in the upper quadrant and right lower quadrant (Figure 3.11B).

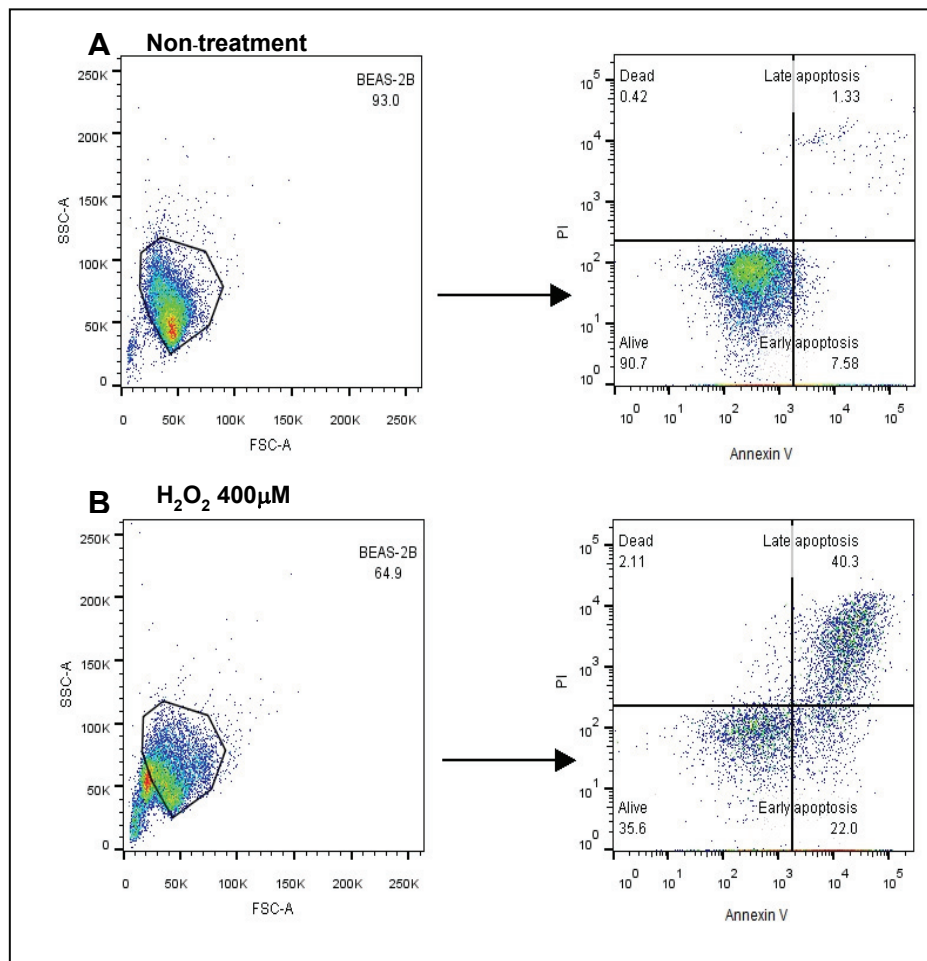


Figure 3.11 Gating strategy for detection of apoptosis in BEAS-2B cells using a high H_2O_2 concentration

First, untreated cells were gated based on forward scatter/side scatter (FSC/SSC) (A) and the gated area selected for analysis of treated samples (circle), $400\mu M H_2O_2$ -treated sample (B), for example. Normal sized cells in the gated area in each sample were then subsequently gated based on fluorescence intensity of Annexin V and PI and grouped as percentage of live cells (Annexin V⁻ PI⁻), early apoptotic cells (Annexin V⁺ PI⁻), late apoptotic cells (Annexin V⁺ PI⁺) and dead cells (Annexin V⁻ PI⁺).

The percentage of labelled cells compared between the untreated group (control) and $400\mu M H_2O_2$ treated group are presented as a bar graph (Figure 3.12). $400\mu M H_2O_2$ significantly ($p < 0.05$) decreased the percentage of live cells ($46 \pm 12\%$) compared to control ($91 \pm 0.4\%$) and increased the percentage of early apoptotic cells ($13 \pm 5\%$) compared to the control group ($7 \pm 0.5\%$). There was a significantly ($p < 0.05$) higher

percentage of late apoptotic/dead cells when treated with 400 μ M H₂O₂ (28 \pm 6%) compared to the untreated control cells (2 \pm 0.2%).

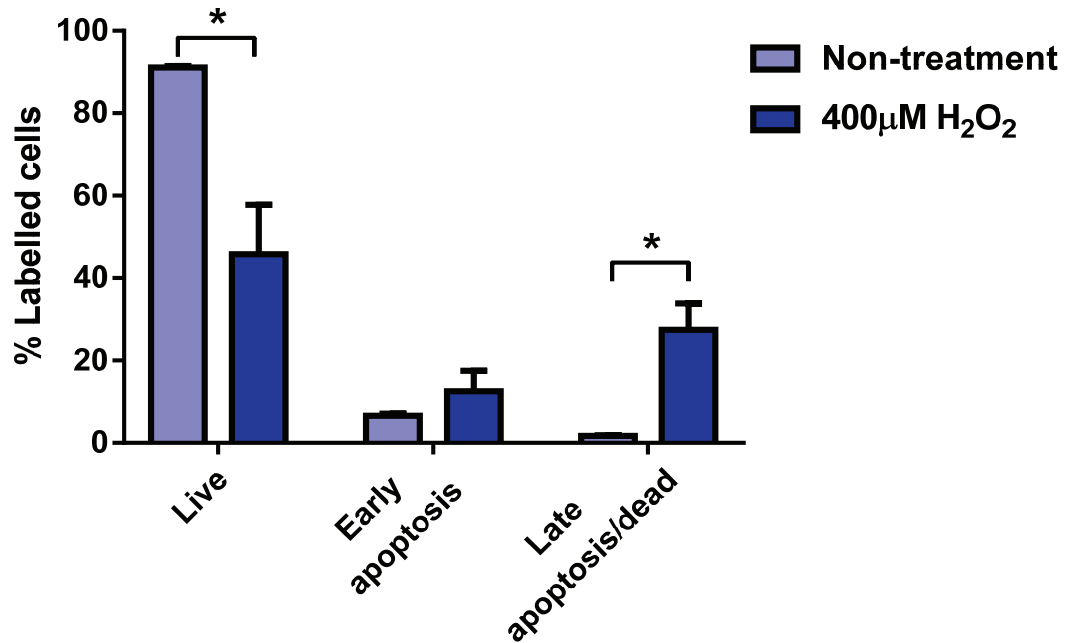


Figure 3.12 Effect of 400 μ M H₂O₂ on apoptosis in BEAS-2B cells

BEAS-2B cells were exposed to 400 μ M H₂O₂ for 30min. Live cells, early apoptotic cells and late apoptotic/dead cells were analysed using FITC Annexin V/Dead Cell Apoptosis kit for flow cytometer. Percentage of live cells, early apoptotic cells and late apoptotic/dead cells from non-treated and 400 μ M H₂O₂ treated groups are presented in light and dark blue bars, respectively. Results are presented as the mean \pm S.E.M of data from three independent experiments. Statistical analysis was performed using a multiple t-test to compare between non-treated and H₂O₂ treated groups in each category. * p <0.05.

This result indicates that 400 μ M H₂O₂ caused BEAS-2B cells to undergo apoptosis and/or die. Therefore, this H₂O₂ concentration was used in further apoptosis experiments with antioxidants.

3.4.6 H₂O₂ and IL-1 β stimulated inflammatory cytokine secretion (CXCL8) in BEAS-2B cells

To confirm that stimulation of BEAS-2B cells with H₂O₂ and IL-1 β caused an inflammatory response, BEAS-2B cells were treated with 25-400 μ M H₂O₂ or 0.1-10ng/ml IL-1 β for 24h. The inflammatory cytokine, CXCL8, was measured using a human CXCL8 ELISA. An MTT assay was used to determine cell viability. Stimulation of BEAS-2B cells with H₂O₂ for 24h induced CXCL8 release in a concentration-dependent manner. 200 μ M H₂O₂ significantly increased CXCL8 release compared to the control ($p < 0.01$) groups (Figure 3.13A). However, treatment with 200 and 400 μ M H₂O₂ for 24h caused a significant decrease in BEAS-2B cell viability (Figure 3.13C).

IL-1 β -stimulated BEAS-2B cells released greater amounts of CXCL8 after 24h than cells stimulated with H₂O₂ (Figure 3.13B). CXCL8 release was concentration-dependent with IL-1 β (10ng/ml) significantly ($p < 0.01$) enhancing CXCL8 release compared to control and 0.1ng/ml IL-1 β -treated cells ($p < 0.01$). No decrease in BEAS-2B cell viability was seen with IL-1 β (Figure 3.13D). Therefore, 100 μ M H₂O₂ and a submaximal concentration of IL-1 β (1ng/ml) were used in further experiments to examine the effects of antioxidants on inflammation.

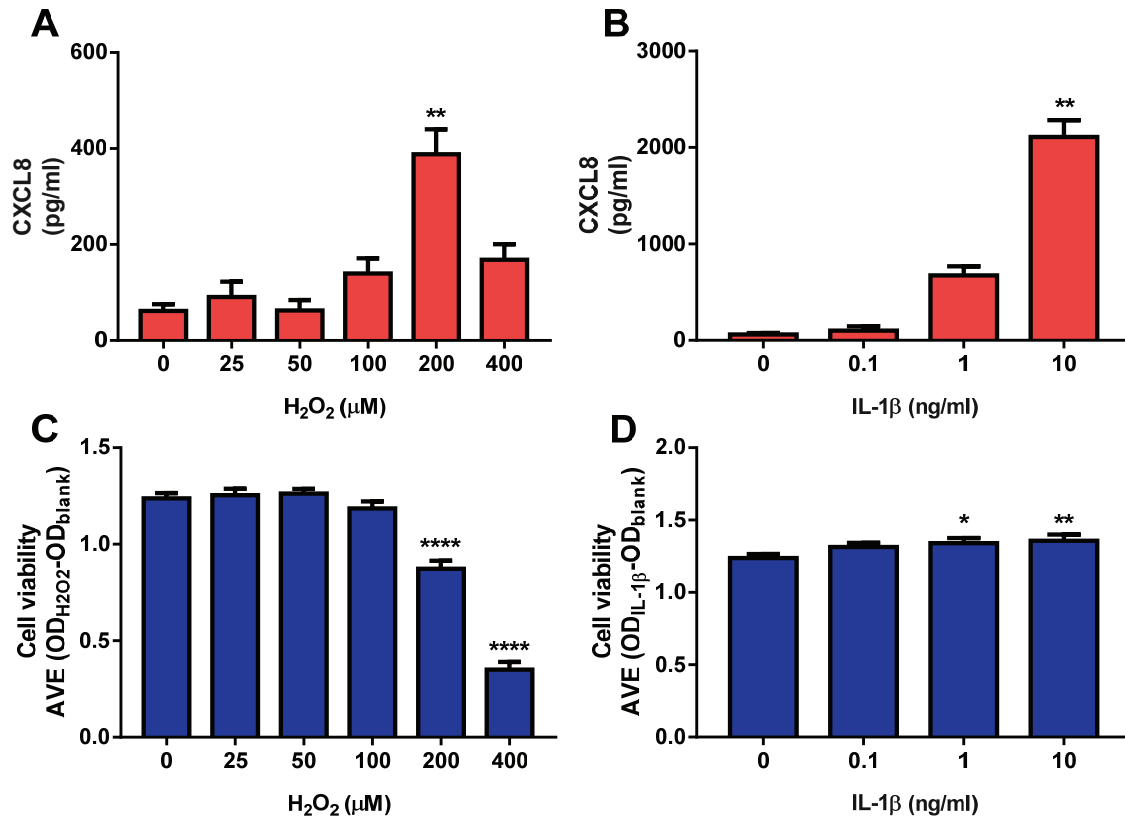


Figure 3.13 CXCL8 release and cell viability from BEAS-2B stimulated with H₂O₂ or IL-1β

BEAS-2B were stimulated with 25-400μM H₂O₂ or 0.1-1.0ng/ml IL-1β. CXCL8 levels and cell viability were measured using ELISA and MTT assay respectively. CXCL8 levels increased in a concentration-dependent manner with both H₂O₂ (A) and IL-1β (B). Cell viability was decreased in the 200 and 400μM H₂O₂ groups (C) but remained over the control in the IL-1β-stimulated group (D) compared to their controls. Results are presented as the mean ± S.E.M of six independent experiments. For CXCL8, statistical analysis was performed using Friedman's test with a Dunn's post-test, and a repeated measures one-way ANOVA with a Dunnett's multiple comparisons test was used for cell viability data analysis. **p*<0.05, ***p*<0.01, *****p*<10⁻⁴.

IL-8 mRNA levels were not analysed as previous data from the group showed that CXCL8 release in BEAS-2B cells correlates with a change in mRNA at earlier time points (2h) (Khan et al., 2014). In summary, both H₂O₂ and IL-1β induced release of CXCL8 in concentration dependent manner in BEAS-2B cells; however, H₂O₂ has lower potency to induce inflammation compared to IL-1β in this cell type.

3.4.7 Effect of H₂O₂ and IL-1 β stimulation on BEAS-2B cell proliferation

We investigated whether H₂O₂ or IL-1 β stimulation could affect BEAS-2B cell proliferation. A previous study showed that 100 μ M H₂O₂ elevated *Wnt4* expression (a gene highly expressed in lung epithelium and is involved in abnormal lung development) which was the driver of proliferation in BEAS-2B cells (Durham et al., 2013). In our experiment, 100 μ M H₂O₂ caused cell death rather than enhanced cell proliferation (Figure 3.14A). As a result, lower concentrations (12.5-50 μ M) of H₂O₂ were used to examine the effect on BEAS-2B cell proliferation. IL-1 β had no effect on BEAS-2B cell proliferation (Figure 3.14B) and 5ng/ml was chosen for use in further experiments.

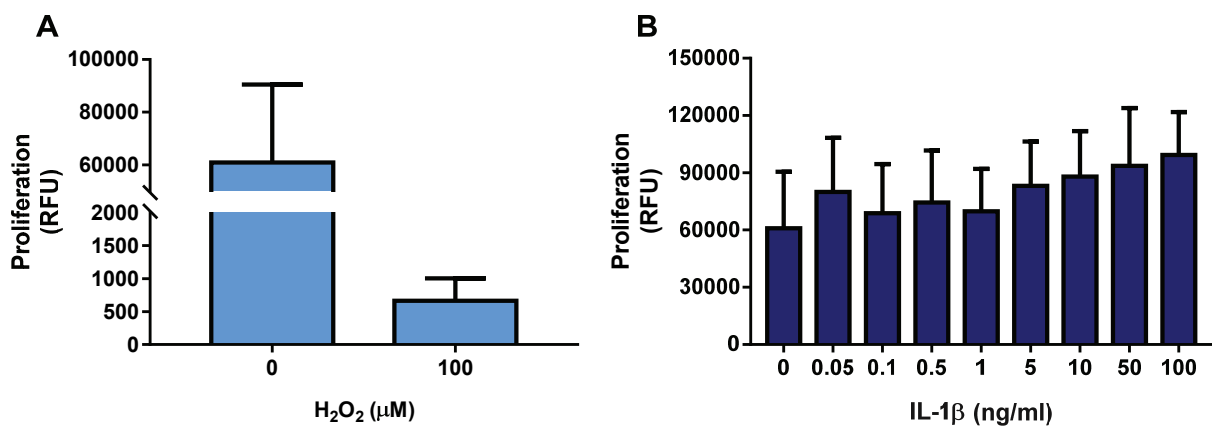


Figure 3.14 Effect of H₂O₂ and IL-1 β on proliferation in BEAS-2B

BEAS-2B cells were incubated with 100 μ M H₂O₂ in serum free media (A) or incubated with 0.05-100ng/ml IL-1 β for 24h (B) followed by BrdU incorporation. Data are presented as the mean \pm S.E.M of relative fluorescence units (RFU) from three independent experiments. Statistical analysis was performed using the Wilcoxon's test for (A) and a repeated measures one-way ANOVA with Dunnett's multiple comparisons test for (B).

Cells were treated with 0-50 μ M H₂O₂ alone for 30min or in combination with 5ng/ml IL-1 β in serum free media for 48h followed by adding BrdU reagent and incubated for a further 24h. There was a significant decrease in BEAS-2B cell proliferation when cells were treated with 50 μ M H₂O₂ compared to untreated cells ($p < 0.01$) (Figure 3.15).

When cells were stimulated with 5ng/ml IL-1 β alone or in combination with H₂O₂ (12.5-25 μ M) an significant increase in BEAS-2B cell proliferation was seen when compared within the same H₂O₂ concentration ($p < 0.05$ and $p < 0.01$) (Figure 3.15). 50 μ M H₂O₂ significantly reduced BEAS-2B cell proliferation when given alone or in combination with IL-1 β ($p < 0.01$). Since H₂O₂ decreased cell proliferation, therefore, 5ng/ml IL-1 β alone was used in further proliferation experiments with antioxidants.

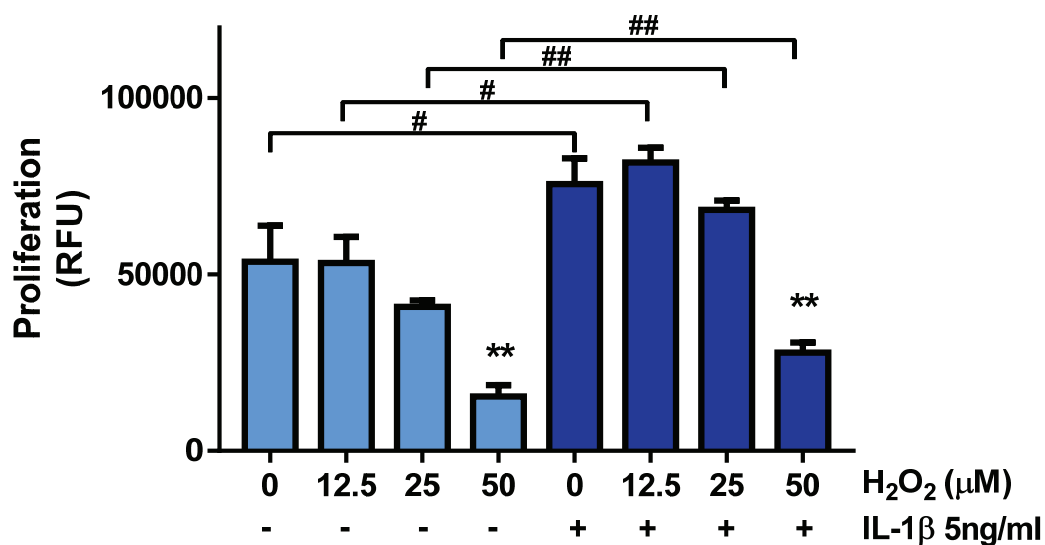


Figure 3.15 Effect of H₂O₂ and IL-1 β stimulation on BEAS-2B cell proliferation

Cells were treated with 0-50 μ M H₂O₂ alone for 30min or in combination with 5ng/ml IL-1 β in serum free media for 48h. Cell proliferation was measured using BrdU assay. Data are presented as the mean \pm S.E.M of relative fluorescence unit (RFU) from three independent experiments. Statistical analysis were performed using a repeated measures one-way ANOVA with a Dunnett's multiple comparisons test to compare within H₂O₂ alone group and H₂O₂+IL-1 β group, and using a paired t-test to compare the same H₂O₂ concentration with and without IL-1 β . ** $p < 0.01$ vs control (H₂O₂ alone group & H₂O₂+IL-1 β group), # $p < 0.05$, ## $p < 0.01$.

In summary, H₂O₂ decreased BEAS-2B cell proliferation whereas IL-1 β increased the proliferation. A high concentration of H₂O₂ (400 μ M) can induce BEAS-2B cell apoptosis whereas at lower H₂O₂ concentrations BEAS-2B cells are viable but their rate of proliferation is decreased compared to untreated cells. In addition, the H₂O₂ repressed the effect of IL-1 β on BEAS-2B proliferation. Furthermore, incubation of

BEAS-2B cells with H₂O₂ caused mitochondrial dysfunction as shown by increases of intracellular ROS, mitochondrial superoxide, a decrease $\Delta\Psi_m$ and induced inflammatory cytokine release (CXCL8).

3.4.8 Optimisation of antioxidant concentrations used in BEAS-2B cells

Since ROS elimination and antioxidant defence systems have been shown to be defective in COPD and lung cancer; focusing on antioxidants is one of the promising treatments for these diseases (Apostolova & Victor, 2015; Domej et al., 2014; Sanguinetti, 2015). I therefore wanted to investigate the effect of antioxidants on these parameters. I chose to use NAC, a precursor for the synthesis of GSH which is important in the elimination of cellular H₂O₂ (Matera et al., 2016), along with other antioxidants that specifically target superoxide within the mitochondria. These were mitoTEMPO, which has a molecular structure which mimics SOD activity by scavenging O₂⁻ (Trnka et al., 2008); SS31 which has an alternating aromatic-cationic structure that allows passage across the cell and mitochondrial membranes, binds to cardiolipin and is concentrated several hundred fold in MIM (Zhao et al., 2004) and AP39 which contains a H₂S donor portion for ROS scavenging whereas AP219 which is the AP39 backbone without the H₂S donor portion which is used as the control compound for AP39 (Karwi et al., 2017; Zhao et al., 2014).

BEAS-2B cells were incubated with different concentrations of antioxidants as follows; 0.1-10mM NAC, 0.1-10 μ M mitoTEMPO, 5-500 μ M SS31, 0.1-10 μ M AP39 and 0.1-10 μ M AP219 for 24h. Stock solution of NAC, mitoTEMPO and SS31 were prepared in HBSS. Lyophilised AP39 and AP219 were first dissolved in DMSO and further diluted in basal media. DMSO final concentration used in the experiments was below 0.5% as

a previous study showed no effect of DMSO on mitochondrial damage and ROS production in BEAS-2B cells (Holme et al., 2014). Cell viability was determined using MTT and trypan blue assays (Figure 3.16). Treatment with NAC (5 and 10mM), mitoTEMPO (5-500 μ M) and AP39 (10 μ M) resulted in significant decreases in BEAS-2B cell viability compared to their control when using MTT assay (Figure 3.16 A, B & E respectively). The loss of cell viability was not seen when using the trypan blue assay (Figure 3.16, lower panel) except with 10 μ M AP39 (Figure 3.16I) suggesting that most of the antioxidants were affecting mitochondrial function rather than cell death per se.

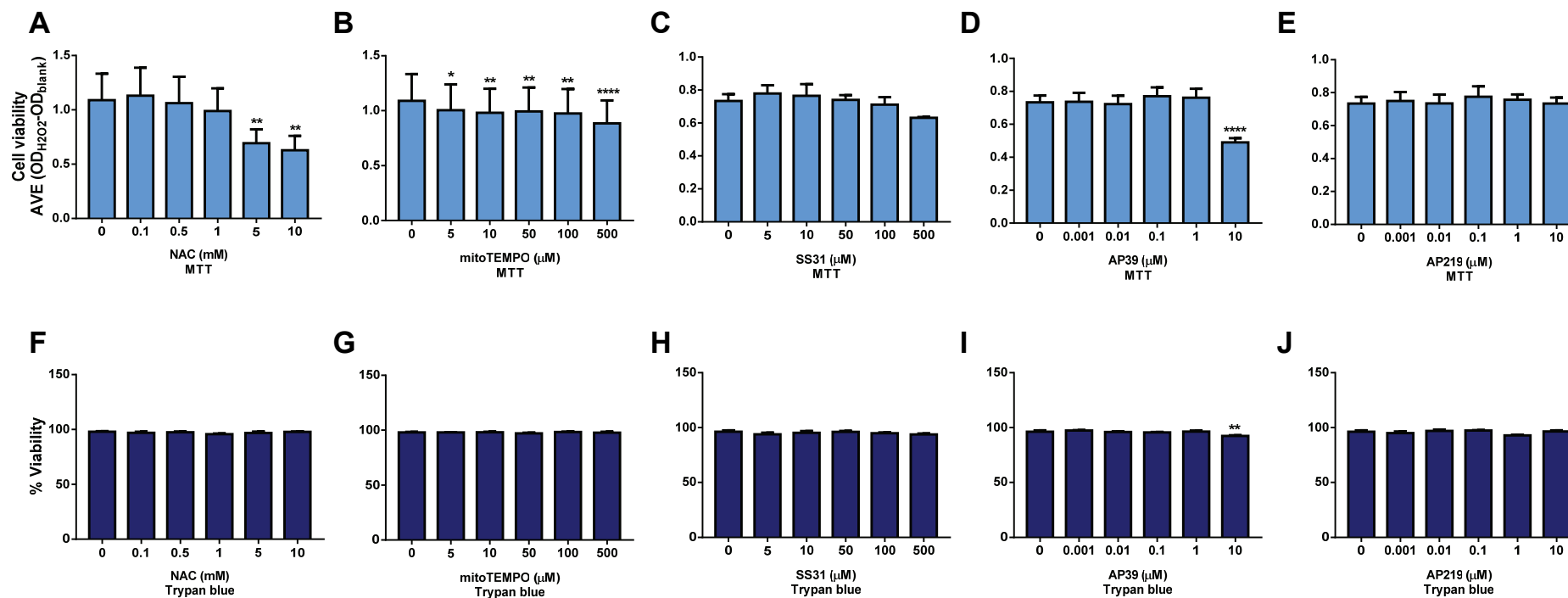


Figure 3.16 Cell viability in NAC, mitoTEMPO, SS31, AP39 and AP219 treated BEAS-2B cells

BEAS-2B cells were treated with different concentrations of NAC, mitoTEMPO, SS31, AP39 and AP219 for 24h. Cell viability was measured using MTT assay (A-E) and trypan blue assay (F-J). Results are presented as the mean \pm S.E.M of three independent experiments. Statistical analysis was performed using a repeated measures one-way ANOVA with Bonferroni's multiple comparisons test. * $p < 0.05$, ** $p < 0.01$ and **** $p < 10^{-4}$ vs control.

Because there were differences in the results obtained using the MTT assay and trypan blue assay, propidium iodide (PI) assay using a flow cytometer was chosen to confirm that the antioxidant-treated cells were viable. BEAS-2B cells were treated with the same concentrations of antioxidants as before for 24h followed by incubation with 1µl of 100µg/ml PI for 10min before measuring MFI (red fluorescence, PE channel) using a flow cytometer with fluorescence excitation/emission set at 535/617nm. Cells previously heated at 70°C for 5min were used as a positive control. The percentage of cell viability was measured and compared to the untreated cell sample (Figure 3.17). Heat killed cells showed only 10±5% viability but there was no change in cell viability among different concentrations of antioxidants compared to their controls except 10µM AP39.

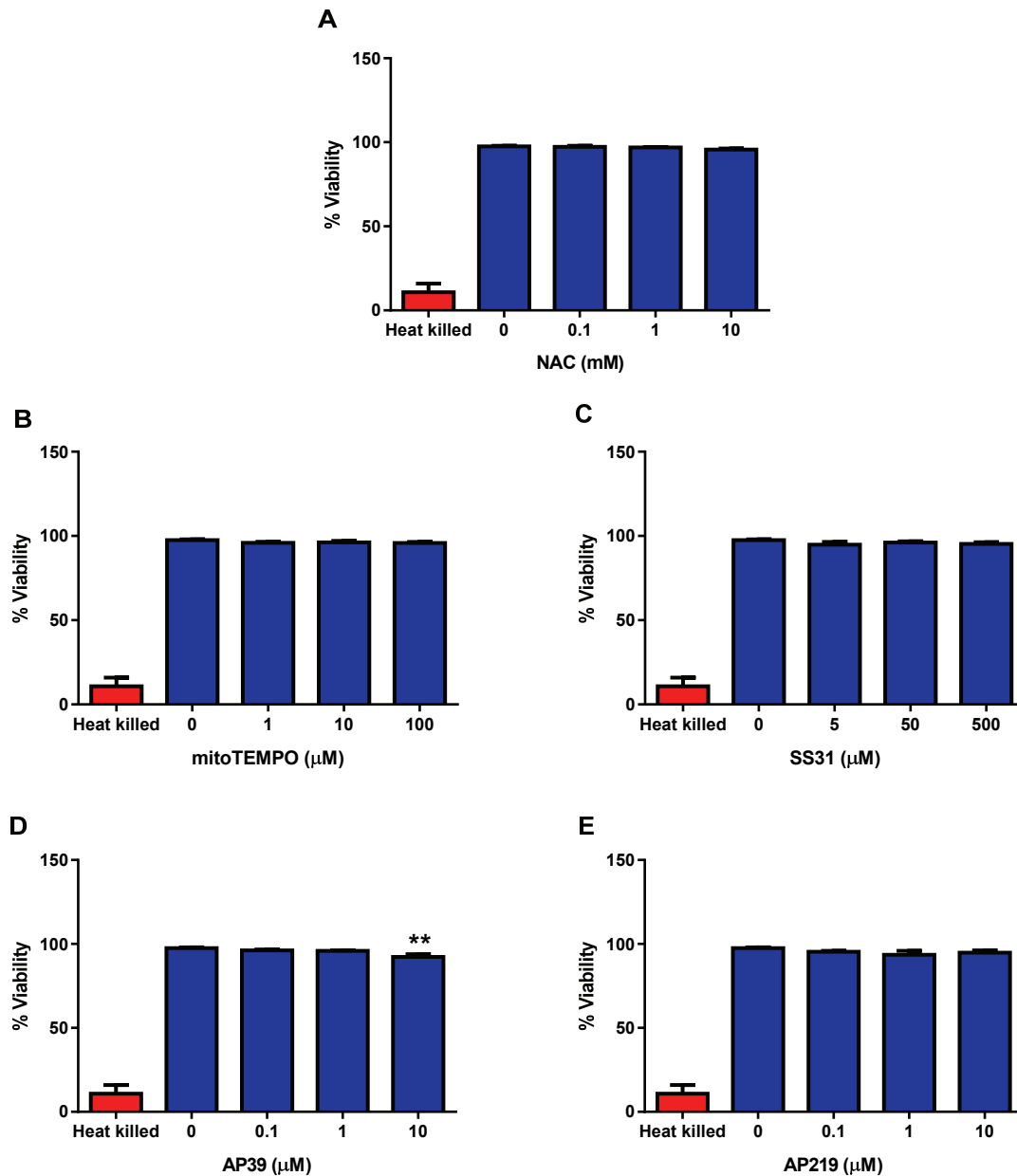


Figure 3.17 Cell viability of antioxidant treated BEAS-2B cells using propidium iodide (PI) assay
 Cells were treated with different concentrations of NAC (A), mitoTEMPO (B), SS31 (C), AP39 (D) and AP219 (E) for 24h. Cell viability was measured using PI assay. Heat killed cell sample was used as positive control (red bar). Data are presented as the mean \pm S.E.M of three independent experiments. Statistical analysis was performed using a repeated means one-way ANOVA with Bonferroni's multiple comparisons test. ** $p < 0.01$ vs untreated cell sample.

From these cell viability experiments, it indicated that most of these antioxidant concentration ranges for 24h did not affect the BEAS-2B viability.

3.4.9 Effect of antioxidants on H₂O₂ stimulated mitochondrial superoxide production in BEAS-2B cells

To investigate whether antioxidants decrease superoxide production in H₂O₂ treated BEAS-2Bs, the cells were pre-treated with various concentrations of antioxidants (as described in section 3.4.8). Previous *in vitro* studies have shown that 1-2h incubation with AP39 provides an antioxidative effect (Szczesny et al., 2014; Zhao et al., 2016). Therefore, BEAS-2B cells were incubated with antioxidants for 3h followed by incubation with 200µM H₂O₂ for 30min. In these experiments, 200µM H₂O₂ was selected despite the previously described decrease in cell viability (Figure 3.1) as 200µM H₂O₂, rather than 100µM, increased superoxide production (Figure 3.4). Before treatment with antioxidants and H₂O₂, BEAS-2B cells were pre-incubated with a final concentration of 2.5µM MitoSOX™ for 30min. At the end of the experiment fluorescence intensity was measured using flow cytometer.

There was a decrease in H₂O₂-stimulated mitochondrial superoxide production when cells were pre-treated with 10mM NAC (Figure 3.18A). No effect on H₂O₂ stimulated mitochondrial superoxide levels was observed with the other antioxidants at any concentration used (Figure 3.18B-E).

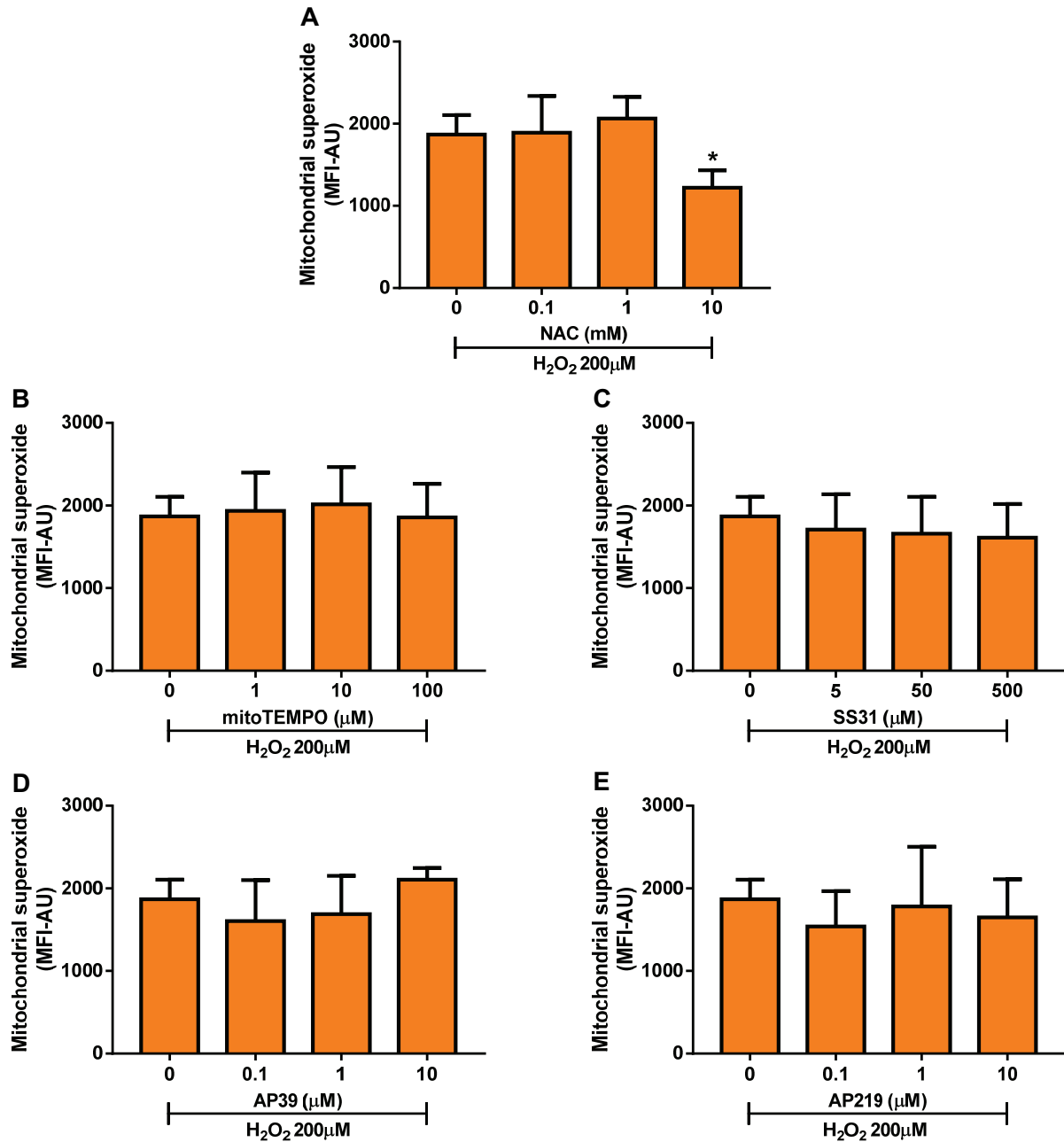


Figure 3.18 Effect of antioxidants on H_2O_2 stimulated mitochondrial superoxide production in BEAS-2B cells

Cells were pre-treated with antioxidants (0.1-10mM NAC (A), 1-100μM mitoTEMPO (B), 5-500μM SS31 (C), 0.1-10μM AP39 (D) and 0.1-10μM AP219 (E)) for 3h followed by 200μM H_2O_2 for 30min. Mitochondrial superoxide was detected using mitoSOX™ staining and fluorescence intensity was measured using flow cytometer. Data are presented as the mean \pm S.E.M of the average mean fluorescence intensity-arbitrary unit (MFI-AU) from three independent experiments. Statistical analysis was performed using a repeated measures one-way ANOVA with Dunnett's multiple comparisons test (A-C), Friedman's test with Dunn's post-test (D&E). * $p < 0.05$ vs H_2O_2 alone.

From these experiments, pre-incubation of BEAS-2B cells with antioxidants did not attenuate the H₂O₂ stimulated increase in mitochondrial superoxide; however, 10mM NAC significantly decreased mitochondrial superoxide levels ($p < 0.05$).

3.4.10 Effect of antioxidants on the H₂O₂ stimulated decrease in mitochondrial membrane potential in BEAS-2B cells

To investigate whether antioxidants restore mitochondrial membrane potential in H₂O₂-stimulated BEAS-2B, the cells were pre-incubated with a final concentration of 2 μ M JC-1 for 30min before treatment with various concentrations of the antioxidants for 3h followed by incubation with H₂O₂ for 30min. As in the previous section, 200 μ M rather than 100 μ M H₂O₂ was used despite decreased cell viability as shown in previous section 3.4.1 because $\Delta\Psi_m$ noticeably decreased at this concentration (Figure 3.9). BEAS-2B cells treated with 50 μ M CCCP were used as a positive control. The fluorescence intensity was measured by flow cytometry.

Cells pre-treated with 10 μ M AP39 showed an increase in $\Delta\Psi_m$ compared to H₂O₂ alone which was not seen with the control compound AP219 (Figure 3.19D&E). Pre-treatment with SS31 (5-500 μ M) showed a small increase in $\Delta\Psi_m$ compared with H₂O₂-treated cells (Figure 3.19C). There was no change in $\Delta\Psi_m$ when BEAS-2B cells were pre-treated with NAC or mitoTEMPO (Figure 3.19A&B).

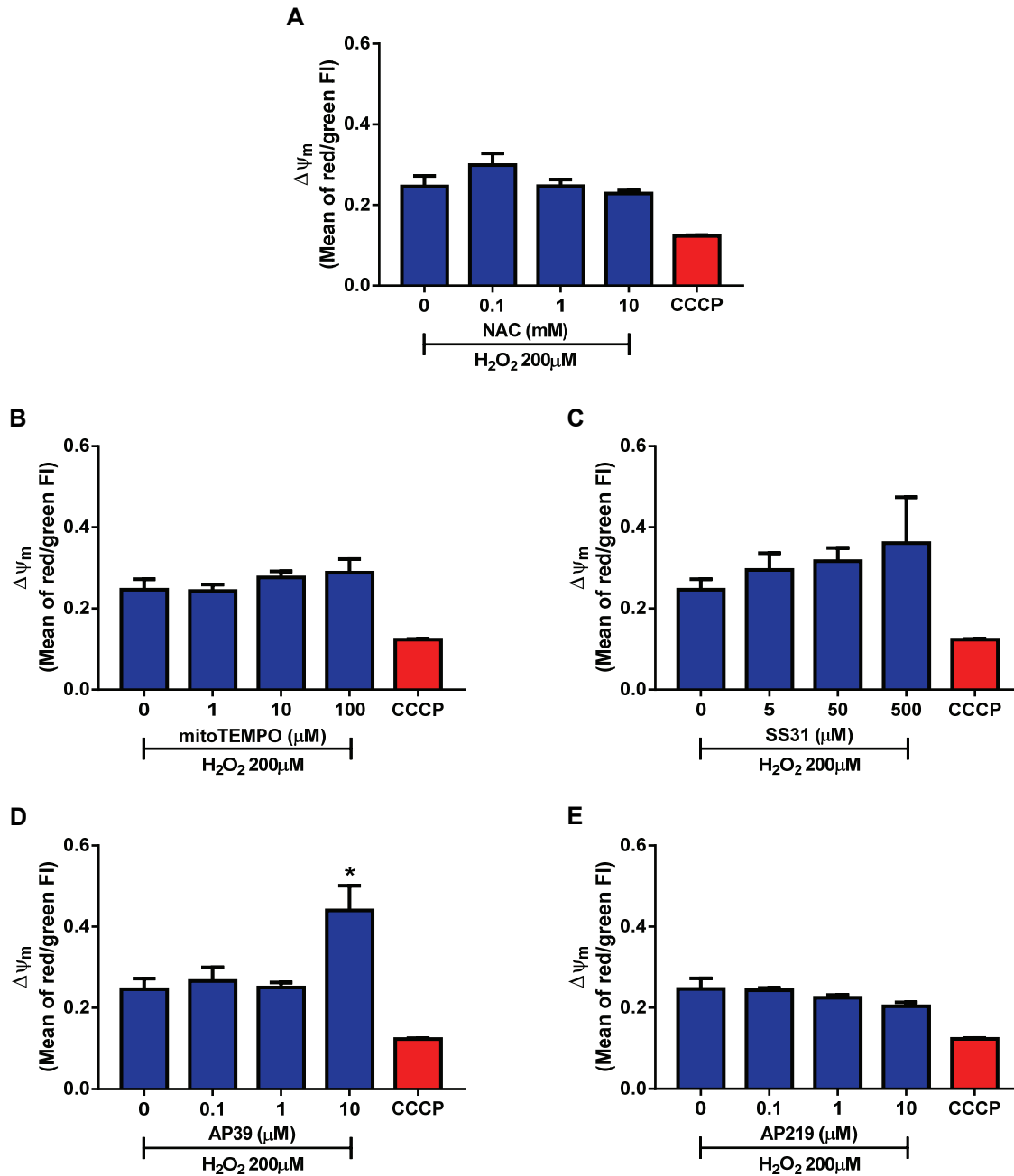


Figure 3.19 Effect of antioxidant pre-treatment on mitochondrial membrane potential ($\Delta\Psi_m$) of H_2O_2 induced BEAS-2B

Cells were pre-treated with antioxidants (0.1-10mM NAC (A), 1-100 μM mitoTEMPO (B), 5-500 μM SS31 (C), 0.1-10 μM AP39 (D) and 0.1-10 μM AP219 (E) for 3h followed by 200 μM H_2O_2 for 30min. CCCP treated cell sample was used as positive control (red bar). $\Delta\Psi_m$ was calculated from means of the ratio of red and green fluorescence intensity. Data are presented as the mean \pm S.E.M of the average $\Delta\Psi_m$ from three independent experiments. Statistical analysis was performed using Friedman's test with Dunn's post-test for (C) whereas the remaining analysis was performed using a repeated measures one-way ANOVA with Dunnett's multiple comparisons test. * $p < 0.05$ vs H_2O_2 alone.

Generally, the antioxidants tested were unable to reverse the H₂O₂-stimulated reduction in $\Delta\Psi_m$ in BEAS-2B cells although the highest concentration of AP39 significantly increase $\Delta\Psi_m$ ($p < 0.05$). This result suggests that the antioxidant with the H₂S donor would work better at ROS scavenging than other antioxidants with different molecular structures. Further research using different H₂S donor compounds should be tested to confirm this.

3.4.11 Effect of antioxidants on H₂O₂ stimulated BEAS-2B cell apoptosis

Previous experiments showed that 400 μ M H₂O₂ caused apoptosis in BEAS-2B cells. We investigated whether antioxidants could reduce the effect of H₂O₂ on apoptosis in BEAS-2B cells. Cells were pre-incubated with various concentrations of NAC, mitoTEMPO, SS31, AP39 and AP219 for 3h (Section 3.4.8). After washing with HBSS the cells were then incubated with 400 μ M H₂O₂ for 30min. The equal number of cells were counted in every sample and then incubated with Annexin V and PI as shown in the Methods chapter (Section 2.2.4). The stained cells were distinguished into 3 groups: live cells, early apoptotic cells and late apoptotic/dead cells and analysed using flow cytometer as the gate setting shown in the result section 3.4.5.

Pre-incubation with NAC showed an increase in the percentage of live cells and a decrease in the percentage of late apoptotic cells compared to 400 μ M H₂O₂-treated BEAS-2B cells, but no change was seen in the percentage of early apoptotic cells (Figure 3.20A). Pre-incubation with SS31 or with higher concentrations of AP39 increased the percentage of late apoptotic/dead cells in 400 μ M H₂O₂-treated BEAS-2B cells (Figure 3.20D&E). mitoTEMPO had no significant effect on

the percentage of cells in each group compared to 400 μ M H₂O₂ treatment (Figure 3.20B).

In summary, it shows that NAC has a trend to have a protective effect on H₂O₂ stimulated apoptosis in BEAS-2Bs whereas the effect of the mitochondrial-directed drugs was variable.

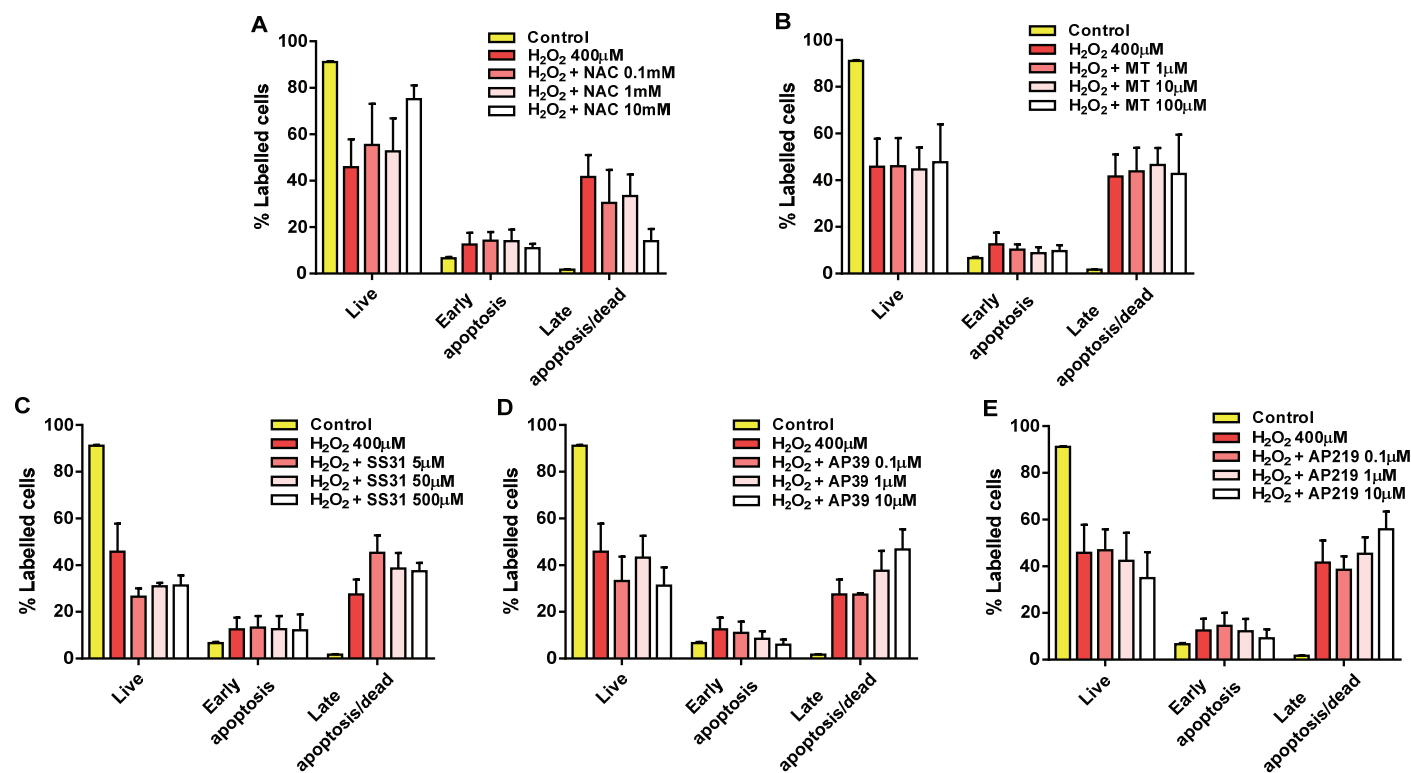


Figure 3.20 Effect of antioxidants on apoptosis in H₂O₂ induced BEAS-2B

Cells were pre-incubated with various concentrations of antioxidants (NAC (A), mitoTEMPO (B), SS31 (C), AP39 (D), AP219 (E)) for 3h followed by 400μM H₂O₂ for 30min. Live cells, early apoptotic cells and late apoptotic/dead cells were analysed using FITC Annexin V/Dead Cell Apoptosis kit for flow cytometer. Results were divided into three main groups: live cells, early apoptotic cells and late apoptotic/dead cells which were subdivided into control (yellow), H₂O₂ alone (red) and H₂O₂+different concentrations of antioxidants. Data are presented as the mean ± S.E.M of the percentage of labelled cells in three independent experiments. Statistical analysis was performed using a repeated measures one-way ANOVA with Dunnett's multiple comparisons test for the live cell experiments with SS31 and for late apoptosis/dead groups for AP39 and AP219. For all other anti-oxidant data, the Friedman's test with Dunn's post-test was used to compare against their respective H₂O₂ alone groups.

3.4.12 Effect of antioxidants on H₂O₂ and IL-1 β induced inflammation

To investigate whether mitochondrial stress impacts upon inflammation induced by H₂O₂ and pro-inflammatory cytokine, the effect of mitochondrial antioxidants on inflammatory mediator expression was examined. As for the previous experiments (Figure 3.13A) that showed an increase in CXCL8 release from BEAS-2B cells incubated with 100 μ M H₂O₂, we then used this concentration for these antioxidant experiments. BEAS-2B cells were pre-incubated with different concentrations of antioxidants for 3h and then treated with 100 μ M H₂O₂ for 30min followed by the addition of 1ng/ml IL-1 β stimulation for 2h before measuring *IL8* mRNA expression and CXCL8 release at 24h. The fold-change responses to treatments were compared to that of H₂O₂- and IL-1 β -stimulated cells.

There was a trend towards the decrease in *IL8* mRNA expression when BEAS-2B cells were pre-treated with NAC (0.1 and 10mM), mitoTEMPO (0-100 μ M) and SS31 (5 μ M) compared to the combination of H₂O₂ and IL-1 β . However, the higher concentration of SS31 had no effect on *IL8* expression (Figure 3.21C). At the maximal concentration of AP39 and AP219 (10 μ M), *IL8* expression significantly decreased compared to the cells treated with combination of H₂O₂ and IL-1 β ($p < 0.05$ and $p < 0.01$, respectively) (Figure 3.21D&E). This suggests that the effect of AP39 may be an off-target effect or due to the mitochondrial targeting moiety alone.

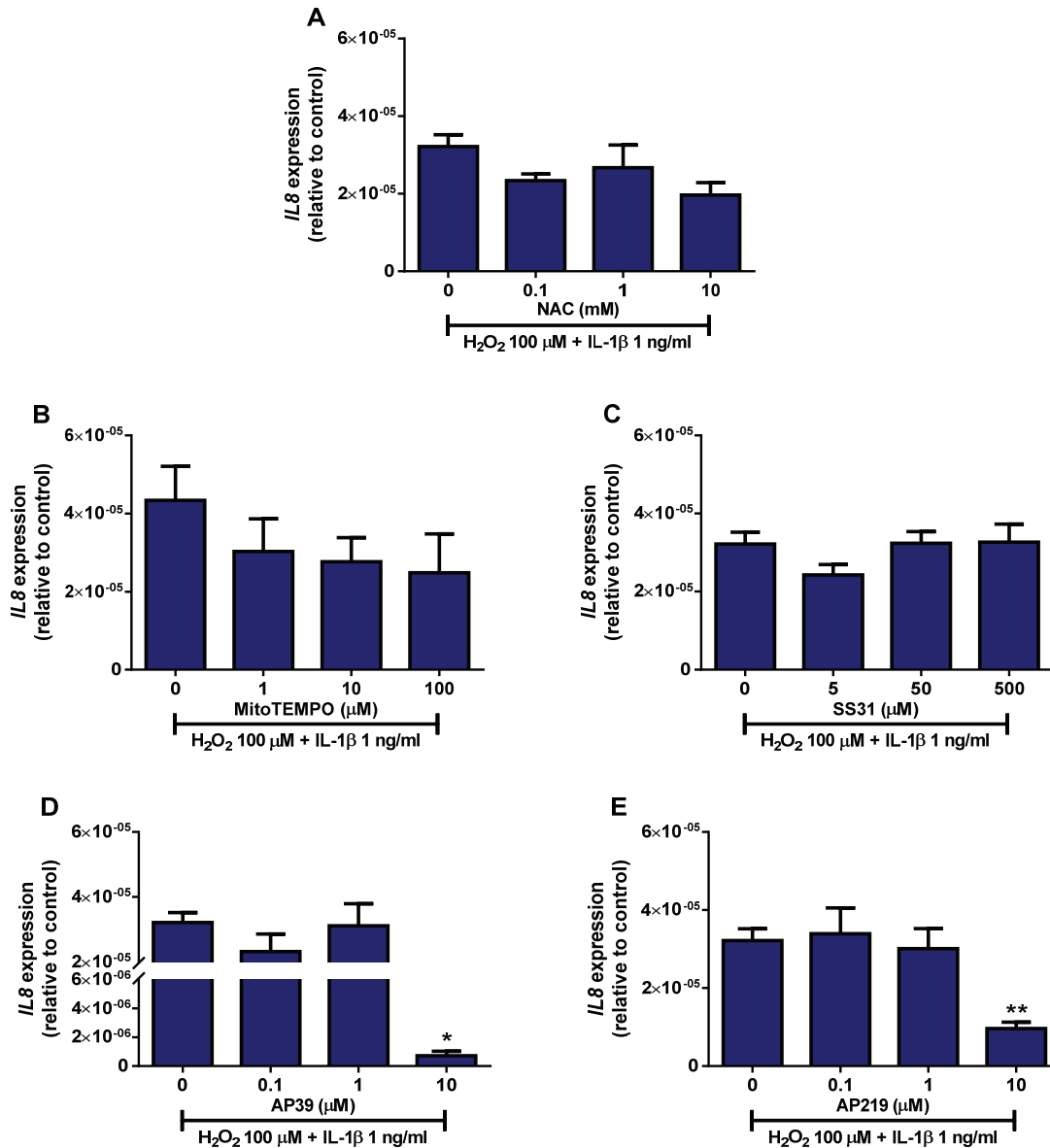


Figure 3.21 Effect of antioxidants on H₂O₂ and IL-1β stimulated IL8 mRNA expression in BEAS-2B cells

Cells were pre-treated with various concentrations of NAC (A), mitoTEMPO (B), SS31 (C), AP39 (D) and AP219 (E) for 3h followed by 100μM H₂O₂ for 30min and 1ng/ml IL-1β for 2h. Cells were collected and mRNA extracted and then PCR performed. Data are presented as the mean ± S.E.M of the IL8 mRNA expression level compared to H₂O₂-and to IL-1β treated cells from four independent experiments. Statistical analysis was performed using the Friedman's test with Dunn's post-test analysis for the mitoTEMPO and AP39 groups. Results from the other antioxidants were analysed using a repeated measures one-way ANOVA with Dunnett's multiple comparisons test. *p<0.05 and **p<0.01 vs H₂O₂-and-IL-1β treated group.

When BEAS-2B cells were pre-treated with NAC a concentration-dependent decrease in CXCL8 release was seen compared to the H₂O₂ and IL-1 β stimulated cells and had a significant decrease at 10mM NAC ($p < 0.01$) (Figure 3.22A) whereas mitoTEMPO decreased CXCL8 release at 1 μ M ($p < 0.05$) but increased its release at 100 μ M ($p < 10^{-3}$) suggesting no effect on CXCL8 induction at high dose (Figure 3.22B). SS31 had a trend towards decreasing CXCL8 release following H₂O₂ and IL-1 β stimulation (Figure 3.22C). Both AP39 and its control compound AP219 decreased CXCL8 levels compared to the H₂O₂ and IL-1 β stimulated cells although the decrease was more evident with AP39 ($p < 10^{-3}$) than AP219 ($p < 0.01$) (Figure 3.22D&E).

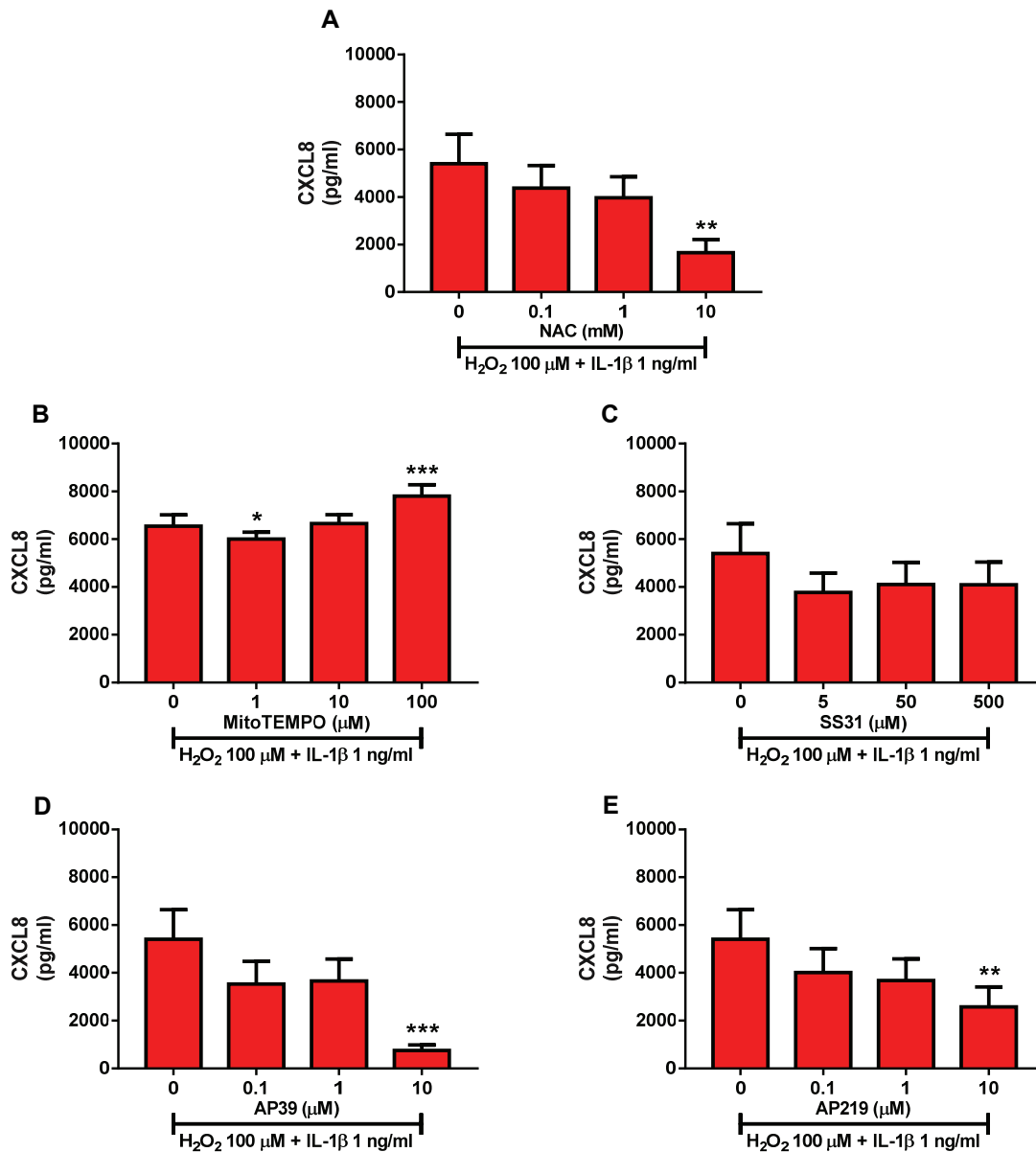


Figure 3.22 Effect of antioxidants on H_2O_2 and $IL-1\beta$ stimulated CXCL8 release in BEAS-2B cells

Cells were pre-treated with various concentrations of NAC (A), mitoTEMPO (B), SS31 (C), AP39 (D) and AP219 (E) for 3h followed by $100\mu M H_2O_2$ for 30min and $1ng/ml IL-1\beta$ for 24h. Media was collected and CXCL8 measured by ELISA. Data are presented as the mean \pm S.E.M of CXCL8 levels from five independent experiments. Statistical analysis was performed using a repeated measures one-way ANOVA with a Dunnett's multiple comparison test for the mitoTEMPO group. Other data was analysed using Friedman's test and Dunn's post-test. ** $p < 0.01$ and *** $p < 10^{-3}$ vs H_2O_2 -and- $IL1\beta$ treated group.

To conclude from this section: some antioxidants decreased the *IL8* expression and CXCL8 release induced by H_2O_2 and $IL-1\beta$ in BEAS-2B cells. NAC reduced CXCL8

release in concentration-dependent manner whereas the mitochondrial antioxidants we used had different effects. SS31 did not reduce the *IL8* expression but had a trend to decrease CXCL8 release but both AP39 and AP219 pre-incubation had some effect at high dose. Since AP219 lacks the active group of AP39 and also shows a similar reduction of *IL8* and CXCL8, it might indicate that H₂S does not play a role in this inflammatory response in BEAS-2B cells or could be a non-specific effect. The possible differential effect on CXCL8 release requires further investigation.

3.4.13 Effect of antioxidants on BEAS-2B cell proliferation

To investigate whether antioxidants themselves had an influence on BEAS-2B cell proliferation, the cells were incubated with different concentrations of antioxidants (section 3.4.8) for 48h followed by incubating with BrdU reagent for 24h and then proliferation measured by spectrofluorometer. There was a significant decrease in BEAS-2B cell proliferation at 5 and 10mM NAC treatment ($p<0.05$ and $p<10^{-3}$, respectively) and at 1, 5 and 10 μ M of AP39 compared to untreated cells ($p<0.05$, $p<0.05$ and $p<10^{-3}$, respectively) (Figure 3.23A&D). BEAS-2B cell proliferation was not affected when incubated with mitoTEMPO from 5-100 μ M, SS31 or AP219 (Figure 3.23B, C&E).

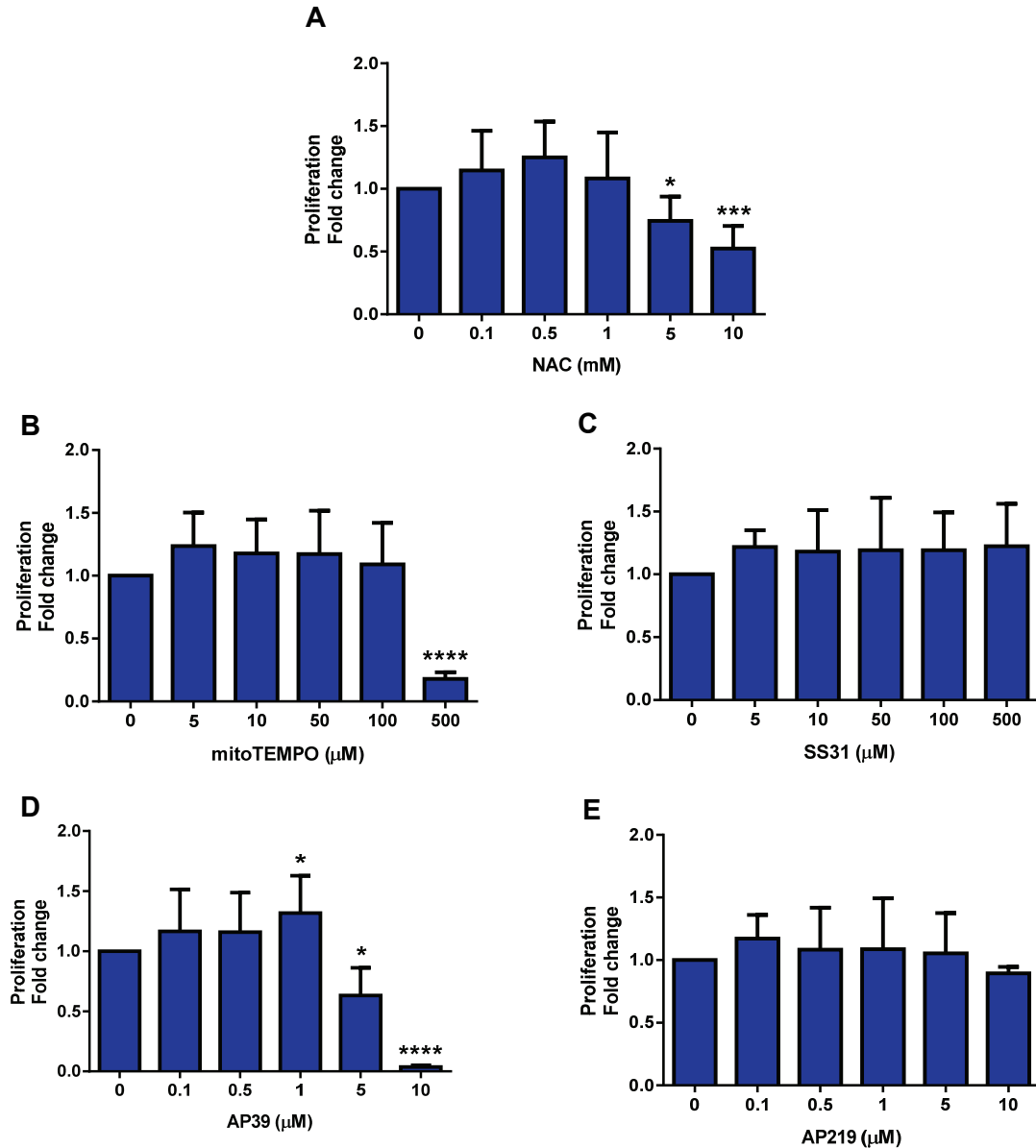


Figure 3.23 Effect of antioxidants on BEAS-2B cell proliferation

Cells were incubated with various concentrations of NAC (A), mitoTEMPO (B), SS31 (C), AP39 (D) and AP219 (E) for 48h followed by incorporating with BrdU for 24h. Results are presented as the mean \pm S.E.M of the fold change compared to control in three independent experiments. Statistical analysis was performed using a repeated measures one-way ANOVA with a Dunnett's multiple comparisons test. * $p < 0.05$, *** $p < 10^{-3}$ and **** $p < 10^{-4}$ vs control.

3.4.14 Effect of antioxidants pre-treatment on IL-1 β induced BEAS-2B cell proliferation

Previous experiments showed that IL-1 β induced BEAS-2B cell proliferation (Section 3.4.7), we further investigated whether antioxidants could decrease IL-1 β induced BEAS-2B proliferation. BEAS-2B cells were pre-incubated with different concentrations of antioxidants (section 3.4.8) for 3h, and then incubated with 5ng/ml IL-1 β for 48h followed by BrdU incorporation for 24h and then performed the BrdU assay.

IL-1 β alone increased BEAS-2B cell proliferation compared to the control (Figure 3.24). Pre-treatment of BEAS-2B cells with NAC showed significant decreases in IL-1 β stimulated cell proliferation which reached significance with 1, 5 and 10mM NAC ($p < 0.05$, $p < 10^{-4}$ and $p < 10^{-4}$, respectively) compared to the IL-1 β alone treated group (Figure 3.24A). BEAS-2B cells preincubated with 50 and 100 μ M mitoTEMPO had a significant decreased proliferation compared to the IL-1 β alone group ($p < 0.05$ and $p < 0.01$, respectively), and no proliferation was observed in cells pre-treated with 500 μ M (Figure 3.24B). SS31 and AP219 had no effect on the proliferation of IL-1 β stimulated cells (Figure 3.24C&E). There was no proliferation observed when BEAS-2B cells were pre-incubated with 5 and 10 μ M AP39 (Figure 3.24D) which has a similar result shown in Figure 3.23D. These results possibly indicate that the hydrogen sulfide (H₂S)-releasing group in AP39 itself inhibited the proliferation since AP219, (AP39 without H₂S), did not affect the proliferation (Figure 3.24E).

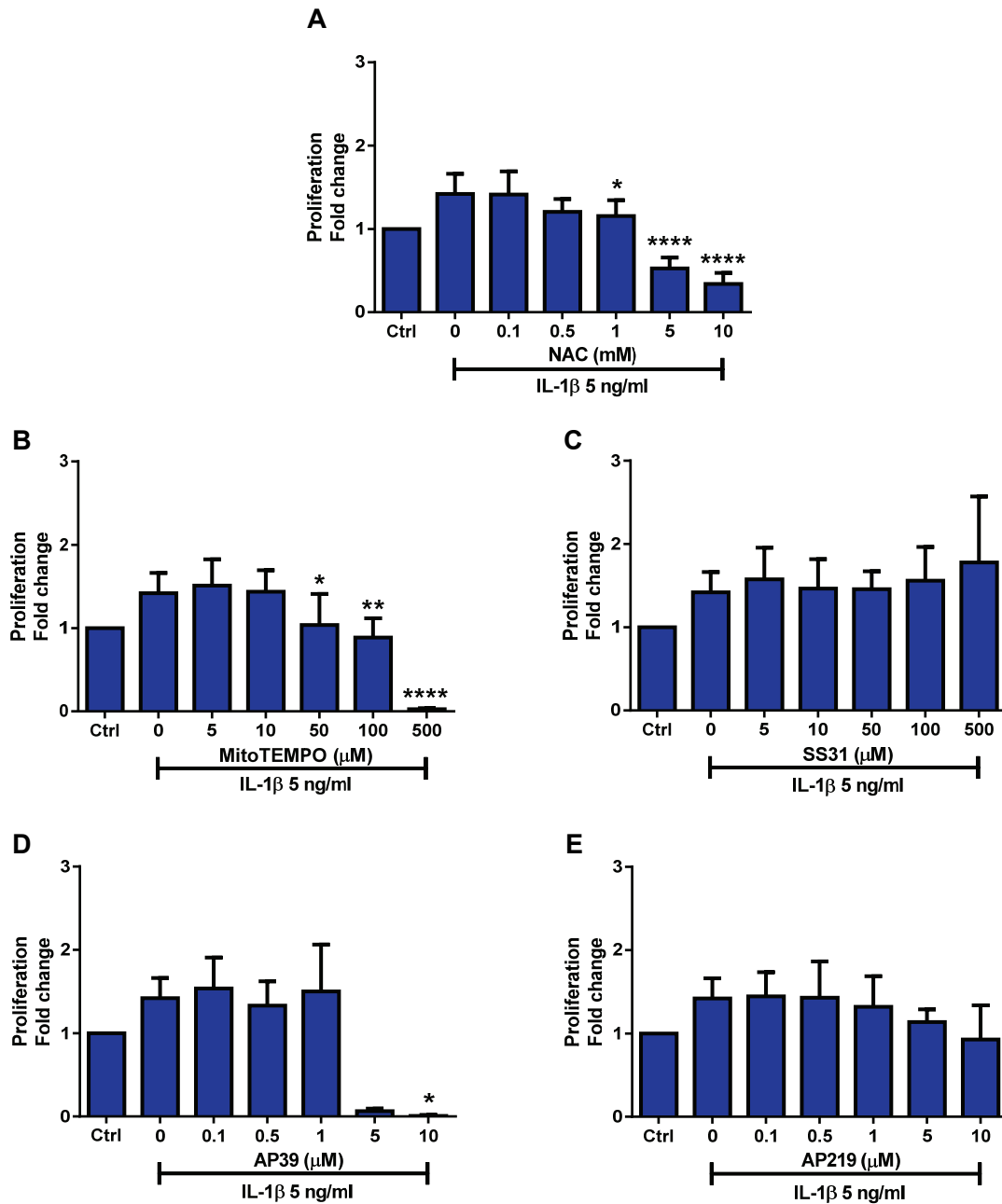


Figure 3.24 Effect of antioxidants on IL-1 β induced BEAS-2B cell proliferation

Cells were incubated with various concentrations of NAC (A), mitoTEMPO (B), SS31 (C), AP39 (D) and AP219 (E) for 3h, then incubated with 5ng/ml IL-1 β for 48h followed by incorporating with BrdU for 24h. Results are presented as the mean \pm S.E.M of the fold change compared to control in three independent experiments. Statistical analysis was performed using Friedman's test with Dunn's post-test analysis for the AP39 treated group. Data from other antioxidant treated groups were analysed using RM one-way ANOVA with Dunnett's multiple comparisons test. * $p < 0.05$, ** $p < 0.01$ and **** $p < 10^{-4}$ vs IL-1 β alone group.

In summary, some antioxidants (NAC, mitoTEMPO and AP39) possess the inhibitory effect on BEAS-2B cell proliferation in both basal condition and IL-1 β stimulation where a greater extent of proliferation was shown in IL-1 β stimulation.

3.5 Discussion

This chapter shows that H₂O₂ alters mitochondrial function by inducing mitochondrial superoxide production, intracellular ROS and decreasing $\Delta\Psi_m$ in BEAS-2B cells. H₂O₂ also induces BEAS-2B cell apoptosis at high concentrations and increases CXCL8 release. In addition, H₂O₂ inhibits basal and IL-1 β -induced proliferation in BEAS-2B cells. Pre-treatment of cells with cellular and mitochondrial-directed antioxidants had differential effects on H₂O₂-perturbed mitochondrial function. N-acetyl cysteine (NAC) decreased mitochondrial superoxide production but had no effect on $\Delta\Psi_m$. Mitochondrial-directed antioxidants with the possible exception of AP39 also failed to restore H₂O₂-suppressed $\Delta\Psi_m$. H₂O₂-induced apoptosis was prevented by NAC pre-incubation. The antioxidants tested had a diverse effect on H₂O₂- and-IL-1 β induced CXCL8 mRNA expression and release in BEAS-2B cells. NAC decreased *IL8* expression and CXCL8 release, but no significant effect was seen following pre-incubation with mitoTEMPO and SS31. Both AP39 and its control compound AP219 reduced *IL8* expression and CXCL8 release. NAC, mitoTEMPO and AP39 inhibited both basal and IL-1 β -stimulated proliferation of BEAS-2B cells.

Epithelial cells lining the airways and the lung are the first sites exposed to exogenous ROS such as cigarette smoke which is the main driver of COPD and can induce epithelial cell metaplasia leading to lung cancer (Barnes, 2016).

In addition, persistent oxidative stress can lead to the induction of inflammation in the lungs of COPD patients (Rahman & Adcock, 2006). Studies investigating the role(s) of the mitochondria in lung disease models have demonstrated that mitochondrial dysfunction may underlie COPD and/or lung cancer pathogenesis (Aravamudan et al., 2013; Cloonan & Choi, 2016; Nam et al., 2017). The effect of oxidative stress on mitochondrial function was demonstrated in the lung of ozone-induced mice (Wiegman et al., 2015) and in ASM cells of COPD patients (Wiegman et al., 2015). Therefore, it is important to understand the effect of oxidative stress on lung epithelial cells. We examined this *in vitro* in this chapter using an immortalised bronchial epithelial cell line (BEAS-2B) and investigated the ability of a cellular antioxidant, NAC, and mitochondrial-directed antioxidants to restore dysregulated mitochondrial function, inflammation, apoptosis and proliferation evoked by oxidative stress.

H₂O₂ as a representative of reactive oxygen species is used in many *in vitro* studies investigating ROS-induced mitochondrial dysfunction and inflammation in airway epithelial cells, ASM cells and lung fibroblasts (Jaspers, Zhang, Fraser, Samet, & Reed, 2001; Thannickal & Fanburg, 1995; Wang et al., 2015; Wiegman et al., 2015). The present study demonstrated that treatment of BEAS-2B cells with 200µM H₂O₂ for 4h increased intracellular ROS without loss of cell viability. This is in contrast to a study in BEAS-2B cells that showed a concentration dependent increase in intracellular ROS with H₂O₂ exposure albeit with decreased cell viability at concentrations >100µM for 2h (Khan et al., 2014). In C6 glioma cells, increasing the cell density decreased the cytotoxic effect of H₂O₂ in the concentration-dependent manner with an increased rate of H₂O₂ elimination present at higher

cell densities (Gülden, Jess, Kammann, Maser, & Seibert, 2010). This suggests that the difference in the ability of H₂O₂ to induce ROS may be due to the different cell densities used.

Previous studies have reported an increase in mitochondrial superoxide production in cigarette smoke extract (CSE)-treated human ASM cells (Li et al., 2017), isolated mitochondria from the skeletal muscles of patients with COPD (Puente-Maestu et al., 2012) and ozone-exposed mice (Wiegman et al., 2015). Increased mitochondrial superoxide was reported in ASM cells of patients with COPD treated with 100µM H₂O₂ which indicated that excessive oxidative stress leads to mitochondrial dysfunction (Wiegman et al., 2015). In this study, BEAS-2B cells incubated with 200µM H₂O₂ increased mitochondrial superoxide level compared to the control which reflects similar results in BEAS-2B cells stimulated with CSE, a source of oxidative stress (Mizumura et al., 2014). This thesis also reports a decrease in $\Delta\Psi_m$ following H₂O₂ treatment of BEAS-2B cells suggesting that ROS can affect mitochondrial function in the bronchial epithelium.

A previous study has shown that H₂O₂ (200-500µM) decreased $\Delta\Psi_m$ in a time- and concentration-dependent manner (Fujii et al., 2002). Similar, but not identical results, were shown in this study but the large drop in $\Delta\Psi_m$ seen at high H₂O₂ concentrations at 2 and 4h was associated with a reduction in cell viability.

Increased apoptosis is involved in the development of COPD and excessive oxidative stress in the lung induces apoptosis and structural cell destruction (Demedts et al., 2006; Lin et al., 2014). In human foetal lung fibroblasts 10-100µM H₂O₂ induced apoptosis which was inhibited by GSH supplementation (Teramoto et

al., 1999). In BEAS-2B cells, CSE exposure caused a concentration-dependent increase in apoptosis which was regulated via the ROS-dependent apoptosis regulating signal kinase 1/p38 MAPK signalling cascade (Lin et al., 2014). In the present study, a high percentage of cells were driven to a late apoptotic stage when exposed to a high H₂O₂ concentration (400µM). These findings are in agreement with the report of increased apoptosis in airway epithelial cells and T-lymphocytes from COPD patients (Hodge et al., 2005).

Oxidative stress can enhance the expression of inflammatory mediators and signalling pathways by immune and structural cells in the lungs and airways of COPD patients (Rahman & Adcock, 2006). ROS increase the activation of NF-κB and inflammatory gene expression in lung epithelial cell lines (Rahman et al., 2001; Rahman, Gilmour, Jimenez, & MacNee, 2002). In BEAS-2B cells, H₂O₂ alone had no effect on *IL8* mRNA expression and CXCL8 protein release but enhanced IL-1β-induced gene expression and release (Khan et al., 2014). In the present study, both H₂O₂ and IL-1β separately induced CXCL8 release in a concentration-dependent manner; however, H₂O₂ had a lower efficacy compared to IL-1β. Further studies are required to confirm whether the enhanced expression seen with combined treatment is additive or synergistic.

Exposure of lung epithelial cells to oxidative stress can result in apoptosis or necrosis whereas any viable cells continue to undergo proliferation (Smit-de Vries, van der Toorn, Bischoff, & Kauffman, 2007). H₂O₂ induces proliferation in primary ATII and A549 cells (Sigaud, Evelson, & González-Flecha, 2005; Smit-de Vries et al., 2007); however, H₂O₂ (100-500µM) treatment of BEAS-2B cells for 1h decreased

cell proliferation in a concentration-dependent manner (Fujii et al., 2002). This result is similar to those in the present study whereby 2h H₂O₂ (12.5-50µM) decreased BEAS-2B cell proliferation.

Studies in multicellular organisms have shown that H₂O₂ can act as a signaling molecule to modulate the activity of transcription factors such as HIF-1 and NF-κB depending on the H₂O₂ concentration and the cell type. The increased proliferation of basal epithelial cells found in the airway in COPD leads to squamous metaplasia (Barnes, 2016). A higher expression of inflammatory mediators (*TNF-α*, *IL-1β* and *IL-6*) was reported in tracheobronchial tissues from smokers as well as the activation of NF-κB and MAPK signalling pathway. In mice exposed to cigarette smoke treatment using anti-TNF-α, anti-IL-1β and anti-IL-6 decreased lung epithelial hyperplasia (Herfs et al., 2012). IL-1β is markedly elevated in serum from patients with NSCLC; it also promotes proliferation and migration of NSCLC cell lines indicating the importance of IL-1β in tumour transformation (Wang et al., 2014). In concordance with the results of these studies, the present study shows that IL-1β increased BEAS-2B cell proliferation in a concentration-dependent manner. However, the current study demonstrates that H₂O₂ attenuated IL-1β-induced proliferation of BEAS-2B cells. This may reflect the concurrent effect of H₂O₂ on cell survival seen in this study but further studies utilising CSE may determine whether factors in addition to ROS alone are required to enhance epithelial cell proliferation and lead to a pre-cancerous state.

Increased ROS from external sources in combination with an ineffective antioxidant response in COPD pathogenesis results in the accumulation of ROS which may damage the mitochondria of bronchial epithelial cells (Hara et al., 2013; Heijink et al.,

2014; Rahman & MacNee, 1996; Sureshababu & Bhandari, 2013; van der Toorn et al., 2009). A number of different antioxidants have been investigated in clinical trials in COPD patients with variable outcomes reported (Rahman, 2008). This may reflect patient heterogeneity, a lack of antioxidant efficacy or the use of antioxidants targeting the wrong cellular compartment.

Previous studies have demonstrated that NAC pre-treatment restored complex IV activity and ATP synthesis in LPS/aspirin-induced toxicity in a liver cancer cell line (HepG2) (Raza, John, & Shafarin, 2016). NAC also prevented the increase in BAL macrophages and reduced the expression of the oxidative marker (8-OHdG) in ozone-induced COPD mice; however, it did not decrease the expression of *IL-1 β* and *TGF- β* when given preventively or therapeutically (Papi et al., 2004). In a human tubular epithelial cell line (HK2) study, NAC protected against hydroquinone metabolite toxicity including decreased cell death, reduced ROS production as well as maintaining $\Delta\Psi_m$ (Zhang, Lau, & Monks, 2011) which is partially consistent with the present study. Pre-treatment with NAC (10mM) prevented the increased mitochondrial superoxide level in H₂O₂-treated BEAS-2B cells. In addition, NAC protects against oxidative stress-induced HK-2 cell death (Zhang et al., 2011) and from ROS-induced apoptosis of BEAS-2B cells via the glyoxalase system (a cellular defence by detoxification) (Antognelli, Gambelunghe, Talesa, & Muzi, 2014). These findings are similar to that of the present study in that NAC protected BEAS-2B cells from apoptosis induced by H₂O₂.

NAC (10mM) suppressed the expression and release of *IL8*, *IL6* and *TNF- α* in viral respiratory infected A549 cells (Mata, Morcillo, Gimeno, & Cortijo, 2011) and a clinical study showed a significant decrease in plasma IL8 and TNF- α levels in patients with COPD who had received a high dose of NAC (1,200mg/day) (El-Hafiz et al, 2013). Further studies could investigate whether NAC inhibits virus-induced CXCL8 expression as reported here with IL-1 β and/or H₂O₂ stimulation.

Evidence of the inhibitory effect of NAC on cell proliferation has been demonstrated in a study using rat oral mucosal cells which showed that NAC (2.5-10mM) decreased cell proliferation and increased intracellular GSH and improved the GSH redox balance (Sato et al., 2009). In NSCLC cell lines treated with NAC (5mM) there was decreased lung tumour growth possibly due to a reduction of PDK1, a metabolic gene highly expressed in cancers (Hann, Zheng, & Zhao, 2013). These findings agree with the present study where NAC showed a concentration-dependent decrease in IL-1 β -stimulated BEAS-2B cell proliferation.

The results describing cell viability were dependent upon the method used. ROS and antioxidants modulated cell viability according to the MTT assay but no loss of viability was seen with the other two assays. This probably reflects the fact that MTT is a measure of mitochondrial function rather than cell death per se. In addition, there may be a direct chemical or enzymatic interaction between antioxidants and MTT since previous studies have shown that thiol-containing compounds can reduce MTT in the absence of cells (Lim, Loh, Ting, Bradshaw, & Allaudin, 2015; Natarajan, Mohan, Martinez, Meltz, & Herman, 2000). This suggests that the results from MTT assays should be interpreted with caution.

The mitochondrial-targeted antioxidants MitoTEMPO, SS31, AP39 and AP219 (the control for AP39) had differing abilities to protect against oxidative stress-induced BEAS-2B dysfunction in this study. MitoTEMPO (1-100 μ M) pre-treatment for 3h had no effect on oxidative stress-induced mitochondrial function, the number of apoptotic cells or the effect on the inflammation (CXCL8 release) pre-treated with mitoTEMPO 5-500 μ M. This is contrary to previous studies that show that a 3h pre-incubation of mitoTEMPO (100 μ M) reduced mitochondrial superoxide production in CSE-exposed primary bronchial epithelial cells (Hara et al., 2013) and the effect of 200 μ M mitoTEMPO on TGF- β 1-induced mitochondrial superoxide in BEAS-2B cells (Patel et al., 2015).

MitoTEMPO (5 μ M, 2h) reduced *TNF- α* in LPS-stimulated human umbilical vein endothelial cells (HUVEC) and decreased cell death when exposed to H₂O₂ (200 μ M) for 24h in a pre-eclampsia study (McCarthy & Kenny, 2016). These findings contrast with those in the present study which may reflect the difference in H₂O₂ incubation time. In my study, cells were incubated with H₂O₂ for only 30mins and extending the incubation time might enhance the damage due to H₂O₂ and have a greater opportunity to demonstrate a protective effect of mitoTEMPO.

SS31 is a small peptide antioxidant which accumulates in the inner mitochondrial membrane (Zhao et al., 2004). Previous studies by Szeto and Schiller's group have shown that SS31 has a protective effect against oxidative stress. One of their studies shows that 4h SS31 (100 μ M) treatment decreased intracellular ROS and increased cell viability after *t*-butylhydroperoxide (*t*BHP) treatment in neuroblastoma (N₂A) cell lines. Additionally SS31 was found to inhibit mitochondrial swelling and

ROS production in Ca^{2+} -activated isolated mitochondria from rat liver (Zhao et al., 2004). Another study also shows that SS31 (1nM) decreased tBHP-induced apoptosis and prevented mitochondrial depolarisation in a neuroblastoma cell line (Zhao, Luo, Giannelli, & Szeto, 2005). It is likely that the SS31 concentration was adjusted depending on the experimental methods. No protective effect of SS31 in BEAS-2B cells in this present study could be detected, this may result from the altered sequence of antioxidant and oxidant treatment of the study which was different from the previous studies and possibly the need to extend the range of concentrations tested.

AP39, a mitochondrially targeted H_2S donor, has shown a protective effect in hyperglycaemic injury, Alzheimer's disease, acute renal injury, burn injury, and myocardial ischemia both *in vitro* and in animal models (Ahmad et al., 2016; Ahmad & Szabo, 2016; Gerő et al., 2016; Karwi et al., 2017; Zhao et al., 2016). In hyperglycaemic endothelial cells, it has been shown that AP39 (0.03-3 μM) inhibited mitochondrial ROS production and improved $\Delta\Psi_m$ (Gerő et al., 2016). In addition, AP39 (0.03-3 μM) pre-treatment attenuated glucose oxidase (GOx)-induced oxidative stress in a normal rat kidney epithelial cell line (NRK) as it showed decreased intracellular ROS and necrosis. Moreover, AP39 was found to inhibit inflammation as shown by a reduction in plasma levels of IL-12 in renal ischemia-reperfusion rat model (Ahmad et al., 2016).

In a burn injury mouse model study, AP39 decreased plasma inflammatory mediator production (IL-6 and IL-10) and decreased malondialdehyde (MDA) levels and myeloperoxidase activity (Ahmad & Szabo, 2016). In comparison to previous

studies, the higher range of AP39 and AP219 concentrations from 0.1-10 μ M was used in the present study. 3h pre-treatment with AP39 slightly decreased mitochondrial superoxide levels in H₂O₂ treated BEAS-2B cells but 10 μ M AP39 did not decrease mitochondrial superoxide level. No change in the mitochondrial superoxide level was observed when pre-treating with AP219. These data are consistent with a previous study in isolated rat cardiac mitochondria which demonstrated that the lower AP39 concentration (1 μ M) inhibited mitochondrial ROS production but that this inhibitory effect was lost with higher AP39 concentrations (Karwi et al., 2017).

This effect has also been shown in a study of primary neuronal cells from transgenic mice studied Alzheimer's disease that the lower AP39 (25-100nM) decreased cell death (LDH release level); however, more cell death was found at the higher AP39 (250nM) (Zhao et al., 2016). In a study of GOx induced NRK cells the highest concentration of AP39 (3 μ M) was less effective at preventing cell death as shown by increased LDH and intracellular ROS (Ahmad et al., 2016).

The effect of AP39 from these previous studies and from the present study are consistent with an earlier study which showed that the toxic effects of high-dose H₂S inhibits cytochrome C oxidase in mitochondrial complex IV but has a protective effect in lower-dose H₂S suggesting that the protective effect of AP39 may have a bell-shaped concentration-response curve (Ahmad et al., 2016; Zhao et al., 2016). This may occur in my study which showed that mitochondrial dysfunction as well as cellular dysfunction leads to cell death in H₂O₂/IL-1 β treated BEAS-2B cells pre-treated with a high concentration (10 μ M) of AP39 which contributed to

the sudden drop of *IL-8* expression, CXCL8 release and proliferation whereas there was no change in these parameters in H₂O₂/IL-1 β treated BEAS-2B when pre-treated with the control compound AP219. Other studies have used additional controls such as ADT-OH (H₂S donor part of AP39) in addition to AP219 as a control (Geró et al., 2016; Karwi et al., 2017) whereas only AP219 was used in this study. Each control compound controls for different aspects of AP39 biology such as the release of H₂S between AP39 and ADT-OH (Geró et al., 2016) and distinguishing the mitochondrial improvement effect between AP39 and AP219 as shown in the present study. ADT-OH may have provided additional information as to the mechanism of AP39 functions in my study.

Interestingly, there was a concentration-dependent decrease of *IL8* and CXCL8 in AP219 pre-treated H₂O₂-and-IL-1 β induced BEAS-2B cells. Since IL-1 β induces the *IL8* mRNA transcription and CXCL8 synthesis via NF- κ B signalling pathway (Eskan et al., 2008; Kim et al., 2010; Kunsch, Lang, Rosen, Shannon, & Proud, 1994), this raises the question whether AP219 alone could inhibit inflammatory responses in BEAS-2B cells.

In summary, this study presented as an *in vitro* model of oxidative stress stimulated bronchial epithelium in the airway has demonstrated the effect of H₂O₂ in BEAS-2B cells that H₂O₂ decreased $\Delta\Psi_m$ and induced mitochondrial superoxide production as well as induced apoptosis. In addition, H₂O₂ had a synergistic effect in the inflammatory induction in combination with IL-1 β but repressed the proliferation stimulation of IL-1 β . The protective effect of antioxidants in response to H₂O₂ and IL-1 β was variable because the antioxidant incubation time was set to finish at

the same time for all studied parameters and experimental setting, and the antioxidant concentration range might be too broad which may have caused some unexpected results. Alternatively, genetic modulation of oxidant/antioxidant expression could have been performed to validate or enhance the results from this chapter.

Investigating the mitochondrial function and cellular function in only a bronchial epithelial cell line is a main limitation in this chapter. Many cell lines have demonstrated alterations in response to oxidative stress such as upregulation of antioxidant systems that allow them to survive, inflammatory signalling in epithelial injury and modulation of mitochondrial redox signalling (Lin et al., 2014; McCarthy & Kenny, 2016; Rahman et al., 2001; Teramoto et al., 1999). The investigation of these functions in primary cells will demonstrate which is more relevant to physiological condition to human. Therefore, in the next chapter the comparison of cellular function and metabolism in different lung epithelial cell types in response to the oxidative stress will be investigated in the BEAS-2B cell line and in human primary bronchial epithelial cells (NHBE) and also in a lung cancer cell line (A549). The protective effect of antioxidants will also be investigated by oxygen consumption rate (OCR) measurement using extracellular flux (XF) analyser.

**Chapter 4 Differences in
cellular function among
lung epithelial cell types
(BEAS-2B, NHBE, and A549)**

4.1 Introduction

Airway epithelial cells from COPD patients are more susceptible to becoming cancerous than cells from smokers without obstruction with the most prevalent outcome being NSCLC (Rooney & Sethi, 2011). Cigarette smoking induced oxidative stress is a common risk factor in both COPD and lung cancer; in addition, cellular pathogenic mechanisms are found to be similar in both diseases (Caramori et al., 2011). The infiltration of inflammatory cells in the airways of patients with COPD as well as in lung tumour tissue was first noticed by Rudolf Virchow in 19th century. The release of inflammatory mediators to the microenvironment can promote characteristics of cancer including proliferation, alteration of signalling pathways and changes in cellular respiration (Adcock et al., 2011; Nam et al., 2017; Rooney & Sethi, 2011). Two lung epithelial cell lines and primary bronchial epithelial cells are used in our experiments as representatives of epithelial cells in the human lungs to investigate the effect of oxidative stress on mitochondrial function, inflammatory response and cellular proliferation. Cell types consist of a human bronchial epithelial cell line (BEAS-2B), primary normal human bronchial epithelial cells (NHBE) and a human lung adenocarcinoma cell line (A549). General characteristics of BEAS-2B, NHBE and A549 are summarised in Chapter 2 (Table 2.11).

Several studies have used primary cells from the lung to investigate the effect of oxidative stress on mitochondrial function. Primary bronchial epithelial cells from asthmatic patients compared to non-asthmatics when exposed to CSE showed increased apoptosis due to increased nuclear translocation of an apoptosis-inducing factor from the mitochondria, which was reduced by GSH indicating that CSE

can alter mitochondrial activity (Bucchieri et al., 2015). Primary airway smooth muscle cells (ASM) from patients with COPD have defects of mitochondrial function ($\Delta\Psi_m$, ATP production and mitochondrial complex expression); moreover, H_2O_2 caused ASM mitochondrial dysfunction in non-smokers (Wiegman et al., 2015). In addition to the assessment of mitochondrial function in BEAS-2B cells presented in the previous chapter, this chapter investigates mitochondrial function in the three different cell types. Besides the fluorescent methods used in the previous chapter to assess mitochondrial function, cellular respiration will be measured using an Extracellular Flux (XF) analyser. This refined technology determines cell respiratory control and mitochondrial function-related parameters as oxygen consumption rate. Moreover, the sequential additions of mitochondrial inhibitor reagents (Mito Stress test) during cell respiration enable monitoring of the mitochondrial respiration parameters which represent the mitochondrial function as mentioned previously in Chapter 2.

The effect of H_2O_2 with/without pro-inflammatory stimulation on the expression of the mitochondrial related genes AMP-activated protein kinase (*AMPK*), hypoxia inducible factor alpha (*HIF1A*) and interleukin-8 (*IL8*) are also investigated as they have been implicated in the pathogenesis of both COPD and lung cancer. Finally, the effect of antioxidants on the above parameters will be evaluated in the three cell types as well.

4.2 Hypothesis

Mitochondrial function and proliferation of BEAS-2B, NHBE, and A549 cells are different at baseline and in response to H₂O₂ exposure.

H₂O₂ and pro-inflammatory stimulation can induce alterations in gene (*AMPK*, *HIF-1A* and *IL8*) expression in BEAS-2B, NHBE, and A549 cells.

Mitochondrial targeted antioxidants will restore changes in H₂O₂-stimulated mitochondrial function in these three cell types.

4.3 Aims

- To compare mitochondrial function and proliferation among BEAS-2B, NHBE, and A549 cells at baseline and after exposure to H₂O₂.
- To determine the mitochondrial respiration rate of BEAS-2B, NHBE, and A549 cells at baseline and after exposure to H₂O₂ using Extracellular Flux analyser (Seahorse Technology).
- To compare gene expression (*AMPK*, *HIF-1A* and *IL8*) and inflammatory cytokine release in response to H₂O₂ in combination with/without pro-inflammatory stimulation.
- Evaluate the effect of antioxidants on H₂O₂ stimulated changes in mitochondrial respiration parameters.

4.4 Results

4.4.1 Mitochondrial superoxide, intracellular ROS and mitochondrial membrane potential ($\Delta\Psi_m$), in BEAS-2B, NHBE and A549 cells (baseline and after H₂O₂ exposure)

To examine any differences in mitochondrial function between normal bronchial epithelial cells and lung cancer cells and to investigate how they respond to H₂O₂, seeding plates were coated with 30µg/ml collagen type I and bronchial epithelial cell growth medium (BEGM) was used for all cell types. 2.5x10⁵/well of BEAS-2B, NHBE, and A549 cells were seeded into 24-well plates for mitochondrial superoxide, intracellular ROS and $\Delta\Psi_m$ measurement. Cells were starved for 16h for cell cycle synchronisation followed by treatment with basal media with or without 100µM H₂O₂ for 4h.

At baseline, higher basal mitochondrial superoxide levels were observed in A549 cells compared to NHBE cells, and this was also significantly higher than that seen in BEAS-2B cells ($p<0.05$) (Figure 4.1A). In contrast, the maximum basal total intracellular ROS level was observed in NHBE cells (Figure 4.1B). The basal $\Delta\Psi_m$ of NHBE cells was higher than that of BEAS-2B and significantly higher compared to that of A549 cells ($p<0.05$) (Figure 4.1C).

H₂O₂-treated BEAS-2B cells had a significantly increased mitochondrial superoxide level compared to A549 cells ($p<0.05$) (Figure 4.1D) whereas there was no significant difference of intracellular ROS between cell types (Figure 4.1E). When cells were treated with 100µM H₂O₂ for 4h, no significant difference in $\Delta\Psi_m$ was observed in the three cell types (Figure 4.1F) confirming data in BEAS-2B cells in Chapter 3.

In summary, the data shows that BEAS-2B, NHBE and A549 at baseline had different levels of mitochondrial superoxide, intracellular ROS and $\Delta\Psi_m$. In response to H_2O_2 , these parameters changed differently between the cell types. Mitochondrial superoxide and intracellular ROS increased in BEAS-2B and NHBE cells whereas levels remained the same in A549 cells. This may be because A549 cells have a high baseline ROS level or have an efficient mechanism for ROS removal.

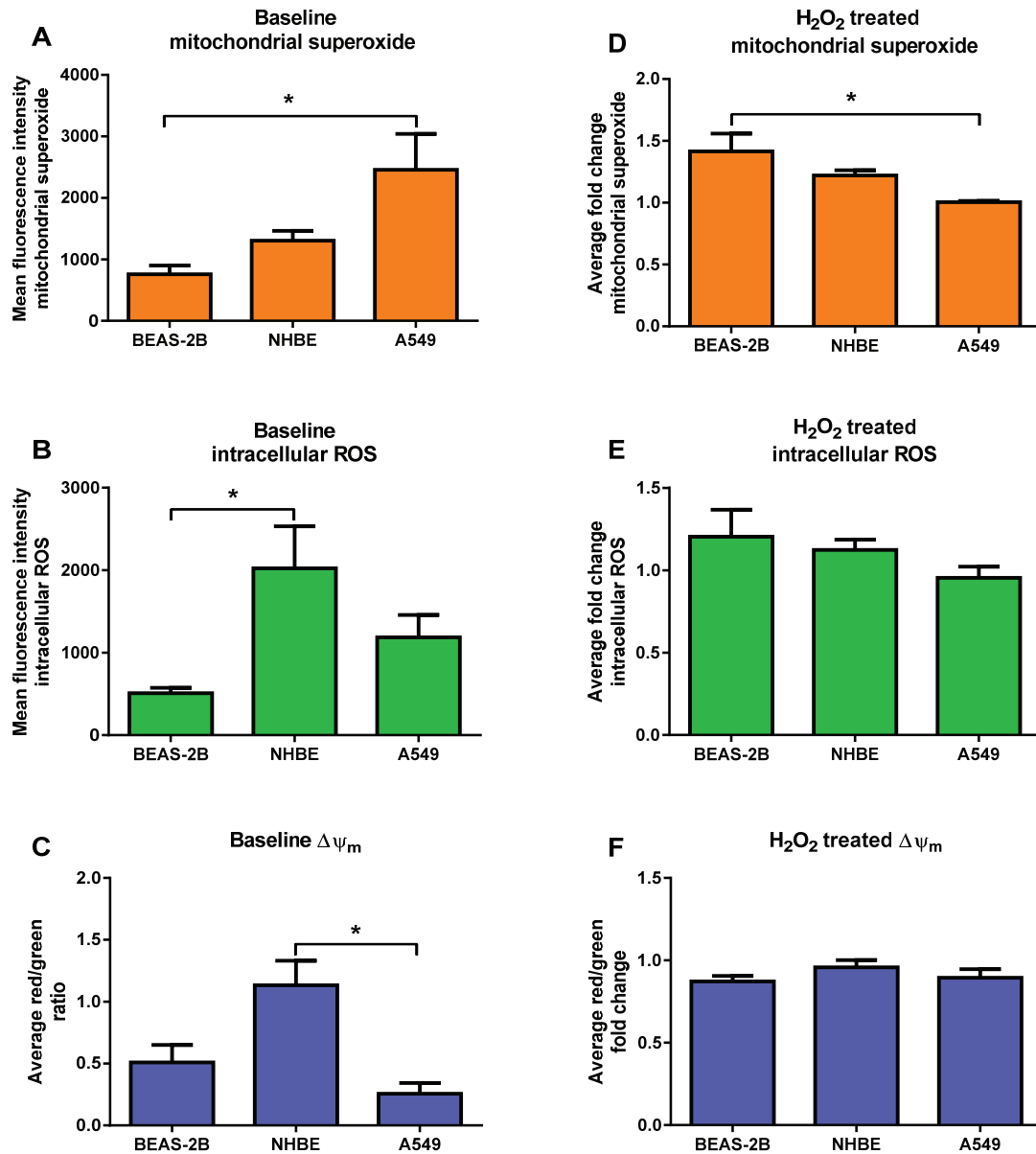


Figure 4.1 Mitochondrial function of BEAS-2B, NHBE and A549 cells at baseline and after H₂O₂ exposure

Cells were exposed to 100 μ M H₂O₂ for 4h or left untreated and were then stained with MitoSOX (mitochondrial superoxide), DCFH-DA (intracellular ROS) and JC-1 ($\Delta\psi_m$) prior to measuring fluorescence intensity using flow cytometer. The basal mitochondrial superoxide (A) and intracellular ROS (B) are presented as mean fluorescence intensity (MFI). $\Delta\psi_m$ is presented as the ratio of red and green fluorescence intensity (C). The mitochondrial superoxide, intracellular ROS levels and $\Delta\psi_m$ of 100 μ M H₂O₂ treated groups are presented as fold change compared to their controls shown in (D), (E), and (F), respectively. The data are presented as mean \pm S.E.M of three independent experiments. Comparisons were analysed using the Kruskal-Wallis test with Dunn's post-test for (A). For other comparisons, one-way ANOVA was used. * p <0.05.

Next the mitochondrial function in these cell types was investigated by mitochondrial respiration measurement using Seahorse XFe96 analyser which provides additional mitochondrial function parameters including basal respiration, ATP production, mitochondrial reserve capacity and proton leak can be obtained from cell respiration rate which monitors along with Mito Stress test compounds added during the experiment.

4.4.2 Characteristics of mitochondrial respiration in BEAS-2B, NHBE and A549 cells using Extracellular Flux Analyser (Seahorse technology)

4.4.2.1 Cell density optimisation

To detect basal oxygen consumption rate (OCR) and to observe any alteration in OCR to the Mito Stress test effectively, BEAS-2B cells were plated at 2, 4 and 6×10^4 cells/well. Both NHBE and A549 were plated at 1.5, 3.0 and 4.5×10^4 cells/well in collagen coated XFe96 cell culture microplates in supplemented BEGM for 24h, then starved overnight before the day of experiment. Each cell density was plated in triplicates. To compare the OCR among different cell densities and cell types, the obtained values were normalised to the total protein per well.

At baseline, the higher the cell density, the higher OCR was detected but was still relatively low in NHBE (Figure 4.2). According to the concentrations of reagents used for Mito Stress test in previous studies, oligomycin (ATP synthase inhibitor) concentration was used at $1 \mu\text{M}$ (Ju et al., 2016; Zhao & Klimecki, 2015). After oligomycin injection, the OCR instantly dropped and remained low until FCCP stimulation. In the first experiment, $0.5 \mu\text{M}$ FCCP was used as stated in previous studies (Ju et al., 2016; Zhao & Klimecki, 2015). The OCR after FCCP injection

increased above the basal OCR level; however, this concentration was unable to maintain this high OCR until before the injection of antimycin A and rotenone (Figure 4.2A&C). Instead of 0.5 μ M, 1.5 μ M FCCP was applied in NHBE experiments (Figure 4.2B); the OCR level sustained before the last injection. Therefore, I subsequently used 1.5 μ M FCCP in experiments for all cell types. To shut down the mitochondrial respiration completely at the end of the analysis to achieve non-mitochondrial respiration, the highest possible concentration of antimycin A/rotenone (0.9 μ M) was used because the suggested concentration (0.5 μ M) from the Mito Stress test kit protocol might partially suppress mitochondrial respiration.

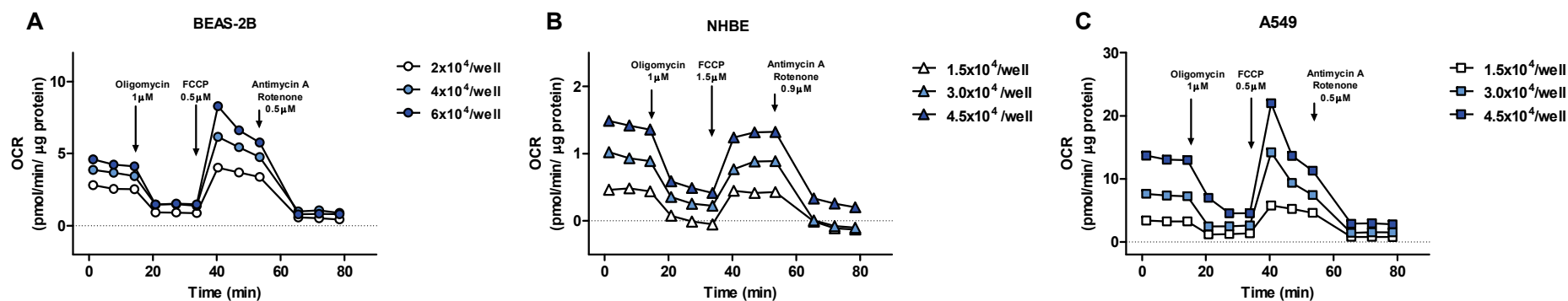


Figure 4.2 Cell density optimisation for mitochondrial respiration analysis in BEAS-2B, NHBE and A549 cells

BEAS-2B were plated at 2-6x10⁴/well (A), NHBE and A549 cells were plated at 1.5-4.5x10⁴/well (B, C) in XFe96 cell culture plates in supplemented BEGM for 24h then starved overnight before the day of experiment. Data as OCR were obtained with the XF Analyser (Seahorse Bioscience). The concentrations of reagents used for Mito Stress tests are shown in the graphs; 1µM oligomycin for all cell types. Due to being unable to elevate OCR for a certain time as the results shown in BEAS-2B and A549, the higher concentration of FCCP was applied from 0.5 to 1.5µM, and to shut down mitochondrial respiration completely, antimycin A/rotenone was changed from 0.5 to 0.9µM in a further NHBE density experiment and subsequent antioxidant experiments.

4.4.2.2 Basal mitochondrial respiratory profiles of BEAS-2B, NHBE and A549 cells

To observe whether BEAS-2B, NHBE and A549 cells show any difference in mitochondrial respiration parameters in response to the Mito Stress test, BEAS-2B cells were plated at 6×10^4 cells/well and both NHBE and A549 cells were plated at 4.5×10^4 cells/well, in supplemented BEGM for 24h and then starved overnight before the day of experiment. Each cell type was plated in triplicate. The respiration profiles were plotted separately as shown in Figure 4.3A-C.

In the experiments, compounds in the Mito Stress test kit were used at the same concentration for all cell types as follow; $1 \mu\text{M}$ oligomycin, $1.5 \mu\text{M}$ FCCP, and $0.9 \mu\text{M}$ antimycin A/rotenone, based on the previous cell density optimisation experiments. To compare the OCR among these cell types, the obtained values were normalised to the total protein per well.

BEAS-2B and NHBE cells showed a similar OCR level in response to Mito Stress tests throughout the analysis (Figure 4.3D). The OCR of NHBE cells after oligomycin injection gradually dropped (Figure 4.3B) whereas the OCR of BEAS-2B and A549 cells rapidly dropped and was maintained at the same level before FCCP injection (Figure 4.3A&C). The OCR of BEAS-2B cells reached a maximum immediately after the FCCP injection (the 7th time point) as shown in Figure 4.3A, which differed from those of NHBE and A549 where the maximal OCR was at the 9th time point (Figure 4.3B&C).

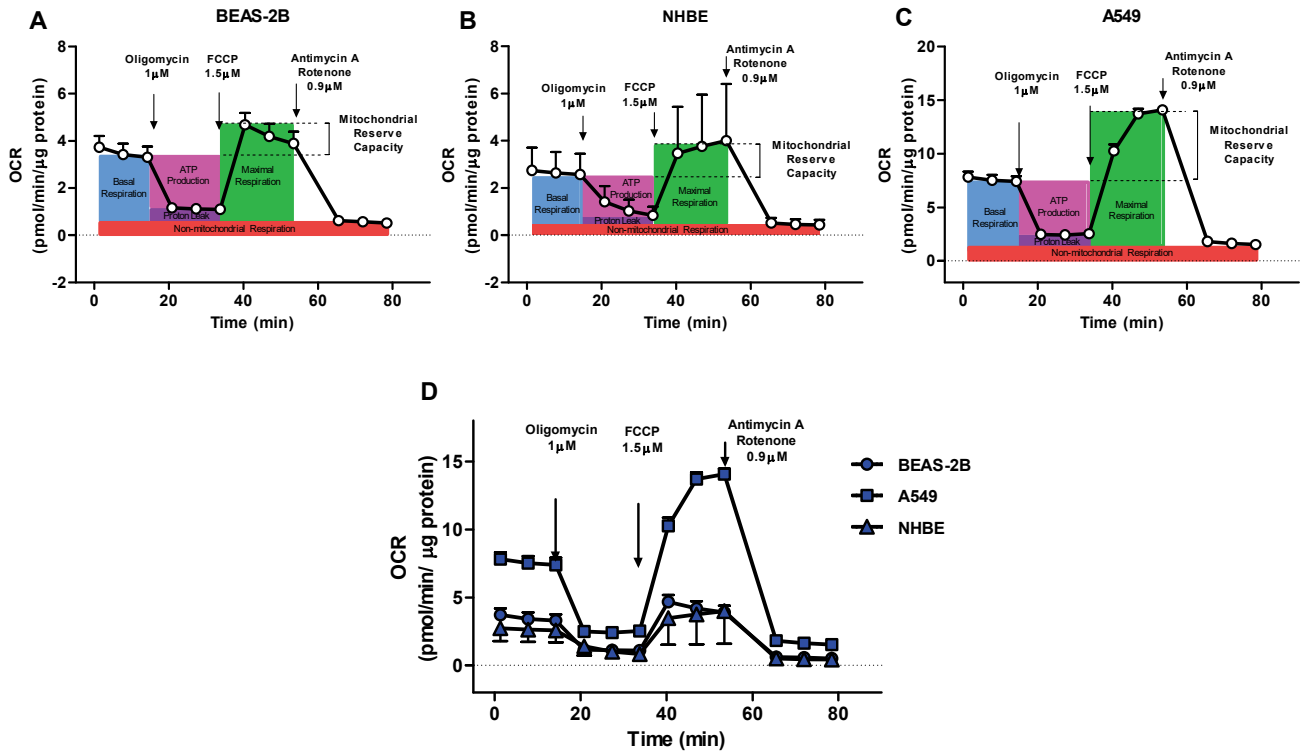


Figure 4.3 Mitochondrial respiration profiles of BEAS-2B, NHBE and A549 cells
 BEAS-2B 6×10^4 /well, NHBE and A549 4.5×10^4 /well were plated in supplemented BEGM in collagen coated XFe 96-well plate for 24h and starved overnight prior to the day of Mito Stress test. Mitochondrial respiration profiles of BEAS-2B (A), NHBE (B) and A549 (C) cells were plotted as OCR for 12 time-points. The same concentrations of oligomycin, FCCP and antimycin A/rotenone were administered to all cell types. The differential respiration profiles were plotted in (D). The data were obtained from independent experiments of four for BEAS-2B, three for NHBE and three for A549 and presented as the mean \pm S.E.M.

4.4.2.3 Basal mitochondrial respiration parameters of BEAS-2B, NHBE and A549 cells

The mitochondrial respiration parameters including basal respiration, ATP production, mitochondrial reserve capacity and proton leak were calculated and analysed using Seahorse XF Cell Mito Stress Test Report Generator (Methods section 2.2.14, Table 2.18).

At baseline, A549 cells had a higher basal OCR compared to BEAS-2B cells and significantly ($p < 0.05$) greater than NHBE cells (Figure 4.4A). The ATP production is calculated from the difference between the basal OCR and the lowest OCR after oligomycin injection. A549 cells produced more ATP compared to BEAS-2B and NHBE cells (Figure 4.4B).

The mitochondrial reserve capacity is calculated from the difference between the maximal respiration and the basal respiration. Due to the high level of maximal respiration, A549 had a higher mitochondrial reserve capacity compared to that of BEAS-2B and NHBE cells ($p < 0.05$) (Figure 4.4C). Proton leak (protons entering the mitochondrial matrix without producing ATP) was calculated by subtraction of the lowest OCR after oligomycin injection from the lowest OCR after antimycin A/rotenone injection. Mitochondria of A549 cells had a higher proton leak compared to BEAS-2B and NHBE cells but this did not reach significance (Figure 4.4D).

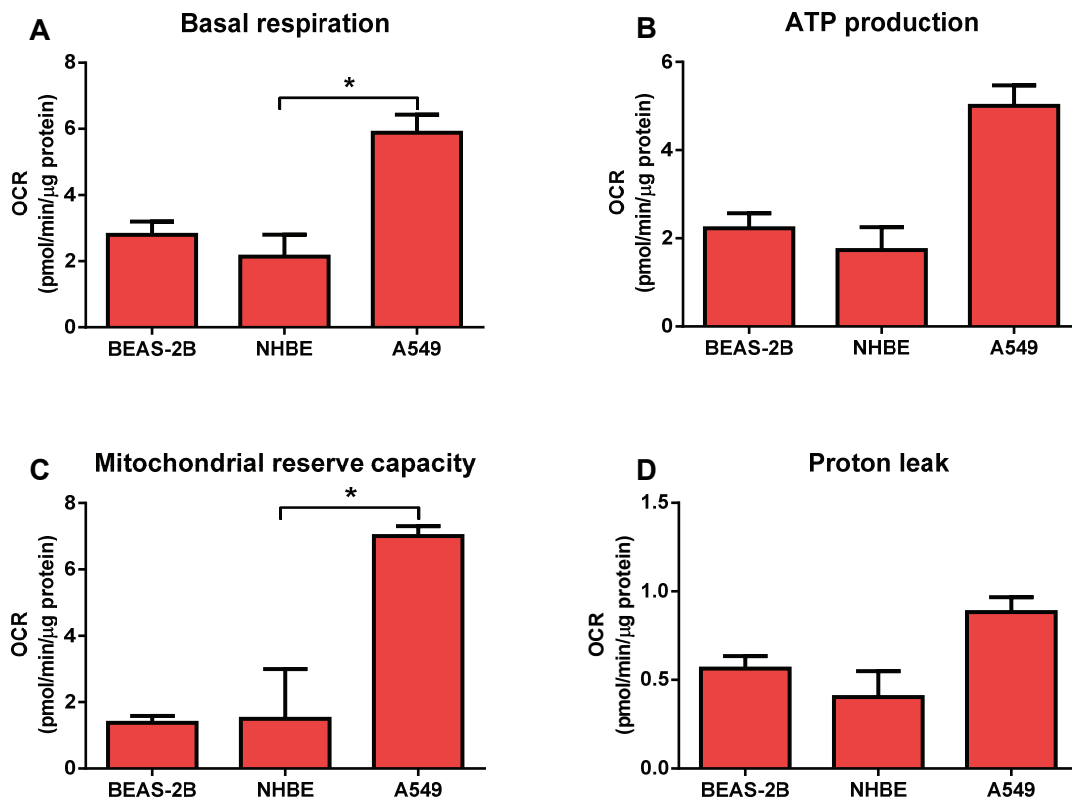


Figure 4.4 Comparison of mitochondrial respiration parameters of BEAS-2B, NHBE and A549 cells

Mitochondrial parameters calculated from OCR obtained from mitochondrial respiration profiles are presented as bar graphs of basal respiration (A), ATP production (B), mitochondrial reserve capacity (C) and proton leak (D). The data were obtained from four independent experiments for BEAS-2B cells, three independent experiments for NHBE cells and three independent experiments for A549 cells and presented as the mean \pm S.E.M. Comparisons were calculated using the Kruskal-Wallis test with Dunn's post-test analysis. * $p < 0.05$.

This data indicates differences in mitochondrial function in the three airway/lung epithelial cells tested. I wished to examine whether these differences had any functional consequences at baseline or in response to oxidative stress/inflammation. Therefore, I investigate whether the stimulation of BEAS-2B, NHBE and A549 cells with H_2O_2 and/or $IL-1\beta$ had differential effects on cell functions: proliferation and inflammatory cytokine (CXCL8) release.

4.4.2.4 Cell proliferation in BEAS-2B, NHBE and A549 cells (baseline and after H₂O₂ exposure)

To investigate whether ROS exposure affected cell proliferation differently in each cell type, BEAS-2B, NHBE and A549 cells were plated at 2,000 cells/well in collagen coated black 96-well plates. Due to nearly undetectable proliferation when incubating the cells in non-supplemented BEGM (Figure 4.5A), after starving for 16h, the cells were treated with 100 μ M H₂O₂ in supplemented BEGM and incubated for 48h prior to performing BrdU assay. The data is presented as relative fluorescence units (RFU) for cell type comparison and as percentage change when compared to their controls. At baseline, NHBE cells showed the lowest rate of proliferation whereas BEAS-2B and A549 cells were more proliferative (Figure 4.5B). Comparing with their own control groups, H₂O₂ treated NHBE cell proliferation was decreased whereas there was no change in BEAS-2B and A549 cell treated groups (Figure 4.5C). The difference in proliferation seen here with BEAS-2B cells compared with the data in Chapter 3 for these cells may reflect the presence of serum in these studies as compared to the use of serum-free media in Chapter 3.

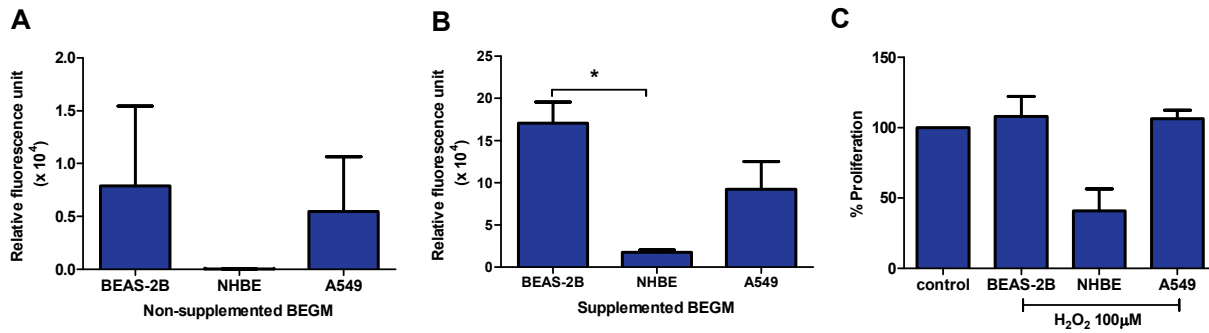


Figure 4.5 Proliferation of BEAS-2B, NHBE and A549 cells in basal state and after H_2O_2 exposure

BEAS-2B, NHBE and A549 cells were incubated in non-supplemented BEGM (A) or supplemented BEGM (B) for 48h as well as cells in supplemented BEGM were exposed to 100 μ M H_2O_2 (C) for 48h. Proliferation was measured using BrdU assay. Values are reported as relative fluorescence units (RFU) (A, B) and percentage of proliferation compared to control (C). The data are presented as the mean \pm S.E.M of three independent experiments. Comparison was calculated using the Kruskal-Wallis test with Dunn's post-hoc test. * $p < 0.05$.

4.4.3 Changes in gene expression in response to H₂O₂ and pro-inflammatory cytokine exposure in BEAS-2B, NHBE and A549 cells

To investigate whether H₂O₂ alone and in combination with an inflammatory stimulus would affect expression of genes, which have roles in metabolic control, BEAS-2B, NHBE and A549 cells were plated at 1x10⁶ cell/ well in collagen coated 6-well plates. After 16h of starvation, cells were treated with 100μM H₂O₂ for 30min followed by addition of IL-1β to give a final concentration of 1ng/ml. Cells were collected after 2h of treatment for gene expression. Real-time PCR was performed on cDNA using SYBR green probes for *AMPK*, *HIF1A* and *IL8*.

At baseline *AMPK* mRNA expression was low in all three cell types (Figure 4.6A-C). *AMPK* mRNA levels did not change in BEAS-2B and NHBE after incubation with H₂O₂ or IL-1β alone compared to control. *AMPK* mRNA expression in BEAS-2B and NHBE cells treated with the combination of H₂O₂ and IL-1β were higher than those treated with H₂O₂ or IL-1β alone (Figure 4.6A&B) whereas the expression in A549 cells treated with the combination were not changed (Figure 4.6C).

Similar to *AMPK*, low expression levels of *HIF1A* mRNA were detected at baseline in all cell types and no change in expression levels was detected with H₂O₂ or IL-1β alone when compared to the control. The *HIF1A* expression was elevated in the BEAS-2B and NHBE cells treated with the combination of H₂O₂ and IL-1β but this was not observed in A549 cells (Figure 4.6D-F).

In contrast to the *AMPK* and *HIF1A*, high levels of *IL8* mRNA expression were detected in all three cell types at baseline (Figure 4.6G-I). H₂O₂ and IL-1β exposure alone enhanced *IL8* expression in BEAS-2B cells, and the level was significantly

increased in the combination treated group compared to the control ($p < 0.05$) (Figure 4.6G). *IL8* expression showed a non-significant increase in NHBE cells when treated with H_2O_2 or IL-1 β alone and was further increased in cells exposed to combined H_2O_2 and IL-1 β treatment (Figure 4.6H). In A549 cells, *IL8* expression was increased in the IL-1 β group only ($p < 0.05$) compared to its expression in control un-treated cells. The increase in *IL8* expression in the combination treated group compared to the H_2O_2 -treated group did not reach significance (Figure 4.6I).

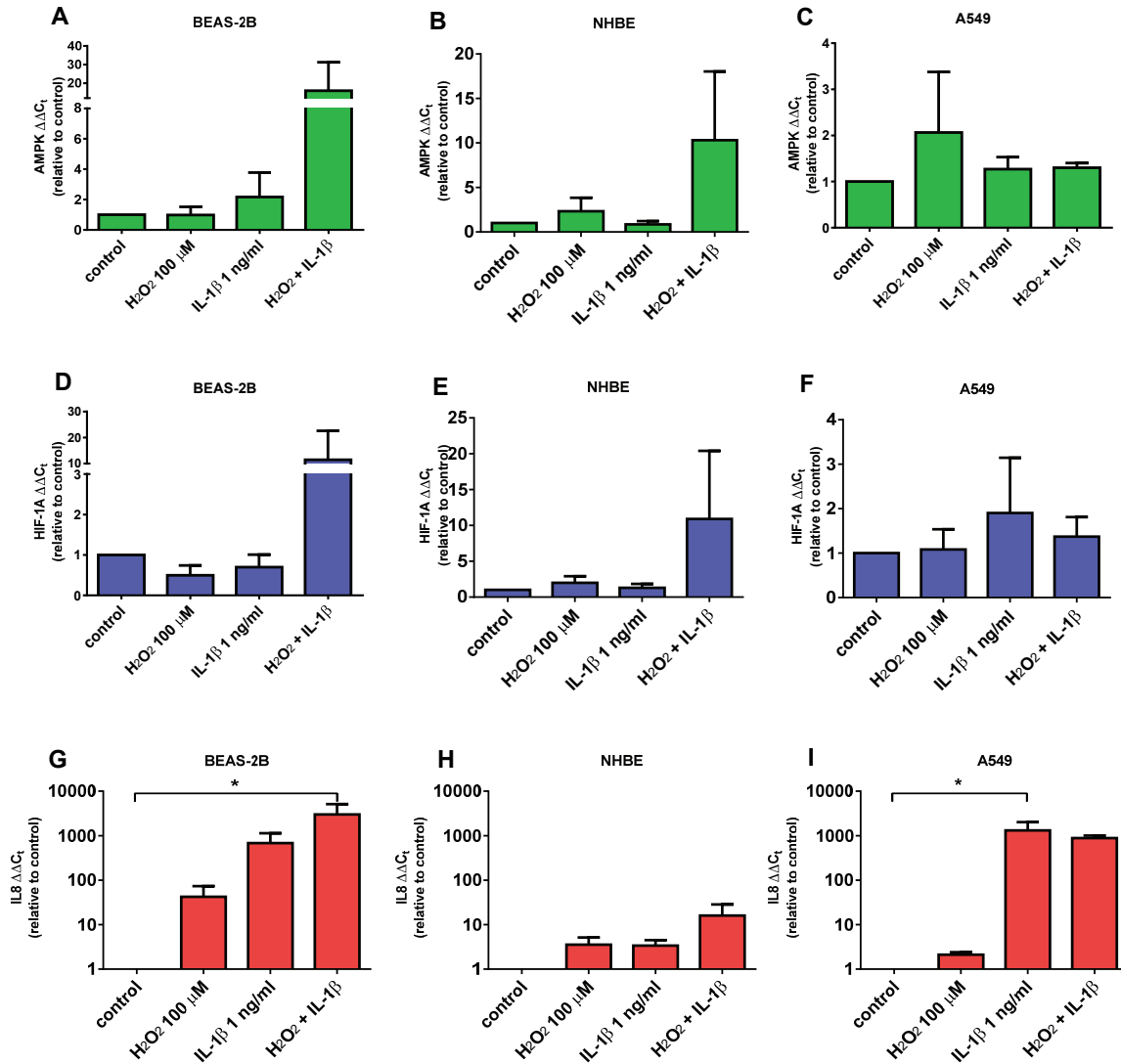


Figure 4.6 Gene expression in response to H₂O₂ and pro-inflammatory cytokine exposure in BEAS-2B, NHBE and A549 cells

Cells were plated at 1×10^6 cells/ well in collagen coated 6-well plates. After 16h starvation, cells were treated with 100 μ M H₂O₂ for 30min followed by the final concentration of 1ng/ml IL-1 β for 2h. AMPK (top panel), HIF1A (middle panel) and IL8 (bottom panel) expression were measured using RT-PCR. Data are presented as $\Delta\Delta C_t$ compared to control. The data are presented as the mean \pm S.E.M of three independent experiments. Comparisons were calculated using the Friedman's test and Dunn's post-test analysis. * $p < 0.05$ vs control.

4.4.4 Change in CXCL8 release in response to H₂O₂ and pro-inflammatory cytokine exposure in BEAS-2B, NHBE and A549 cells

Since *IL8* expression was obviously detected compared to that of other genes, CXCL8 release was determined. For the detection of CXCL8, the cells were plated

at 1.5×10^5 cell/ well in collagen coated 96-well plates. Supernatants were collected after 24h of treatment.

Increased CXCL8 release was detected in BEAS-2B and A549 cells stimulated with IL-1 β alone and in combination with H₂O₂ compared to control and H₂O₂ alone treated group (Figure 4.7A&C) whereas primary cells, NHBE, showed a high basal CXCL8 level which did not increase with treatment conditions (Figure 4.7B). This high basal CXCL8 level mean in NHBE is due to the very high basal CXCL8 level (<1,000ng/ml) of the cells used in one of the three experiments.

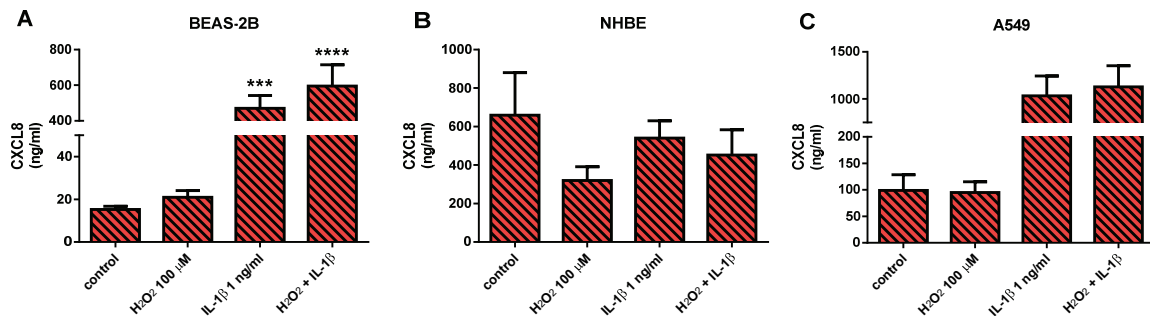


Figure 4.7 CXCL8 release in response to H₂O₂ and pro-inflammatory cytokine exposure in BEAS-2B, NHBE and A549 cells

BEAS-2B, NHBE and A549 cells (A-C) were plated at 1.5×10^5 cells/ well in collagen coated 96-well plates. After 16h starvation, cells were treated with 100 μ M H₂O₂ for 30min followed by final concentration of 1ng/ml IL-1 β for 24h. CXCL8 release was measured in the supernatants using ELISA. The data are presented as the mean \pm S.E.M of three independent experiments. Comparisons were calculated using a one-way ANOVA with Dunnett's multiple comparisons post-test analysis. *** $p < 10^{-3}$ and **** $p < 10^{-4}$ vs control.

In this section, the *IL8* expression by BEAS-2B increased in response to H₂O₂ or IL-1 β and was higher when treating with both in combination. This is in contrast to the *AMPK* and *HIF1A* mRNA expression levels which were higher only in the combination treatment. While the gene expression in NHBE were lower, an increase in response to the combination treatment was seen. These responses in NHBE cells may reflect the variable baseline response seen with

individual subject's cells as suggested by the CXCL8 release. In A549 cells, *AMPK* and *HIF1A* mRNA expression levels had minimal changes in response to the treatments but *IL8* mRNA levels increased in response to IL-1 β . The pattern of increased CXCL8 release from BEAS-2B cells was similar to that seen in A549; however, the levels were lower in BEAS-2B cells. NHBE cells did not respond to any of the treatments. Regarding these findings of the three cell types, it might indicate that the changes of metabolism, homeostatic and inflammatory responses when stimulation with oxidative stress or/and proinflammatory cytokine are different. The data suggests that neither A549 cells nor BEAS-2B can be considered good models of NHBEs at least with respect to these outputs.

This section demonstrates the differences in characteristics between these cell types including mitochondrial aspect (mitochondrial superoxide level and $\Delta\Psi_m$), basal mitochondrial respiration using Seahorse XFe96 analyser, intracellular ROS and cell functions at baseline and after H₂O₂ and/or IL-1 β treatment conditions. Next the effect of antioxidants on mitochondrial function in these cell types was also investigated using Seahorse XFe96 analyser and the mitochondrial parameters mentioned in section 4.4.2.

4.4.5 Effect of antioxidants on mitochondrial respiration parameters in H₂O₂ stimulated BEAS-2B, NHBE and A549 cells

To investigate whether the mitochondrial respiration profiles of BEAS-2B, NHBE and A549 cells respond differentially to antioxidant pre-treatment, the same antioxidants as described in Chapters 2 and 3 were studied (e.g. Methods section Chapter 2 Table 2.9). The concentrations of antioxidants used were based on the highest concentration found in Chapter 3 that did not affect BEAS-2B cell viability (Section 3.4.1).

BEAS-2B, NHBE and A549 cells were plated at 6×10^4 , 4.5×10^4 and 4.5×10^4 cells/well respectively in supplemented BEGM for 24h and starved overnight. On the day of analysis, the cells were pre-treated with 10mM NAC, 100 μ M mitoTEMPO, 500 μ M SS31, 10 μ M AP39 or 10 μ M AP219 for 1h followed by 100 μ M H₂O₂ for 4h.

4.4.5.1 Basal respiration

As shown previously, A549 cells had a higher basal respiration compared to BEAS-2B and NHBE cells. When exposed to 100 μ M H₂O₂, there was no significant change in cellular respiration in any cell type (Figure 4.8A). Pre-incubation with NAC had no significant effect on basal respiration of H₂O₂-treated NHBE, BEAS-2B or A549 cells compared to those treated with H₂O₂ alone (Figure 4.8B). Similar results were obtained when cells were pre-incubated with mitoTEMPO (Figure 4.8C), SS31 (Figure 4.8D), AP39 or its control AP219 (Figure 4.8E&F).

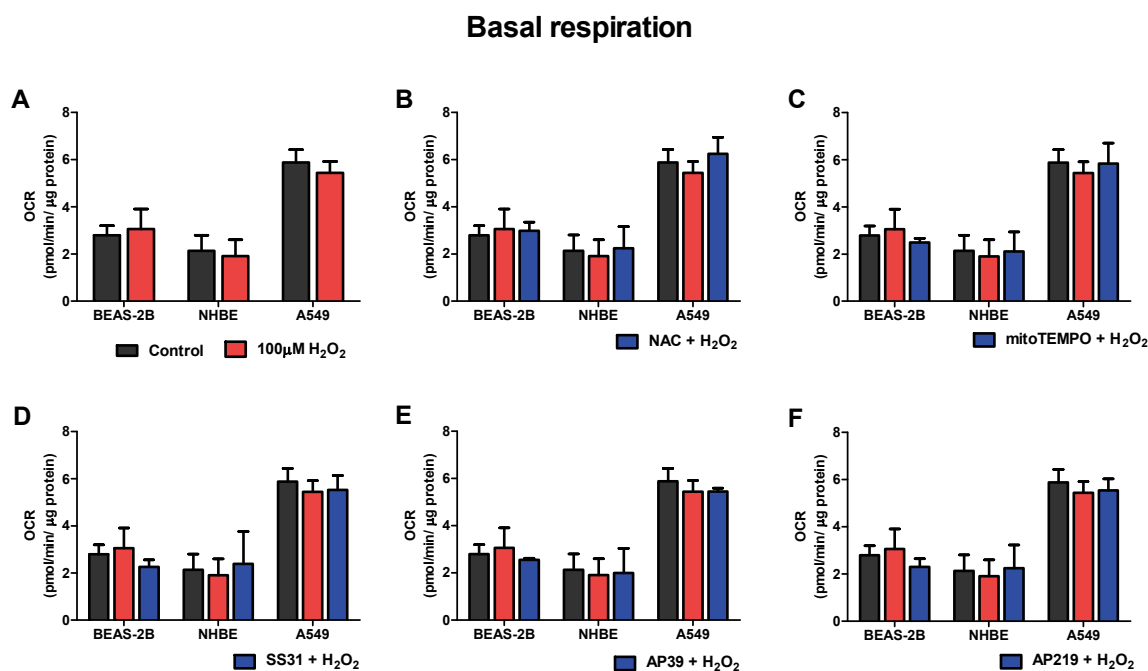


Figure 4.8 Effect of antioxidants on basal respiration of BEAS-2B, NHBE and A549

BEAS-2B 6×10^4 /well, NHBE and A549 4.5×10^4 /well were plated in supplemented BEGM in collagen coated XFe 96-well plate for 24h and starved overnight prior to the day of Mito Stress test. Basal respiration was measured prior to Mito Stress test. Bar graphs present the basal respiration as OCR of control (black), H₂O₂ (red) and antioxidant + H₂O₂ (blue). All cells were pre-treated with 10mM NAC (B) or 100μM MitoTEMPO (C) or 500μM SS31 (D) or 10μM AP39 (E) or 10μM AP219 (F) for 1h followed by 4-h 100μM H₂O₂ exposure. The data were obtained from 3-4 independent experiments and presented as the mean \pm S.E.M. Comparison was calculated using Kruskal-Wallis test and Dunn's post-hoc test.

4.4.5.2 ATP production

ATP production by A549 cells was higher than that of BEAS-2B and NHBE at baseline. There was no significant effect of H₂O₂ on ATP production in any cell type at the time-point investigated (Figure 4.9A). In addition, there were no significant effects on ATP production when these cells were pre-incubated with the antioxidants NAC and mitoTEMPO (Figure 4.9B&C), SS31 (Figure 4.9D) or AP39 and its control compound AP219 compared to the controls and H₂O₂-treated cells (Figure 4.9E&F).

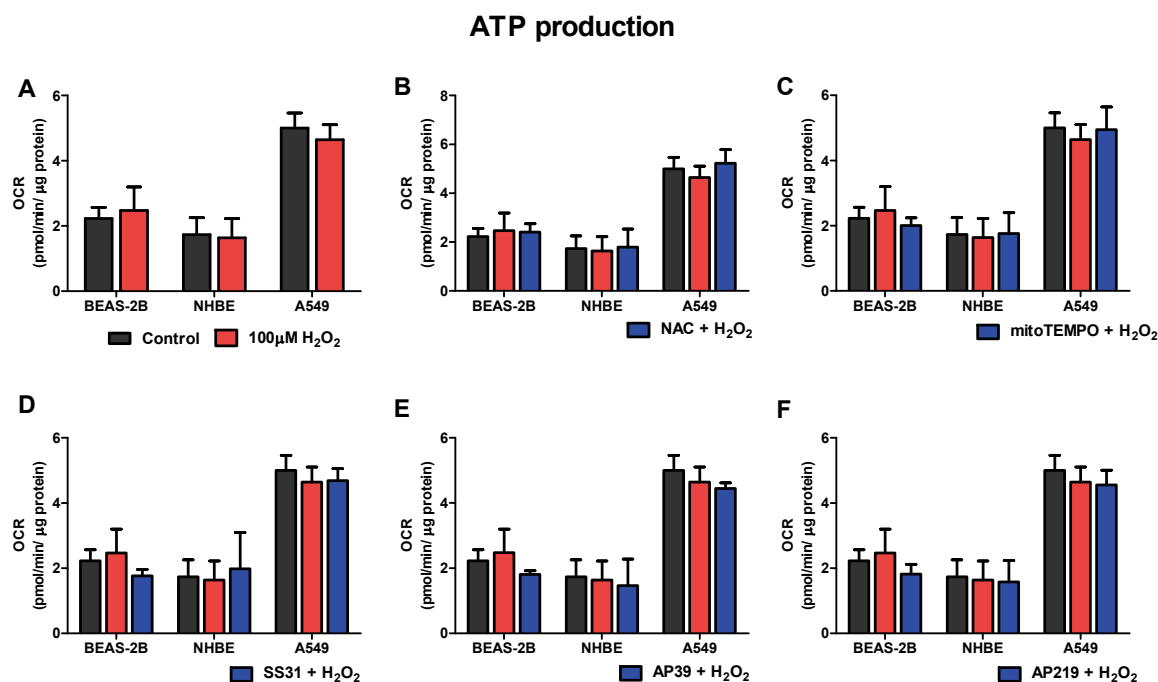


Figure 4.9 Effect of antioxidants on ATP production of BEAS-2B, NHBE and A549

BEAS-2B 6×10^4 /well, NHBE and A549 4.5×10^4 /well were plated in supplemented BEGM in collagen coated XFe 96-well plate for 24h and starved overnight prior to the day of Mito Stress test. ATP production was obtained by the difference between OCR of basal respiration and the lowest OCR after oligomycin injection. Bar graphs present the ATP production of control (black), H₂O₂ (red) and antioxidant + H₂O₂ (blue). All cells were pre-treated with 10mM NAC (B) or 100μM MitoTEMPO (C) or 500μM SS31 (D) or 10μM AP39 (E) or 10μM AP219 (F) for 1h followed by 4-h 100μM H₂O₂ exposure. The data were obtained from 3-4 independent experiments and presented as the mean \pm S.E.M. Comparison was calculated using Kruskal-Wallis test and Dunn's post-hoc test.

4.4.5.3 Mitochondrial reserve capacity

Mitochondrial reserve capacity represents the fitness of the mitochondria. At baseline, A549 cells had a much higher reserve capacity than BEAS-2B and NHBE cells and these differences were unaltered by exposure to H₂O₂ (Figure 4.10A). Although there was a trend for an increase in mitochondrial reserve capacity in H₂O₂ treated A549 cells in the presence of NAC and mitoTEMPO, this did not reach significance (Figure 4.10B&C) and no change was seen in BEAS-2B and NHBE cells with these drugs. SS31 had no effect on the reserve capacity of H₂O₂-treated A549, BEAS-2B or NHBE cells (Figure 4.10D).

A similar lack of effect was observed for pre-incubation NHBE and A549 cells with AP39. However, AP39 (Figure 4.10E), but not AP219 (Figure 4.10F), significantly reduced the reserve capacity in BEAS-2B cells.

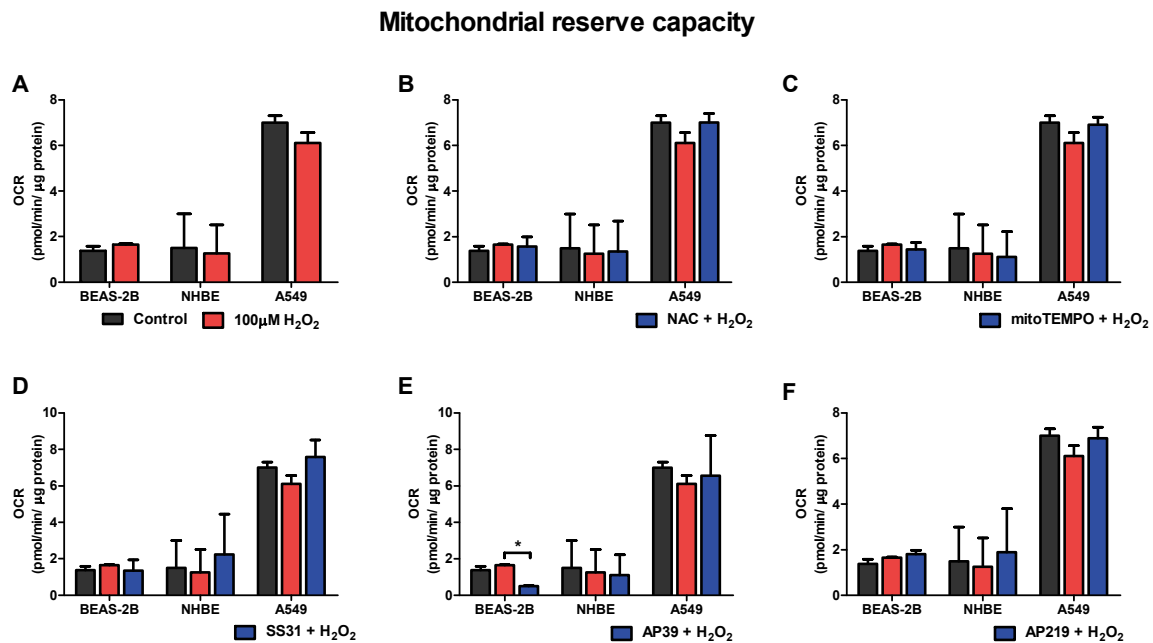


Figure 4.10 Effect of antioxidants on mitochondrial reserve capacity of BEAS-2B, NHBE and A549

BEAS-2B 6×10^4 /well, NHBE and A549 4.5×10^4 /well were plated in supplemented BEGM in collagen coated XFe 96-well plate for 24h and starved overnight prior to the day of Mito Stress test. Mitochondrial reserve capacity was obtained by the difference between maximal respiration and basal respiration. Bar graphs present the mitochondrial reserve capacity of control (black), H₂O₂ (red) and antioxidant + H₂O₂ (blue). All cells were pre-treated with 10mM NAC (B) or 100μM MitoTEMPO (C) or 500μM SS31 (D) or 10μM AP39 (E) or 10μM AP219 (F) for 1h followed by 4-h 100μM H₂O₂ exposure. The data were obtained from 3-4 independent experiments and presented as the mean ± S.E.M. Comparison was calculated using Kruskal-Wallis test and Dunn's post-hoc test. * $p < 0.05$.

4.4.5.4 Proton leak

Proton leak represents the inefficiency of oxygen consumption by mitochondria to synthesize ATP. Similar to the other mitochondrial respiration parameters compared in these cell types, the proton leak in A549 cells was higher than in the other two cell types but this difference was not as great as that seen with the other parameters.

When treated with H₂O₂, there was no change in proton leak in any cell type

compared to non-treated condition (Figure 4.11A). Pre-incubation with NAC did not significantly affect proton leak level in H₂O₂-treated cells (Figure 4.11B). Similarly, no effect was seen with MitoTEMPO and SS31 in any H₂O₂-treated cell type (Figure 4.11C&D). Finally, neither AP39 (Figure 4.11E) or AP219 (Figure 4.11F) significantly affected proton leak in any cell type studied.

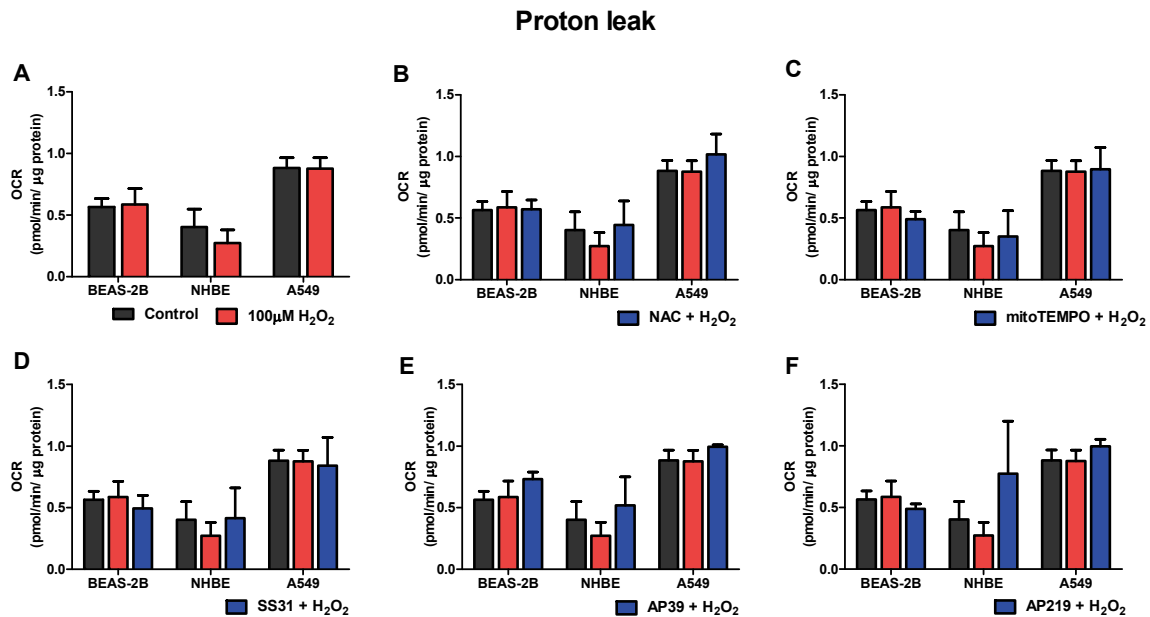


Figure 4.11 Effect of antioxidants on proton leak of BEAS-2B, NHBE and A549

BEAS-2B 6×10^4 /well, NHBE and A549 4.5×10^4 /well were plated in supplemented BEGM in collagen coated XFe 96-well plate for 24h and starved overnight prior to the day of Mito Stress test. Proton leak was obtained by the difference between the lowest OCR after oligomycin injection and the lowest OCR after antimycin A/rotenone injection. Bar graphs present the mitochondrial reserve capacity of control (black), H₂O₂ (red) and antioxidant + H₂O₂ (blue). All cells were pre-treated with 10mM NAC (B) or 100µM MitoTEMPO (C) or 500µM SS31 (D) or 10µM AP39 (E) or 10µM AP219 (F) for 1h followed by 4-h 100µM H₂O₂ exposure. The data were obtained from 3-4 independent experiments and presented as the mean \pm S.E.M. Comparison was calculated using Kruskal-Wallis test and Dunn's post-hoc test.

In summary, the data shows that at baseline A549 cells exhibit a greater level of mitochondrial respiration, ATP production, mitochondrial reserve capacity and proton leak compared to BEAS-2B and NHBE cells. Incubation of the three cell types with 100µM H₂O₂ had minimal effects on these parameters and no parameter reached significance. Pre-treatment with antioxidants, either mitochondrial-directed

or non-selective, also had no significant effect on these mitochondrial respiration parameters.

4.5 Discussion

This chapter compared the basal state and effect of H₂O₂ on non-cancerous bronchial epithelial cell line (BEAS-2B), primary bronchial epithelial cells (NHBE) and a lung cancer cell line (A549). The same procedure was used to expose all cell types as well as the same medium, exposure duration and concentration of reagents and antioxidants. The results showed different levels of mitochondrial superoxide, intracellular ROS and $\Delta\Psi_m$ between BEAS-2B, NHBE and A549 cells at baseline. In addition, the assessment of mitochondrial respiration parameters using XF analysis demonstrates that at baseline, A549 cells possess a higher basal respiration, ATP production, reserve capacity and proton leak compared to BEAS-2B and NHBE cells.

I then assessed whether these baseline differences were reflected in any functional differences. At baseline, BEAS-2B and A549 cells are more proliferative than NHBE cells. After H₂O₂ exposure, the levels of mitochondrial superoxide and intracellular ROS increased in BEAS-2B, was slightly elevated in NHBE cells, and no change in A549 cells. H₂O₂ did not alter the $\Delta\Psi_m$ in any of the cell types. No change in proliferation was seen in response to H₂O₂ in BEAS-2B and A549 cells but a decrease in proliferation was seen in NHBE cells.

These three cell types had differential levels of *AMPK*, *HIF1A* and *IL8* mRNA expression in response to H₂O₂ and/or IL-1 β . The combination of H₂O₂ and IL-1 β stimulation elevated all gene expression levels in BEAS-2B cells.

This synergistic effect was also found in NHBE cells despite low expression levels. In contrast, a change in *AMPK* and *HIF1A* expression is minimal in A549 cells with H₂O₂ and/or IL-1 β stimulation but has a greater fold change of *IL8* expression when stimulated with IL-1 β . CXCL8 release in an individual cell type in response to the stimulations follow their *IL8* expression patterns.

However, it was not possible to link these functional differences to changes in mitochondrial status as incubation with H₂O₂ caused no significant effect on mitochondrial reserve capacity or other parameters in A549 cells for example and similar to the previous chapter, mitochondrial-directed antioxidants had no effect on basal respiration in any cell type. NAC and mitoTEMPO pre-incubation provoked a small non-significant increase in ATP production and mitochondrial reserve capacity in H₂O₂ treated A549 cells while SS31 pre-incubation had minimal effect on increased mitochondrial reserve capacity in H₂O₂-treated A549 and NHBE cells. AP39, not AP219, decreased the mitochondrial reserve capacity in H₂O₂ treated BEAS-2B cells. In contrast, pre-incubation with NAC caused increases of all parameters in A549 cells although these effects were not significant. Considering the results of mitochondrial-directed antioxidants in other systems (see Chapter 1), these data were surprising and may reflect either a timing or concentration issue. In addition, the effect of mitochondrial-directed antioxidants on these functional outputs was not determined.

Cancer cells have various characteristics that distinguish them from non-cancerous cells including morphological differences such as increased nucleus/cytoplasm ratio, change in size and shape and poor differentiation. These are reflected in changes

in their functional characteristics including quickened cell cycle, gene mutations and metabolic changes that together constitute the hallmarks of cancer as proposed by Hanahan and Weinberg (Hanahan & Weinberg, 2011). These differences are driven by underlying changes in several processes including growth suppressor expression, invasion and metastasis, replicative immortality, angiogenesis induction, resistance to cell death and sustained proliferative signalling (Hanahan & Weinberg, 2011). In a similar manner, the different metabolic responses of normal and cancer cells has also been widely studying in regard to alterations in gene expression in response to oxidative stress (Cortes et al., 2011), the differential response to cytotoxic effects of anticancer agents (Babich, Krupka, Nissim, & Zuckerbraun, 2005) and the bi-phasic effect of anticancer having cytoprotective effect in normal cells and cytotoxic effect against cancer cells (Nair, Li, & Kong, 2007).

In the present study incubating cells with H₂O₂ for 4h had no effect on cell viability in any cell types. Cell viability following longer H₂O₂ treatment periods should have been performed; however, incubation of NHBE and A549 cells with H₂O₂ (100µM) for 24h has been shown to have no effect on cell viability (Jaspers et al., 2001; Shao et al., 2012; Wu, Pollack, Panos, Sporn, & Kamp, 1998). The differences seen between cell types at baseline might result from the different characteristics and the tissue of origin between cell lines and primary cells. Even though both BEAS-2B and A549 are immortalised cell lines, BEAS-2B cells were immortalised using an infection by adenovirus and represent a normal bronchial epithelial cell line (Reddel et al., 1989) whereas A549 cells originated from a patient with lung adenocarcinoma and represent a cancerous lung epithelial cell (Giard et al., 1973). NHBE cells are primary cells collected from different

healthy donors (Lechner & LaVeck, 1985) with donor-to-donor variation leading to divergence of the data.

Mutations of mitochondrial involved DNA in cancer cells leads to mitochondrial function defects and alters metabolism from OXPHOS to aerobic glycolysis known as Warburg's effect (Brandon, Baldi, & Wallace, 2006). However, cancer cell lines: A549 cells, glioblastoma cells (M059K) and breast cancer cells (MCF-7) exhibit high $\Delta\Psi_m$ and decreased oxidative metabolism compared to those of their non-cancerous cell lines: small airway epithelial cells (SAEC), fibroblasts and pulmonary smooth muscle cells (PMSC) respectively; both the $\Delta\Psi_m$ and metabolic shift of cancer cells are reversed by dichloroacetate (DCA), a PDK inhibitor (Bonnet et al., 2007).

Lower ROS levels and an elevated ROS scavenging system were found in breast cancer stem cells compared to normal stem cells suggesting that cancer cells contain a high antioxidant capacity to prevent ROS induced cellular damage (Diehn et al., 2009; Zhang, Wang, Guo, & Xuan, 2015). In lung epithelial cells (BEAS-2B), 3-month CSE exposure resulted in altered mitochondrial dynamics and morphology accompanied by increased pro-inflammatory cytokine expressions (*IL1 β* , *IL6* and *IL8*) (Hoffmann et al., 2013). Additionally H_2O_2 (200-1,000 μ M) caused a reduction in $\Delta\Psi_m$ in a concentration-dependent manner in BEAS-2B cells and increased DNA fragmentation when incubated in 500 μ M H_2O_2 for 1h (Fujii et al., 2002). In A549 cells, the treatment of 100 μ M H_2O_2 for 24h resulted in a decrease of $\Delta\Psi_m$, an increase in DNA fragmentation, and a reduced mitochondrial aconitase activity leading to apoptosis (Panduri et al., 2009). Moreover, after pre-exposure to hypoxia,

A549 cells were highly sensitive to H₂O₂ leading to DNA damage, mitochondrial activity inhibition and decreased intracellular ATP production (Erdélyi, Pacher, Virág, & Szabó, 2013).

The findings in the present study, in contrast, present lower $\Delta\Psi_m$ of A549 cells at baseline compared to BEAS-2B and NHBE cells. More ROS production occurs in cancer cells than in normal cells (Trachootham, Alexandre, & Huang, 2009) as shown in this study with A549 cells showing a higher superoxide level produced by mitochondria. The lower intracellular ROS seen in A549 cells may result from the high capacity of cellular oxidative defence system. However, oxidative-antioxidative homeostasis in various cell types are different. In a study of BEAS-2B and A549 cells there was a delayed response of DNA repair in titanium dioxide nanoparticles (TiO₂-NP) induced A549 cells compared to BEAS-2B cells; this TiO₂-NP also downregulated *NRF2* in A549 compared to BEAS-2B cells (Biola-Clier et al., 2017), indicating that A549 cells also might have a higher basal oxidative status compared to BEAS-2B.

Erlemann et al. demonstrated that a shorter duration of H₂O₂ (100µM for 20-30min) exposure was sufficient to induce 5-oxo-eicosatetraenoic acid (5-oxo-ETE, an eosinophilic chemoattractant) synthesis in A549 cells with an even greater effect seen in NHBE cells. This suggests the possibility of having a more effective ROS response pathway in NHBE cells compared to A549 cells. Thus, the higher expression of catalase activity in A549 compared to NHBE cells results in a comparatively greater ability to increase 5-oxo-ETE production in response to H₂O₂ in NHBE cells (Erlemann et al., 2006). This study has also shown that in

the presence of H₂O₂, the GSH redox cycle in NHBE cells was activated which, in turn, can accelerate H₂O₂ effects (Erlemann et al., 2006). These findings possibly explain the unchanged level of mitochondrial superoxide and intracellular ROS in H₂O₂ treated A549 cells in the present study. In contrast, another study showed increased mitochondrial superoxide and intracellular ROS levels in A549 cells induced with 500µM H₂O₂ for 24h together with the depolarisation of mitochondrial membrane. It indicates that prolonged incubation period and higher concentrations of H₂O₂ might contribute to an adequate induction.

In addition, the concentration of H₂O₂ selected may not have been optimal. H₂O₂ has a short duration of action and longer exposure to ROS by incubation with CSE or with butathione sulphoxide or knockdown of glutathione or peroxireductase using siRNA or CRISPR/Cas9 may have provided a greater stimulus. In addition, the concentrations of H₂O₂ selected were based on its effects on cell survival as determined by MTT assay – a measure of mitochondrial function. Other methods for assessing cell survival such as Trypan Blue or lactate dehydrogenase assay may have given a rationale for the use of higher concentrations of H₂O₂ for longer duration and thus given a clearer functional readout.

In the present study under the same incubation period and supplemented with BEGM, the basal proliferation rates of BEAS-2B and A549 cells were higher than in NHBE cells. At 100µM H₂O₂, all cell types were viable, but the proliferation of NHBE cells was found to be inhibited which is consistent with a previous study which showed a reduced growth rate when exposed to 6h H₂O₂ and decreased DNA synthesis in NHBE cells (Saladino et al., 1985). Due to the availability of primary

NHBE cells, viability assays were not performed concomitantly with the BrdU assay. However, in a previous study NHBE cells were found to be viable when exposed to 100 and 500 μ M H₂O₂ for 24h (Jaspers et al., 2001).

In the present study, the effects of H₂O₂ and IL-1 β stimulation on *AMPK*, *HIF1A* and *IL8* mRNA expression levels were compared between BEAS-2B, NHBE and A549 cells. AMPK is an important regulator of cellular metabolism (Mihaylova & Shaw, 2011) and is involved in the regulation of cell proliferation in NSCLC (Hardie, 2011). AMPK was found to reduce the inflammatory response in CSE-treated BEAS-2B cells and in an *in vivo* mouse study (Cheng, Li, Huang, Li, & Yao, 2017; Lee et al., 2015). In the present study, a combination of H₂O₂ and IL-1 β stimulation enhanced *AMPK* expression in BEAS-2B and NHBE cells which might suggest an effect on mitochondrial function in response to oxidative stress-induced inflammation. AMPK has a role in tumourigenesis prevention as the AMPK activator metformin decreased the incidence of cancer and reduced AMPK levels were reported in highly aggressive cancer (Hadad et al., 2009). A growth hormone-releasing hormone (GHRH) antagonist inhibited antioxidant enzymes in a prostate cancer cell line (LNCaP) (Barabutis & Schally, 2008) and also elevated AMPK protein expression in A549 cells (Siejka, Barabutis, & Schally, 2011). The variable induction/reduction of *AMPK* mRNA induction with different stimuli in A549 cells may possibly explain the unchanged *AMPK* level of A549 cells in response to the oxidative stress (H₂O₂) and IL-1 β exposure in this study.

HIF1 is a transcription factor that has a role in cellular adaptation to low oxygen conditions (hypoxia) (Majmundar, Wong, & Simon, 2010). HIF1 is upregulated by inflammatory stimuli including TNF α /IL4 in BEAS-2B cells (Jiang, Zhu, Xu, Sun, & Li, 2010) and is associated with a poor prognosis in NSCLC patients (Yohena et al., 2009). Similarly, in the present study, the combination of oxidative stress and inflammatory stimulation increased *HIF1A* mRNA levels in BEAS-2B cells whereas NHBE and A549 cells had a minimal increase in *HIF1A*. However, HIF1A expression was found to be increased in A549 cells under hypoxic conditions and inhibition of HIF1A by LW6 induced apoptosis through an increase in mitochondrial ROS formation (Sato et al., 2015). Therefore, *HIF1A* expression might contribute to oxidative stress under hypoxic conditions.

IL8 is an inflammatory cytokine involved in the pathogenesis of COPD (Zhang et al., 2011). *IL8* expression is increased in H₂O₂ treated BEAS-2B (Khan et al., 2014) and A549 cells which requires the binding of redox-responsive transcription factors (AP-1 and NF- κ B) to the *IL8* promoter (Lakshminarayanan et al., 1998) and is attenuated by carbocysteine (an indirect antioxidant) (Wang et al., 2015). *IL8* mRNA levels are upregulated in response to NF- κ B-mediated induction in BEAS-2B and NHBE cells (Khan et al., 2014), and in response to carbon nanotubes via ROS production in A549 cells (Ye, Wu, Hou, & Zhang, 2009).

AMPK, HIF1A and IL8 can all regulate/modulate inflammatory processes in response to oxidative stress. CSE as an oxidative stress increased the phosphorylation of AMPK and IL8 production in A549 cells (Lee et al., 2015). Evidence showing the effect of oxidative stress and pro-inflammatory stimulation from these previous

studies might support the present study demonstrating that incubation with H₂O₂ increases *IL8* in BEAS-2B but not in NHBE and A549 cells whereas IL-1 β stimulation increases *IL8* expression in BEAS-2B and A549 cells. Despite the lower *IL8* expression of NHBE cells compared to other cell types, its expression was also significantly enhanced by IL-1 β compared to control. The 2h incubation time was fixed for all cell types in these experiments as this was the optimal time point for induction in BEAS-2B cells (Chapter 3). Future experiments should optimise the time-course and concentration-response required to obtain detectable expression of *AMPK* and *HIF1A* in each cell type.

In the assessment of respiration, key parameters including basal respiration, ATP production, mitochondrial reserve capacity and proton leak were obtained by analysing OCR. This was in contrast to the fluorescence methods used in the earlier experiments which assess mitochondrial function using $\Delta\Psi_m$ and mitochondrial superoxide production (Brand & Nicholls, 2011). Although an effect of H₂O₂ was observed with the less sensitive fluorescent approaches, the more accurate XF analysis did not report any effect. This is despite the functional effect observed with these concentrations of H₂O₂.

The number of cells required for XF analysis experiments were determined from previous studies of BEAS-2B (2-3x10⁴/well) (Koo et al., 2015; Zhao & Klimecki, 2015; Zhao, Severson, Pacheco, Futscher, & Klimecki, 2013) and A549 (2-6x10⁴/well) (Jia, Gu, Chen, & Jiao, 2016; Ju et al., 2016; Wang et al., 2015). Also the ranges of cell numbers were optimised to obtain a certain level of OCR in the experiments. Owing to there being no published data on primary lung

epithelial cells, optimisation of NHBE cell number was performed and found to be between $1.5-4.5 \times 10^4$ /well. The recommended FCCP and antimycin A/rotenone concentrations failed to have the expected effect on OCR parameters and higher concentrations had to be used (Figure 4.3). This may reflect specific issues with the cell types used and impact upon the efficacy of the mitochondrial-directed antioxidants used in the study.

Differences of bioenergetic profiles between normal cells and cancer cells have been demonstrated in ovarian cancer cell lines which demonstrate a higher mitochondrial respiration rate and ATP production compared to normal ovarian surface epithelial cells (Dier, Shin, Hemachandra, Uusitalo, & Hempel, 2014). These findings are similar to a study which measured mitochondrial respiration by detection of dissolved O_2 concentration in a cell chamber in normal bronchial epithelial cells (HBEC30KT) and a NSCLC cell line (HCC4017), in which heme biosynthesis enhanced energy production leading to increased proliferation and progression of cancer cells (Hooda et al., 2013). The different basal metabolic state of BEAS-2B, NHBE and A549 cells has been reported in a study examining the effect of anoxia (Shahriary, Chin, & Nussbaum, 2012). By measuring ATP activity in mitochondria, A549 cells had the highest level of mitochondrial activity at baseline (normoxia) whereas under anoxia, all cell types showed decreased mitochondrial activity. However, a longer anoxic incubation period to decrease cellular metabolism was required in BEAS-2B and NHBE cells (2 days) compared to A549 cells (1 day). Oxygen deprivation creates cell stress causing the accumulation of free radicals which leads to cellular dysfunction and damage (Majmundar et al., 2010).

In spite of using different methods for stress induction and detection methods (Shahriary et al., 2012), these findings are partially consistent with mitochondrial parameters in that I show that A549 cells possess the highest level of basal respiration, ATP production and reserve capacity compared to BEAS-2B and NHBE cells in the basal state. However, there was no significant change in these parameters in all cell types studied when exposed to 4h H₂O₂. This might be due to the short period of stress-induced incubation time and the different times-to-react required in the individual cell types. Due to limited access to the XF analyser, I was unable to perform full a time-course analysis of OCR changes in response to H₂O₂ in each different cell type. These experiments, along with a full concentration response analysis of H₂O₂ alone and in combination with IL-1 β , might provide greater clarity of the role of oxidative stress and inflammation on mitochondrial function.

Studies of the bioenergetic effect of mitochondrial-directed antioxidants using the extracellular flux analyser have investigated AP39-treated primary neurons from transgenic mice in an Alzheimer's disease model and in murine endothelial cells in a hyperglycaemic injury prevention model (Gerő et al., 2016; Zhao et al., 2016). These studies found that AP39 increased basal respiration and maximal respiration capacity at a low concentration, but that the effect was reversed at higher concentrations as mentioned in the discussion in previous chapter. Similar to the result of this chapter that pre-incubation with AP39, but not with AP219, significantly decreased the mitochondrial reserve capacity in BEAS-2B cells. However, using a single concentration of AP39 in the present study, I was unable to see any effect of AP39 on other basal respiration parameters in the presence or absence of H₂O₂.

This may be in part due to the lack of effect of the concentration of H_2O_2 used here but may also be due to the differential effect seen in OCR parameters at different AP39 concentrations. The incubation time in this study is also a consideration since a prolonged incubation period of antioxidant will affect the cytotoxicity of NHBE cells especially with AP39. The incubation was shortened from 3h in Chapter 3 to 1h as a study showed the protective effect by maintaining ATP production of a kidney epithelial cell line when pre-incubated with AP39 for 30 min (Ahmad et al., 2016). In addition, as access to the analyser was limited, I decided to decrease the incubation time. A time course experiment for each antioxidant and each cell type would need to be performed to see their effect clearly. A full concentration response analysis should be performed for these inhibitors for each cell type studied at baseline and after exposure to H_2O_2 . Interestingly, the decreased mitochondrial reserve capacity in H_2O_2 treated A549 cells are reversed by the antioxidant pre-incubation which possibly causes an effective coupling of the respiration process between OXPHOS and ATP synthesis.

Comparing the mitochondrial function between normal and cancer cells in the present study requires further investigation to explore the mechanisms underlying their differences with respect to mitochondrial respiration at baseline and in response to other oxidative stresses such as cigarette smoke or with a greater H_2O_2 concentration range. It may be important to re-examine the effect of each mitochondrial-directed antioxidant in cell type individually in concentration-dependent and time-dependent experiments. In addition, the data highlights the problem of using A549 and BEAS-2B cells as models of NHBE redox functions. Although I was unable to demonstrate a clear link between

oxidative stress, inflammation and mitochondrial function in a reproducible *in vitro* model in airway/lung epithelial cells, the clinical data discussed in Chapter 1 supports a link between mitochondrial dysfunction and cancer. Therefore, in the next chapter I used tumour and non-tumour samples from patients with lung cancer with and without COPD to determine whether there were changes in mitochondrial genes, proteins and functional aspects that linked cancer and COPD.

**Chapter 5 Investigation of
mitochondrial function,
gene expression and morphology
in lung tissue of lung cancer
patients**

5.1 Introduction

In the previous results chapters I have shown that H₂O₂, as an oxidative stress, impaired mitochondrial function and increased mitochondrial superoxide production accompanied with increased inflammatory responses in BEAS-2B. In cellular models, there was a modest effect of some antioxidants such as NAC and AP39 on mitochondrial superoxide (Figure 3.18) and mitochondrial function levels (Figure 3.19). In primary bronchial epithelial cells (NHBE) and a lung cancer cell line (A549) I demonstrated differences in mitochondrial function and ROS production at the basal state. Furthermore, I found that A549 (adenocarcinoma cell line) had reduced mitochondrial function (increased proton leak) and a higher mitochondrial respiration capacity than NHBE and BEAS-2B cells. Contrary to expectations there was no significant effect of H₂O₂ on mitochondrial parameters as determined by Seahorse analysis at the time and concentration used.

The overall hypothesis is that mitochondrial dysfunction links the higher incidence of NSCLC in COPD patients. This chapter will use matched lung tissue (tumour and non-tumour) from patients with lung cancer (with/without COPD) to investigate the association of genes involved in mitochondrial structure and function in COPD and in relation to smoking. Firstly, I examined and analysed metabolic pathway signatures from published data sets studied in patients with COPD and lung cancer using Gene Set Variation Analysis (GSVA). Previous studies have shown that the glucose metabolic pathway of cancer cells shifted from the production of ATP from the OXPHOS pathway to that from the glycolysis pathway. This is due to the increased activation of glycolytic enzymes e.g. GLUT1 and PKM2 which increase glucose uptake and pyruvate production respectively, and of PDK which inhibits

acetyl CoA production which feeds the Krebs's cycle (Cairns, Harris, & Mak, 2011; Younes, Lechago, Somoano, Mosharaf, & Lechago, 1996). Secondly, I focused on investigating the expression of specific mitochondrial genes between matched non-tumour and tumour tissues from lung cancer patients. Since mitochondrial dysfunction in cancer also results from mutations in mitochondrial proteins (Brandon et al., 2006; Roberts & Thomas, 2013), I screened mitochondrial gene candidates using a public database providing RNA expression profiles (Cancer RNA-Seq Nexus). I selected a mitochondrial protein, NDUFA9, from the protein expression public database analysis to compare the protein expression in alveolar macrophages and bronchial epithelial cells between background and tumour tissues, and to investigate whether smoking habits and COPD alter the expression of this protein.

Observing mitochondrial structural changes using electron microscopy can determine the mitochondrial dynamics of the cells (Yaffe, 1999). A study in lung tissue samples from COPD patients showed that the shape of the mitochondria in the bronchial epithelium was changed under long-term exposure to CSE *in vitro* which is consistent with the abnormal mitochondrial morphology observed in bronchial epithelium from COPD patients (Hoffmann et al., 2013). More fragmented and swollen mitochondria were found in smokers with COPD compared to non-smokers with COPD (Hara et al., 2013) suggesting the effect of oxidative stress on mitochondrial morphology could possibly be involved in cancer development. However, the structure of mitochondria within the lung epithelium of patients with lung cancer has not been investigated. Therefore, I also assessed mitochondrial structure within the bronchial epithelium, alveolar epithelium, and alveolar

macrophages of non-smokers, healthy smokers and COPD subjects who have lung cancer.

5.2 Hypothesis

Metabolic alterations in the lung of smoking/COPD patients results in changes in mitochondrial function which may lead to the development of lung cancer.

5.3 Aims

- To assess the enrichment of gene signatures defining cellular metabolism pathways in lung cancer patients with and without COPD

- To investigate mitochondrial function in lung tissue collected from lung cancer patients comparing between matched non-tumour and tumour tissue

- To investigate the differences in metabolic gene expression between matched non-tumour and tumour tissue from lung cancer patients

- To compare mitochondrial protein expression between background lung tissue and tumour tissue from lung cancer patients with different smoking habits

- To illustrate the morphology of mitochondria in different cell types in lung tissue from non-smokers, smokers and COPD subjects who have lung cancer

5.4 Results

5.4.1 Enrichment scores in metabolic pathway signatures by gene set variation analysis (GSVA)

GSVA was used to determine whether the expression of genes relating to key metabolic pathways (pathway signature) was enriched as a group in patients with COPD and lung cancer. GSVA calculates sample-wise enrichment scores (ES) irrespective of any group labels, thus enabling the implementation of null hypothesis-based statistical analysis (Hänzelmann, Castelo, & Guinney, 2013). The ES in each subject is a summarization of the genes related to the pathway and was used to compare the overall expression of the set of genes between groups.

OXPPOS, KEGG.glycolysis and Biocarta.glycolysis signatures (Table 5.1) were used to analyse gene array data from each subject in two datasets. Both glycolysis signatures were used due to some genes in the KEGG signature not being present in Biocarta and vice versa. The datasets used were from an investigation of differential gene expression profiles in normal bronchial epithelium and in squamous cell carcinoma (SCC) (GSE12428 and GSE12472) (Boelens et al., 2009, 2011) and another study investigating antioxidant response gene expression in bronchial airway epithelial cells of smokers at risk of lung cancer (GSE19027) (Wang et al., 2010).

Table 5.1 Gene sets representing specific processes and cell signature

Signatures	Genes in signature
OXPPOS	<i>ND1 ND2 ND3 ND4 ND4L ND5 ND6 NDUFS1 NDUFS2 NDUFS3 NDUFS4 NDUFS5 NDUFS6 NDUFS7 NDUFS8 NDUFV1 NDUFV2 NDUFV3 NDUFA1 NDUFA2 NDUFA3 NDUFA4 NDUFA4L2 NDUFA5 NDUFA6 NDUFA7 NDUFA8 NDUFA9 NDUFA10 NDUFAB1 NDUFA11 NDUFA12 NDUFA13 NDUFB1 NDUFB2 NDUFB3 NDUFB4 NDUFB5 NDUFB6 NDUFB7 NDUFB8 NDUFB9 NDUFB10 NDUFB11 NDUFC1 NDUFC2 NDUFC2-KCTD14 SDHA SDHB SDHC SDHD UQCRC1 CYTB CYC1 UQCRC1 UQCRC2 UQCRH UQCRHL UQCRB UQCRQ UQCR10 UQCR11 COX10 COX3 COX1 COX2 COX4I2 COX4I1 COX5A COX5B COX6A1 COX6A2 COX6B1 COX6B2 COX6C COX7A1 COX7A2 COX7A2L COX7B COX7B2 COX7C COX8C COX8A COX11 COX15 COX17 ATP5A1 ATP5B ATP5C1 ATP5D ATP5E ATP5O ATP6 ATP5F1 ATP5G1 ATP5G2 ATP5G3 ATP5H ATP5I ATP5J2 ATP5L ATP5J ATP8 ATP6V1A ATP6V1B1 ATP6V1B2 ATP6V1C2 ATP6V1C1 ATP6V1D ATP6V1E2 ATP6V1E1 ATP6V1F ATP6V1G1 ATP6V1G3 ATP6V1G2 ATP6V1H TCIRG1 ATP6V0A2 ATP6V0A4 ATP6V0A1 ATP6V0C ATP6V0B ATP6V0D1 ATP6V0D2 ATP6V0E1 ATP6V0E2 ATP6AP1 ATP4A ATP4B ATP12A PPA2 PPA1 LHPP ENO1</i>
Biocarta.glycolysis	<i>ENO1 ALDOB GAPDH GPI HK1 PFKL PGAM1 PGK1 PKLR TPI1</i>
KEGG.glycolysis	<i>ENO2 ENO3 GAPDH PGAM1 PGAM2 PGAM4 PGK1 PGK2 PKLR PKM TPI1</i>

The first dataset (GSE12428) contained expression profiles of 28 normal bronchial epithelium samples (16 without smoking at least 1 year before surgery and 12 with smoking until surgery) compared with 35 squamous cell carcinoma (SCC) samples in which 15 did not smoke at least 1 year before surgery and 19 smoked until surgery. Using GSVA, there was a significant increase in the OXPPOS signature in SCC compared to patients without SCC (Figure 5.1A). There was no difference in the OXPPOS signature in SCC tumour samples when segregated according to smoking status (Figure 5.1B). This indicates that although smoking affects OXPPOS, smoking cessation for a year might not change the expression of OXPPOS genes.

GSE12428

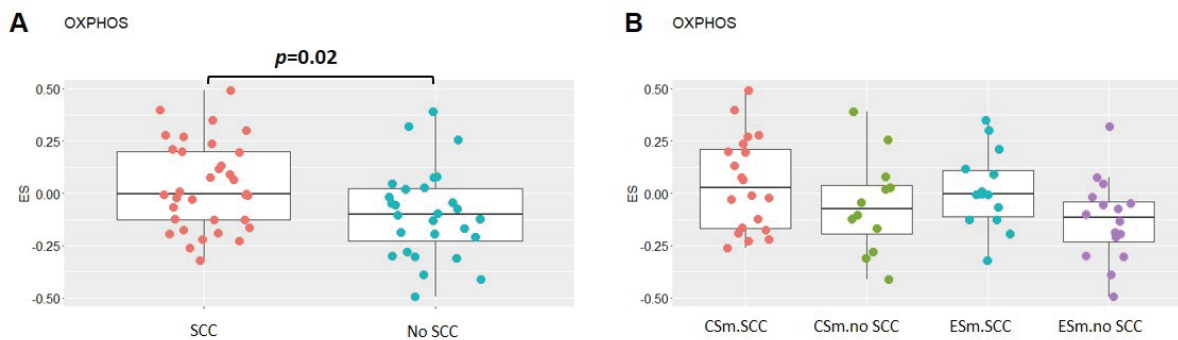


Figure 5.1 Enrichment scores (ES) of the OXPPOS signature in squamous cell tumour of both current smokers and ex-smokers (GSE12428)

Each dot represents enrichment in a single subject of expression in samples of squamous cell carcinoma (SCC, red) and of no SCC (blue) patients (A), and in squamous cell tumour of current smokers (CSm.SCC) and of ex-smokers (ESm.SCC) (red & blue respectively) versus normal bronchial epithelium in current smokers (CSm.no SCC) and of ex-smokers (ESm.no SCC) (green & purple respectively) (B). Data are presented as individual data point for each subject, box-and-whisker plot showing median and interquartile range. The ES differences between the two medians were analysed using Student's t-test and across group medians were analysed using ANOVA.

There was a significantly higher ES of both Biocarta and KEGG glycolysis signatures in the SCC group compared to non-SCC group (Figure 5.2A&B). With smoking status, there was no difference in ES between current smokers (CSm) and ex-smokers (ESm) either in SCC samples or in the normal bronchial epithelium samples (no SCC) (Figure 5.2C&D).

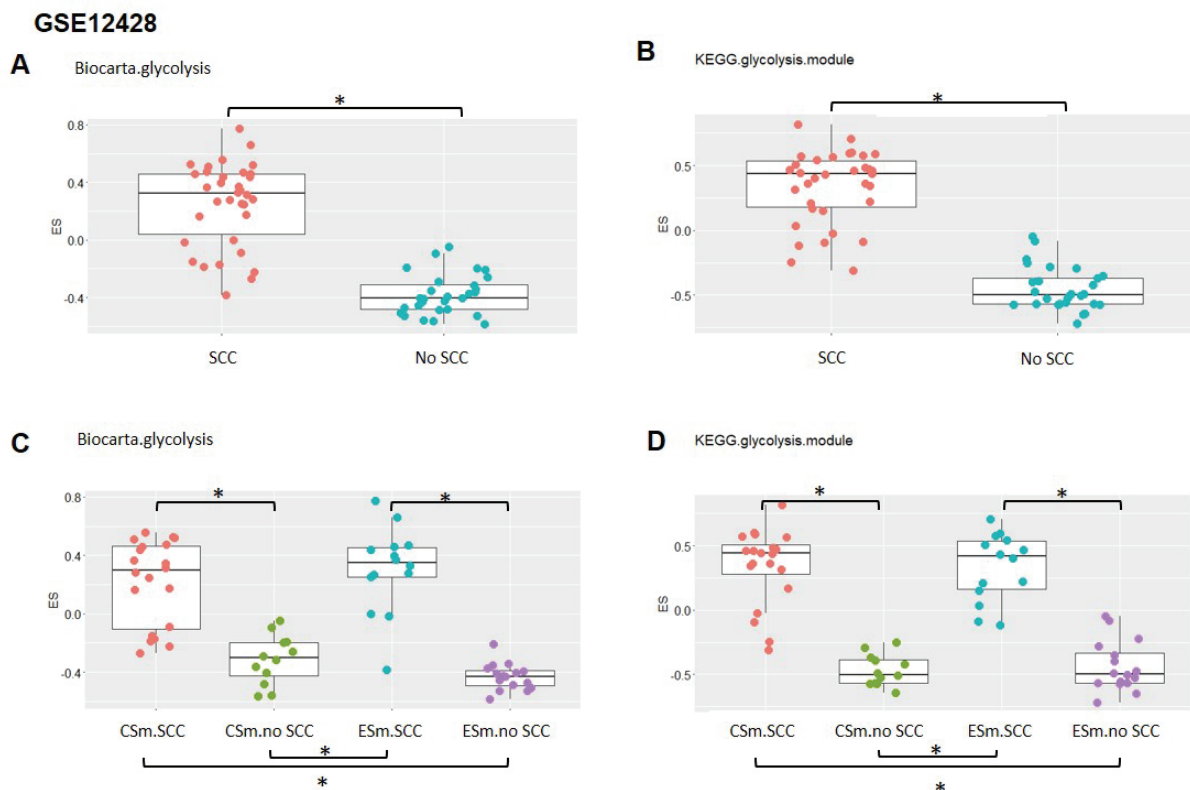


Figure 5.2 Higher enrichment scores (ES) of glycolysis signatures in squamous cell tumour of both current smokers and ex-smokers (GSE12428)

Each dot represents enrichment in a single subject of expression in samples of squamous cell carcinoma (SCC, red) and of no SCC (blue) patients analysed using Biocarta.glycolysis and KEGG.glycolysis (A & B respectively), and in SCC of current smokers (CSm.SCC) and of ex-smokers (ESm.SCC) (red and blue respectively) versus normal bronchial epithelium in current smokers (CSm.no SCC) and ex-smokers (ESm.no SCC) (green and purple respectively) (C & D). Data are presented as individual data points for each subject, box-and-whisker plot showing median and interquartile range. The ES differences between the two medians were analysed using Student's *t*-test and across group medians were analysed using ANOVA. * $p < 10^{-4}$.

To determine whether the expression of OXPHOS and glycolysis signatures in COPD patients is altered with lung cancer, I examined a second dataset (GSE12472) which contained expression profiles from 28 normal bronchial epithelium samples (10 without COPD and 18 with COPD) compared with 35 SCC samples in which 17 did not have COPD and 18 had COPD. Using GSVA, there was a greater spread of data within the groups compared to that seen with the GSE12428 data set and no significant difference in ES of OXPHOS signature was observed between SCC patients and patients who do not have cancer (no SCC) irrespective of COPD status (Figure 5.3A). With separation between COPD and non-COPD patients, there was again no difference in ES between the no SCC group and SCC groups. The SCC patients without COPD group (no COPD.SCC) displayed the lowest ES median for OXPHOS (Figure 5.3B). However, current smoking status was not available for this dataset. Overall, this data indicates that OXPHOS expression is maintained despite chronic exposure to oxidative stress from smoking.

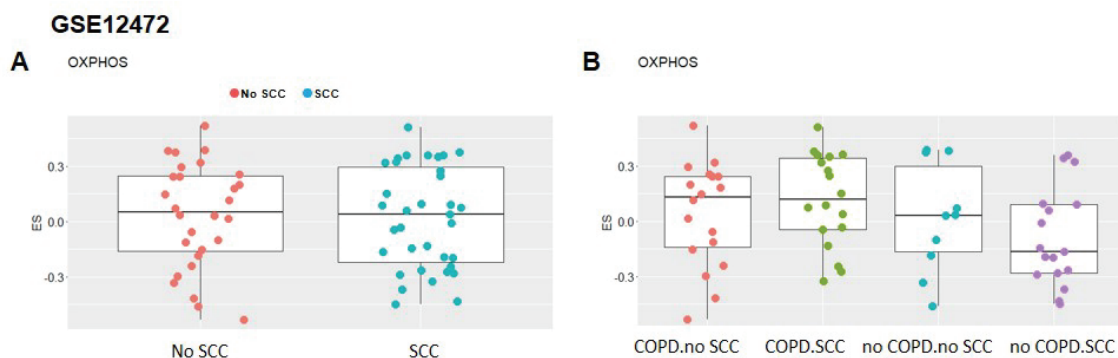


Figure 5.3 Enrichment scores (ES) of the OXPHOS signature in squamous cell tumour of both non-COPD and COPD patients (GSE12472)

Each dot represents enrichment in a single subject of expression in samples of no squamous cell carcinoma (no SCC, red) and of SCC (blue) patients (A), and in normal bronchial epithelium of COPD and of non-COPD patients (red & blue respectively) versus squamous cell tumour in COPD and non-COPD patients (green & purple respectively) (B). Data are presented as individual data points for each subject, box-and-whisker plot showing median and interquartile range. The ES differences between the two medians were analysed using Student's *t*-test and across group medians were analysed using ANOVA.

There was a significantly higher median ES of both Biocarta and KEGG glycolysis signatures in the SCC group compared to normal (no SCC) group (Figure 5.4A&B). However, there was no difference in ES between non-COPD and COPD patients when compared with the no SCC or SCC groups. The ES in SCC groups regardless of COPD are significantly higher compared to no SCC groups suggesting that the switch of metabolic pathways from OXPHOS to glycolysis in SCC is not dependent on COPD status (Figure 5.4C&D).

GSE12472

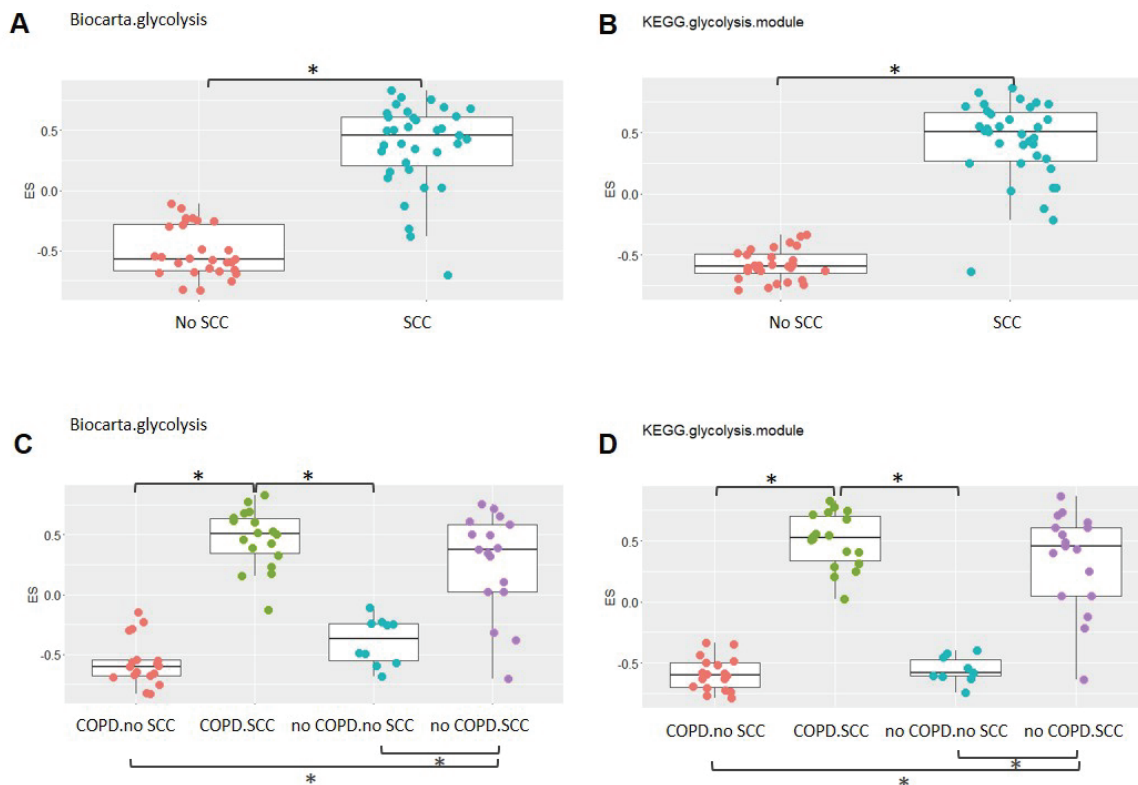


Figure 5.4 Higher enrichment scores (ES) of glycolysis signatures in squamous cell tumour of both non-COPD and COPD patients (GSE12472)

Each dot represents enrichment in a single subject of expression in samples of no squamous cell carcinoma (no SCC, red) and of SCC (blue) patients analysed using Biocarta.glycolysis and KEGG.glycolysis (A & B respectively), and in no SCC of COPD (COPD.no SCC) and of non-COPD (no COPD.no SCC) patients (red and blue respectively) versus squamous cell tumour in COPD (COPD.SCC) and non-COPD (no COPD.SCC) patients (green and purple respectively) (C & D). Data are presented as individual data points for each subject, box-and-whisker plot showing median and interquartile range. The ES differences between the two medians were analysed using Student's *t*-test and across group medians were analysed using ANOVA. * $p < 10^{-4}$.

Enrichment of the OXPHOS pathway was also examined in GSE19027. This dataset comprises gene expression profiles from airway epithelial cells of 20 smokers (8 current smokers, CSm; 12 ex-smokers, ESm) with lung cancer, 24 smokers (17 CSm and 7 ESm) without lung cancer and 8 non-smoker subjects. The OXPHOS signature was elevated in CSm cancer patients compared to the ES without cancer (Figure 5.5A) suggesting an effect of smoking per se on mitochondrial

function. The OXPHOS ES scores between subject groups was wide ranging and no differences between other groups was observed.

There was also considerable variability in ES values for glycolysis (Figure 5.5B&C) which again suggested an effect of cigarette smoke on metabolic function (CSm with or without cancer is elevated compared to ESm with or without cancer). This was similar whichever glycolysis signature was used. In contrast, ex-smokers, with or without cancer, showed no difference in glycolysis ES values possibly suggesting that the smoking effects in these subjects may be transient.

GSE19027

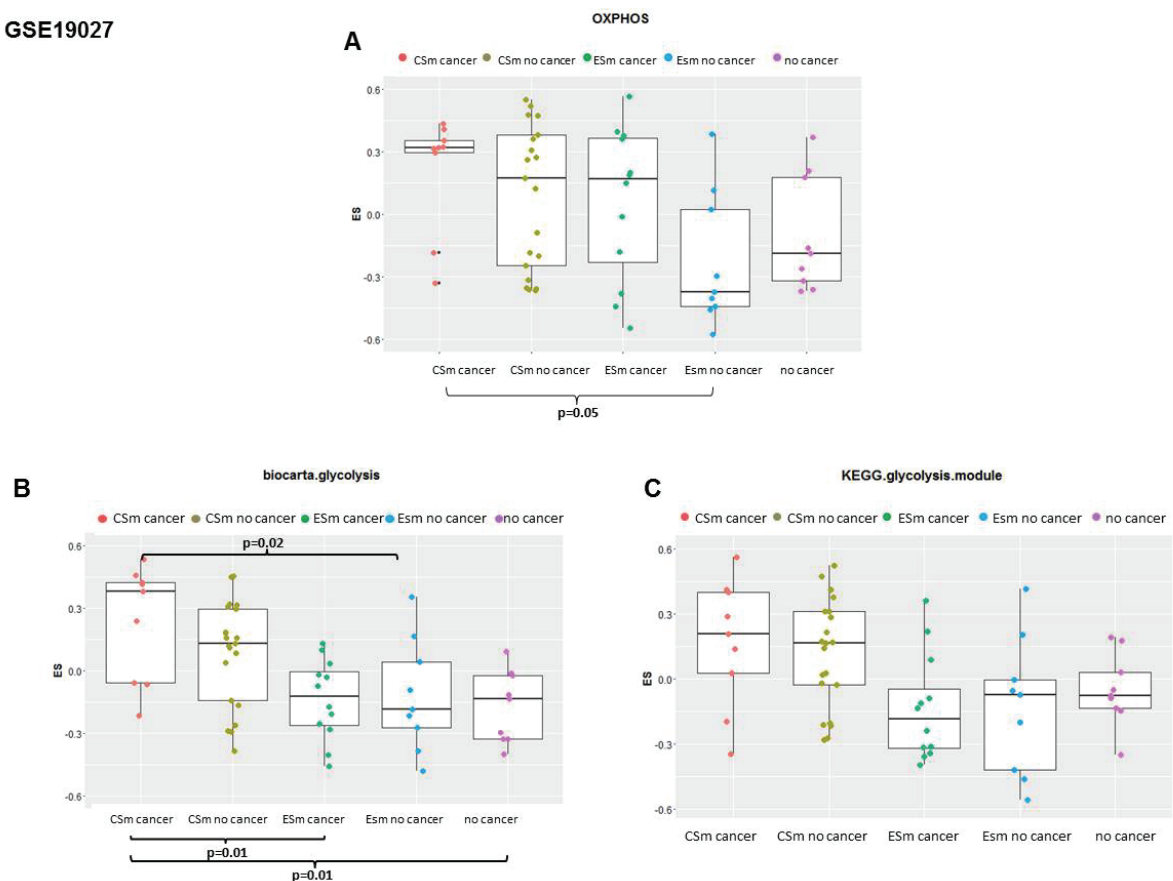


Figure 5.5 Enrichment scores (ES) of OXPHOS and glycolysis signatures in bronchial epithelial cells of smokers with or without lung cancer (GSE19027)

Patients were divided into current smokers (CSm) with or without cancer, ex-smokers (ESm) with or without cancer, and non-smoker without cancer. Gene sets of OXPHOS (A), Biocarta.glycolysis (B) and KEGG.glycolysis (C) were used to analyse gene array data. Data are presented as individual data points for each subject, box-and-whisker plot showing median and interquartile range. The ES differences across group medians were analysed using ANOVA.

It was not possible to determine the COPD status of the patients in this dataset and a direct comparison with the data in Figure 5.5 was not possible.

Overall, this data indicates that glycolysis is enhanced in lung cancer although there were variable effects of active smoking and no enhancement of glycolysis with COPD alone. This may reflect the lack of metadata available to completely interrogate the datasets. However, I propose that these changes may be due to smoking acting through an oxidative stress mechanism which reflects a metabolic switch as a consequence of altered mitochondrial function. It was not possible conclusively to ascribe these effects as being linked to COPD. Furthermore, due to the variability in the ES for OXPHOS and glycolysis and the incomplete clinical variables available using these published datasets I decided to compare mitochondrial function in clinical samples available from the respiratory biobank of the Biomedical Research Unit at the Royal Brompton Hospital. Due to practical and structural changes to the RBH BRU and changes in staff at the BRU biobank, the numbers of NSCLC paired samples available was restricted whilst I was performing these analyses.

5.4.2 Comparison of mitochondrial function and metabolic gene expression between tumour and matched non-tumour tissue in lung cancer patients

The different ES of OXPHOS and glycolysis in lung cancer and non-lung cancer patients analysed from published datasets were shown in section 5.4.1. I further investigated whether there was a difference in $\Delta\Psi_m$ and mitochondrial superoxide levels between lung tumour and matched non-tumour tissue from 7 lung cancer patients in this pilot study.

Individual characteristics and demographic data of the 7 lung cancer patients are presented in Table 5.2. The patients, 4 males and 3 females were all ex-smokers with an age range of 52-75 years. Some patient lung function profiles were missing but two patients also had COPD (% of FEV1/FVC less than 70). There were 3 adenocarcinoma (ADC), 2 squamous cell carcinoma (SCC), 1 colorectal carcinoma with lung metastasis and 1 soft tissue sarcoma cases in this group.

Table 5.2 Individual characteristics and demographic data of lung cancer patients

Patient No.	Age (year)	Weight (kg)	Height (cm)	Gender	FEV1	FEV1/FVC (%)	Smoking status	Pack years	Type of lung cancer
1	52	61.5	166.0	Male	2.8	62.0*	Ex-smoker	30	Adenocarcinoma
2	63	60.0	152.0	Female	0.9	53.0*	Ex-smoker	N/A	Adenocarcinoma
3	75	83.0	170.0	Male	1.7	47.0*	Ex-smoker	20	Adenocarcinoma
4	74	73.0	166.0	Male	3.3	N/A	Ex-smoker	20	Colorectal carcinoma with lung metastasis
5	73	75.4	165.5	Female	N/A	N/A	Ex-smoker	20	Soft tissue sarcoma
6	71	64.6	152.0	Female	1.7	74.0	Ex-smoker	N/A	Squamous cell carcinoma
7	68	79.7	166.8	Male	2.5	76.0	Ex-smoker	40	Squamous cell carcinoma
Mean ± S.D.	68.0 ± 8.2	71.0 ± 9.1	162.2 ± 7.4	F=3, M=4		<70, COPD*			

5.4.2.1 Mitochondrial membrane potential and mitochondrial superoxide levels

To measure $\Delta\Psi_m$ and mitochondrial superoxide levels in lung tissue samples, mitochondria were isolated and protein content determined see Chapter 2 (Sections 2.2.15 & 2.2.9, respectively). 30 μ g of mitochondrial protein per sample was added in a black 96-well plate and stained with JC-1 and mitoSOX for $\Delta\Psi_m$ and mitochondrial superoxide measurement, respectively. I compared the value between matched non-tumour and tumour tissue within the same patient as intra-subject comparison. 6 out of the 7 patient tumour samples had a lower $\Delta\Psi_m$ compared to their matched non-tumours tissue (Figure 5.6A). All 3 ADC tumours (blue) had lower $\Delta\Psi_m$ whereas the $\Delta\Psi_m$ of one of SCC remained the same (red square) but the $\Delta\Psi_m$ of a soft tissue sarcoma tumour was higher compared to its matched non-tumour control tissue (black diamond). In contrast, regardless of the type of tumour, the mitochondrial superoxide level in 4 out of 7 tumour tissues were lower compared to their match non-tumours whereas those of the others were higher (Figure 5.6B).

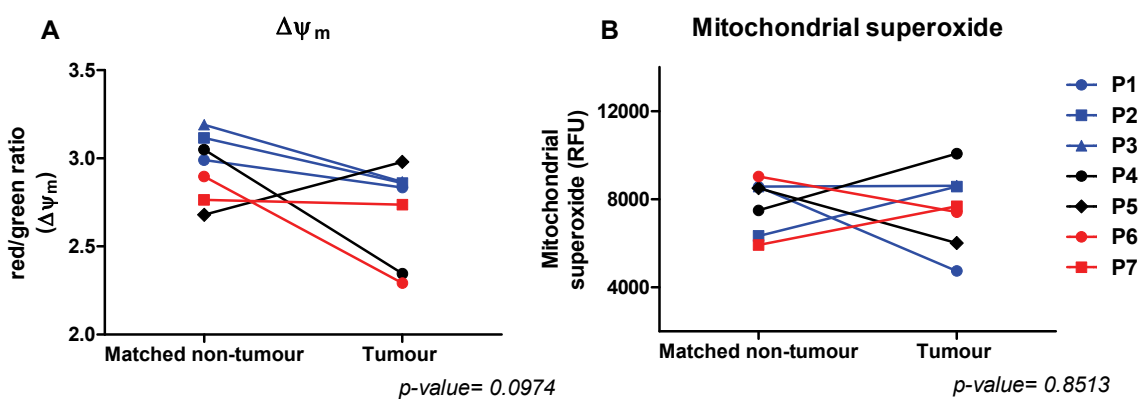


Figure 5.6 Comparison of $\Delta\Psi_m$ and mitochondrial superoxide levels between tumour and matched non-tumour tissue from lung cancer patients

Isolated mitochondria from tumour and matched non-tumour tissue from 7 lung cancer patients were stained with JC-1 and mitoSOX and $\Delta\Psi_m$ and mitochondrial superoxide levels measured, respectively using microplate reader. The $\Delta\Psi_m$ is presented as red/green fluorescence intensity ratio (A). The mitochondrial superoxide is presented as relative fluorescence unit (RFU) (B). P1-3: ADC (blue), P4: colorectal carcinoma with lung metastasis (round black), P5: soft tissue sarcoma (diamond black), P6-7: SCC (red). Means of fold change between the two groups were analysed using Wilcoxon's test.

5.4.2.2 Expression of cancer related genes (*EGFR* and *KRAS*)

Mutations in epidermal growth factor receptor (*EGFR*) and *KRAS* are involved in carcinogenesis pathways in smokers and non-smokers respectively (Kadara et al., 2016). I therefore investigated whether there was any alteration in the gene expression levels of *EGFR* and oncogenic *KRAS*, between tumour and matched non-tumour tissue in this group of patients. Regardless of the type of cancer, tumour tissue from 5 patients had lower *EGFR* expression level compared to their matched non-tumours (Figure 5.7A). Similarly, the *KRAS* expression in tumours of 4 patients was lower compared to their matched non-tumours (Figure 5.7B). Noticeably, there were 3 patients, P1, P2 and P4 who had lower expression levels of both *EGFR* and *KRAS*. However, the expression level of both *EGFR* and *KRAS* were diverse among tumours of this small group of patients.

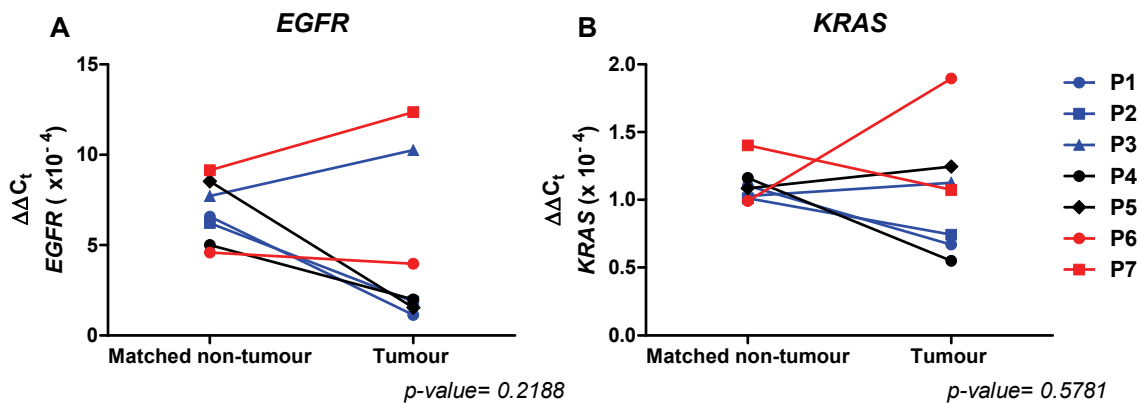


Figure 5.7 *EGFR* and *KRAS* gene expression levels of tumour and matched non-tumour tissue from lung cancer patients

Tumours and matched non-tumour tissue from 7 lung cancer patients were reverse transcribed and RT-PCR performed. The *EGFR* (A) and *KRAS* (B) gene expression levels are presented as fold change ($\Delta\Delta C_t$) compared to housekeeping gene (18S). P1-3: ADC (blue), P4: colorectal carcinoma with lung metastasis (round black), P5: soft tissue sarcoma (diamond black), P6-7: SCC (red). Means of fold change between the two groups were analysed using Wilcoxon's test.

5.4.2.3 Expression of energy metabolism and mitochondrial related genes (*GLUT1*, *PDK1*, *PKM2*, *HK2*, *PGC1a* and *PGC1b*)

Because cancer metabolism is shifted from OXPHOS to glycolysis resulting in altered metabolic related gene expression, I examined whether there was any difference in expression levels of these genes between tumour and matched non-tumour tissue. Gene expression of *GLUT1*, *PDK1* and *PKM2* was significantly ($p < 0.05$) higher in the tumour tissue compared to matched non-tumour tissue (Figure 5.8A-C) whereas expression of *PGC1a* was significantly lower in tumour tissue compared to non-tumour ($p = 0.03$) (Figure 5.8D). The increase in the expression of genes involved in glycolysis and the lower *PGC1a* gene expression in lung tumour tissues may reflect enhanced glycolysis during carcinogenesis. There was no difference in the expression of *HK2* and *PGC1b* between the matched tissue groups (Figure 5.8E&F).

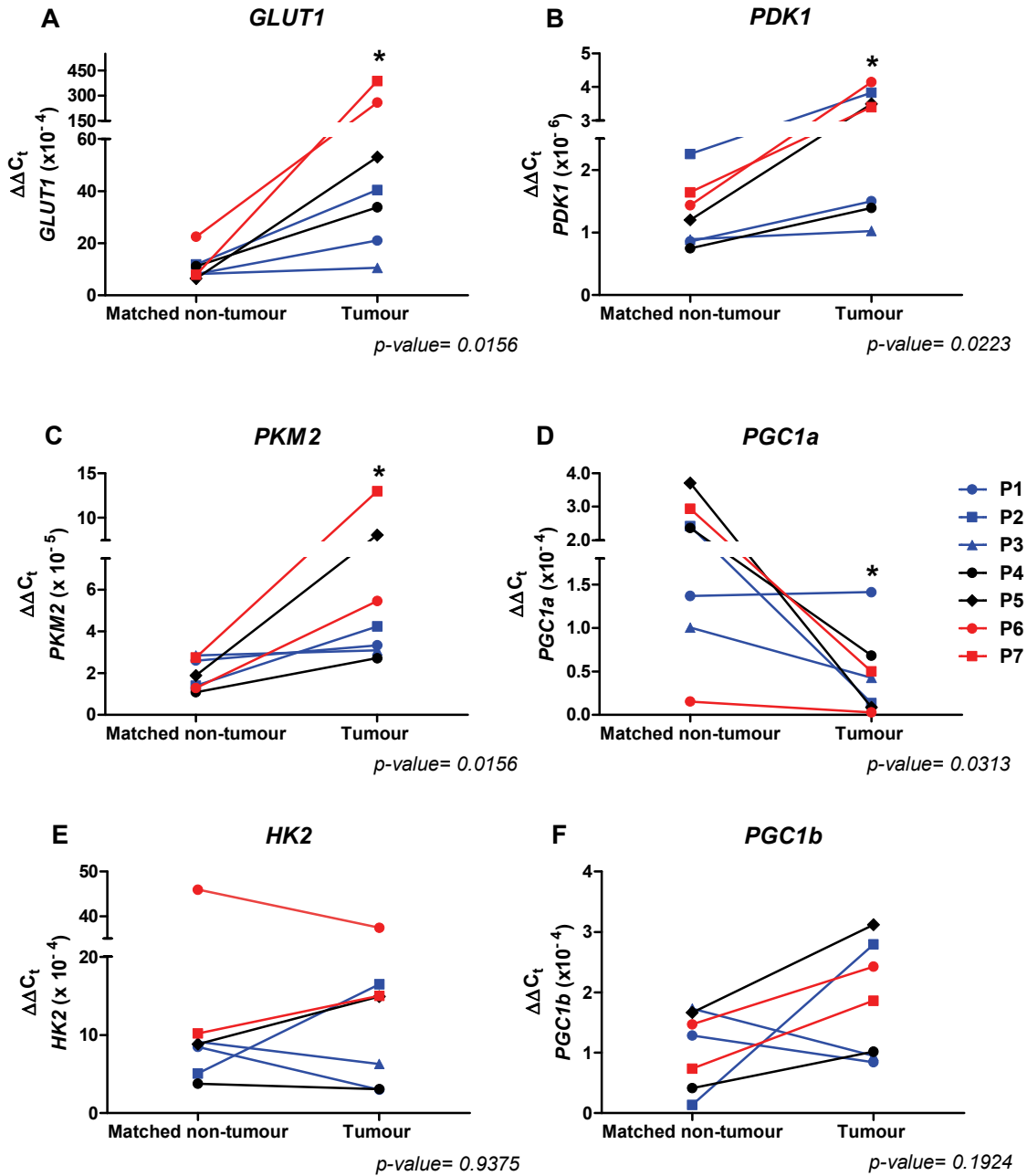


Figure 5.8 Metabolic related gene expression levels in tumour and matched non-tumour tissue from lung cancer patients

Tumours and matched non-tumour tissues from 7 lung cancer patients were reverse transcribed and RT-PCR performed. The GLUT1 (A), PDK1 (B), PKM2 (C), PGC1a (D), HK2 (E) and PGC1b (F) gene expression levels were presented as fold change ($\Delta\Delta C_t$) compared to housekeeping gene (18S). P1-3: ADC (blue), P4: colorectal carcinoma with lung metastasis (round black), P5: soft tissue sarcoma (diamond black), P6-7: SCC (red). Means of fold change between the two groups were analysed using Wilcoxon's test. * $p < 0.05$

In summary, this pilot study in a small group of patients with lung cancer who are ex-smokers there is a lower $\Delta\Psi_m$ in lung tumour whereas there was no difference in the mitochondrial superoxide level compared to matched non-tumour tissue. Similarly, the cancer related genes *EGFR* and *KRAS* present diverse expressions individually between lung tumour and matched non-tumour tissue. The overall expression levels of the metabolism-related genes *GLUT1*, *PDK1* and *PKM2* show a significant increase in tumour tissue and a significantly lower *PGC1a* expression whereas the difference expression of *HK2* and *PGC1b* between tumour and matched non-tumour groups were not different. These changes may account for the differences in glycolysis/metabolic switching seen in the lung cancer versus matched non-cancer tissue.

5.4.3 Mitochondrial protein expression in lung tissue from lung cancer patients

To investigate whether mitochondrial protein expression between tumour tissue and normal adjacent tissue was different, I wanted to select a mitochondrial protein candidate. Over 140 metabolism-related genes were selected from the oxidative phosphorylation pathway in Kyoto Encyclopedia of Genes and Genomes (KEGG) and from the list of glucose metabolism-related genes provided in the Human Glucose Metabolism RT² Profiler PCR Array (Qiagen®). Then screening of these mitochondrial related genes was performed using public databases.

5.4.3.1 Selection of mitochondrial gene and its protein expression candidate

First, the gene candidates were screened using the RNA-Seq Nexus database [<http://syslab4.nchu.edu.tw>]. The RNA expression ratio was determined from the data of 151 squamous cell lung cancer stage IB (SCC) and 140 adenocarcinoma

stage IB (ADC) compared to the data from 51 normal adjacent lung tissues. Next, the genes which had >2-fold change were determined using another public database, Prediction of Clinical Outcomes from Genomic Profiles (PRECOG), to check whether the gene expression was related to survival outcome data in both types of cancer. The genes were then considered when the meta Z-score was <-1.96 or >1.96 either in SCC or ADC or both which suggested the higher degree of gene expression has an impact on survival probability. The candidate genes are shown in Table 5.3.

Table 5.3 RNA expression ratio and PRECOG Z-score of candidate genes

Gene	RNA expression ratio (Fold change >2)		PRECOG Z-score (significant when < -1.96 or >1.96) p-value <0.05	
	SCC/normal adjacent tissue	ADC/ normal adjacent tissue	SCC	ADC
<i>ATP5I</i>	4.78	4.84	2.63*	2.14*
<i>ATP6V1B1</i>	5.33	3.28	1.58	-2.04*
<i>ATP6V1H</i>	2.84	2.71	2.11*	1.08
<i>NDUFV1</i>	7.30	2.76	2.01*	-0.74
<i>NDUFA9</i>	2.43	2.34	1.18	3.39*

ATP5I: ATP synthase, H⁺ transporting, mitochondrial Fo complex subunit; *ATP6V1B1*: ATPase H⁺ transporting V1 subunit B1; *ATP6V1H*: ATPase H⁺ transporting V1 subunit H1; *NDUFV1*: NADH:ubiquinone oxidoreductase core subunit V1; *NDUFA9*: NADH:ubiquinone oxidoreductase subunit A9

From the genes listed in Table 5.3, I determined whether their protein expression was differentially expressed between lung tumour tissue and normal lung tissue using IHC staining from ProteinAtlas.org as shown in Table 5.4. *NDUFA9* encoded protein is a structural protein within a subunit of the hydrophobic protein fraction of the NADH (complex I) of the electron transport chain which is a potential target for anti-cancer drugs (García-Ruiz et al., 2013; Stroud et al., 2013; Wheaton et al., 2014). *NDUFA9* was therefore selected to examine its protein expression in patients' lung tissues.

Table 5.4 Level of protein expression (IHC) of candidate genes in lung cancer tissue and normal lung tissue

[Data derived from the Human Protein Atlas (www.ProteinAtlas.org)]

Gene	Protein expression of tumour	Protein expression of normal tissue (bronchus/lung)
<i>ATP5I</i>	Medium to high	High/medium
<i>ATP6V1B1</i>	Low to medium	Not detected
<i>ATP6V1H</i>	Medium	Medium/low
<i>NDUFA9</i>	Low to medium	Medium/low
<i>NDUFV1</i>	Low	Low/not detected

NDUFA9 protein expression was analysed by IHC in a small group of lung cancer patients. All patients were pathologically diagnosed with lung cancer. Patient characteristics are listed in Table 5.5. Lung cancer patients were divided into three groups; non-smokers, healthy smokers and COPD patients, by lung function and cigarette smoking.

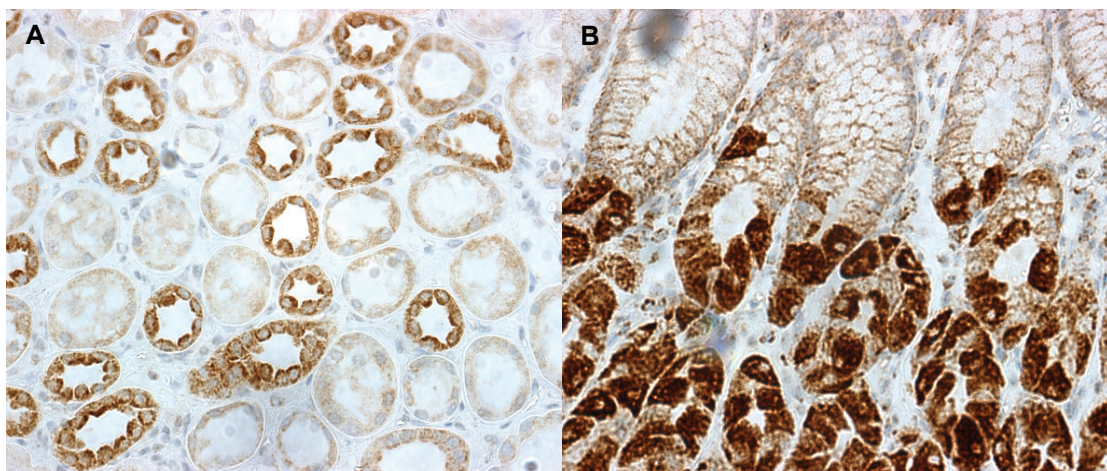
Table 5.5 Demographic data, histopathology characteristics and cancer stage of non-smoker, smoker and COPD groups of patients

	Non-smoker	Smoker	COPD
No. of patients	7	5	7
Age (year)	73.9 ± 10.5	73.2 ± 8.3	67.1 ± 8.7
Gender			
Male	2	4	5
Female	5	1	2
Pack years	N/A	46.5 ± 5.1	64.7 ± 31.4
FEV1	1.8 ± 0.3	2.4 ± 0.6	1.9 ± 0.5
FVC	2.3 ± 0.5	3.2 ± 0.7	3.5 ± 1.0 ^{*a}
FEV1/FVC (%)	76.3 ± 9.8	75.4 ± 4.6	55.7 ± 9.2 ^{*b, **}
Histopathology	6 ADC 1 SCC	3 ADC 2 SCC	2 ADC 4 SCC 1 NSCLC
Cancer stage	5 stage I 2 stage II	4 stage I 1 stage II	3 stage I 2 stage II 2 stage III

^{*a} $p < 0.05$ (Non-smoker VS COPD), ^{*b} $p < 0.05$ (Smoker VS COPD), ^{**} $p < 0.01$ (Non-smoker VS COPD)
ADC: Adenocarcinoma, SCC: Squamous cell carcinoma, NSCLC: Non-small cell lung carcinoma

5.4.3.2 NDUFA9 immunohistochemistry scoring assessment

For assessment, bronchial epithelium and alveolar macrophages were scored in normal adjacent lung tissue slides whilst for the matched tumour slides only staining of tumour cells was assessed. Staining intensity of NDUFA9 was scored as 0, negative; 1, weak; 2, moderate; 3, strong. Tubular epithelium from kidney and glandular epithelium from stomach were used as positive control (score=3) (Figure 5.9A&B).



Positive control

Figure 5.9 Positive control for immunohistochemistry assessment of NDUFA9
Cytoplasmic stained tubular epithelium from kidney (A) and glandular epithelium from stomach (B) were used as positive controls (score=3). (IHCx40)

Isotype control, a negative control that has the same isotype as the primary antibody but not specific to any antigen in human body, was used in lung tissues to compare with our primary antibody and ensure that the primary antibody has a specific antibody signal as shown in Figure 5.10. There was moderate staining in the cytoplasm of alveolar macrophages in both negative control and NDUFA9 stained samples (Figure 5.10A&B) but no staining was shown in the negative control of both bronchial epithelium and tumour cells (Figure 5.10C&E) compared to

their NDUFA9 samples (Figure 5.10D&F). Tissue slides were blinded and scored randomly. The average score was calculated from scores given by two assessors.

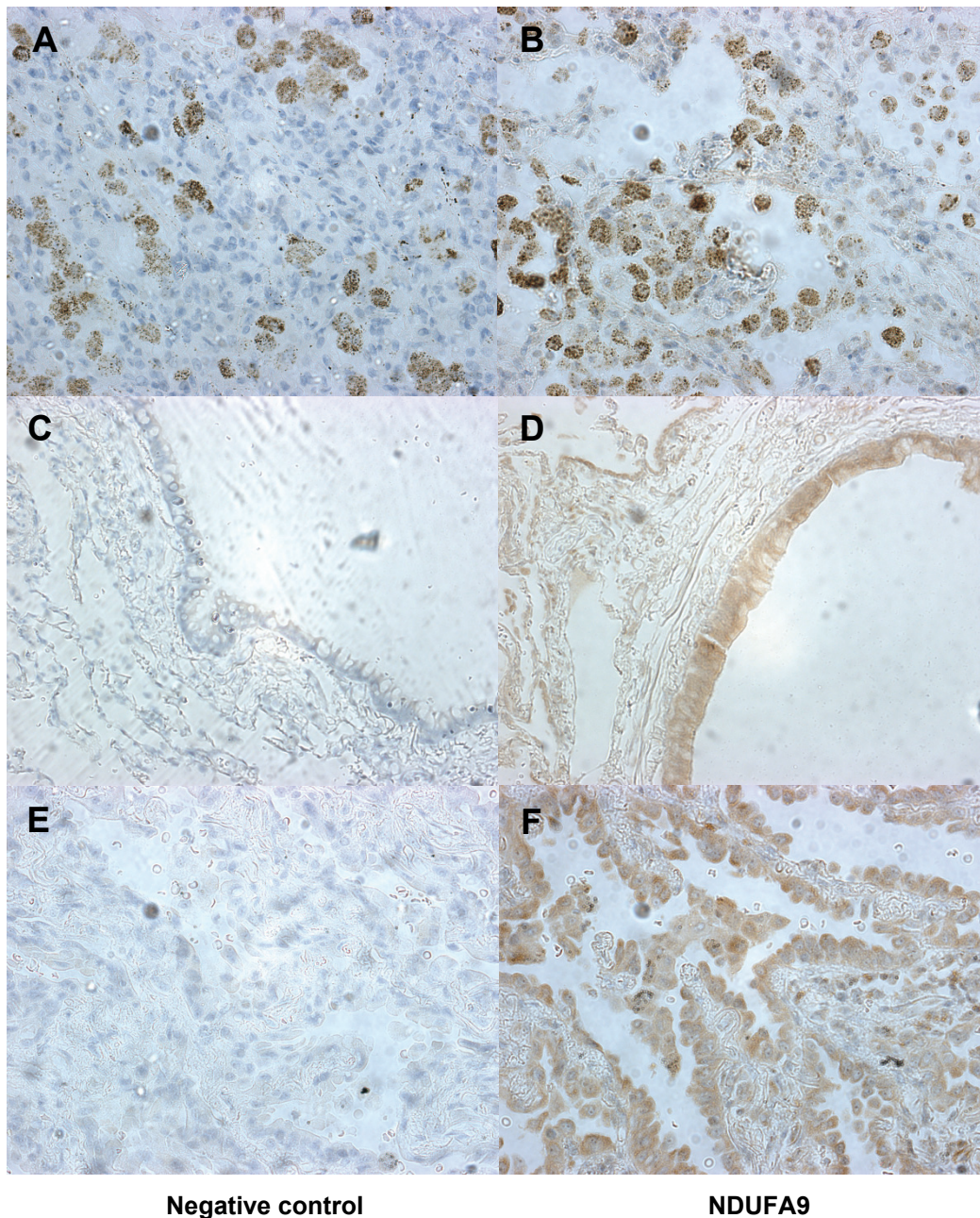


Figure 5.10 Negative control for NDUFA9 in lung tissue slides

A negative isotype control was performed on some of lung tissue slides. Negative controls (left column) and NDUFA9 stained slides (right column) were from the same patients shown in horizontal panel. Alveolar macrophages (negative control, A, and NDUFA9, B) (IHCx40). Normal bronchial epithelium (negative control, C, and NDUFA9, D) (IHCx20). Tumour epithelium (negative control, E and NDUFA9, F) (IHCx40).

The representative images of NDUFA9 expression in lung tissue samples are shown in Figure 5.11 and Figure 5.12. There was variation in staining intensity (0-1.5) in both alveolar macrophage (Figure 5.11A&B, arrows) and bronchial epithelium (Figure 5.11C&D).

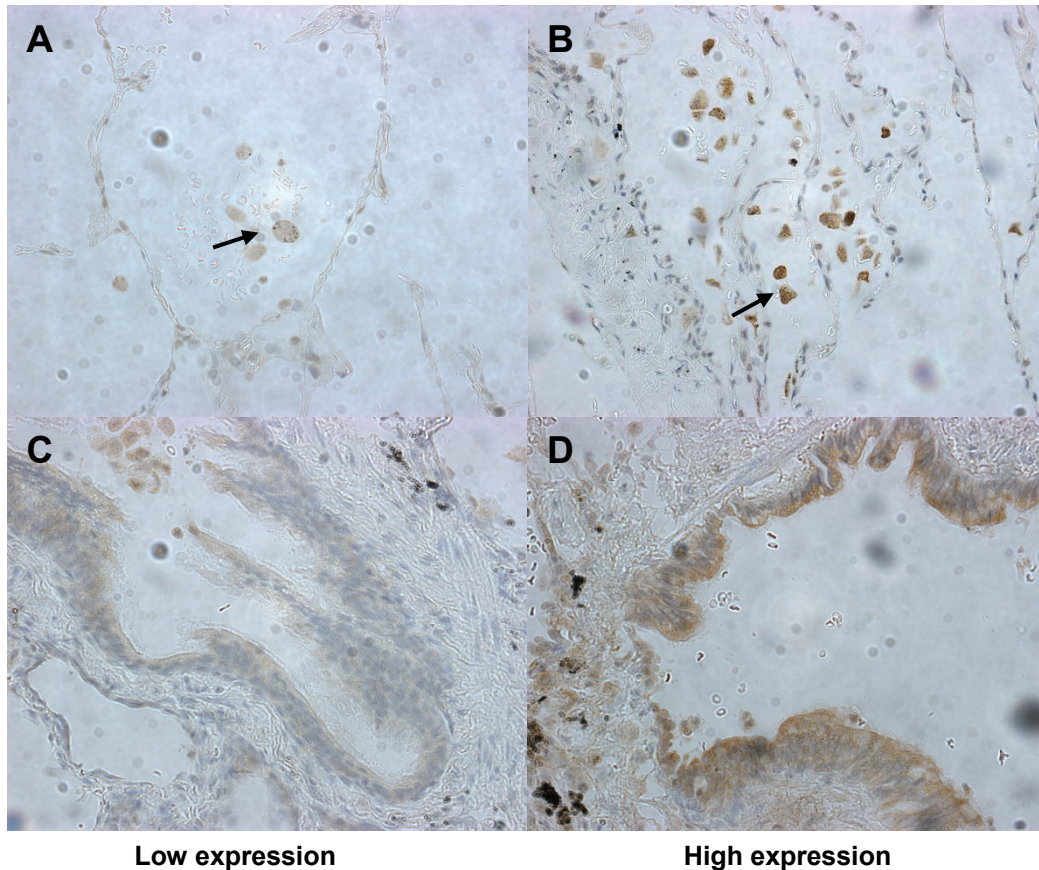


Figure 5.11 NDUFA9 expressions in alveolar macrophages and bronchial epithelium from background lung tissue of patients

Representative images show examples of low expression (left panels) and high expression (right panels) of NDUFA9 in alveolar macrophages (arrows in A and B with average score of 0 and 1.5, respectively) and in bronchial epithelium (C and D with average score of 0 and 1.5, respectively). (IHCx40)

The expression of NDUFA9 was also variable in both adenocarcinoma (Figure 5.12A&B) and squamous cell carcinoma (Figure 5.12C&D).

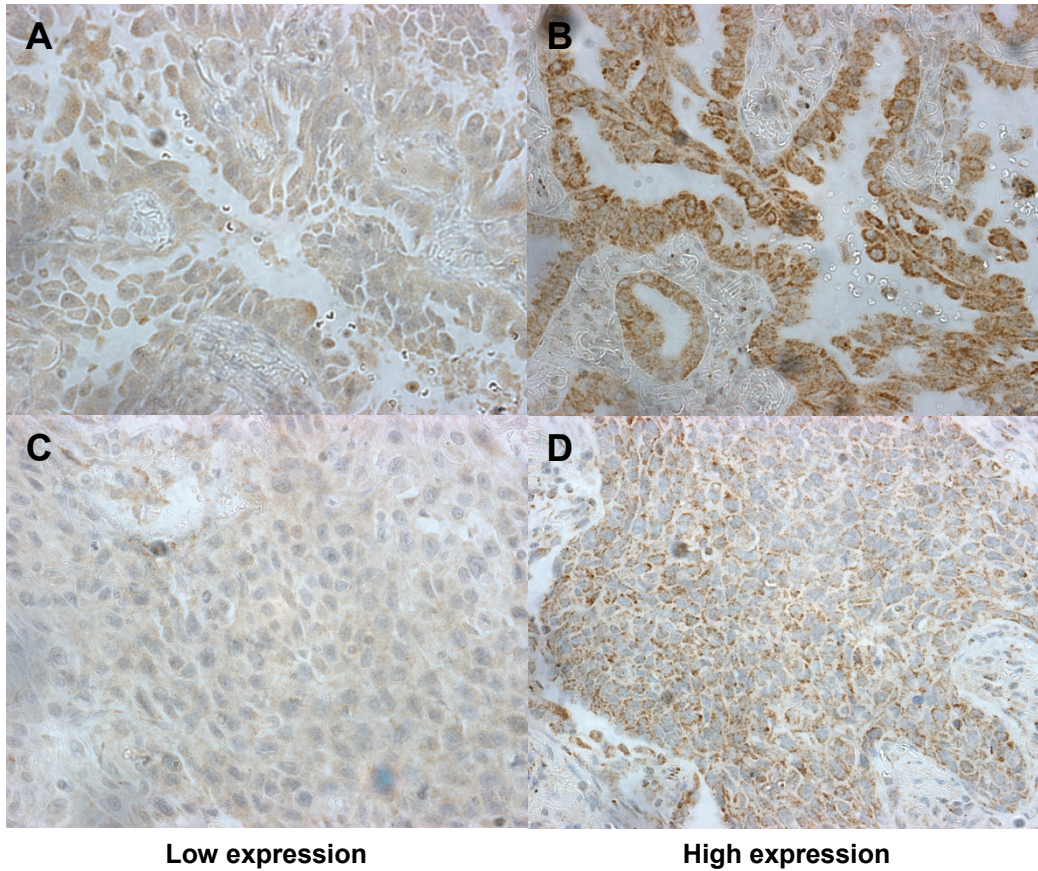


Figure 5.12 NDUFA9 expressions in tumour epithelium from lung tumour tissue of patients

Representative images show examples of low expression (left panels) and high expression (right panels) of NDUFA9 in adenocarcinoma (A and B with average score of 0 and 1.5, respectively) and in squamous cell carcinoma (C and D with average score of 0 and 1, respectively). (IHCx40)

5.4.3.3 NDUFA9 expression between background tissue and tumour tissue

The average staining score for alveolar macrophage and normal bronchial epithelium was compared between background lung tissue and tumour tissue.

The average score of NDUFA9 in alveolar macrophages from the non-smoker group was significantly higher in the tumour tissue compared to background lung tissue ($p < 0.05$). Whereas alveolar macrophages in tumour tissue from the smoker group had a lower staining score, compared to the background lung tissue. In the COPD group, there was no difference in the staining score for alveolar macrophages between background and tumour tissue (Figure 5.13A).

The average score of NDUFA9 in normal bronchial epithelium from non-smokers, similar to alveolar macrophages, was significantly higher in tumour tissue compared to those in background lung tissue ($p < 0.05$). There was no difference between the average staining score in background lung tissue and tumour tissue in smokers which may be due to the variability of staining score in the tumour group. In the COPD group, background lung tissue presented a lower average score compared to that in tumour tissue but was not significant (Figure 5.13B).

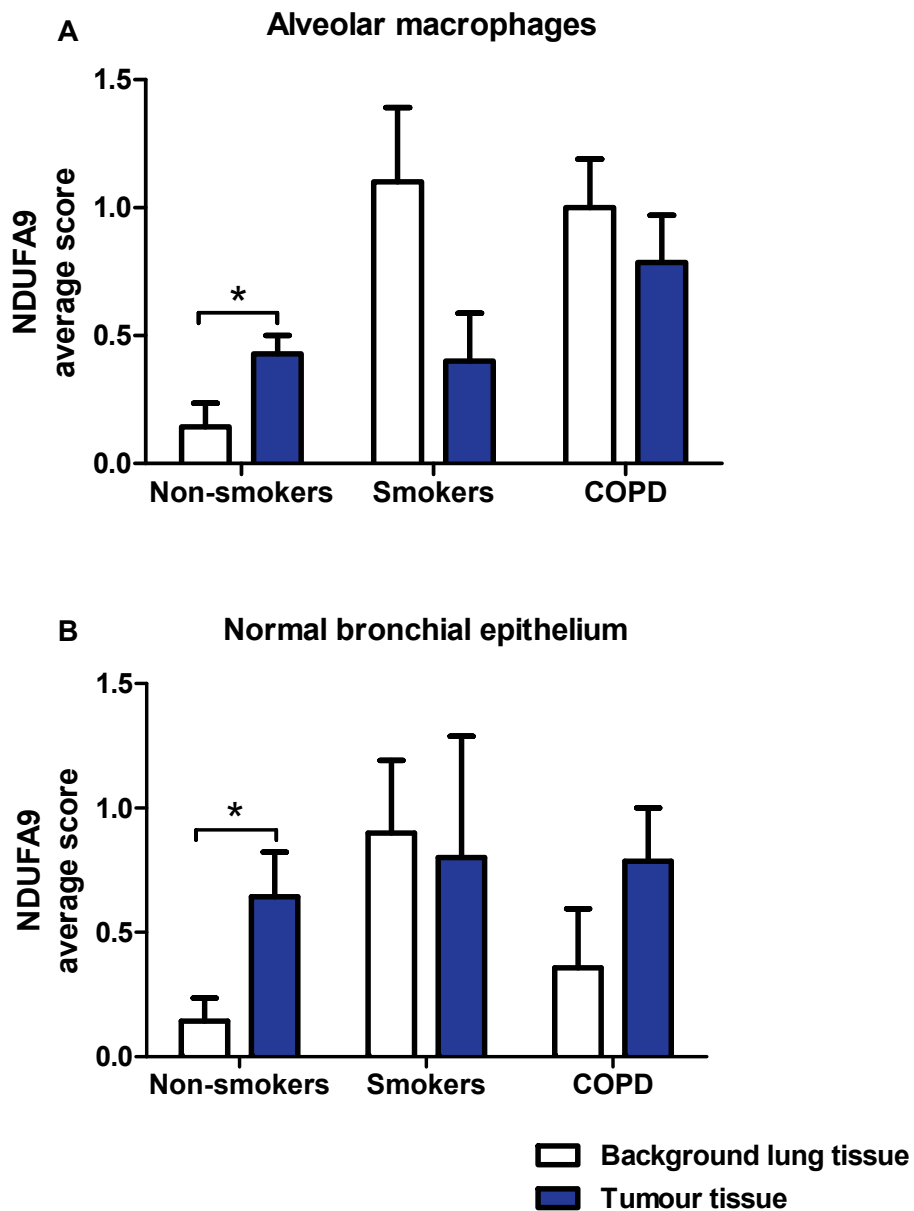


Figure 5.13 NDUFA9 average staining score of alveolar macrophage and normal bronchial epithelium in lung tissue of lung cancer patients

Staining score of alveolar macrophage and normal bronchial epithelium was assessed in background lung tissue (white bars) and tumour tissue (blue bars) of non-smokers ($n=7$), smokers ($n=5$) and COPD ($n=7$) patients. Each bar graph is presented as mean \pm S.D. Comparison between background lung tissue and tumour tissue in each group was calculated using Mann-Whitney test. * $p<0.05$.

5.4.3.4 NDUFA9 expression between non-smokers, smokers and COPD patients

To see whether there was a difference of protein expression among non-smokers, healthy smokers and COPD groups, I plotted the mean staining score of tumour epithelium among these groups, the average staining score of alveolar macrophages and of normal bronchial epithelium in the background lung tissue and in tumour tissue.

There was no difference in the average staining score of tumour epithelium among these patient groups (Figure 5.14A). In COPD group, the mean average score was the lowest compared to other groups.

In Figure 5.14B, in background lung tissues the average staining score of alveolar macrophages in smokers and COPD patients was significantly higher compared to that in non-smokers ($p < 0.05$). There was no difference in the staining score for alveolar macrophages in tumour tissue among these groups.

In Figure 5.14C, the staining score of normal bronchial epithelium in the background lung tissue of smokers was significantly ($p < 0.05$) higher compared to non-smokers whereas there was no difference in the average score in COPD compared to non-smokers. There was no difference in the average staining score of bronchial epithelium in tumour tissue among these groups.

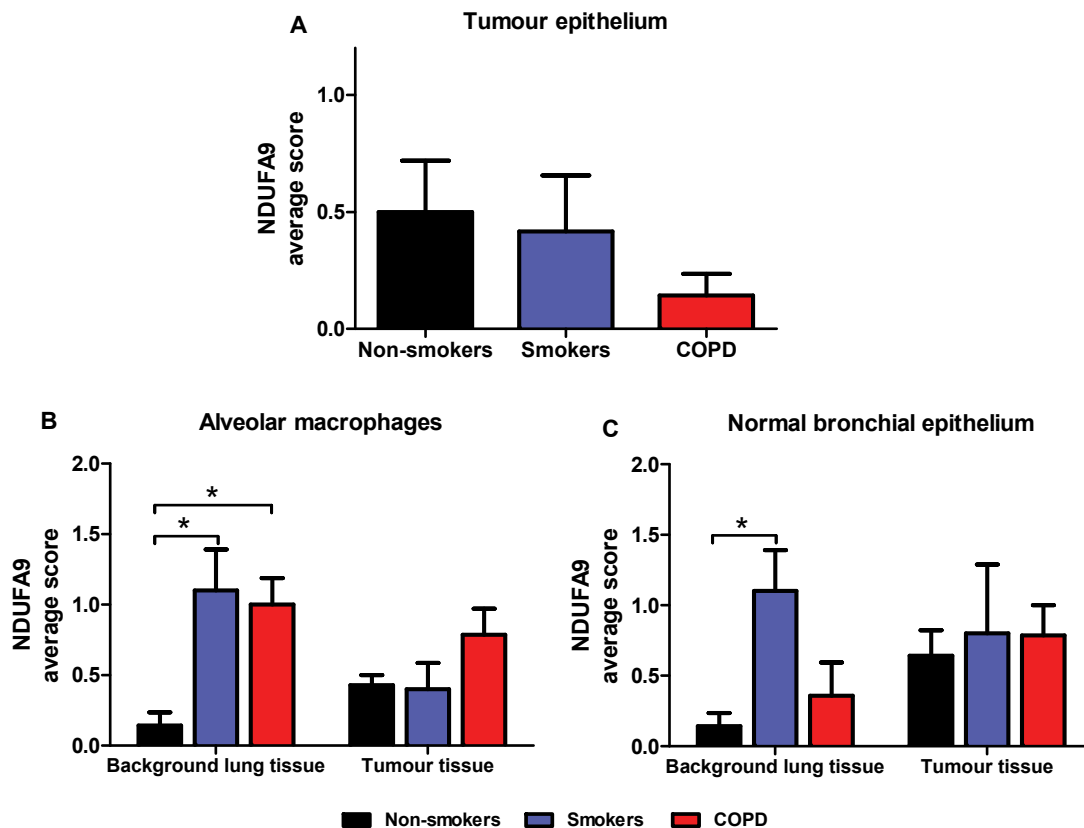


Figure 5.14 NDUF9 average staining score compared among non-smokers, smokers and COPD groups

Average NDUF9 staining score was assessed comparing among non-smokers ($n=7$) (black), healthy smokers ($n=5$) (blue) and COPD ($n=7$) (red) subjects in tumour epithelium within tumour tissue (A), in alveolar macrophages from control non-disease background lung tissue and tumour tissue (B) and within normal bronchial epithelium (C). Bar graphs are presented as mean \pm S.D. Comparison was calculated using Kruskal-Wallis test with Dunn's multiple comparisons test. * $p<0.05$.

There was a trend towards a reduction in NDUF9 expression in tumour epithelium of COPD patients compared to controls although this did not reach significance. In addition, NDUF9 expression was significantly higher in the alveolar macrophages of healthy smokers and COPD patients within background lung tissue whilst this did not differ within tumour tissue. However, there was no significant difference between smokers and COPD patients (Figure 5.13). Normal-looking epithelial cells within background tissue also expressed higher levels of NDUF9 although this was not elevated in COPD. Tumour tissue had a trend towards greater

NDUFA9 expression across all subject groups compared to non-tumour tissue although this was not significant (Figure 5.14). This might suggest that smoking could possibly affect NDUFA9 expression in alveolar macrophages and epithelial cells within control 'healthy' lung tissue of lung cancer patients and that this ability was lost in COPD.

5.4.4 Mitochondrial morphology in cells from lung tissue of lung cancer patients

As shown by immunohistochemical analysis (section 5.4.3), NDUFA9 expression levels differed with respect to tumour presence and smoking status in this pilot study. To observe whether there was any change in mitochondrial structure of cells in lung tissue resulting from cigarette smoke exposure and to compare the mitochondrial structural change between background normal tissue and tumour tissue, samples from one representative patient in each group of non-smokers, healthy smokers and COPD patients was selected for electron microscopy.

Mitochondria with normal structure were seen in alveolar macrophages within the normal healthy background lung tissue from the non-smoker sample (Figure 5.15, top left) whereas there were fewer mitochondria in the smoker sample which also appeared swollen with less cristae (Figure 5.15, top right). Similar to smoker's mitochondria, alveolar macrophages in 'healthy' tissue from the COPD patient had swollen mitochondria with a lack of cristae and mitochondrial membrane disruption (Figure 5.15, bottom left). An increase in dark particles, presumably carbon particles from smoking, was observed in cytoplasm of the cell of the COPD patient

(Figure 5.15, bottom right). This data agrees with the decrease in $\Delta\Psi_m$ seen in COPD tissue as reported earlier in this chapter.

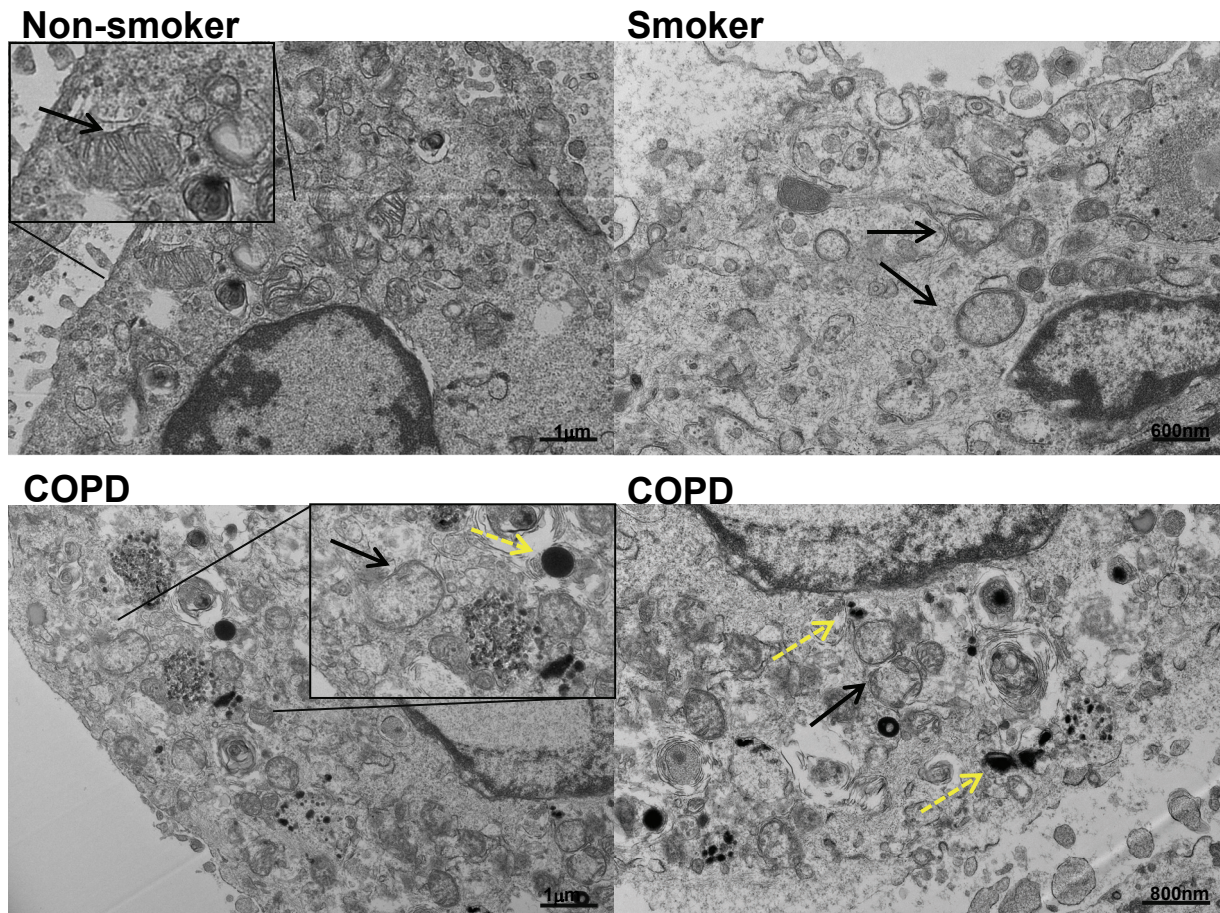


Figure 5.15 Mitochondrial morphology in alveolar macrophage of non-smoker, smoker and COPD patients with lung cancer

Images of alveolar macrophages from a non-smoker shows normal mitochondria (black arrow, top left). Alveolar macrophages from a 'healthy' smoker shows swollen mitochondria with a lack of cristae (black arrows, top right). Alveolar macrophages of a COPD patient show swollen mitochondria (black arrows) with increasing dark particles (dotted yellow arrows, bottom left & right).

In both the smoker and COPD patients, mitochondria in normal bronchial epithelium were irregular, swollen and had less cristae (Figure 5.16). An abnormal mitochondrial shape was observed in the smoker's tissue (Figure 5.16, left). The mitochondria in the bronchial epithelium from the COPD subject were more swollen and more irregular e.g. club-shaped (Figure 5.16, right). I was unable to

obtain an electron micrograph of normal bronchial epithelium from the non-smoker due to its absence in the lung tissue sample obtained from the peripheral lung section.

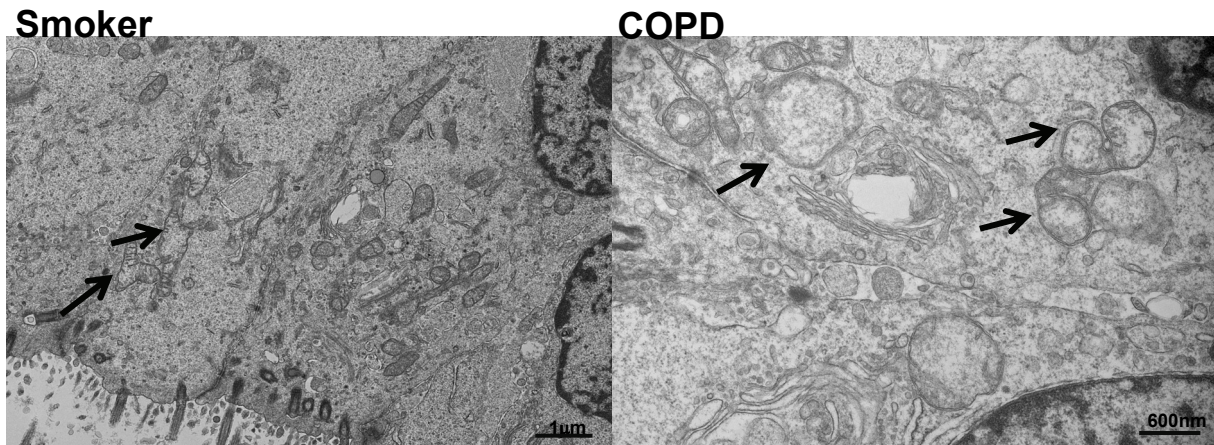


Figure 5.16 Mitochondrial morphology in normal bronchial epithelium of smoker and COPD patients with lung cancer

Image of bronchial epithelium from smoker shows irregular shape of mitochondria (arrows, left) and loss of cristae. Mitochondria in bronchial epithelium from COPD are swollen and have less cristae, some have clubbing shape (arrows, right).

As most adenocarcinoma cancers originate from alveolar type II epithelium (ATII), mitochondrial structures of tumour cells were compared to those of normal ATII in background tissue. In the non-smoker, the mitochondria in ATII cells appeared to be normal with dense cristae (Figure 5.17, upper left) whereas swollen mitochondria with uncleared cristae inside were packed into tumour cells (Figure 5.17, upper right). Similar to the non-smoker, the appearance of mitochondria in ATII cells in the smoker remained normal but with fewer cristae (Figure 5.17, middle left). Less mitochondria with even fewer cristae were observed in tumour cells (Figure 5.17, middle right). In COPD, the mitochondrial membrane in ATII cells remained intact but they had less cristae (Figure 5.17, lower left) whereas

the mitochondria within tumour cells were more irregular and swollen with a further loss of cristae (Figure 5.17, lower right).

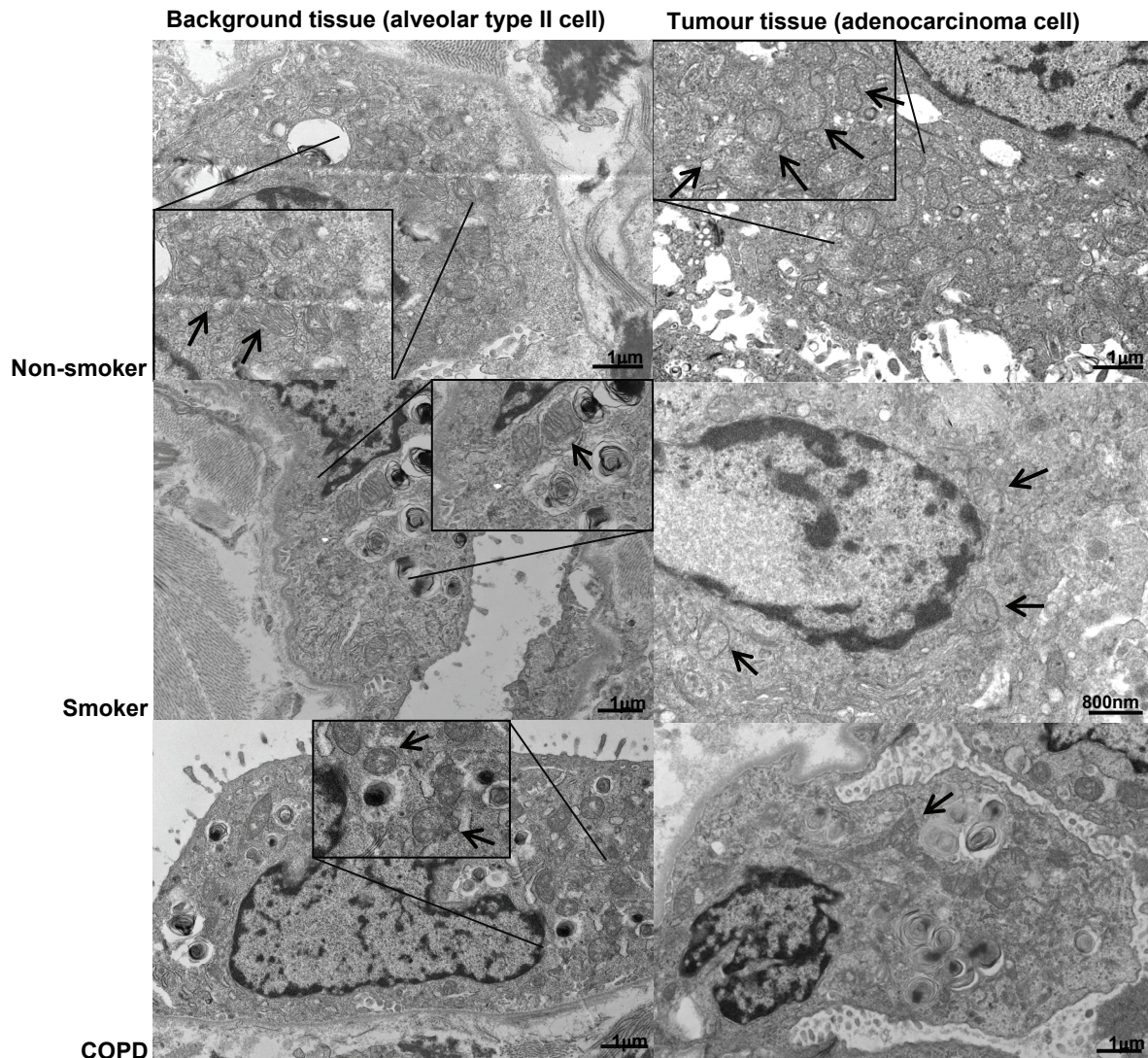


Figure 5.17 Differences in mitochondrial morphology between alveolar type II epithelium (ATII) and adenocarcinoma cell in non-smoker, smoker and COPD

ATII from background tissue and adenocarcinoma cell from tumour tissue present in left and right column, respectively. Arrows locate the mitochondria in the cells. Non-smoker (upper panel): normal mitochondria with dense cristae in background tissue (left); packed swollen mitochondria in tumour (right). Smoker (middle panel): intact mitochondria with less cristae (left); less mitochondria with less cristae (right). COPD (lower panel): intact mitochondrial membrane but less cristae (left); irregular shaped and swollen mitochondria with less cristae (right).

The observed mitochondrial morphology in cells of background lung tissue from these samples showed that smoking appears to change/damage the mitochondria of AII cells and the bronchial epithelium. Moreover, there were more pronounced changes in the shape of the mitochondria in adenocarcinoma in the smoker and COPD patients compared to their background AII cells. To some extent, these findings possibly suggest the influence of smoking on changes in the mitochondria structure in lung epithelial cell types which could drive cancer development.

In summary, this chapter provides evidence of altered mitochondrial structure and function in lung cancer and that this may be associated with disease prognosis. There was some evidence for a major effect of active smoking on these processes but less so for any effect of COPD per se.

5.5 Discussion

Data in this chapter presents the alteration of the glycolysis signature in lung cancer patients from published datasets which varied according to smoking status but not COPD depending upon the dataset analysed. Data regarding OXPHOS signatures values in epithelial cells were more variable compared to those for glycolysis. In addition, samples from current smokers were enriched for the OXPHOS signature compared to ex-smokers without lung cancer. Current smokers also possessed a greater enrichment of the glycolysis signature compared to ex-smokers regardless of the presence of lung cancer.

Lung tissues from two groups of lung cancer patients were separately examined. One group comparing lung tumour and its matched non-tumour individually demonstrates the diverse levels of $\Delta\Psi_m$, mitochondrial superoxide and

the expression of cancer related genes (*EGFR* and *KRAS*). The metabolic related genes showed significantly increased expression in *GLUT1*, *PDK1*, *PKM2* whereas *PGC1a* expression decreased in lung tumours. No significant change in *HK2* and *PGC1b* expression was found in this patient group. Overall, this is indicative of an enhanced glycolytic process within the lung cancer tissue compared to matched 'healthy' tissue.

Lung tissue from the second group was divided into non-smokers, healthy smokers and COPD subgroups and again tumour tissues were compared to their background tissues. A mitochondrial protein (NDUFA9) was highly expressed in the bronchial epithelium and alveolar macrophages in tumour tissues compared to their background tissues of non-smokers. There was a high NDUFA9 expression in bronchial epithelium in background tissue of smokers as well as in alveolar macrophages of smokers and COPD patients. NDUFA9 is linked to complex I stability and function and its altered expression may impact on mitochondrial membrane potential.

This chapter also described preliminary data examining mitochondrial structure in cells from lung cancer patients with different smoking status. Swollen mitochondria with less cristae were observed in alveolar macrophages, bronchial epithelial cells and ATII cells from the current smoker which was more pronounced in those cells from the COPD patient. Mitochondrial shapes in adenocarcinoma cells are also different and more irregular from their origin, ATII cells.

Gene sets analysis related to pathway signatures has been used in many studies to investigate the molecular phenotypes involved in inflammation in severe asthma (Kuo et al., 2018), identifying pathways causing persistent airflow limitation in severe asthma patients (Hekking et al., 2017), and determining pathway activation in breast cancer subtypes (Chung et al., 2017) as well as drug targeting pathway activation in renal cancer (Kim et al., 2016). Datasets used in the present study were derived from previous studies which investigated gene expression involved in lung cancer. The study by Boelens et al. (GSE12428) reported upregulation of oxidative stress response genes which control oxidoreductase activity in normal bronchial epithelium of current smokers compared to ex-smokers but no significant difference in lung cancer (SCC) cells (Boelens et al., 2009). Using the dataset, higher levels of the OXPHOS and glycolysis signatures were obtained in SCC tissues compared to normal tissues. Smoking status showed no difference in the OXPHOS gene sets which may result from focusing on electron transport chain-related genes which is the focus of the present study. However, there is an increase enrichment of glycolysis pathway signature value in lung cancer patients regardless of current and ex-smoking history.

Boelens et al. (GSE12472) reported a high expression in genes related to mitochondrial localisation and function in SCC tissue from patients with COPD compared to non-COPD patients (Boelens et al., 2011). This finding is only partially consistent with the GSVA data reported in the present study in which the SCC tissues from patients with COPD had a higher OXPHOS signature level compared to those from non-COPD patients although this was variable and did not reach statistical significance. This may reflect the strong influence of active smoking on

OXPHOS which we could not disentangle in some of these datasets without the associated metadata. The data is suggestive of, but not conclusive for, the overarching hypothesis. Again a higher glycolysis signature level in SCC tissues regardless of the existence of COPD was found in the present study which suggests greater glycolysis pathway activity in cancer cells - the Warburg effect (Liberti & Locasale, 2016).

GSVA from the GSE19027 dataset also presents an increased OXPHOS signature enrichment in normal bronchial epithelium from current smokers with SCC compared to ex-smokers without SCC which emphasizes the role of smoking on driving mitochondrial function. However, a study by Wang et al. which analysed this dataset revealed a significantly lower expression of genes related to NFE2L2 (Nrf2)-mediated antioxidant response in smokers with SCC compared to those without SCC. This suggests the limitation of NFE2L2 induction influenced by a binding molecule of NFE2L2 which is affected by different smoking history (Wang et al., 2010). The increased glycolysis signatures were observed in current smokers compared to ex-smokers regardless of lung cancer existence; however, the effect of smoking on glycolysis may be temporary as no difference was seen in the glycolysis signature between cancer and non-cancer patients after smoking cessation. However, the duration of smoking cessation was not available.

6 out of 7 tumours had a lower $\Delta\Psi_m$ compared to matched non-tumour tissue. The lower $\Delta\Psi_m$ in tumour tissues indicates that mitochondria have an altered function particularly with respect to ATP production and subsequently the tumour cell changes its bioenergetic pathways to obtain ATP from aerobic glycolysis. This was

reflected in the data seen with A549 cancer cells in Chapter 4. A study of mitochondrial function between lung adenocarcinoma tissue and normal adjacent tissue demonstrated that mitofusin 2 (MFN2) protein was overexpressed in the tumour tissue suggesting a possible role of MFN2 in lung cancer development (Lou et al., 2015). These findings support a previous study which indicated that alterations in mitochondrial function in lung cancer cells is possibly caused by a mutation in mtDNA which was found in over 40% of patients with NSCLC (Wang et al., 2015). These mtDNA mutations can reduce OXPHOS and enhance metabolic reprogramming (Liu & Chen, 2017).

Mitochondrial superoxide levels were variable with 4 out of 7 tumours having lower levels and was cell-type independent. Previous studies showed that lower antioxidant capacity (GPx and CAT activities) are found in tumour tissues compared to normal tissues (Bentley, Emrani, & Cassano, 2008). Moreover, there were inter-individual variation in the expression of antioxidant genes in normal bronchial epithelial cells leading to individual variation in risk of bronchogenic carcinoma (Crawford et al., 2000). This may be due to variation of individual oxidant defence systems such as the risk of having COPD that has been shown to be influenced by genetic variation in antioxidant enzymes (Bentley et al., 2008) and which may cause reduction in mitochondrial superoxide elimination capability. Variability in these pathways may explain the results seen in the previous chapter in response to H₂O₂ in different epithelial cell types.

As these small number of lung samples had lower $\Delta\Psi_m$ in tumour tissues without any significantly altered mitochondrial superoxide levels between the tumours and

their matched non-tumour tissues, it might reflect the unaltered OXPHOS gene ES seen using GSVA.

Oxidant generation in different lung cancer subtypes may affect lipid metabolism pathways. Lipid peroxidation is more involved in adenocarcinoma whereas the cannabinoid pathway is involved in SCC development (Gęgotek et al., 2016). Therefore, antioxidant genes, oxidant defence system and oxidant generation pathways may affect the ROS level and the up-or-down regulation of antioxidants involved in mitochondrial genes observed in tumour tissue. These should be studied in the samples obtained in this thesis from cancer and matched non-cancer tissue.

Mutations in *EGFR* and *KRAS* are involved in the molecular pathways of carcinogenesis in the lungs of smokers and non-smokers respectively (Kadara et al., 2016). Mutations in *EGFR* and its abnormal protein production occur in NSCLC and are associated with non-smoking status, gene amplification and protein overexpression (Tang et al., 2008). In this study, the diversity in the level of *EGFR* expression in matched pair of non-tumours and tumours suggested tumour heterogeneity but confirmed previous data demonstrating overexpression of EGFR protein in the normal bronchiolar epithelium within adenocarcinoma tissue compared to sites adjacent to the tumours (Tang et al., 2008). This abnormality may be subject to the field cancerisation phenomenon suggested in an earlier study in oral cancer which demonstrated that there was the abnormality in EGFR levels in histologically normal tissue adjacent to the tumour (Slaughter, Southwick, & Smejkal, 1953).

A recent study reported that the mutation of *EGFR* was higher in NSCLC patients without COPD while *KRAS* mutations were not associated with COPD status

in NSCLC patients (Saber et al., 2016). The determination of EGFR phosphorylation status would be a better approach to investigate pathway activation in lung tissues. In COPD primary human airway epithelial cells increased EGFR phosphorylation elevated IL8 protein expression via the regulation of nuclear forkhead transcription factor class O (FoxO)3A (Ganesan et al., 2013). Therefore, in future studies it would be interesting to investigate the genetic mutation and phosphorylation status in the matched normal-tumour pairs and increase the number of patient samples to decrease the variability of data.

Metabolic adaptation has been observed in many tumour cell types where cells produce ATP via glycolysis despite sufficient O₂ levels (Koppenol et al., 2011; Warburg et al., 1927). This present study showed higher gene expression levels of glycolytic enzymes in lung tumours compared to matched non-tumour tissue. In comparison to normal tissues, overexpression of GLUT1 has been reported in lung, oesophagus, ovary, pancreas, skin and liver cancers using immunohistochemistry (IHC) (Sun et al., 2016; Younes et al., 1996). This is consistent with the present study which demonstrated a significantly higher *GLUT1* expression in the lung tumour tissue group compared to matched non-tumour group.

Similarly, in this study the *PKM2* expression is higher in the tumour group compared to matched non-tumour group indicating increased activity of the glycolysis pathway. PKM2 is an important enzyme in the last step of glycolysis controlling the production of pyruvate prior to entry into mitochondria (Israelsen & Vander Heiden, 2015). PKM2 overexpression also has been shown to correlate with the poor prognosis in lung cancer (Schneider, Neu, Velcovsky, Morr, & Eigenbrodt, 2003),

osteosarcoma (Liu et al., 2016) and invasiveness in cervical cancer (Landt et al., 2010) indicating that PKM2 may play important roles in cancer progression.

PDK1, an isoform of pyruvate dehydrogenase kinase, phosphorylates PDH leading to an inhibition of acetyl-CoA synthesis from pyruvate (Gray et al., 2014). An IHC study in NSCLC showed evidence that the PDH/PDK ratio was decreased in tumours but found increased PDH activity and a reduced PDK1 expression in fibroblasts surrounding the tumour tissue (Koukourakis et al., 2005). Therefore, in future studies it would be interesting to investigate *PDH* expression level that could support the finding of higher *PDK1* expression in lung tumours compared with matched non-tumours demonstrated in this thesis.

The gene expression of *PGC1a* is another gene expressed differently between matched non-tumour and tumour tissue. This transcriptional co-activator is involved in mitochondrial biogenesis by regulating the transcription of the mitochondrial transcription factor A (TFAM) (D'Errico et al., 2011; Erkstrand MI et al., 2004). Moreover, mitochondrial numbers in the cell may be controlled by *PGC1a* as the number of mitochondria in osteosarcoma is significantly lower than in normal tissue and the overexpression of *PGC1a* enhanced mitochondrial numbers in these cells (Onishi et al., 2014). Decreased *PGC1a* expression has been found in various types of cancers but not analysed with respect to mitochondrial number or function. Further studies in this area are required. A study in A549 cells showed that *PGC1a* was down-regulated which caused a decrease in a cell fate control protein: receptor-interacting protein 1 (RIP1). This resulted in decreased mitochondrial OXPHOS and increased glycolysis activity and elevation of p53

tumour suppressor protein (Chen et al., 2014). In addition, *PGC1a* was higher in p53 wild-type adenocarcinoma lung cancer cell lines compared to other p53-mutated cell lines (Taguchi et al., 2014). This suggests a role for PGC1a in enhancing oxidative metabolism and controlling cell proliferation via p53 modulation. Data in this thesis demonstrates a significantly lower *PGC1a* mRNA expression in lung tumour tissue samples compared to matched non-tumour samples suggesting a shift of metabolism pathway in cancer cells. *PGC1a* expression was independent of cigarette smoke (CS) as similar levels were expressed in myocardium from control and 2-month cigarette smoke exposed rats (Santos et al., 2014). This may indicate that the alteration in *PGC1a* expression may occur during carcinogenesis. These data may underpin the enhanced glycolysis in lung cancer tissues reported in this thesis but do not explain the lack of effect on OXPHOS.

Conversely, higher *PGC1b* was found in 5 out of 7 lung tumours compared to matched non-tumours in this study. In contrast to PGC1a, this PGC1a homologue does not have a metabolic role in brown fat tissue in response to low temperatures (Scarpulla, 2011). From a bioenergetics perspective, PGC1a and PGC1b control metabolic efficiency differently as demonstrated in myoblasts (C2C12). PGC1b expressing cells increased mitochondrial respiration by increasing ATP production rather than increasing proton leak whereas PGC1a expressing cells increase mitochondrial respiration by increasing proton leak (St-Pierre et al., 2003). The different trends in the alteration of gene expression of PGC1a and PGC1b in the present study may explain, at least in part, the differential regulation of mitochondrial metabolism observed in lung cancer.

Hexokinase (HK) is the enzyme which phosphorylates glucose into G6P at the beginning of the glycolysis pathway (Calmettes et al., 2015). Increased HK activity has been reported in many types of cancer suggesting a role in facilitating ATP production via glycolysis (Kwee et al., 2012; Palmieri et al., 2009; Suh et al., 2014). Normal bronchial epithelium and lung cancer cell lines (NCI-H460 and NCI-H661) differently expressed HK2 in response to glucose, insulin and glucagon. Maintenance of HK2 expression in lung cancer cells following exposure to these stimuli may allow cancer cells to continue active glycolysis (Katabi, Chan, Karp, & Batist, 1999). A study of 39 patients with lung cancer showed an increase in lung tumour/normal lung tissue ratio in HK2 protein expression which was negatively associated with a microRNA (miR-143) regulation.

In this thesis, the expression of HK2 between lung tumours and matched non-tumour tissue was highly variable. Comparison between the tumours and matched non-tumours of mitochondrial function and expression levels of some genes (*EGFR*, *KRAS*, *HK2* and *PGC1b*) was also not significant suggesting that the sample size needs to be increased that the suitable sample size should be in between 10 and 30 as stated elsewhere (Hertzog, 2008; Julious, 2005; van Belle, 2008). Being able to study each lung cancer type in further investigations would hopefully help to see a clearer difference between matched non-tumour and tumour tissues.

NDUFA9 has a role in structural stabilisation in complex I where it has been suggested as the target for anti-cancer drugs (García-Ruiz et al., 2013; Stroud et al., 2013; Wheaton et al., 2014). Using whole human genome microarrays *NDUFA9* gene was shown to be highly expressed in tumours from patients with SCC who also

have COPD compared to non-COPD patients (Boelens et al., 2011) suggesting that COPD may cause alteration in genes involved in mitochondrial function. Data presented in this chapter extended this earlier work to show that the average staining score of NDUFA9 in both alveolar macrophages and normal bronchial epithelium in tumour tissues were significantly higher than those in background lung tissues in the non-smoker group. The mitochondrial function activity might be altered in these normal-appearance cells as they reside in the tumour microenvironment.

Interestingly, the protein expression levels of NDUFA9 in alveolar macrophages, in tumour tissues from smokers and COPD groups were lower than in background tissues in the same groups. Whereas the expression level in normal bronchial epithelium in tumour tissues from COPD group was higher than in background tissues. This may be due to the ability to reprogram the metabolic pathway in the individual cell types in response to oxidative stress. Indeed, the NDUFA9 expression in both alveolar macrophages and normal bronchial epithelium in background tissue from smokers are significantly higher than those from non-smokers. It may indicate that instead of complex I dysfunction, this complex can be up-regulated/activated by excessive oxidative stress exposure like cigarette smoking. The shift of metabolism pathway to glycolysis in cancer cells and the impaired mitochondrial function as found in COPD lung (Jiang, Wang, & Hu, 2017; Wiegman et al., 2015) might explain the low expression observed in tumour epithelium in the COPD group. However, since there was high variation in NDUFA9 protein expression in tumour cells and background tissues, more samples need to be studied to provide a reliable conclusion.

This study also provided preliminary data illustrating changes in mitochondrial morphology in lung cells from lung cancer patients with different smoking status. In the absence of cancer, Hara et al. reported that bronchial epithelial cells in COPD patients possess more fragmented and swollen mitochondria than cells from smokers. In primary bronchial epithelial cells exposed to CSE for 48h, mitochondrial ROS caused mitochondrial fragmentation (Hara et al., 2013). A study by Hoffmann et al. also demonstrated that in BEAS-2B cells prolonged CSE exposure (3 months) caused swollen and fragmented mitochondria, and a reduction of cristae in a concentration dependent manner (Hoffmann et al., 2013). Whereas primary bronchial epithelial cells from COPD patients showed mitochondria with elongated and branched appearance. However, there was a compensatory mechanism at the molecular level as an increase of OXPHOS was accompanied by enhanced antioxidant protein levels compared to non-smokers (Hoffmann et al., 2013). Preliminary data from this thesis showed swollen mitochondria with loss of cristae in alveolar macrophages and normal bronchial epithelial cells in both background tissue and tumour tissue from the smoker which was more pronounced in those from COPD patients.

In a mouse alveolar epithelial cell line (MLE12) exposed to CSE for 6-48h there was an increase in mitochondrial fusion and elongation accompanied with increased $\Delta\psi_m$. In primary mouse ATII cells exposed to CSE up-regulation of MFN2 was seen suggesting an early response to CSE (Ballweg, Mutze, Königshoff, Eickelberg, & Meiners, 2014). Healthy smokers and most patients with COPD can be defined as persons who are, or have been, chronically expose to cigarette smoke, therefore the morphological findings of mitochondria in ATII cells in background tissues

of tumour cells may be different from those found in the mouse A11 cell study. An ultrastructural study of cancer cells from patients with bronchiolo-alveolar carcinoma showed numerous mitochondria in their cytoplasm (Bedrossian, Weilbaecher, Bentinck, & Greenberg, 1975). In the present study, the cytoplasm of tumour cells from the non-smoking patient are fully filled with swollen mitochondria. However, in tumour cells from smoking and COPD patients less mitochondria but with more damage, swelling, less cristae and irregular shape are found. This suggests that cigarette smoke may be a crucial factor in mitochondrial damage.

The duration of ROS exposure also appears critical for the metabolic and mitochondrial changes reported here. This temporal effect may explain, in part, the lack of significant effects seen with acute H₂O₂ exposure seen in the earlier chapters. Exposure of cells to CSE or to other methods of creating high, long-lasting changes in intracellular ROS such as exposure of cells to butathione sulphoxide for example may help understand the role, if any, of mitochondrial dysfunction in the association between COPD and lung cancer. Overall, the hypothesis is only partially supported by the current data but the study limitations indicate that further studies are required to resolve this.

Chapter 6 General Discussion and Future Directions

6.1 General Discussion

6.1.1 Roles of oxidative stress in COPD and lung cancer involving mitochondria

Oxidant-antioxidant imbalance has been proposed as a driver mechanism in several chronic respiratory diseases particularly COPD (Gao et al., 2015; El-Hafiz et al., 2013; Rahman & Adcock, 2006). Besides production of endogenous ROS, chronic cigarette smoke exposure, for example, contributes exogenous ROS which can overwhelm the capacity of the oxidant defence system causing an oxidant-antioxidant imbalance (Domej et al., 2014). The existence of excessive oxidative stress in the lung, results not only in the protective responses including induction of inflammatory processes in immune cells, hypersecretion in goblet cells and airway smooth muscle cell hypertrophy but also the destruction of the epithelial lining and alveoli leading to epithelial metaplasia (Barnes et al., 2015). A clinical relationship between COPD and lung cancer has been observed in a retrospective review in that 40-70% of lung cancer patients had previously been diagnosed with COPD (Young et al., 2009).

There is growing evidence for the involvement of many potential mechanisms involved in lung carcinogenesis linked to COPD. These include; a chronic inflammatory microenvironment inducing carcinogenesis, divergent effects of oxidative stress between cancer cell apoptosis and airway epithelial cell proliferation, tissue injury and repair repetitive cycle induced by chronic inflammation accompanied with epigenetic change and suppressed anti-tumour immunity. All these processes may lead to dysregulated cell proliferation associated with oxidative stress-induced mitochondrial gene mutations resulting in mitochondrial dysfunction and bioenergetic dysregulation (Boland et al., 2013; Caramori et al.,

2011; Khan et al., 2008; Sekine et al., 2014; Vermaelen & Brusselle, 2013).

H₂O₂ is a representative of oxidants commonly used in the investigation of the effect of oxidative stress in *in vitro* models of inflammatory lung diseases particularly in COPD (Khan et al., 2014; Wang et al., 2015). Several studies have reported increased levels of H₂O₂ in exhaled breath of patients with COPD (De Benedetto et al., 2005; Dekhuijzen et al., 1996; Ferreira, Hazari, Gutierrez, Zamel, & Chapman, 2001). The production of H₂O₂ in the cell occurs when superoxide (O₂⁻) is catalysed by superoxide dismutase (SOD), which is then converted into the hydroxyl radical (·OH) by catalytic metal ions inside the mitochondria. However, excessive free radicals can cause cellular and organelle damage (Andreyev et al., 2005; Rosanna & Salvatore, 2012).

Mitochondria are the main source of endogenous ROS which can be eliminated using antioxidant enzymes in redox homeostasis (Espinosa-Diez et al., 2015). However, many diseases including Alzheimer's disease, chronic renal diseases, diabetes and fatty liver disease have reported that oxidative stress can result in mitochondrial dysfunction. This includes loss of membrane potential, overproduction of ROS and abnormal mitochondrial dynamics (Patti & Corvera, 2010; Che, Yuan, Huang, & Zhang, 2014; Hroudová et al., 2014; Paradies, Paradies, Ruggiero, & Petrosillo, 2014). Moreover, signalling pathways modulated by mitochondrial ROS such as inflammatory pathways, MAPK and NF-κB, NFE2L2/Nrf2-mediated antioxidant system and caspase pathways have been found to be affected when mitochondria dysfunction occurs (Guo et al., 2012; Hroudová et al., 2014; Lin et al., 2014; Park et al., 2015).

Mitochondrial targeted antioxidants such as TPP⁺ conjugated antioxidants and SS-tetrapeptides have been shown to protect against cell and mitochondria damage from excessive ROS in *in vitro* and *in vivo* pathological models (Gerő et al., 2016; Hara et al., 2013; Zhao et al., 2004). The development of lung cancer in COPD patients may partially result from the defect of redox homeostasis and a change in mitochondrial bioenergetics. Therefore, it was hypothesised that mitochondrial dysfunction, resulting in an abnormal metabolic profile, causes COPD patients to develop lung cancer.

The epithelial lining of the lung is the first site directly exposed to cigarette smoke-generated oxidants. The BEAS-2B cell line was therefore used at the beginning of this thesis as a representative of bronchial epithelial cells to investigate the effect of H₂O₂ on mitochondrial function and cellular function and to optimise the concentration of antioxidants. At a non-cytotoxic concentration of H₂O₂ I found slightly increased mitochondrial superoxide and intracellular ROS levels with a decrease in $\Delta\Psi_m$. These findings were supported by previous studies in BEAS-2B cells which demonstrated decreased $\Delta\Psi_m$ and increased intracellular ROS in a time and concentration dependent manner (Fujii et al., 2002; Khan et al., 2014). Despite a difference in cell type, increased mitochondrial superoxide level was reported in H₂O₂-treated ASM cells of COPD patients (Wiegman et al., 2015) indicating the role of oxidative stress on mitochondrial function in lung cells.

A recent statement from the American Heart Association (Griendling et al., 2016) has cautioned against the use of some dyes for the detection of intracellular and mitochondrial oxidative stress. In particular, they stated that care should also be

taken with MitoSox as its distribution across the mitochondrial membrane may be affected by mitochondrial membrane potential. Although all the various methods to assess oxidative stress in biological samples have their weaknesses (Cheng et al., 2018), the guidelines were designed to highlight the limitations of each approach and thereby avoid experimental error and ensure the best quality measurements possible within the experimental constraints (Griendling et al., 2016). The data presented here using dyes should be interpreted with these limitations in mind.

The effect of H₂O₂ on apoptosis, proliferation and the inflammatory response was investigated in BEAS-2B cells since these cellular processes occur in the pathogenesis of COPD. Previous studies in BEAS-2B cells have shown an effect of H₂O₂ and CSE on the induction of apoptosis via ROS regulating signal kinase 1/p38 signalling cascade and increased apoptosis has been demonstrated in airway epithelial cells from COPD patients (Hodge et al., 2005; Lin et al., 2014). Using Annexin V/PI assay in this thesis, data demonstrated that H₂O₂ induced apoptosis in BEAS-2B cells; however, late apoptotic cells were the main population which potentially included dead cells. Lowering the H₂O₂ concentration and adding time course experiments may clarify the apoptotic effect of H₂O₂. Other studies have treated BEAS-2B cells with cigarette smoke extract for many months (Liu et al., 2010; Rahman et al., 2016) and this type of chronic exposure using H₂O₂ may provide a better link to chronic inflammation and metabolic dysregulation.

Structural cells in the airway like bronchial epithelial cells release inflammatory mediators such as IL-1, IL-8 and GM-CSF via oxidative pathways in response to proinflammatory stimulation (Chung, 2005). There is evidence showing that H₂O₂

activates inflammation via NF- κ B in lung epithelial cell lines (Rahman et al., 2001; Rahman, Gilmour, et al., 2002) which supports my findings which demonstrated that H₂O₂ and IL-1 β co-stimulation provides the synergistic effect on inflammatory response induced *IL8* expression and CXCL8 release in BEAS-2B cells.

Increased expression of inflammatory mediators such as IL-1 β , IL-6 and TNF- α are found in the airway of smokers, additionally IL-1 β promoted the proliferation of lung cancer cell lines from NSCLC patients (Nanavaty et al., 2002; Wang et al., 2014). We demonstrated that IL-1 β increased BEAS-2B proliferation. In spite of the absence of oxidative stress, the ongoing chronic inflammation could increase proliferation and subsequently become squamous metaplasia as increased proliferation of basal airway epithelial cells shown in chronic bronchitis and COPD (Barnes, 2014).

There is an increased risk of all-cause mortality and of lung cancer in COPD patients who are frequent exacerbators (GOLD, 2017). Chronic inflammation and infection probably provide the link between COPD and the increased risk of lung cancer. Although the inflammasome is not activated in stable disease (Di Stefano et al., 2014), there is evidence that it is in a primed state and more able to respond to the second hits (Faner et al., 2016). Recent evidence has suggested that newly synthesised oxidised mitochondrial DNA triggers inflammasome activation (Zhong et al., 2018). The inflammasome is a multi-protein complex involved in innate host defence and located in many immune cell types but particularly the macrophage. When macrophages sense a foreign molecule, they respond by increasing the expression of CMPK2, a mitochondrial deoxyribonucleotide kinase, which

localises to the mitochondrial membrane and increases the levels of CTP (cytidine triphosphate) and mitochondrial DNA synthesis. This freshly synthesised DNA is oxidised by ROS, exits the mitochondria and binds to the NLRP3 inflammasome leading to its activation. The downstream effect of inflammasome activation is the production of IL-1 β and IL-18. The recent CANTOS study examines the effect of 3-year treatment with canakinumab, an anti-IL-1 β mAb on over 10,000 lung cancer patients and demonstrated a significant increase in survival time (Ridker et al., 2017). There was no effect on survival in patients with COPD, but it would have been interesting to examine this in the context of frequent exacerbators and in patients with high levels of IL-1 β in their airways.

Mitochondria also release non-oxidised mtDNA which can function as a signalling molecule and unmethylated CpG within mtDNA can activate TLR9 and modify the immune response and cell proliferation in COPD and lung cancer patients (Hemmi et al., 2000). Overall, it seems that measuring the release of modified and un-modified mtDNA may give further insight into the effect of ROS in COPD and how this may impact on epithelial cell proliferation in lung cancer.

The lower mtDNA copy number of peripheral leukocytes is associated with COPD development (Liu et al., 2015). Investigation of the alteration of mtDNA copy number in background tissues versus lung tumours in patients with different smoking status may provide understanding of the association between COPD and lung cancer related to this organelle.

TNF α also induces ASM proliferation via endothelin 1/GM-CSF/IL-6 (Knobloch et al., 2016) and increased IL-6 production in the presence of Wnt1-inducible signalling

protein 1 in lung fibroblasts proliferation (Klee, Lehmann, Wagner, Baarsma, & Königshoff, 2016). The Wnt signalling pathways are involved in tissue repair and remodelling in the lung (Zhu et al., 2016). The role of Wnt4 signalling on inflammatory induction has been reported to be associated with airway inflammation in COPD (Durham et al., 2013). Activation of Wnt4 aggravates the progression of gastric and colorectal cancer (Novellademunt, Antas, & Li, 2015; Zhu et al., 2016). D-type cyclins play important roles in regulating the cell cycle. These cyclins are overexpressed in cancers and also have roles in glycolytic enzyme regulation and control of oxidant-antioxidant homeostasis (Wang et al., 2017). Therefore, dysregulation of these signalling pathways, related to proliferation, might occur during cell metaplasia in COPD, it may be interesting to examine whether they can be activated via ROS and associated with mitochondrial dysfunction in primary human airway epithelial cells from COPD patients.

6.1.2 Protective effect of antioxidants on cellular functions

In my experiments, pre-treatment with different antioxidants showed variable protective effects in H₂O₂ ± IL-1β treated BEAS-2B cells. N-acetyl cysteine (NAC) decreased H₂O₂-induced mitochondrial superoxide level, IL-1β-induced proliferation and *IL8* mRNA expression and prevented H₂O₂ induced apoptosis. These findings agree with data obtained in previous studies that NAC prevents ROS production and cell death as well as maintains ΔΨ_m in oxidative stress induced cells (Antognelli et al., 2014; Papi et al., 2004; Zhang et al., 2011). However, the mitochondrial targeted antioxidants used in my study failed to show any protective effects. Previous studies demonstrated the effect of mitoTEMPO on the reduction of mitochondrial superoxide, inflammation and cell death in cell lines and primary bronchial epithelial cells

(Hara et al., 2013; McCarthy & Kenny, 2016; Patel et al., 2015). SS-31 had a protective effect against oxidative stress resulting in decreased mitochondrial dysfunction and damage as well as less apoptosis in brain cancer cell lines (Zhao et al., 2004, 2005).

AP39, a H₂S donor, has been shown to improve mitochondrial function, decrease mitochondrial superoxide and cell death in human renal epithelial cells and mouse cortical neurons with non-toxic concentrations, but had an inverse effect at higher concentrations reflecting a bell-shaped concentration response curve (Ahmad et al., 2016; Zhao et al., 2016). This may explain the results reported here in this thesis which shows that a high concentration of AP39 caused mitochondrial dysfunction but with no cytotoxic effect, suppressed IL-1 β -stimulated proliferation and decreased H₂O₂-and-IL-1 β induced *IL8* gene expression and CXCL8 release. The mitochondrial targeted antioxidants did not show the improvement of mitochondrial function compared to non-pretreatment condition in my study although I optimised the drug concentrations and pre-incubation times using data from previous studies (Geró et al., 2016; Hara et al., 2013; Mata et al., 2011; Zhao et al., 2016; Zhao et al., 2013). My data suggests that optimisation for efficacy in different cell types is essential and there is a need for additional optimisation with respect to the pre-incubation times used and the concentrations of each mitochondrial-directed antioxidant in each cell type. In addition, it may be best to perform these studies using the Extracellular Flux (XF) analyser as a better read-out of mitochondrial function. Indeed, differences in molecular structures and the anti-oxidative mechanism of mitoTEMPO, SS31 and AP39 as well as different aspects of investigation require different pre-incubation periods for further investigation.

In addition, in light of the data from Rahman and colleagues (Rahman et al., 2016) the duration of H₂O₂ treatment could be extended from the acute studies here to chronic studies lasting many months. Furthermore, other sources of ROS could be used such as chronic cigarette smoke exposure or modulation of glutathione levels.

In addition, cellular damage as well as mitochondrial dysfunction has been reported to be affected by some pro-inflammatory cytokines such as TNF α and IFN γ but not IL-1 β which increased ROS production and mitochondrial damage in normal bronchial epithelial cells (Kampf, Relova, Sandler, & Roomans, 1999); however, all of these cytokines induced mitochondrial-generated ROS in human retinal pigment epithelial cells (Yang et al., 2007). Therefore, in future it may be worth investigating the effect of TNF α or IFN γ on mitochondrial function and its activation which may help to distinguish the protective effect of mitochondrial-targeted antioxidants in oxidative stress-induced lung epithelial cell experiments.

6.1.3 Comparison of mitochondrial and cellular functions between airway epithelial cell types

Comparing between a bronchial epithelial cell line, primary bronchial epithelial cells and a lung cancer cell line (A549 cells) has provided evidence of different baseline functions and their functional changes in response to oxidative stress. The demonstration of different mitochondrial function at baseline which demonstrated lower $\Delta\Psi_m$ and higher mitochondrial superoxide level in lung adenocarcinoma cell line (A549) compared to the other two normal cell types (BEAS-2B and NHBE) are partially in agreement with other studies. These showed a higher $\Delta\Psi_m$ in A549 cells, at baseline, compared to small airway epithelial cell line

(SAEC) detected by tetramethyl rhodamine methyl ester (TMRM) fluorescence intensity (Bonnet et al., 2007); but this decreased when exposed to H₂O₂ (Panduri et al., 2009). The higher capacity of ROS elimination in A549 cells compared to NHBE cells when exposed to H₂O₂ in a previous study (Erlemann et al., 2006) supports the finding that mitochondrial superoxide and intracellular ROS levels were unchanged in H₂O₂-treated A549 cells. This suggests that survival mechanisms such as endogenous antioxidant expression control to maintain physiological ROS level in cancer cells from being damaged by oxidative stress (Nogueira & Hay, 2013).

The different epithelial cell models I investigated all express *IL8* mRNA in detectable levels in response to IL-1 β stimulation (Eskan et al., 2008). Inflammatory responses can be inhibited by AMPK activation via the NF- κ B pathway as demonstrated by increased AMPK protein expression in CSE induced A549 cells (Lee et al., 2015). This may explain the elevation of *AMPK* mRNA seen in H₂O₂+IL-1 β -treated BEAS-2B and NHBE cells in order to counteract the inflammatory response and maintain redox status (Xie, Zhang, Wu, Viollet, & Zou, 2008). HIF1A is also activated in response to inflammation and is ROS-dependent (Daijo et al., 2016). However, there was minimal expression of both *AMPK* and *HIF1A* mRNAs which made data interpretation difficult. Possible reasons for this issue could be the different response times for gene transcription among cell types and various incubation times among genes. Therefore, re-investigation of the gene expression profiles starting with time-course experiments for each cell type may provide greater mechanistic insights.

Monitoring of oxygen consumption (respiration rate) in cell populations using XF analyser is an indirect technique for assessing mitochondrial function with respect to their ability to respond to mitochondrial inhibitors within a single experiment (Brand & Nicholls, 2011). This is considered one of the best ways of measuring many aspects of mitochondrial function although it does not measure metabolic flux and the XF analyser with Mito Stress test assay is more useful in comparing the respiration rate in different cell types. This approach shows differentiation of bioenergetics profiles: basal respiration, ATP production, respiratory reserve capacity and proton leak between normal cells and cancer cells. A549 cells showed a higher respiration capacity in relation to mitochondria compared to the other two normal epithelial cell types. The H₂O₂ incubation time and concentrations in individual cell types should be optimised using this approach. This may also provide a better marker of cell survival than the non-optimal MTT assay.

The metabolic switch from OXPHOS to glycolysis known as Warburg effect occurs in tumourigenesis (Hirschhaeuser et al., 2011). It would be of interest to investigate this feature with the Glycolysis Rate Assay in these three cell types at baseline and in oxidative stress exposure. In contrast to Mito Stress test, this assay monitors extracellular acidification rate (proton efflux) with additions of rotenone/antimycin A to shut down OXPHOS and 2-deoxy glucose which is phosphorylated by hexokinase leading to inhibition of G6P production and blocks the glycolysis pathway. These additions help examine the capacity of cell in the compensatory glycolysis. Moreover, investigation of metabolic switch towards glycolysis could be important in examining in primary bronchial epithelial cells from patients with various smoking status.

The results of the effect of H₂O₂/IL-1 β and antioxidants on mitochondrial and cellular functions of BEAS-2B cells and mitochondrial parameters of BEAS-2B, NHBE and A549 at basal state are summarised in Figure 6.1.

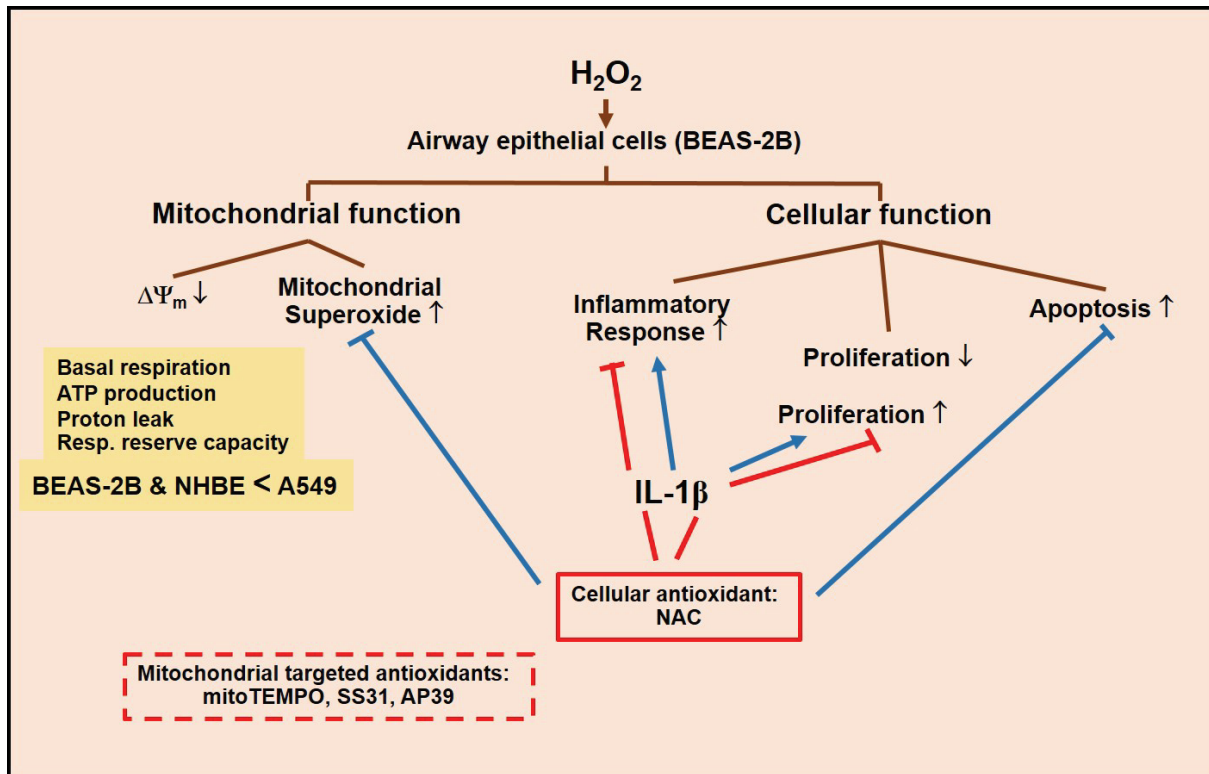


Figure 6.1 Diagram summarising main results from BEAS-2B cells with H₂O₂ exposure and mitochondrial parameters between BEAS-2B, NHBE and A549 cells

Exposure of H₂O₂ caused the alteration of mitochondrial function and cellular function in BEAS-2B cells. H₂O₂ decreased $\Delta\Psi_m$ proliferation, increased mitochondrial superoxide and apoptosis. Combination treatment of H₂O₂ and IL-1 β increased inflammatory response compared to H₂O₂ alone while IL-1 β induced proliferation (blue arrows). Pre-treatment of NAC reduced mitochondrial superoxide and apoptosis before H₂O₂ exposure (blue bar-headed lines) while it reduced inflammatory response and proliferation in IL-1 β treated cells (red bar-headed lines). However, these effects from mitochondrial targeted antioxidants used in the experiments were still unclear. Mitochondrial parameters measured by XF analyser: basal respiration, ATP production, proton leak and respiratory reserve capacity of A549 were higher than those of BEAS-2B and NHBE.

6.1.4 Importance of genomic and proteomic approaches in genes and pathway identification

Using published datasets, our GSVA shows that SCC tissues had higher levels of the OXPHOS and glycolysis signatures compared to normal tissues. Regardless of existence of smoking, an enrichment of glycolysis pathway signature value was high

in lung cancer patients. Furthermore, we found an increase of glycolysis signature level in SCC tissues regardless of COPD status which indicates hyperactivity of glycolysis pathway in cancer cells.

Smoking affects mitochondrial function as the GSVA presents an increased OXPHOS signature enrichment in normal bronchial epithelium from current smokers with SCC compared to ex-smokers without SCC. Besides OXPHOS, glycolysis pathway was affected by smoking as the increased signature level observed in current smokers.

A shotgun proteomic analysis of airway epithelial cells from patients stratified as at-risk for lung cancer identified 2,869 proteins of which 312 were significantly differentially expressed in patients at high risk (Rahman et al., 2016). The dysregulated pathways identified included those involved in metabolic re-wiring such as the glycolytic pathway, TCA cycle, pentose phosphate pathway and galactose and glycogen metabolism and also the antioxidant glutathione pathway. The data across risk categories indicated metabolic reprogramming as an early event in lung cancer. These changes in metabolic reprogramming were re-capitulated in human BEAS-2B cells after exposure to cigarette smoke for 7 months. This confirms the importance of oxidative stress induced changes but highlights the need for chronic exposure to reflect disease pathogenesis. Similar results regarding the importance of these pathways were obtained using GSVA analysis of transcriptomic signatures. It would be interesting to see whether a top hit signature from the shotgun proteomic analysis by Rahman and colleagues could be detected in other transcriptomic databases of COPD and lung cancer.

6.1.5 Sources of ROS and cell culture models in *in vitro* studies for airway epithelial cells

H₂O₂ is commonly used for oxidative stress induction *in vitro*; however, its concentration in the media can change over time, since it quickly decomposes within 1-2 h in monolayer cell culture (Kaczara, Sarna, & Burke, 2010; Makino, Mise, & Sagara, 2008). Instead of H₂O₂, previous studies have used other reagents such as the H₂O₂-generating agent: glucose oxidase (GOx) (Kaczara et al., 2010; Khan et al., 2008), the superoxide anion donor: potassium superoxide (Maioli et al., 2015), redox cycling agent: menadione (Broniowska et al., 2015; Järvinen et al., 2000) and a folic acid metabolite: 6-formylpterin (Wada et al., 2005) to generate H₂O₂ continuously to sustain an oxidative effect in the system which can mimic the chronic oxidative stress exposure. Cigarette smoke extract (CSE) is another reagent *in vitro* which simulates oxidative stress exposure in the airway epithelium. In BEAS-2B cells cigarette smoke exposure increased mitochondrial superoxide production (Mizumura et al., 2014). However, in submerged culture conditions like monolayer cell culture as well as particulates-based exposure, CSE might not mimic human lungs. Therefore, an air-liquid interface culture model would be more suitable and whole smoke exposure system which provides both particulate and vapour phases may be considered for further investigation (Thorne & Adamson, 2013). A549 cells are an alveolar epithelial cell and ideally the results from these cells should be compared with normal alveolar epithelial cells. Comparing the results in BEAS-2B and NHBE cells with squamous cell lung carcinoma cell lines would also be of interest as would the use of small airway epithelial cells.

6.1.6 Differences in mitochondrial function and metabolic gene expression in matched normal-tumour pairs

The activation of oncogenes such as *EGFR*, *KRAS* and *C-MYC* results in mitochondrial dysfunction and increases in ROS production which induces changes in metabolic pathways (Hu et al., 2012; Jose & Bellance, 2011). In the study of matched normal-tumour pairs, the changes in $\Delta\Psi_m$, mitochondrial superoxide level and *EGFR* and *KRAS* expression are variable among subjects. There are several possible reasons for this. Firstly, the number of lung cancer patients was small and included various lung cancer subtypes. Insufficient demographic data was available to clearly sub-phenotype COPD patients. Therefore, increasing sample size and grouping cancer cell subtypes could reduce the inter subject variation, and careful demographic data collection can help result interpretation. Secondly, individual patients might have a difference in their capacity for switching from OXPHOS to glycolysis. This is seen in cancer cell lines whereby different cancer cell types have a unique individualised capacity to produce energy via OXPHOS and/or glycolysis (Jose & Bellance, 2011). A recent study has demonstrated the different metabolic phenotypes in lung cancer between adenocarcinoma and squamous cell subtypes (Jose & Bellance, 2011). Elevation of *GLUT1* expression was observed in squamous cell cancer subtypes. This is consistent with our result which showed that patients with squamous cell tumours had the greatest increase in *GLUT1* level compared to other cancer cell types. The higher expression of some metabolic genes in lung tumour tissues compared to their background tissues emphasises the importance of metabolic changes in tumorigenesis. I observed higher gene expression levels of key glycolytic enzymes in the tumours. This indicates that

lung tumours prefer this metabolic pathway to the OXPHOS pathway as indicated by the lower *PGC1a* mRNA expression in tumour tissues. However, PGC1a can regulate OXPHOS indirectly by acting as a transcriptional activator. An investigation of OXPHOS related genes would be of interest.

A combination of bioinformatic analysis and immunohistochemical examination of the mitochondrial protein NDUFA9 in lung tissue demonstrated higher expression in normal bronchial epithelium and alveolar macrophages in tumour tissues from non-smokers but lower protein expression in smokers which may indicate the role of oxidative stress in the alteration of mitochondrial function. Away from the tumour area, higher NDUFA9 expression was observed in background tissues of smokers suggesting an early compensatory mechanism by up-regulating OXPHOS. Lower NDUFA9 expression in tumours from patients with COPD might be due to metabolic shift towards glycolysis due to defective mitochondria.

However, there are some limitations when investigating protein expression in tissue and when interpreting the results. Firstly, the antibodies directed against the selected candidate protein antibodies might not provide optimal staining in the target cell types in the tissue of interest. Secondly, there are a small number of patients with heterogeneous lung cancer subtypes might result in scoring misinterpretation. Thirdly, IHC scoring assessment is a subjective evaluation even with blinded labelling, therefore human experience and personal bias can affect the results. Considering objective evaluation such as image analysis may better quantify the staining score. Future analysis in this area will involve artificial intelligence (AI) and machine or deep learning as demonstrated recently for retinal

disease imaging (De Fauw et al., 2018). This will be integrated with large database screens of omics and clinical data to reveal key driver pathways/proteins which are then analysed in tissue using automated staining.

6.1.7 Mitochondrial morphological studies and their biogenesis in COPD and lung cancer

Abnormalities in mitochondria, such as abnormal structure, altered mitochondrial dynamic proteins, increased ROS production and changes in mitochondrial related metabolic modulation, can be considered as one of COPD pathogenesis which increase the risk of having lung cancer (Hoffmann et al., 2013; Jiang et al., 2017; Ng Kee Kwong et al., 2017). Mitochondrial related investigations in lung epithelium from non-smokers, smokers and patients with COPD have demonstrated that significant changes in OXPHOS and mitochondrial marker expressions level together with abnormal mitochondrial structure were observed in tissue from patients with COPD (Hoffmann et al., 2013). Interventions with antioxidants targeting the mitochondria could be undertaken in primary airway epithelial cells from COPD patients to determine whether they can improve mitochondrial function and/or morphology.

Mitochondrial responses also depend upon fission-fusion dynamics that aid the cell in removing damaged mitochondria (Eisner, Picard, & Hajnóczky, 2018). This aspect of mitochondrial regulation was not examined in this thesis although this has been reported to be abnormal in COPD epithelial cells (Hoffmann et al., 2013). The release of factors such as pyruvate from damaged mitochondria has profound effects on cellular metabolism and function (Spinelli & Haigis, 2018). Further work

should examine the effects of ROS on cellular metabolites (metabolomics) and on mitochondrial flux.

Mitochondrial-derived peptides may also affect cell signalling via the mitochondrial unfolded protein response (UPR) and subsequent signalling to the nucleus (Hill, Sataranatarajan, & Remmen, 2018). Bioinformatics analysis of lung cancer and COPD transcriptomic profiles as performed in this thesis for mitochondrial proteins may reveal the distinct gene activation pattern of the mitochondrial UPR response which could be subsequently analysed in detail using wet-lab experiments.

The ability of mitochondria to move around the cell and interact with other organelles such as the lysosome is now appreciated as a key factor in mitochondrial control of cellular function. This area of research has not been studied in COPD or lung cancer to my knowledge and may provide a fertile area of research. This may include live-cell video microscopy of mitochondrial movement in HBECs in response to ROS and the effect of mutations in fission/fusion proteins introduced by CRISPR/Cas9. Work in this area has been hampered by the lack of a good animal model of lung cancer with most models using cancer cell lines injected into the tail vein of mice. The development of a cigarette smoke-induced lung cancer animal model is critical and would provide a system to determine the effects of mitochondrial-directed antioxidants in preventing lung cancer.

Oxidative stress and chronic inflammation resulting in genetic mutation in COPD are the main factors for malignant transformation. Many mechanisms have been shown to be involved in driving carcinogenesis in the pathogenesis of COPD. These include genetic mutation, altered cell cycle, persistent inflammation and

redox imbalance (Bozinovski et al., 2016; D'Anna et al., 2015; Goldkorn et al., 2014; Vermaelen & Brusselle, 2013). Mitochondrial dysfunction results in an imbalance of redox homeostasis and oxidant accumulation which can then activate oncogenic related pathways (Weinberg et al., 2010). The aim of this thesis was to explore a cause that COPD develops lung cancer focusing on mitochondrial dysfunction and metabolism change and to assess the effect of mitochondrial targeted antioxidants in improving mitochondrial function. The changes in levels of metabolic genes and a mitochondrial protein shown in lung tissue samples in this study may suggest, in part, the role of the metabolic pathway in cancer development. Understanding the mechanism(s) which cause mitochondrial dysfunction in COPD and identification of mitochondrial related proteins may lead to the establishment of a specific biomarker for lung cancer prediction in COPD patients. Further investigation regarding the effect of mitochondrial targeted antioxidants in lung cancer prophylaxis could be worth studying in COPD-animal models accompanied with oncogene activation which can implicate to clinical study in the future.

(A proposed mechanism of metabolic pathway and mitochondrial function in lung cancer development and intervention of antioxidants is illustrated in Figure 6.2)

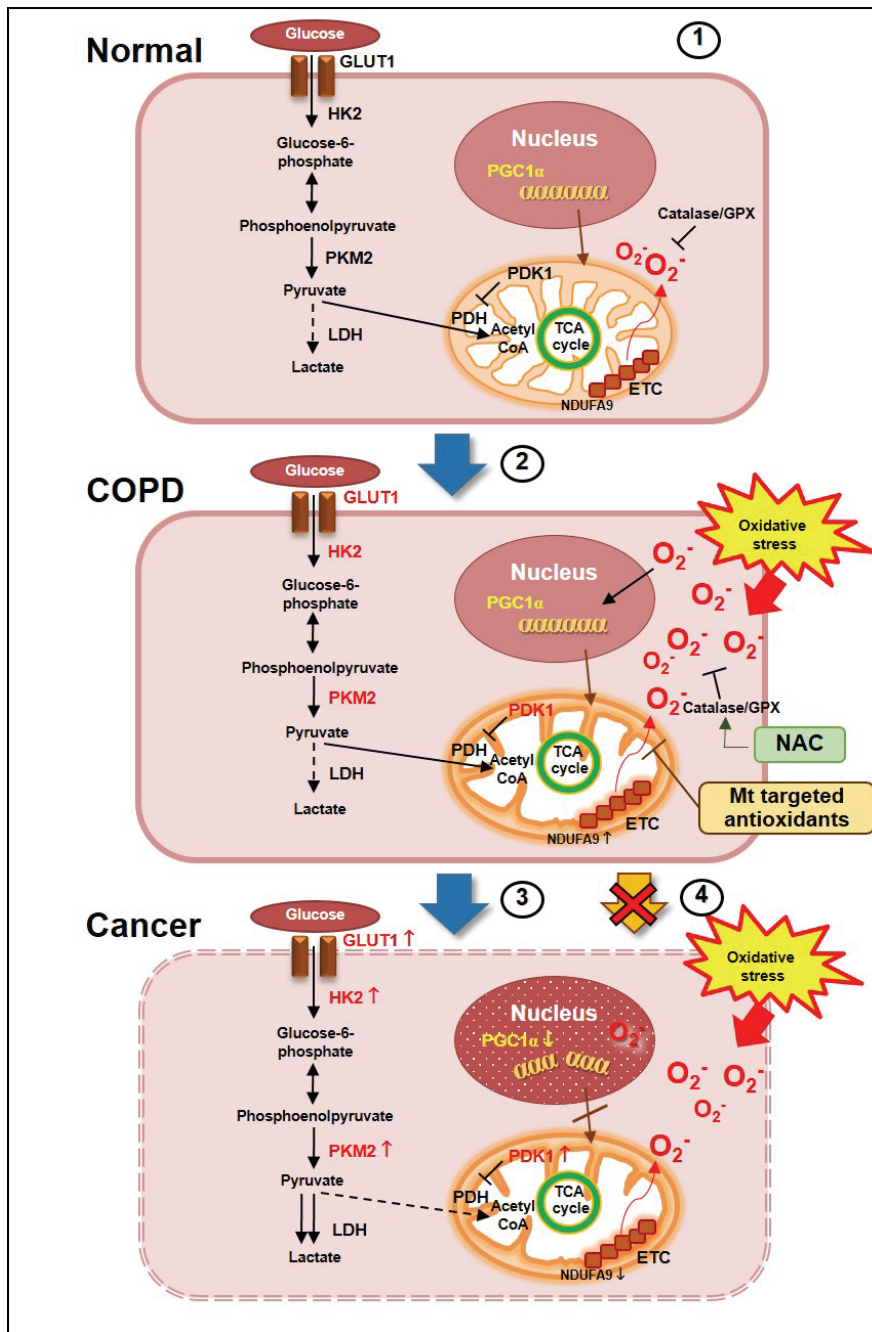


Figure 6.2 Summary of proposed mechanism involving in some metabolic pathways, relationship between COPD and lung cancer

In normal cell, metabolism occurs via glycolysis pathway in cytoplasm and subsequently via TCA cycle and ETC in mitochondria. O_2^- produced from ETC is eliminated by catalase/GPX system (1). In COPD, overexposure to O_2^- from smoking, for example, combination with mitochondrial dysfunction leads to alteration of expression of enzymes in glycolysis pathway, mitochondrial transcriptional coactivator (PGC1 α) and ETC protein expression (NDUFA9) (2). DNA damage occurs by O_2^- causing gene mutation and develops cancer (3), PGC1 α expression decreases leading to mitochondrial dysfunction while expression of key enzymes in glycolysis are increased (GLUT1, HK2 and PKM2) herewith the increased inhibition of acetyl CoA production by PDK1 contributed to aerobic glycolysis. Therefore, using antioxidants such as NAC or mitochondrial targeted antioxidants to reduce O_2^- as lung cancer prevention might be useful in COPD patients (4).

In my study, I observed the mitochondrial function between BEAS-2B, NHBE and A549 using XF analyser which has shown different bioenergetics which can be a model for further investigation regarding these cells in response to other stress conditions. However, doing experiment of three cell types with the same treatment duration would be difficult to compare and interpret. Investigation in clinical samples have shown the differences of metabolic gene expression involving glycolysis and mitochondrial biogenesis between normal adjacent tissues and lung tumour tissues; however, increasing the number of samples analysed for each group of cancer cell types should give a better indication of the importance of mitochondrial dysfunction in COPD and in the evolution of COPD-associated lung cancer.

6.2 Future plans

The following is a summary of experiments that should be considered based on this thesis:

- Investigate the effect of chronic exposure of CSE/H₂O₂ on mitochondrial function in BEAS-2B cells using XF analyser
- Investigate the effect of CSE/H₂O₂ on the release of modified and un-modified mtDNA and cell proliferation in lung cancer cells
- Re-investigate the effect of proinflammatory cytokine on *AMPK* and *HIF1A* expressions by time-course experiments for individual cell types to get the suitable time points for further experiments regarding the effect of mitochondrial targeted antioxidants
- Investigate whether other cytokines (TNF α and IFN γ) affect mitochondrial ROS production and mitochondrial function in airway epithelial cells

General Discussion and Future directions

- Investigate whether signaling pathways regulating cell cycle such as cyclin and Wnt can be activated via ROS and associated with mitochondrial function in primary airway epithelial cells from COPD patients
- Investigate whether mitochondrial targeted antioxidants help improve mitochondrial function and their morphology in primary airway epithelial cells in COPD patients
- Compare the copy number of mtDNA of airway epithelial cells in normal background tissue versus tumour tissue in patients with different smoking status
- Examine transcriptomic signatures involving metabolic pathways and OXPHOS pathway in other available transcriptomic databases of COPD and lung cancer using GSVA

References

- Adcock, I. M., Caramori, G., & Barnes, P. J. (2011). Chronic obstructive pulmonary disease and lung cancer: new molecular insights. *Respiration*, 81, 265–84.
- Adekola, K., Rosen, S. T., & Shanmugam, M. (2012). Glucose transporters in cancer metabolism. *Curr Opin Oncol*, 24(6), 650–4.
- Aerts, J. G., & Hegmans, J. P. (2013). Tumor-specific cytotoxic T cells are crucial for efficacy of immunomodulatory antibodies in patients with lung cancer. *Cancer Res*, 73(8), 2381–8.
- Agarwal, A. R., Yin, F., & Cadenas, E. (2014). Short-term cigarette smoke exposure leads to metabolic alterations in lung alveolar cells. *Am J of Respir Cell Mol Biol*, 51(2), 284–93.
- Agusti, A. (2018). Filling the gaps in COPD: the TRIBUTE study. *Lancet*, 391(10125), 1004–6.
- Agustí, A. G. N., Sauleda, J., Miralles, C., Gomez, C., Togores, B., Sala, E., Batle, S., & Busquets, X. (2002). Skeletal muscle apoptosis and weight loss in chronic obstructive pulmonary disease. *Am J of Respir Crit Care Med*, 166(4), 485–9.
- Ahmad, A., Olah, G., Szczesny, B., Wood, M. E., Whiteman, M., & Szabo, C. (2016). AP39, a mitochondrially targeted hydrogen sulfide donor, exerts protective effects in renal epithelial cells subjected to oxidative stress in vitro and in acute renal injury in vivo. *Shock*, 45(1), 88–97.
- Ahmad, A., & Szabo, C. (2016). Both the H₂S biosynthesis inhibitor aminooxyacetic acid and the mitochondrially targeted H₂S donor AP39 exert protective effects in a mouse model of burn injury. *Pharmacol Res*, 113, 348–55.
- Allegra, L., Cordaro, C. I., & Grassi, C. (1996). Prevention of acute exacerbations of chronic obstructive bronchitis with carbocysteine lysine salt monohydrate: a multicenter, double-blind, placebo-controlled trial. *Respiration*, 63(3), 174–80.
- Amann, T., Maegdefrau, U., Hartmann, A., Agaimy, A., Marienhagen, J., Weiss, T. S., Stoeling, O., Warnecke, C., Scholmerich, J., Oefner, P. J., Kreutz, M., Bosserhoff, A. K., & Hellerbrand, C. (2009). GLUT1 expression is increased in hepatocellular carcinoma and promotes tumorigenesis. *Am J Pathol*, 174(4), 1544–52.
- Amrani, Y., & Panettieri, R. A. (2003). Airway smooth muscle: contraction and beyond. *Int J Bioche Cell Biol*, 35(3), 272–6.
- Anastasiou, D., Poulogiannis, G., Asara, J. M., Boxer, M. B., Jiang, J., Shen, M., Bellinger, G., Sasaki, A. T., Locasale, J. W., Auld, D. S., Thomas, C. J., Vander Heiden, M. G., & Cantley, L. C. (2011). Inhibition of pyruvate kinase M2 by reactive oxygen species contributes to cellular antioxidant responses. *Science*, 334(6060), 1278–83.
- Anastasiou, D., Yu, Y., Israelsen, W. J., Jiang, J., Boxer, M. B., Hong, B. S., Tempel, W., Dimov, S., Shen, M., Jha, A., Yang, H., Mattaini, K. R., Metallo, C. M., Fiske, B. P., Courtney, K. D., Malstrom, S., Khan, T. M., Kung, C., Skoumbourdis, A. P., Veith, H., Southall, N., Walsh, M. J., Brimacombe, K. R., Leister, W., Lunt, S.

- Y., Johnson, Z. R., Yen, K. E., Kunii, K., Davidson, S. M., Christofk, H. R., Austin, C. P., Inglese, J., Harris, M. H., Asara, J. M., Staphanopoulos, G., Salituro, F. G., Jin, S., Dang, L., Auld, D. S., Park, H., Cantley, L. C., Thomas, C. J., & Vander Heiden, M. G. (2012). Pyruvate kinase M2 activators promote tetramer formation and suppress tumorigenesis. *Nat Chem Biol*, 8(10), 839–47.
- Andreyev, A. Y., Kushnareva, Y. E., & Starkov, A. A. (2005). Mitochondrial metabolism of reactive oxygen species. *Biochemistry (Mosc)*, 70(2), 200–14.
- Antognelli, C., Gambelunghe, A., Talesa, V. N., & Muzi, G. (2014). Reactive oxygen species induce apoptosis in bronchial epithelial BEAS-2B cells by inhibiting the antiglycation glyoxalase I defence: involvement of superoxide anion, hydrogen peroxide and NF- κ B. *Apoptosis*, 19(1), 102–16.
- Apostolova, N., & Victor, V. M. (2015). Molecular strategies for targeting antioxidants to mitochondria: therapeutic implications. *Antioxid Redox Signal*, 22(8), 686–729.
- Aravamudan, B., Thompson, M. A., Pabelick, C. M., & Prakash, Y. S. (2013). Mitochondria in lung diseases. *Expert Rev Respir Med*, 7, 631–46.
- Arnold, R. S., Sun, Q., Sun, C. Q., Richards, J. C., O'Hearn, S., Osunkoya, A. O., Wallace, D. C., & Petros, J. A. (2013). An inherited heteroplasmic mutation in mitochondrial gene COI in a patient with prostate cancer alters reactive oxygen, reactive nitrogen and proliferation. *BioMed Res Int*, 2013, 239257.
- Assi, H. I., Kamphorst, A. O., Moukalled, N. M., & Ramalingam, S. S. (2017). Immune checkpoint inhibitors in advanced non-small cell lung cancer. *Cancer*, 124(2), 248–61.
- Babich, H., Krupka, M. E., Nissim, H. A., & Zuckerbraun, H. L. (2005). Differential in vitro cytotoxicity of (-)-epicatechin gallate (ECG) to cancer and normal cells from the human oral cavity. *Toxicology In Vitro*, 19(2), 231–42.
- Baertling, F., Sánchez-Caballero, L., van den Brand, M. A. M., Fung, C. W., Chan, S. H. S., Wong, V. C., Hellebrekers, D. M. E., de Coo I. F. N., Smeitink J. A. M., Rodunburg, R. J. T., & Nijtmans, L. G. J. (2018). *NDUFA9* point mutations cause a variable mitochondrial complex I assembly defect. *Clin Genet*, 93(1), 111–8.
- Baglole, C. J., Bushinsky, S. M., Garcia, T. M., Kode, A., Rahman, I., Sime, P. J., & Phipps, R. P. (2006). Differential induction of apoptosis by cigarette smoke extract in primary human lung fibroblast strains: implications for emphysema. *Am J Physiol Lung Cell Mol Physiol*, 291(1), L19-29.
- Ballweg, K., Mutze, K., Königshoff, M., Eickelberg, O., & Meiners, S. (2014). Cigarette smoke extract affects mitochondrial function in alveolar epithelial cells. *Am J Physiol Lung Cell Mol Physiol*, 307(11), L895-907.
- Banat, G. A., Tretyn, A., Pullamsetti, S. S., Wilhelm, J., Weigert, A., Olesch, C., Ebel, K., Stiwe, T., Grimminger, F., Seeger, W., Fink, L., & Savai, R. (2015). Immune and Inflammatory Cell Composition of Human Lung Cancer Stroma. *PLoS One*,

10(9), e0139073.

- Barabutis, N., & Schally, A. V. (2008). Antioxidant activity of growth hormone-releasing hormone antagonists in LNCaP human prostate cancer line. *Proc Natl Acad Sci U S A*, 105(51), 20470–5.
- Barnes, P. J. (2004). Alveolar macrophages as orchestrators of COPD. *COPD*, 1(1), 59–70.
- Barnes, P. J. (2010). Mechanisms and resistance in glucocorticoid control of inflammation. *J Steroid Biochem Mol Biol*, 120(2–3), 76–85.
- Barnes, P. J. (2014). Cellular and molecular mechanisms of chronic obstructive pulmonary disease. *Clin Chest Med*, 35(1), 71–86.
- Barnes, P. J. (2016). Inflammatory mechanisms in patients with chronic obstructive pulmonary disease. *J of Allergy Clin Immunol*, 138(1), 16–27.
- Barnes, P. J. (2017). Cellular and molecular mechanisms of asthma and COPD. *Clin Sci (Lond)*, 131(13), 1541–58.
- Barnes, P. J., Burney, P. G. J., Silverman, E. K., Celli, B. R., Vestbo, J., Wedzicha, J. A., & Wouters, E. F. M. (2015). Chronic obstructive pulmonary disease. *Nat Rev Dis Primers*, 1, 15076.
- Barth, P. J., Koch, S., Müller, B., Unterstab, F., von Wichert, P., & Moll, R. (2000). Proliferation and number of Clara cell 10-kDa protein (CC10)-reactive epithelial cells and basal cells in normal, hyperplastic and metaplastic bronchial mucosa. *Virchows Arch*, 437(6), 648–55.
- Basma, H., Gunji, Y., Iwasawa, S., Nelson, A., Farid, M., Ikari, J., Liu, X., Wang, X., Michalski, J., Smith, L., Igbal, J., El Behery, R., West, W., Yelamanchili, S., Rennard, D., Holz, O., Mueller, K. C., Magnussen, H., Rabe, K., Castaldi, P. J., & Rennard, S. I. (2014). Reprogramming of COPD lung fibroblasts through formation of induced pluripotent stem cells. *Am J Physiol Lung Cell Mol Physiol*, 306(6), L552–65.
- Bedrossian, C. W. M., Weilbaecher, D. G., Bentinck, D. C., & Greenberg, S. D. (1975). Ultrastructure of human bronchiolo-alveolar cell carcinoma. *Cancer*, 36(4), 1399–413.
- Beeh, K. M. (2016). The role of bronchodilators in preventing exacerbations of chronic obstructive pulmonary disease. *Tuberc Respir Dis (Seoul)*, 79(4), 241–7.
- Bell, E. L., Klimova, T. A., Eisenbart, J., Moraes, C. T., Murphy, M. P., Budinger, G. R., & Chandel, N. S. (2007). The Qo site of the mitochondrial complex III is required for the transduction of hypoxic signaling via reactive oxygen species production. *J Cell Biol*, 177(6), 1029–36.
- Bentley, A. R., Emrani, P., & Cassano, P. A. (2008). Genetic variation and gene expression in antioxidant related enzymes and risk of COPD: a systematic review. *Thorax*, 63(11), 956–61.

- Bernardini, J. P., Lazarou, M., & Dewson, G. (2017). Parkin and mitophagy in cancer. *Oncogene*, 36(10), 1315–27.
- Bewley, M. A., Budd, R. C., Ryan, E., Cole, J., Collini, P., Marshall, J., Kolsum, U., Beech, G., Emes, R. D., Tcherniaeva, I., Berbers, G. A. M., Walmsley, S. R., Donaldson, G., Wedzicha, J. A., Kilty, I., Rumsey, W., Sanchez, Y., Brightling, C. E., Donnelly, L. E., Barnes, P. J., Singh, D., Whyte, M. K. B., Dockrell, D. H., & COPDMAP. (2018). Opsonic phagocytosis in chronic obstructive pulmonary disease is enhanced by Nrf2 agonists. *Am J Respir Crit Care Med*, 198(6), 739–50.
- Bhat, T. A., Panzica, L., Kalathil, S. G., & Thanavala, Y. (2015). Immune dysfunction in patients with chronic obstructive pulmonary disease. *Ann Am Thorac Soc*, 12 Suppl 2, S169–75.
- Bhowmick, R., & Gappa-Fahlenkamp, H. (2016). Cells and culture systems used to model the small airway epithelium. *Lung*, 194(3), 419–28.
- Binnewies, M., Roberts, E. W., Kersten, K., Chan, V., Fearon, D. F., Merad, M., Coussens, L. M., Gabrilovich, D. I., Ostrand-Rosenberg S., Hedrick, C. C., Vonderheide, R. H., Pittet, M. J., Jain, R. K., Zou, W., Howcroft, T. K., Woodhouse, E. C., Weinberg, R. A., & Krummel, M. F. (2018). Understanding the tumor immune microenvironment (TIME) for effective therapy. *Nat Med*, 24(5), 541–50.
- Biola-Clier, M., Beal, D., Caillat, S., Libert, S., Armand, L., Herlin-Boime, N., Sauvaigo, S., Douki, T., & Carriere, M. (2017). Comparison of the DNA damage response in BEAS-2B and A549 cells exposed to titanium dioxide nanoparticles. *Mutagenesis*, 32(1), 161–72.
- Boelens, M. C., Gustafson, A. M., Postma, D. S., Kok, K., van der Vries, G., van der Vlies, P., Spira, A., Lenburg, M. E., Geerlings, M., Sietsma, H., Timens, W., van den Berg, A., & Groen, H. J. (2011). A chronic obstructive pulmonary disease related signature in squamous cell lung cancer. *Lung Cancer*, 72(2), 177–83.
- Boelens, M. C., van den Berg, A., Fehrmann, R. S., Geerlings, M., de Jong, W. K., te Meerman, G. J., Sietsma, H., Timens, W., Postma, D. S., & Groen, H. J. (2009). Current smoking-specific gene expression signature in normal bronchial epithelium is enhanced in squamous cell lung cancer. *J Pathol*, 218(2), 182–91.
- Boland, M. L., Chourasia, A. H., & Macleod, K. F. (2013). Mitochondrial dysfunction in cancer. *Front Oncol*, 3, 292.
- Bonnet, S., Archer, S. L., Allalunis-Turner, J., Haromy, A., Beaulieu, C., Thompson, R., Lee, C. T., Lopaschuk, G. D., Puttagunta, L., Bonnet, S., Harry, G., Hashimoto, K., Porter, C. J., Andrade, M. A., Thebaud, B., & Michelakis, E. D. (2007). A mitochondria-K⁺ channel axis is suppressed in cancer and its normalization promotes apoptosis and inhibits cancer growth. *Cancer Cell*, 11(1), 37–51.
- Bozinovski, S., Vlahos, R., Anthony, D., McQualter, J., Anderson, G., Irving, L., & Steinfort, D. (2016). COPD and squamous cell lung cancer: aberrant

- inflammation and immunity is the common link. *Br J Pharmacol*, 173(4), 635–48.
- Brand, M. D. (2016). Mitochondrial generation of superoxide and hydrogen peroxide as the source of mitochondrial redox signaling. *Free Radic Biol Med*, 100, 14–31.
- Brand, M. D., & Nicholls, D. G. (2011). Assessing mitochondrial dysfunction in cells. *Biochem J*, 435(2), 297–312.
- Brandon, M., Baldi, P., & Wallace, D. C. (2006). Mitochondrial mutations in cancer. *Oncogene*, 25(34), 4768–76.
- Bridgeman, M. M., Marsden, M., Selby, C., Morrison, D., & MacNee, W. (1994). Effect of N-acetyl cysteine on the concentrations of thiols in plasma, bronchoalveolar lavage fluid, and lung tissue. *Thorax*, 49(7), 670–5.
- Bridges, R. B., Fu, M. C., & Rehm, S. R. (1985). Increased neutrophil myeloperoxidase activity associated with cigarette smoking. *Eur J Respir Dis*, 67(2), 84–93.
- Broniowska, K. A., Oleson, B. J., McGraw, J., Naatz, A., Mathews, C. E., & Corbett, J. A. (2015). How the location of superoxide generation influences the β -cell response to nitric oxide. *J Biol Chem*, 290(12), 7952–60.
- Brücher, B. L., & Jamall, I. S. (2014). Cell-cell communication in the tumor microenvironment, carcinogenesis, and anticancer treatment. *Cell Physiol Biochem*, 34(2), 213–43.
- Bucchieri, F., Marino Gammazza, A., Pitruzzella, A., Fucarino, A., Farina, F., Howarth, P., Holgate, S. T., Zummo, G., & Davies, D. E. (2015). Cigarette smoke causes caspase-independent apoptosis of bronchial epithelial cells from asthmatic donors. *PLoS One*, 10(3), e0120510.
- Burney, P., Jithoo, A., Kato, B., Janson, C., Mannino, D., Nizankowska-Mogilnicka, E., Studnicka, M., Tan, W., Bateman, E., Kocabas, A., Vollmer, W. M., Gislason, T., Marks, G., Koul, P. A., Harrabi, I., Gnatiuc, L., Buist, S. (2014). Chronic obstructive pulmonary disease mortality and prevalence: the associations with smoking and poverty—a BOLD analysis. *Thorax*, 69(5), 465–73.
- Cairns, R. A., Harris, I. S., & Mak, T. W. (2011). Regulation of cancer cell metabolism. *Nat Rev Cancer*, 11(2), 85–95.
- Calcinotto, A., Filipazzi, P., Grioni, M., Iero, M., De Milito, A., Ricupito, A., Cova, A., Canese, R., Jachetti, E., Rossetti, M., Huber, V., Parmiani, G., Generoso, L., Santhinami, M., Borghi, M., Fais, S., Bellone, M., Rivoltini, L. (2012). Modulation of microenvironment acidity reverses anergy in human and murine tumor-infiltrating T lymphocytes. *Cancer Res*, 72(11), 2746–56.
- Calmettes, G., Ribalet, B., John, S., Korge, P., Ping, P., & Weiss, J. N. (2015). Hexokinases and cardioprotection. *J Mol Cell Cardiol*, 78, 107–15.
- Camelo, A., Dunmore, R., Sleeman, M. A., & Clarke, D. L. (2014). The epithelium in idiopathic pulmonary fibrosis: breaking the barrier. *Front Pharmacol*, 4, 173.

- Cancer Research UK, <https://www.cancerresearchuk.org/health-professional/cancer-statistics/statistics-by-cancer-type/lung-cancer>, (2017, May). Lung cancer statistics.
- Caramori, G., Casolari, P., Cavallesco, G. N., Giuffre, S., Adcock, I., & Papi, A. (2011). Mechanisms involved in lung cancer development in COPD. *Int J Biochem Cell Biol*, 43, 1030–44.
- Caramori, G., Adcock, I. M., Casolari, P., Ito, K., Jazrawi, E., Tsaprouni, L., Villetti, G., Civelli, M., Carnini, C., Chung, K. F., Barnes, P. J., Papi, A. (2011). Unbalanced oxidant-induced DNA damage and repair in COPD: a link towards lung cancer. *Thorax*, 66(6), 521–7.
- Caramori, G., Casolari, P., Barczyk, A., Durham, A. L., Di Stefano, A., & Adcock, I. (2016). COPD immunopathology. *Semin Immunopathol*, 38(4), 497–515.
- Carpagnano, G. E., Lacedonia, D., Carone, M., Soccio, P., Cotugno, G., Palmiotti, G. A., Scioscia, G., & Foschino Barbaro, M. P. (2016). Study of mitochondrial DNA alteration in the exhaled breath condensate of patients affected by obstructive lung diseases. *J Breath Res*, 10(2), 026005.
- Carter, B. W., Glisson, B. S., Truong, M. T., & Erasmus, J. J. (2014). Small cell lung carcinoma: staging, imaging, and treatment considerations. *Radiographics*, 34(6), 1707–21.
- Carter, E. A., Bonab, A. A., Goverman, J., Paul, K., Yerxa, J., Tompkins, R. G., & Fischman, A. J. (2011). Evaluation of the antioxidant peptide SS31 for treatment of burn-induced insulin resistance. *Int J Mol Med*, 28(4), 589–94.
- Cazzola, M., & Matera, M.G.. (2014). Bronchodilators: current and future. *Clin Chest Med*, 35(1), 191–201.
- Celli, B., Decramer, M., Kesten, S., Liu, D., Mehra, S., & Tashkin, D. P. (2009). Mortality in the 4-year trial of tiotropium (UPLIFT) in patients with chronic obstructive pulmonary disease. *Am J Respir Crit Care Med*, 180(10), 948–55.
- Ceylan, E., Kocyigit, A., Gencer, M., Aksoy, N., & Selek, S.. (2006). Increased DNA damage in patients with chronic obstructive pulmonary disease who had once smoked or been exposed to biomass. *Respir Med*, 100(7), 1270–6.
- Che, R., Yuan, Y., Huang, S., & Zhang, A. (2014). Mitochondrial dysfunction in the pathophysiology of renal diseases. *Am J Physiol Renal Physiol*, 306(4), F367–78.
- Chen, H., Chomyn, A., & Chan, D. C. (2005). Disruption of fusion results in mitochondrial heterogeneity and dysfunction. *J Biol Chem*, 280(28), 26185–92.
- Chen, W., Wang, Q., Bai, L., Chen, W., Wang, X., Tellez, C. S., Leng, S., Padilla, M. T., Nyunoya, T., Belinsky, S. A., & Lin, Y. (2014). RIP1 maintains DNA integrity and cell proliferation by regulating PGC-1 α -mediated mitochondrial oxidative phosphorylation and glycolysis. *Cell Death Differ*, 21(7), 1061–70.
- Cheng, G., Zielonka, M., Dranka, B., Kumar, S. N., Myers, C. R., Bennett, B.,

- Garces, A. M., Dias Duarte Machado, L. G., Thiebaut, D., Ouari, O., Hardy, M., Zielonka, J., & Kalyanaraman, B. (2018). Detection of mitochondria-generated reactive oxygen species in cells using multiple probes and methods: Potentials, pitfalls, and the future. *J Biol Chem*, 293(26), 10363–80.
- Cheng, X. Y., Li, Y. Y., Huang, C., Li, J., & Yao, H. W. (2017). AMP-activated protein kinase reduces inflammatory responses and cellular senescence in pulmonary emphysema. *Oncotarget*, 8(14), 22513–23.
- Chiang, Y. Y., Chen, S. L., Hsiao, Y. T., Huang, C. H., Lin, T. Y., Chiang, I. P., Hsu, W. H., & Chow, K. C. (2009). Nuclear expression of dynamin-related protein 1 in lung adenocarcinomas. *Mod Pathol*, 22(9), 1139–50.
- Chiche, J., Rouleau, M., Gounon, P., Brahim-Horn, M. C., Pouyssegur, J., & Mazure, N. M. (2009). Hypoxic enlarged mitochondria protect cancer cells from apoptotic stimuli. *J Cell Physiol*, 222(3), 648–57.
- Chrysofakis, G., Tzanakis, N., Kyriakoy, D., Tsoumakidou, M., Tsiligianni, I., Klimathianaki, M., & Siafakas, Ni. M. (2004). Perforin expression and cytotoxic activity of sputum CD8+ lymphocytes in patients with COPD. *Chest*, 125(1), 71–6.
- Chung, K. F.. (2005). The role of airway smooth muscle in the pathogenesis of airway wall remodeling in chronic obstructive pulmonary disease. *Proc Am Thorac Soc*, 2(4), 347-54; discussion 371–2.
- Chung, W., Eum, H. H., Lee, H. O., Lee, K. M., Lee, H. B., Kim, K. T., Ryu, H. S., Kim, S., Lee, J. E., Park, Y. H., Kan, Z., Han, W., & Park, W. Y. (2017). Single-cell RNA-seq enables comprehensive tumour and immune cell profiling in primary breast cancer. *Nat Commun*, 8, 15081.
- Cloonan, S. M., & Choi, A. M. (2016). Mitochondria in lung disease. *J Clin Invest*, 126(3), 809–20
- Cooper, Jim. (2012). Cell line profile A549 (ECACC catalogue no. 86012804). *European Collection of Authenticated Cell Cultures*. 1–2
- Cortes, D. F., Sha, W., Hower, V., Blekherman, G., Laubenbacher, R., Akman, S., Torti, S. V., & Shulaev, V. (2011). Differential gene expression in normal and transformed human mammary epithelial cells in response to oxidative stress. *Free Radic Biol Med*, 50(11), 1565–74.
- Craft, B. D., Kerrihard, A. L., Amarowicz, R., & Pegg, R. B. (2012). Phenol-based antioxidants and the in vitro methods used for their assessment. *Compr Rev Food Sci F*, 11(2), 148–73.
- Crawford, E. L., Khuder, S. A., Durham, S. J., Frampton, M., Utell, M., Thilly, W. G., Weaver, D. A., Ferencak, W. J., Jennings, C. A., Hammersley, J. R., Olson, D. A., & Willey, J. C. (2000). Normal bronchial epithelial cell expression of glutathione transferase P1, glutathione transferase M3, and glutathione peroxidase is low in subjects with bronchogenic carcinoma. *Cancer Res*, 60(6), 1609–18.

- Culpitt, S. V., Rogers, D. F., Shah, P., De Matos, C., Russell, R. E., Donnelly, L. E., & Barnes, P. J. (2003). Impaired inhibition by dexamethasone of cytokine release by alveolar macrophages from patients with chronic obstructive pulmonary disease. *Am J Respir Crit Care Med*, 167(1), 24–31.
- D'Anna, C., Cigna, D., Costanzo, G., Ferraro, M., Siena, L., Vitulo, P., Gjomarkaj, M., & Pace, E. (2015). Cigarette smoke alters cell cycle and induces inflammation in lung fibroblasts. *Life Sci*, 126, 10–8.
- D'Errico, I., Salvatore, L., Murzilli, S., Lo Sasso, G., Latorre, D., Martelli, N., Egorova, A. V., Polishuck, R., Madeyski-Bengtson, K., Lelliott, C., Vidal-Puig, A. J., Siebel, P., Villani, G., & Moschetta, A. (2011). Peroxisome proliferator-activated receptor-gamma coactivator 1-alpha (PGC1alpha) is a metabolic regulator of intestinal epithelial cell fate. *Proc Natl Acad Sci U S A*, 108(16), 6603–8.
- Daijo, H., Hoshino, Y., Kai, S., Suzuki, K., Nishi, K., Matsuo, Y., Harada, H., & Hirota, K. (2016). Cigarette smoke reversibly activates hypoxia-inducible factor 1 in a reactive oxygen species-dependent manner. *Sci Rep*, 6(1), 34424.
- Dal Negro, R. W., Wedzicha, J. A., Iversen, M., Fontana, G., Page, C., Cicero, A. F., Pozzi, E., Calverley, P. M., & RESTORE group. RESTORE study. (2017). Effect of erdosteine on the rate and duration of COPD exacerbations: the RESTORE study. *Eur Respir J*, 50(4), 1700711.
- Dasari, S., & Bernard Tchounwou, P. (2014). Cisplatin in cancer therapy: molecular mechanisms of action. *Eur J Pharmacol*, 740, 364–78.
- Dasgupta, S., Soudry, E., Mukhopadhyay, N., Shao, C., Yee, J., Lam, W., Zhang, W., Gazdar, A. F., Fisher, P. B., & Sidransky, D. (2012). Mitochondrial DNA mutations in respiratory complex-I in never-smoker lung cancer patients contribute to lung cancer progression and associated with EGFR gene mutation. *J Cell Physiol*, 227(6), 2451–60.
- Davis, A. S., Chertow, D. S., Moyer, J. E., Suzich, J., Sandouk, A., Dorward, D. W., Logun, C., Shelhamer, J. H., & Taubenberger, J. K. (2015). Validation of normal human bronchial epithelial cells as a model for influenza A infections in human distal trachea. *J Histochem Cytochem*, 63(5), 312–28.
- De Benedetto, F., Aceto, A., Dragani, B., Spacone, A., Formisano, S., Pela, R., Donner, C. F., & Sanguinetti, C. M. (2005). Long-term oral n-acetylcysteine reduces exhaled hydrogen peroxide in stable COPD. *Pulm Pharmacol Ther*, 18(1), 41–7.
- De Craene, B., & Berx, G. (2013). Regulatory networks defining EMT during cancer initiation and progression. *Nat Rev Cancer*, 13(2), 97–110.
- De Fauw, J., Ledsam, J. R., Romera-Paredes, B., Nikolov, S., Tomasev, N., Blackwell, S., Askham, H., Glorot, X., O'Donoghue, B., Visentin, D., van den Driessche, G., Lakshminarayana, B., Meyer, C., Mackinder, F., Bouton, S., Ayoub, K., Chopra, R., King, D., Karthikesalingam, A., Hughes, C. O., Raine, R., Hughes, J., Sim, D. A., Egan, C., Tufial, A., Montgomery, H., Hassabis, D., Ree, G., Back, T., Khaw, P. T., Suleyman, M., Cornebise, J., Keane, P. A., &

- Ronneberger, O. (2018). Clinically applicable deep learning for diagnosis and referral in retinal disease. *Nat Med*, 24(9), 1342–50.
- De Luca, A., Fiorillo, M., Peiris-Pagès, M., Ozsvari, B., Smith, D. L., Sanchez-Alvarez, R., Martinez-Outschoorn, U. E., Cappello, A. R., Pezzi, V., Lisanti, M. P., & Sotgia, F. (2015). Mitochondrial biogenesis is required for the anchorage-independent survival and propagation of stem-like cancer cells. *Oncotarget*, 6(17), 14777–95.
- De Torres, J. P., Marín, J. M., Casanova, C., Cote, C., Carrizo, S., Cordoba-Lanus, E., Baz-Dávila, R., Zulueta, J. J., Aguirre-Jaime, A., Saetta, M., Cosio, M. G., & Celli, B. R. (2011). Lung cancer in patients with chronic obstructive pulmonary disease: Incidence and predicting factors. *Am J Respir Crit Care Med*, 184(8), 913–9.
- Decramer, M., Rutten-van Mólken, M., Dekhuijzen, P. N., Troosters, T., van Herwaarden, C., Pellegrino, R., van Schayck, C. P., Olivieri, D., Del Donno, M., De Backer, W, Lankhorst, I., Ardia, A. (2005). Effects of N-acetylcysteine on outcomes in chronic obstructive pulmonary disease (Bronchitis Randomized on NAC Cost-Utility Study, BRONCUS): a randomised placebo-controlled trial. *Lancet*, 365(9470), 1552–60.
- Dekhuijzen, P. N., Aben, K. K., Dekker, I., Aarts, L. P., Wielders, P. L., van Herwaarden, C. L., & Bast, A. (1996). Increased exhalation of hydrogen peroxide in patients with stable and unstable chronic obstructive pulmonary disease. *Am J Respir Crit Care Med*, 154(3 Pt 1), 813–6.
- Demedts, I. K., Demoor, T., Bracke, K. R., Joos, G. F., & Brusselle, G. G. (2006). Role of apoptosis in the pathogenesis of COPD and pulmonary emphysema. *Respir Res*, 7, 53.
- Di Stefano, A., Caramori, G., Barczyk, A., Vicari, C., Brun, P., Zanini, A., Cappello, F., Garofano, E., Padovani, A., Contoli, M., Casolari, P., Durham, A. L., Chung, K. F., Barnes, P. J., Papi, A., Adcock, I., & Balbi, B. (2014). Innate immunity but not NLRP3 inflammasome activation correlates with severity of stable COPD. *Thorax*, 69(6), 516–24.
- Diehn, M., Cho, R. W., Lobo, N. A., Kalisky, T., Dorie, M. J., Kulp, A. N., Qian, D., Lam, J. S., Ailles, L. E., Wong, M., Joshua, B., Kaplan, M. J., Wapnir, I, Dirbas, F. M., Somlo, G., Garberoglio, C., Paz, B., Shen, J., Lau, S. K., Quake, S. R., Brown, J. M., Weissman, I. L., & Clarke, M. F. (2009). Association of reactive oxygen species levels and radioresistance in cancer stem cells. *Nature*, 458(7239), 780–3.
- Dier, U., Shin, D. H., Hemachandra, L. P., Uusitalo, L. M., & Hempel, N.. (2014). Bioenergetic analysis of ovarian cancer cell lines: profiling of histological subtypes and identification of a mitochondria-defective cell line. *PLoS One*, 9(5), e98479.
- Domej, W., Oettl, K., & Renner, W. (2014). Oxidative stress and free radicals in COPD--implications and relevance for treatment. *Int J Chron Obstruct Pulmon*

- Dis*, 9, 1207–24.
- Dominy, J. E., Lee, Y., Gerhart-Hines, Z., & Puigserver, Pere. (2010). Nutrient-dependent regulation of PGC-1 α 's acetylation state and metabolic function through the enzymatic activities of Sirt1/GCN5. *Biochim Biophys Acta*, 1804(8), 1676–83.
- Domyan, E. T., & Sun, X. (2011). Patterning and plasticity in development of the respiratory lineage. *Dev Dyn*, 240(3), 477–85.
- Drannik, A. G., Pouladi, M. A., Robbins, C. S., Goncharova, S. I., Kianpour, S., & Stämpfli, M. R. (2004). Impact of cigarette smoke on clearance and inflammation after *Pseudomonas aeruginosa* infection. *Am J Respir Crit Care Med*, 170(11), 1164–71.
- Drost, E. M., Skwarski, K. M., Sauleda, J., Soler, N., Roca, J., Agusti, A., & MacNee, W. (2005). Oxidative stress and airway inflammation in severe exacerbations of COPD. *Thorax*, 60(4), 293–300.
- Durham, A. L., & Adcock, I. M. (2015). The relationship between COPD and lung cancer. *Lung Cancer*, 90(2), 121–7.
- Durham, A. L., McLaren, A., Hayes, B. P., Caramori, G., Clayton, C. L., Barnes, P. J., Chung, K. F., Adcock, I. M. (2013). Regulation of Wnt4 in chronic obstructive pulmonary disease. *FASEB J*, 27(6), 2367–81.
- Eigenbrodt, E., & Glossmann, H. (1980). Glycolysis—one of the keys to cancer? *Trends Pharmacol Sci*, 1(2), 240–5.
- Eisner, V., Picard, M., & Hajnóczky, G.. (2018). Mitochondrial dynamics in adaptive and maladaptive cellular stress responses. *Nat Cell Biol*, 20(7), 755–65.
- Ekstrand, M.I., Falkenberg, M., Rantanen, A., Park, C.B., Gaspari, M., Hultenby, K., Rustin, P., Gustafsson, C.M. & Larsson, NG. (2004). Mitochondrial transcription factor A regulates mtDNA copy number in mammals. *Hum Mol Genet*, 13(9), 935–44.
- El-Hafiz, A. M., El-Wakeel, L. M., El-Hady, H. M., & El-Raheem, M. (2013). High dose N-acetyl cysteine improves inflammatory response and outcome in patients with COPD exacerbations. *Egypt J Chest Dis Tuberc*, 62(1), 51–7.
- Epstein, T., Xu, L., Gillies, R. J., & Gatenby, R. A. (2014). Separation of metabolic supply and demand: aerobic glycolysis as a normal physiological response to fluctuating energetic demands in the membrane. *Cancer Metab*, 2, 7.
- Erdélyi, K., Pacher, P., Virág, L., & Szabó, C. (2013). Role of poly(ADP-ribosyl)ation in a “two-hit” model of hypoxia and oxidative stress in human A549 epithelial cells in vitro. *Int J Mol Med*, 32(2), 339–46.
- Erlemann, K. R., Cossette, C., Gravel, S., Lesimple, A., Lee, G. J., Saha, G., Rokach, J., Powell, W. S. (2006). Airway epithelial cells synthesize the lipid mediator 5-oxo-ETE in response to oxidative stress. *Free Radic Biol Med*, 42, 654–64.

- Ernster, L., & Schatz, G. (1981). Mitochondria: a historical review. *J Cell Biol*, 91(3 Pt 2), 227s–55s.
- Eskan, M. A., Benakanakere, M. R., Rose, B. G., Zhang, P., Zhao, J., Stathopoulou, P., Fujioka, D., Kinane, D. F. (2008). Interleukin-1beta modulates proinflammatory cytokine production in human epithelial cells. *Infec Immun*, 76(5), 2080–9.
- Espinosa-Diez, C., Miguel, V., Mennerich, D., Kietzmann, T., Sánchez-Pérez, P., Cadenas, S., & Lamas, S.. (2015). Antioxidant responses and cellular adjustments to oxidative stress. *Redox Biol*, 6, 183–97.
- Faner, R., Sobradillo, P., Noguera, A., Gomez, C., Cruz, T., López-Giraldo, A., Ballester, E., Soler, N., Arostegui, J. I., Pelegrin, P., Rodriguez-Roisin, R., Yagüe, J., Cosio, B. G., Jaun, M., & Agustí, A. (2016). The inflammasome pathway in stable COPD and acute exacerbations. *ERJ Open Res*, 2(3).
- Fang, H. Y., Chen, C. Y., Chiou, S. H., Wang, Y. T., Lin, T. Y., Chang, H. W., Chieang, I. P., Lan, K. J., & Chow, K. C. (2012). Overexpression of optic atrophy 1 protein increases cisplatin resistance via inactivation of caspase-dependent apoptosis in lung adenocarcinoma cells. *Hum Pathol*, 43(1), 105–14.
- Fehrenbach, H. (2001). Alveolar epithelial type II cell: defender of the alveolus revisited. *Respiratory Research*, 2(1), 33–46.
- Ferlay, J., Shin, HR, Bray, F., Forman, D., Mathers, C., & Parkin, D. (2010). Estimates of worldwide burden of cancer in 2008: GLOBOCAN 2008. *Int J Cancer*, 127(12), 2893–917.
- Ferreira, I. M., Hazari, M. S., Gutierrez, C., Zamel, N., & Chapman, K. R. (2001). Exhaled nitric oxide and hydrogen peroxide in patients with chronic obstructive pulmonary disease. *Am J Respir Crit Care Med*, 164(6), 1012–5.
- Fine-Coulson, K., Giguère, S., Quinn, F. D., & Reaves, B. J. (2015). Infection of A549 human type II epithelial cells with Mycobacterium tuberculosis induces changes in mitochondrial morphology, distribution and mass that are dependent on the early secreted antigen, ESAT-6. *Microbes Infect*, 17(10), 689–97.
- Finkel, T. (2011). Signal transduction by reactive oxygen species. *J Cell Biol*, 194(1), 7–15.
- Footitt, J., Mallia, P., Durham, A. L., Ho, W. E., Trujillo-Torralbo, M. B., Telcian, A. G., Del, R. A., Chang, C., Peh, H. Y., Keadze, T., Aniscenko, J., Stanciu, L., Essilfie-Quaye, S., Ito, K., Barnes, P. J., Elkin, S. L., Kon, O. M., Wong, W. S., Adcock, I. M., & Johnston, S. L. (2016). Oxidative and nitrosative stress and histone deacetylase-2 activity in exacerbations of COPD. *Chest*, 149(1), 62–73.
- Forde, P. M., & Ettinger, D. S. (2013). Targeted therapy for non-small-cell lung cancer: past, present and future. *Expert Rev Anticancer Ther*, 13(6), 745–58.
- Forum of International Respiratory Societies (FIRS). (2013). Respiratory diseases in the world. Realities of today—opportunities for tomorrow. *Eur Respir Soc*, 1-35.

- Franks, T. J., Colby, T. V., Travis, W. D., Tuder, R. M., Reynolds, H. Y., Brody, A. R., Cardoso, W. V., Crystal, R. G., Drake, C. J., Engelhardt, J., Frid, M., Herzog, E., Mason, R., Phan, S. H., Randell, S. H., Rose, M. C., Stevens, T., Serge, J., Sunday, M. E., Voynow, J. A., Weinstein, B. M., Whitsett, J., & Williams, M. C. (2008). Resident cellular components of the human lung current knowledge and goals for research on cell phenotyping and function. *Proc Am Thorac Soc*, 5, 763–6.
- Fujii, Y., Tomita, K., Sano, H., Yamasaki, A., Hitsuda, Y., Adcock, I. M., & Shimizu, E. (2002). Dissociation of DNA damage and mitochondrial injury caused by hydrogen peroxide in SV-40 transformed lung epithelial cells. *Cancer Cell Int*, 2, 16.
- Fujino, N., Kubo, H., Suzuki, T., Ota, C., Hegab, A. E., He, M., Suzuki, S., Suzuki, T., Yamada, M., Kondo, T., Kato, H., & Yamaya, M. (2011). Isolation of alveolar epithelial type II progenitor cells from adult human lungs. *Lab Invest*, 91(3), 363–78.
- Gane, E. J., Weilert, F., Orr, D. W., Keogh, G. F., Gibson, M., Lockhart, M. M., Frampton, C. M., Taylor, K. M., Smith R. A., & Murphy, M. P. (2010). The mitochondria-targeted anti-oxidant mitoquinone decreases liver damage in a phase II study of hepatitis C patients. *Liver Int*, 30(7), 1019–26.
- Ganesan, S., Unger, B. L., Comstock, A. T., Angel, K. A., Mancuso, P., Martinez, F. J., & Sajjan, U. S. (2013). Aberrantly activated EGFR contributes to enhanced IL-8 expression in COPD airways epithelial cells via regulation of nuclear FoxO3A. *Thorax*, 68(2), 131–41.
- Gao, W., Li, L., Wang, Y., Zhang, S., Adcock, I. M., Barnes, P. J., Huang, M., & Yao, X. (2015). Bronchial epithelial cells: The key effector cells in the pathogenesis of chronic obstructive pulmonary disease? *Respirology*, 20(5), 722–9.
- Garcia-Canton, C., Minet, E., Anadon, A., & Meredith, C. (2013). Metabolic characterization of cell systems used in in vitro toxicology testing: lung cell system BEAS-2B as a working example. *Toxicol In Vitro*, 27(6), 1719–27.
- Garcia-Heredia, J. M., & Carnero, A. (2015). Decoding Warburg's hypothesis: tumor-related mutations in the mitochondrial respiratory chain. *Oncotarget*, 6(39), 41582–99.
- García-Ruiz, I., Solís-Muñoz, P., Fernández-Moreira, D., Muñoz-Yagüe, T., & Solís-Herruzo, J. A. (2013). Pioglitazone leads to an inactivation and disassembly of complex I of the mitochondrial respiratory chain. *BMC Biol*, 11, 88.
- Gęgotek, A., Nikliński, J., Żarković, N., Żarković, K., Waeg, G., Łuczaj, W., Charkiewicz, R., & Skrzydlewska, E. (2016). Lipid mediators involved in the oxidative stress and antioxidant defence of human lung cancer cells. *Redox Biol*, 9, 210–9.
- Gerő, D., Torregrossa, R., Perry, A., Waters, A., Le-Trionnaire, S., Whatmore, J. L., Wood, M., & Whiteman, M. (2016). The novel mitochondria-targeted hydrogen sulfide (H₂S) donors AP123 and AP39 protect against hyperglycemic injury in

- microvascular endothelial cells in vitro. *Pharmacol Res*, 113(Pt A), 186–98.
- Giangreco, A., Reynolds, S. D., & Stripp, B. R. (2002). Terminal bronchioles harbor a unique airway stem cell population that localizes to the bronchoalveolar duct junction. *Am J Pathol*, 161(1), 173–82.
- Giard, D. J., Aaronson, S. A., Todaro, G. J., Arnstein, P., Kersey, J. H., Dosik, H., & Parks, W. P. (1973). In vitro cultivation of human tumors: establishment of cell lines derived from a series of solid tumors. *J Natl Cancer Inst*, 51(5), 1417–23.
- Global Initiative for Chronic Obstructive Lung Disease (GOLD). (2017). Global strategy for the diagnosis, management, and prevention of chronic obstructive pulmonary disease (2017 report).
- Go, S. I., Lee, W. S., Lee, G. W., Kang, J. H., Kang, M. H., Song, H. N., Lee, A., Lee, U. S., Choi, H. J., & Kim, H. G. (2014). Gemcitabine plus vinorelbine as the second-line treatment and beyond in elderly patients with platinum-pretreated advanced non-small cell lung cancer. *Chemotherapy*, 60(4), 267–73.
- Goldkorn, T., Filosto, S., & Chung, S. (2014). Lung injury and lung cancer caused by cigarette smoke-induced oxidative stress: molecular mechanisms and therapeutic opportunities involving the ceramide-generating machinery and epidermal growth factor receptor. *Antioxid Redox Signal*, 21(15), 2149–74.
- Gosker, H. R., Hesselink, M. K., Duimel, H., Ward, K. A., & Schols, A. M. (2007). Reduced mitochondrial density in the vastus lateralis muscle of patients with COPD. *Eur Respir J*, 30(1), 73–9.
- Gou, L. Y., Niu, F. Y., Wu, Y. L., & Zhong, W. Z. (2015). Differences in driver genes between smoking-related and non-smoking-related lung cancer in the Chinese population. *Cancer*, 121 Suppl 17, 3069–79.
- Gray, L. R., Tompkins, S. C., & Taylor, E. B. (2014). Regulation of pyruvate metabolism and human disease. *Cell Mol Life Sci*, 71(14), 2577–604.
- Griendling, K. K., Touyz, R. M., Zweier, J. L., Dikalov, S., Chilian, W., Chen, Y. R., Harrison, D. G., & Bhatnagar, A. (2016). Measurement of reactive oxygen species, reactive nitrogen species, and redox-dependent signaling in the cardiovascular system: a scientific statement from the American Heart Association. *Circ Res*, 119(5), e39-75.
- Grivennikov, S. I., & Karin, M. (2010). Dangerous liaisons: STAT3 and NF-κB collaboration and crosstalk in cancer. *Cytokine Growth Factor Rev*, 21(1), 11–9.
- Grumelli, S., Corry, D. B., Song, L. Z., Song, L., Green, L., Huh, J., Hacken, J., Espada, R., Bag, R., Lewis, D. E., & Kheradmand, F. (2004). An immune basis for lung parenchymal destruction in chronic obstructive pulmonary disease and emphysema. *PLoS Med*, 1(1), e8.
- Guillot, L., Nathan, N., Tabary, O., Thouvenin, G., Le Rouzic, P., Corvol, H., Amselem, S., & Clement, A. (2013). Alveolar epithelial cells: master regulators of lung homeostasis. *Int J Biochem Cell Biol*, 45(11), 2568–73.

- Gülden, M., Jess, A., Kammann, J., Maser, E., & Seibert, H.. (2010). Cytotoxic potency of H₂O₂ in cell cultures: impact of cell concentration and exposure time. *Free Radic Biol Med*, 49(8), 1298–305.
- Guo, L., Li, L., Wang, W., Pan, Z., Zhou, Q., & Wu, Z. (2012). Mitochondrial reactive oxygen species mediates nicotine-induced hypoxia-inducible factor-1 α expression in human non-small cell lung cancer cells. *Biochim Biophys Acta*, 1822(6), 852–61.
- Hadad, S. M., Baker, L., Quinlan, P. R., Robertson, K. E., Bray, S. E., Thomson, G., Kellock, D., Jordan, L. B., Purdie, C. A., Hardie, D. G., Fleming, S., & Thompson, A. M. (2009). Histological evaluation of AMPK signalling in primary breast cancer. *BMC Cancer*, 9, 307.
- Hallgren, O., Nihlberg, K., Dahlbäck, M., Bjermer, L., Eriksson, L. T., Erjefält, J. S., Löfdahl, C. G., & Westergren-Thorsson, G. (2010). Altered fibroblast proteoglycan production in COPD. *Respir Res*, 11, 55.
- Hamada, S., Sato, A., Hara-Chikuma, M., Satooka, H., Hasegawa, K., Tanimura, K., Tanizawa, K., Inouchi, M., Handa, T., Oga, T., Muro, S., Mishima, M., & Chin, K. (2016). Role of mitochondrial hydrogen peroxide induced by intermittent hypoxia in airway epithelial wound repair in vitro. *Exp Cell Res*, 344(1), 143–51.
- Han, J., Zhang, L., Guo, H., Wysham, W. Z., Roque, D. R., Willson, A. K., Sheng, X., Bae-Jump, V. L. (2015). Glucose promotes cell proliferation, glucose uptake and invasion in endometrial cancer cells via AMPK/mTOR/S6 and MAPK signaling. *Gynecol Oncol*, 138(3), 668–75.
- Hanahan, D., & Weinberg, R. A. (2011). Hallmarks of cancer: the next generation. *Cell*, 144(5), 646–74.
- Hann, S. S., Zheng, F., & Zhao, S. (2013). Targeting 3-phosphoinositide-dependent protein kinase 1 by N-acetyl-cysteine through activation of peroxisome proliferators activated receptor alpha in human lung cancer cells, the role of p53 and p65. *J Exp Clin Cancer Res*, 32, 43.
- Hänzelmann, S., Castelo, R., & Guinney, J. (2013). GSVA: gene set variation analysis for microarray and RNA-seq data. *BMC Bioinformatics*, 14, 7.
- Hara, H., Araya, J., Ito, S., Kobayashi, K., Takasaka, N., Yoshii, Y., Wakui, H., Kojima, J., Shimuzu, K., Numata, T., Kawaishi, M., Kamiya, N., Odaka, M., Morikawa, T., Kaneka, Y., Nakayama, K., & Kuwano, K. (2013). Mitochondrial fragmentation in cigarette smoke-induced bronchial epithelial cell senescence. *Am J Physiol Lung Cell Mol Physiol*, 305(10), L737–L46.
- Hardie, D. G. (2011). AMP-activated protein kinase: an energy sensor that regulates all aspects of cell function. *Genes Dev*, 25(18), 1895–908.
- Harris, A. L. (2002). Hypoxia- a key regulatory factor in tumour growth. *Nat Rev Cancer*, 2(1), 38–47.
- Harris, R. A., Bowker-Kinley, M. M., Huang, B., & Wu, P. (2002). Regulation of the activity of the pyruvate dehydrogenase complex. *Adv Enzyme Regul*, 42, 249–311

59.

- Harrison, R. (2002). Structure and function of xanthine oxidoreductase: where are we now? *Free Radic Biol Med*, 33(6), 774–97.
- Heijink, I. H., Brandenburg, S. M., Noordhoek, J. A., Slebos, D. J., Postma, D. S., & van Oosterhout, A. J. (2011). Role of aberrant metalloproteinase activity in the pro-inflammatory phenotype of bronchial epithelium in COPD. *Respir Res*, 12, 110.
- Heijink, I., van Oosterhout, A., Kliphuis, N., Jonker, M., Hoffmann, R., Telenga, E., Klooster, K., Slebos, D. J., ten Hacken, N., Postma, D., & van den Berge, M. (2014). Oxidant-induced corticosteroid unresponsiveness in human bronchial epithelial cells. *Thorax*, 69(1), 5–13.
- Heikkinen, S., Suppola, S., Malkki, M., Deeb, S. S., Jänne, J., & Laakso, M. (2000). Mouse hexokinase II gene: structure, cDNA, promoter analysis, and expression pattern. *Mamm Genome*, 11(2), 91–6.
- Hekking, P. P., Loza, M. J., Pavlidis, S., De Meulder, B., Lefaudeux, D., Baribaud, F., Auffray, C., Wagener, A. H., Brinkman, P., Lutter, R., Bansal, A. T., Sousa, S. A., Sousa, A. R., Bates, S. A., Pandis, I., Flaming, L. J., Shaw, D. E., Fowler, S. J., Guo, Y., Meister, A., Sun, K., Corfield, J., Howarth, P., Bel, E. H., Adcock, I. M., Chung, K. F., Djukanovic, R., Sterk, P. J. (2017). Transcriptomic gene signatures associated with persistent airflow limitation in patients with severe asthma. *Eur Respir J*, 50(3).
- Hellermann, G. R., Nagy, S. B., Kong, X., Lockey, R. F., & Mohapatra, S. S. (2002). Mechanism of cigarette smoke condensate-induced acute inflammatory response in human bronchial epithelial cells. *Respir Res*, 3(1), 15.
- Hemmi, H., Takeuchi, O., Kawai, T., Kaisho, T., Sato, S., Sanjo, H., Matsumoto, M., Hoshino, K., Wagner, H., Takeda, K., & Akira, S. (2000). A Toll-like receptor recognizes bacterial DNA. *Nature*, 408(6813), 740–5.
- Henson, P. M., Cosgrove, G. P., & Vandivier, R. W. (2006). Apoptosis and cell homeostasis in chronic obstructive pulmonary disease. *Proc Am Thorac Soc*, 3(6), 512–6.
- Herfs, M., Hubert, P., Poirrier, A. L., Vandevenne, P., Renoux, V., Habraken, Y., Cataldo, D., Bonvier, J., & Delvenne, P. (2012). Proinflammatory cytokines induce bronchial hyperplasia and squamous metaplasia in smokers. *Am J Respir Cell Mol Biol*, 47(1), 67–79.
- Hertzog, M. A. (2008). Considerations in determining sample size for pilot studies. *Res Nurs Health*, 31(2), 180–91.
- Hill, S., Sataranatarajan, K., & Remmen, H. V. (2018). Role of signaling molecules in mitochondrial stress response. *Front Genet*, 9, 225.
- Hirschhaeuser, F., Sattler, U. G., & Mueller-Klieser, W. (2011). Lactate: a metabolic key player in cancer. *Cancer Res*, 71(22), 6921–5.

- Hodge, S., Hodge, G., Holmes, M., & Reynolds, P. N. (2005). Increased airway epithelial and T-cell apoptosis in COPD remains despite smoking cessation. *Eur Respir J*, 25(3), 447–54.
- Hodge, S., Hodge, G., Scicchitano, R., Reynolds, P. N., & Holmes, M. (2003). Alveolar macrophages from subjects with chronic obstructive pulmonary disease are deficient in their ability to phagocytose apoptotic airway epithelial cells. *Immunol Cell Biol*, 81(4), 289–96.
- Hoenderdos, K., & Condliffe, A. (2013). The neutrophil in chronic obstructive pulmonary disease. too little, too late or too much, too soon? *Am J Respir Cell Mol Biol*, 48(5), 531–9.
- Hoffmann, R. F., Zarrintan, S., Brandenburg, S. M., Kol, A., de Bruin, H. G., Jafari, S., Dijk, F., Kalicharan, D., Kelders, M., Gosker, H. R., Ten Hacken, N. H., van der Want, J. J., van Oosterhout, A. J., & Heijink, I. H. (2013). Prolonged cigarette smoke exposure alters mitochondrial structure and function in airway epithelial cells. *Respir Res*, 14, 97.
- Hogg, J. C., Chu, F., Utokaparch, S., Woods, R., Elliott, W. M., Buzatu, L., Cherniack, R. M., Rogers, R. M., Sciurba, F. C., Coxson, H. Q., & Paré, P. D. (2004). The nature of small-airway obstruction in chronic obstructive pulmonary disease. *N Engl J Med*, 350(26), 2645–53.
- Hollins, F., Sutcliffe, A., Gomez, E., Berair, R., Russell, R., Szyndralewicz, C., Saunders, R., & Brightling, C. (2016). Airway smooth muscle NOX4 is upregulated and modulates ROS generation in COPD. *Respir Res*, 17(1), 84.
- Holme, J. A., Nyvold, H. E., Tat, V., Arlt, V. M., Bhargava, A., Gutzkow, K. B., Solhaug, A., Lag, M., Becher, R., Schwarze, P. E., Ask, K., Ekeren, L., & Øvrevik, J. (2014). Mechanisms linked to differences in the mutagenic potential of 1,3-dinitropyrene and 1,8-dinitropyrene. *Toxicol Rep*, 1, 459–73.
- Holz, O., Zühlke, I., Jaksztat, E., Müller, K. C., Welker, L., Nakashima, M., Diemel, K. D., Branschied, D., Magnussen, H., & Jörres, R. A. (2004). Lung fibroblasts from patients with emphysema show a reduced proliferation rate in culture. *Eur Respir J*, 24(4), 575–9.
- Hong, K. U., Reynolds, S. D., Watkins, S., Fuchs, E., & Stripp, B. R. (2004). In vivo differentiation potential of tracheal basal cells: evidence for multipotent and unipotent subpopulations. *Am J Physiol Lung Cell Mol Physiol*, 286(4), L643-9.
- Hooda, J., Cadinu, D., Alam, M. M., Shah, A., Cao, T. M., Sullivan, L. A., Brekken, R., & Zhang, L. (2013). Enhanced heme function and mitochondrial respiration promote the progression of lung cancer cells. *PLoS One*, 8(5), e63402.
- Houghton, A. M. (2013). Mechanistic links between COPD and lung cancer. *Nat Rev Cancer*, 13, 233–45.
- Hroudová, J., Singh, N., & Fišar, Z. (2014). Mitochondrial dysfunctions in neurodegenerative diseases: relevance to Alzheimer's disease. *BioMed Res Int*, 2014, 175062.

- Hu, Y., Ju, Y., Lin, D., Wang, Z., Huang, Y., Zhang, S., Wu, C., & Jiao, S. (2012). Mutation of the Nrf2 gene in non-small cell lung cancer. *Mol Biolo Rep*, 39(4), 4743–7.
- Hu, Y., Lu, W., Chen, G., Wang, P., Chen, Z., Zhou, Y., Ogasawara, M., Trachootham, D., Feng, L., Pelicano, H., Chiao, P. J., Keating, M. J., Garcia-Manero, G., & Huang, P. (2012). K-ras(G12V) transformation leads to mitochondrial dysfunction and a metabolic switch from oxidative phosphorylation to glycolysis. *Cell Res*, 22(2), 399–412.
- Hwang, C., Sinskey, A. J., & Lodish, H. F. (1992). Oxidized redox state of glutathione in the endoplasmic reticulum. *Science*, 257(5076), 1496–502.
- Illsley, N. P. (2000). Glucose Transporters in the Human Placenta. *Placenta*, 21(1), 14–22.
- Inonu, H., Doruk, S., Sahin, S., Erkorkmaz, U., Celik, D., Celikel, S., & Seyfikli, Z. (2012). Oxidative stress levels in exhaled breath condensate associated with COPD and smoking. *Respir Care*, 57(3), 413–9.
- Isaacs, J. S., Jung, Y. J., Mole, D. R., Lee, S., Torres-Cabala, C., Chung, Y. L., Merino, M., Trepel, J., Zbar, B., Toro, J., Ratcliffe, P. J., Linehan, W. M., & Neckers, L. (2005). HIF overexpression correlates with biallelic loss of fumarate hydratase in renal cancer: novel role of fumarate in regulation of HIF stability. *Cancer Cell*, 8(2), 143–53.
- Ishikawa, K., Takenaga, K., Akimoto, M., Koshikawa, N., Yamaguchi, A., Imanishi, H., Nakada, K., Honma, Y., & Hayashi, J. (2008). ROS-generating mitochondrial DNA mutations can regulate tumor cell metastasis. *Science*, 320(5876), 661–4.
- Israelsen, W. J., & Vander Heiden, M. G. (2015). Pyruvate kinase: function, regulation and role in cancer. *Semin Cell Dev Biol*, 43, 43–51.
- Ito, K., Lim, S., Caramori, G., Chung, K. F., Barnes, P. J., & Adcock, I. M. (2001). Cigarette smoking reduces histone deacetylase 2 expression, enhances cytokine expression, and inhibits glucocorticoid actions in alveolar macrophages. *FASEB J*, 15(6), 1110–2.
- Ito, K., Ito, M., Elliott, W. M., Cosio, B., Caramori, G., Kon, O. M., Barczyk, A., Hayashi, S., Adcock, I. M., Hogg, J. C., & Barnes, P. J. (2005). Decreased histone deacetylase activity in chronic obstructive pulmonary disease. *N Engl J Med*, 352(19), 1967–76.
- Jaffer, O. A., Carter, A. B., Sanders, P. N., Dibbern, M. E., Winters, C. J., Murthy, S., Ryan, A. J., Rokita, A. G., Prasad, A. M., Zabner, J., Kline, J. N., Grumbach, I. M., & Anderson, M. E. (2015). Mitochondrial-targeted antioxidant therapy decreases transforming growth factor- β -mediated collagen production in a murine asthma model. *Am J Respir Cell Mol Biol*, 52(1), 106–15.
- Jagannathan, L., Jose, C. C., Arita, A., Kluz, T., Sun, H., Zhang, X., Yao, Y., Kartashov, A. V., Barski, A., Costa, M., & Cuddapah, S. (2016). Nuclear factor κ B1/RelA mediates inflammation in human lung epithelial cells at atmospheric

- oxygen levels. *J Cell Physiol*, 231(7), 1611–20.
- Jans, J., van Dijk, J. H., van Schelven, S., van der Groep, P., Willems, S. H., Jonges, T. N., van Diest, P. J., & Bosch, J. L. (2010). Expression and localization of hypoxia proteins in prostate cancer: prognostic implications after radical prostatectomy. *Urology*, 75(4), 786–92.
- Järvinen, K., Pietarinen-Runtti, P., Linnainmaa, K., Raivio, K. O., Krejsa, C. M., Kavanagh, T., & Kinnula, V. L. (2000). Antioxidant defense mechanisms of human mesothelioma and lung adenocarcinoma cells. *Am J Physiol Lung Cell Mol Physiol*, 278(4), L696–L702.
- Jaspers, I., Zhang, W., Fraser, A., Samet, J. M., & Reed, W. (2001). Hydrogen peroxide has opposing effects on IKK activity and I κ B α breakdown in airway epithelial cells. *Am J Respir Cell Mol Biol*, 24(6), 769–77.
- Jia, X., Gu, Z., Chen, W., & Jiao, J. (2016). Tigecycline targets nonsmall cell lung cancer through inhibition of mitochondrial function. *Fundam Clin Pharmacol*, 30(4), 297–306.
- Jiang, H., Sen Zhu, Y., Xu, H., Sun, Y., & Fang Li, Q. (2010). Inflammatory stimulation and hypoxia cooperatively activate HIF-1 α in bronchial epithelial cells: involvement of PI3K and NF- κ B. *Am J Physiol Lung Cell Mol Physiol*, 298, 660–9.
- Jiang, Y., Wang, X., & Hu, D. (2017). Mitochondrial alterations during oxidative stress in chronic obstructive pulmonary disease. *Int J Chron Obstruct Pulmon Dis*, 12, 1153–62.
- Jin, H., Kanthasamy, A., Ghosh, A., Anantharam, V., Kalyanaraman, B., & Kanthasamy, A. G. (2014). Mitochondria-targeted antioxidants for treatment of Parkinson's disease: preclinical and clinical outcomes. *Biochim Biophys Acta*, 1842(8), 1282–94.
- Jonckheere, A. I., Smeitink, J. A., & Rodenburg, R. J. (2012). Mitochondrial ATP synthase: architecture, function and pathology. *J Inherit Metab Dis*, 35(2), 211–25.
- Jose, C., & Bellance, N. (2011). Choosing between glycolysis and oxidative phosphorylation: A tumor's dilemma? *Biochim Biophys Acta*, 1807(6), 552–61.
- Joseph, B., Ekedahl, J., Lewensohn, R., Marchetti, P., Formstecher, P., & Zhivotovsky, B. (2001). Defective caspase-3 relocalization in non-small cell lung carcinoma. *Oncogene*, 20(23), 2877–88.
- Joshi, M., Liu, X., & Belani, C. P. (2014). Taxanes, past, present, and future impact on non-small cell lung cancer. *Anticancer Drugs*, 25, 571–83.
- Ju, R., Guo, L., Li, J., Zhu, L., Yu, X., Chen, C., Chen, W., Ye, C., & Zhang, D. (2016). Carboxyamidotriazole inhibits oxidative phosphorylation in cancer cells and exerts synergistic anti-cancer effect with glycolysis inhibition. *Cancer Lett*, 370(2), 232–41.

- Julious, S. A. (2005). Sample size of 12 per group rule of thumb for a pilot study. *Pharm Stat*, 4(4), 287–91.
- Kaczara, P., Sarna, T., & Burke, J. M. (2010). Dynamics of H₂O₂ availability to ARPE-19 cultures in models of oxidative stress. *Free Radic Biol Med*, 48(8), 1064–70.
- Kadara, H., Scheet, P., Wistuba, I. I., & Spira, A. E. (2016). Early events in the molecular pathogenesis of lung cancer. *Cancer Prev Res (Phila)*, 9(7), 518–27.
- Kagawa, Y., & Racker, E. (1966). Partial resolution of the enzymes catalyzing oxidative phosphorylation. *J Biol Chem*, 241(10), 2461–6.
- Kampf, C., Relova, A. J., Sandler, S., & Roomans, G. M. (1999). Effects of TNF- α , IFN- γ and IL- β on normal human bronchial epithelial cells. *Eur Respir J*, 14(1), 84-91.
- Karwi, Q. G., Bornbaum, J., Boengler, K., Torregrossa, R., Whiteman, M., Wood, M. E., Schulz, R., & Baxter, G. F. (2017). AP39, a mitochondria-targeting hydrogen sulfide (H₂S) donor, protects against myocardial reperfusion injury independently of salvage kinase signalling. *Br J Pharmacol*, 174(4), 287–301.
- Kasahara, M., & Hinkle, P. C. (1977). Reconstitution and purification of the {D}-glucose transporter from human erythrocytes. *J Biol Chem*, 252(20), 7384–90.
- Kasahara, Y., Tuder, R. M., Cool, C. D., Lynch, D. A., Flores, S. C., & Voelkel, N. F. (2001). Endothelial cell death and decreased expression of vascular endothelial growth factor and vascular endothelial growth factor receptor 2 in emphysema. *Am J Respir Crit Care Med*, 163(3), 737–44.
- Kashatus, D. F., Lim, K. H., Brady, D. C., Pershing, N. L., Cox, A. D., & Counter, C. M. (2011). RALA and RALBP1 regulate mitochondrial fission at mitosis. *Nat Cell Biol*, 13(9), 1108–15.
- Kashatus, J. A., Nascimento, A., Myers, L. J., Sher, A., Byrne, F. L., Hoehn, K. L., Counter, C. M., & Kashatus, D. F. (2015). Erk2 phosphorylation of Drp1 promotes mitochondrial fission and MAPK-driven tumor growth. *Mol Cell*, 57(3), 537–51.
- Kasiel, M., & Nowak, D. (2001). Long-term administration of N-acetylcysteine decreases hydrogen peroxide exhalation in subjects with chronic obstructive pulmonary disease. *Respir Med*, 95(6), 448–56.
- Katabi, M. M., Chan, H. L., Karp, S. E., & Batist, G. (1999). Hexokinase type II: a novel tumor-specific promoter for gene-targeted therapy differentially expressed and regulated in human cancer cells. *Hum Gene Ther*, 10, 155–64.
- Kaushik, G., Kaushik, T., Khanduja, S., Pathak, C. M., & Khanduja, K. L. (2008). Cigarette smoke condensate promotes cell proliferation through disturbance in cellular redox homeostasis of transformed lung epithelial type-II cells. *Cancer Lett*, 270(1), 120–31.
- Kazzaz, J. A., Xu, J., Palaia, T. A., Mantell, L., Fein, A. M., & Horowitz, S. (1996).

- Cellular oxygen toxicity. Oxidant injury without apoptosis. *J Biol Chem*, 271(25), 15182–6.
- Kehrer, J. P. (1993). Free radicals as mediators of tissue injury and disease. *Crit Rev Toxicol*, 23(1), 21–48.
- Keilin, D., & Hartree, E. F. (1939). Cytochrome and cytochrome oxidase. *Proc R Soc Lond B Biol Sci*, 127(115), 167–191.
- Kelley, E. E., Hock, T., Khoo, N. K., Richardson, G. R., Johnson, K. K., Powell, P. C., Giles, G. I., Agarwal, A., Lancaster, J. R., & Tarpey, M. M. (2006). Moderate hypoxia induces xanthine oxidoreductase activity in arterial endothelial cells. *Free Radic Biol Med*, 40(6), 952–9.
- Kensler, T. W., & Wakabayashi, N. (2010). Nrf2: friend or foe for chemoprevention? *Carcinogenesis*, 31(1), 90–9.
- Kezic, A., Spasojevic, I., Lezaic, V., & Bajcetic, M. (2016). Mitochondria-targeted antioxidants: future perspectives in kidney ischemia reperfusion injury. *Oxid Med Cell Longev*, 2016, 2950503.
- Khan, E. M., Lanir, R., Danielson, A. R., & Goldkorn, T. (2008). Epidermal growth factor receptor exposed to cigarette smoke is aberrantly activated and undergoes perinuclear trafficking. *FASEB J*, 22(3), 910–7.
- Khan, Y. M., Kirkham, P., Barnes, P. J., & Adcock, I. M. (2014). Brd4 is essential for IL-1 β -induced inflammation in human airway epithelial cells. *PLoS One*, 9(4), e95051.
- Kim, G. Y., Lee, J. W., Ryu, H. C., Wei, J. D., Seong, C. M., & Kim, J. H. (2010). Proinflammatory cytokine IL-1 β stimulates IL-8 synthesis in mast cells via a leukotriene B4 receptor 2-linked pathway, contributing to angiogenesis. *J Immunol*, 184(7), 3946–54.
- Kim, J. W., Gao, P., Liu, Y. C., Semenza, G. L., & Dang, C. V. (2007). Hypoxia-inducible factor 1 and dysregulated c-Myc cooperatively induce vascular endothelial growth factor and metabolic switches hexokinase 2 and pyruvate dehydrogenase kinase 1. *Mol Cellular Biol*, 27(21), 7381–93.
- Kim, J. W., Tchernyshyov, I., Semenza, G. L., & Dang, C. V. (2006). HIF-1-mediated expression of pyruvate dehydrogenase kinase: a metabolic switch required for cellular adaptation to hypoxia. *Cell Metab*, 3(3), 177–85.
- Kim, K. T., Lee, H. W., Lee, H. O., Song, H. J., Jeong, D. E., Shin, S., Kim, H., Shin, Y., Nam, D. H., Jeong, B. C., Kirch, D. G., Joo, K. M., & Park, W. Y. (2016). Application of single-cell RNA sequencing in optimizing a combinatorial therapeutic strategy in metastatic renal cell carcinoma. *Genome Biol*, 17, 80.
- Kim, S. R., Kim, D. I., Kim, S. H., Lee, H., Lee, K. S., Cho, S. H., & Lee, Y. C. (2014). NLRP3 inflammasome activation by mitochondrial ROS in bronchial epithelial cells is required for allergic inflammation. *Cell Death Dis*, 5, e1498.
- Kirkham, P. A., & Barnes, P. J. (2013). Oxidative stress in COPD. *Chest*, 144(1),

266–73.

- Klee, S., Lehmann, M., Wagner, D. E., Baarsma, H. A., & Königshoff, M. (2016). WISP1 mediates IL-6-dependent proliferation in primary human lung fibroblasts. *Sci Rep*, 6, 20547.
- Knobloch, J., Yanik, S. D., Körber, S., Stoelben, E., Jungck, D., & Koch, A. (2016). TNF α -induced airway smooth muscle cell proliferation depends on endothelin receptor signaling, GM-CSF and IL-6. *Biochem Pharmacol*, 116, 188–99.
- Koo, M. J., Rooney, K. T., Choi, M. E., Ryter, S. W., Choi, A. M., & Moon, J. S. (2015). Impaired oxidative phosphorylation regulates necroptosis in human lung epithelial cells. *Biochem Biophys Res Commun*, 464(3), 875–80.
- Koppenol, W. H., Bounds, P. L., & Dang, C. V. (2011). Otto Warburg's contributions to current concepts of cancer metabolism. *Nat Rev Cancer*, 11(5), 325–37.
- Koranyi, L., Bourey, R. E., James, D., Mueckler, M., Fiedorek, F. T., & Permutt, M. A. (1991). Glucose transporter gene expression in rat brain: pretranslational changes associated with chronic insulin-induced hypoglycemia, fasting, and diabetes. *Mol Cell Neurosci*, 2(3), 244–52.
- Koukourakis, M. I., Giatromanolaki, A., Sivridis, E., Gatter, K. C., & Harris, A. L. (2005). Pyruvate dehydrogenase and pyruvate dehydrogenase kinase expression in non small cell lung cancer and tumor-associated stroma. *Neoplasia*, 7(1), 1–6.
- Krebs, H. A., & Cohen, P. P. (1939). Metabolism of α -ketoglutaric acid in animal tissues. *Biochem J*, 33(11), 1895–9.
- Křepela, E., Procházka, J., Liu, X., Fiala, P., & Kinkor, Z. (2004). Increased expression of Apaf-1 and procaspase-3 and the functionality of intrinsic apoptosis apparatus in non-small cell lung carcinoma. *Biol Chem*, 385(2), 153–68.
- Kunsch, C., Lang, R. K., Rosen, C. A., Shannon, M. F., & Proud, D. (1994). Synergistic transcriptional activation of the IL-8 gene by NF- κ B p65 (RelA) and NF-IL-6. *J Immunol*, 153(1), 153–64.
- Kuo, C. H., Liu, C. Y., Pavlidis, S., Lo, Y. L., Wang, Y. W., Chen, C. H., Ko, H. W., Chung, F. T., Lin, T. Y., Wang, T. Y., Lee, K. Y., Guo, Y. K., Wang, T. H., & Yang, C. T. (2018). Unique immune gene expression patterns in bronchoalveolar lavage and tumor adjacent non-neoplastic lung tissue in non-small cell lung cancer. *Front Immunol*, 9, 232.
- Kwee, S. A., Hernandez, B., Chan, O., & Wong, L. (2012). Choline kinase α and hexokinase-2 protein expression in hepatocellular carcinoma: association with survival. *PLoS One*, 7(10), e46591.
- Kwon, T., Rho, J. K., Lee, J. C., Park, Y. H., Shin, H. J., Cho, S., Kang, Y. K., Kim, B. Y., Yoon, D. Y., & Yu, D. Y. (2015). An important role for peroxiredoxin II in survival of A549 lung cancer cells resistant to gefitinib. *Exp Mol Med*, 47, e165.

- Lababede, O., Meziane, M., & Rice, T. (2011). Seventh edition of the cancer staging manual and stage grouping of lung cancer: quick reference chart and diagrams. *Chest*, 139(1), 183-9.
- Ladjemi, M. Z., Lecocq, M., Weynand, B., Bowen, H., Gould, H. J., Van Snick, J., Detry, B., & Pilette, C. (2015). Increased IgA production by B-cells in COPD via lung epithelial interleukin-6 and TAC1 pathways. *Eur Respir J*, 45(4), 980–93.
- Lai, T., Tian, B., Cao, C., Hu, Y., Zhou, J., Wang, Y., Wu, Y., Li, Z., Xu, X., Zhang, M., Xu, F., Cao, Y., Chen, M., Wu, D., Dong, C., Li, W., Ying, S., Chen, Z., & Shen, H. (2017). HDAC2 suppresses IL17A-mediated airway remodeling in human and experimental modeling of COPD. *Chest*, 153(4), 863-75.
- Lakshminarayanan, V., Drab-Weiss, E. A., & Roebuck, K. A. (1998). H₂O₂ and tumor necrosis factor- α induce differential binding of the redox-responsive transcription factors AP-1 and NF- κ B to the interleukin-8 promoter in endothelial and epithelial cells. *J Biol Chem*, 273(49), 32670–8.
- Landt, S., Jeschke, S., Koeninger, A., Thomas, A., Heusner, T., Korfach, S., Ulm, K., Schmidt, P., Blohmer, J. U., Lichtenegger, W., Sehouli, J., & Kuemmel, S. (2010). Tumor-specific correlation of tumor M2 pyruvate kinase in pre-invasive, invasive and recurrent cervical cancer. *Anticancer Res*, 30(2), 375–81.
- Lang-Lazdunski, L. (2013). Surgery for nonsmall cell lung cancer. *Eur Respir Rev*, 22(129), 382–404.
- Langer, C. J. (2015). Emerging immunotherapies in the treatment of non-small cell lung cancer (NSCLC). *Am J Clin Oncol*, 38(4), 422–30.
- LaRosa, D. F., & Orange, J. S. (2008). 1. Lymphocytes. *J Allergy Clin Immunol*, 121(2), S364–9.
- Lawless, M. W., O'Byrne, K. J., & Gray, S. G. (2009). Oxidative stress induced lung cancer and COPD: opportunities for epigenetic therapy. *J Cell Mol Med*, 13(9a), 2800–21.
- LeBleu, V. S., O'Connell, J. T., Gonzalez Herrera, K. N., Wikman, H., Pantel, K., Haigis, M. C., de Carvalho, F. M., Damascena, A., Domingos Chinen, L. T., Rocha, R. M., Asara, J. M., & Kalluri, R. (2014). PGC-1 α mediates mitochondrial biogenesis and oxidative phosphorylation in cancer cells to promote metastasis. *Nat Cell Biol*, 16(10), 992–1003, 1–15.
- Lechner, J. F., & LaVeck, M. A. (1985). A serum-free method for culturing normal human bronchial epithelial cells at clonal density. *J Tissue Cult Methods*, 9(2), 43–8.
- Lee, D. W., Selamoglu, N., Lanciano, P., Cooley, J. W., Forquer, I., Kramer, D. M., & Daldal, F. (2011). Loss of a conserved tyrosine residue of cytochrome b induces reactive oxygen species production by cytochrome bc1. *J Biol Chem*, 286(20), 18139–48.
- Lee, H. C., Yin, P. H., Lin, J. C., Wu, C. C., Chen, C. Y., Wu, C. W., Chi, C. W., Tam, T. N., & Wei, Y. H. (2005). Mitochondrial genome instability and mtDNA

- depletion in human cancers. *Ann N Y Acad Sci*, 1042, 109–22.
- Lee, J. S., Park, S. J., Cho, Y. S., Huh, J. W., Oh, Y. M., & Lee, S. D. (2015). Role of AMP-activated protein kinase (AMPK) in smoking-induced lung inflammation and emphysema. *Tuberc Respir Dis (Seoul)*, 78(1), 8–17.
- Lee, J., Kim, H. K., Han, Y. M., & Kim, J. (2008). Pyruvate kinase isozyme type M2 (PKM2) interacts and cooperates with Oct-4 in regulating transcription. *Int J Biochem Cell Biol*, 40(5), 1043–54.
- Lee, W. C., Chiu, C. H., Chen, J. B., Chen, C. H., & Chang, H. W. (2016). Mitochondrial fission increases apoptosis and decreases autophagy in renal proximal tubular epithelial cells treated with high glucose. *DNA Cell Biol*, 35(11), 657–65.
- Li, X., Michaeloudes, C., Zhang, Y., Wiegman, C. H., Adcock, I. M., Lian, Q., Mak, J. C., Bhavsar, P. K., & Chung, K. F. (2017). Mesenchymal stem cells alleviate oxidative stress-induced mitochondrial dysfunction in the airways. *J Allergy Clin Immunol*.
- Li, X. B., Gu, J. D., & Zhou, Q. H. (2015). Review of aerobic glycolysis and its key enzymes - new targets for lung cancer therapy. *Thorac Cancer*, 6(1), 17–24.
- Li, Z., Alam, S., Wang, J., Sandstrom, C. S., Janciauskiene, S., & Mahadeva, R. (2009). Oxidized α 1-antitrypsin stimulates the release of monocyte chemoattractant protein-1 from lung epithelial cells: potential role in emphysema. *Am J Physiol Lung Cell Mol Physiol*, 297(2), L388-400.
- Liberti, M. V., & Locasale, J. W. (2016). The Warburg effect: how does it benefit cancer cells? *Trends in Biochem Sci*, 41(3), 211–8.
- Lieber, M., Todaro, G., Smith, B., Szakal, A., & Nelson-Rees, W. (1976). A continuous tumor-cell line from a human lung carcinoma with properties of type II alveolar epithelial cells. *Int J Cancer*, 17(1), 62–70.
- Liloglou, T., Bediaga, N. G., Brown, B. R., Field, J. K., & Davies, M. P. (2014). Epigenetic biomarkers in lung cancer. *Cancer Lett*, 342(2), 200-12.
- Lim, J. U., Yeo, Chang D., Rhee, C. K., Kim, Y. H., Park, C. K., Kim, J. S., Kim, J. W., Lee, S. H., Kim, S. J., Yoon, H. K., Kim, T. J., & Lee, K. Y. (2015). Chronic obstructive pulmonary disease-related non-small-cell lung cancer exhibits a low prevalence of EGFR and ALK driver mutations. *PLoS One*, 10(11), e0142306.
- Lim, S. W., Loh, H. S., Ting, K. N., Bradshaw, T. D., & Allaudin, Z. Na. (2015). Reduction of MTT to purple formazan by vitamin E isomers in the absence of cells. *Trop Life Sci Res*, 26(1), 111–120.
- Lim, S. C., Carey, K. T., & McKenzie, M. (2015). Anti-cancer analogues ME-143 and ME-344 exert toxicity by directly inhibiting mitochondrial NADH: ubiquinone oxidoreductase (Complex I). *Am J Cancer Res*, 5(2), 689–701.
- Lin, X. X., Yang, X. F., Jiang, J. X., Zhang, S. J., Guan, Y., Liu, Y. N., Sun, Y. N., & Xie, Q. M. (2014). Cigarette smoke extract-induced BEAS-2B cell apoptosis and

- anti-oxidative Nrf-2 up-regulation are mediated by ROS-stimulated p38 activation. *Toxicol Mech Methods*, 24(8), 575–83.
- Lipson, D. A., Barnhart, F., Brealey, N., Brooks, J., Criner, G., J., Day, N. C., Dransfield, M. T., Halpin, D. M., Han, M. K., Jones, C. E., Kilbride, S., Lange, P., Lomas, D. A., Martinez, F. J., Singh, D., Tabberer, M., Wise, R. A., & Pascoe, S. J. (2018). Once-daily single-inhaler triple versus dual therapy in patients with COPD. *N Engl J Med*, 378(18), 1671-80.
- Liu, F., Killian, J. K., Yang, M., Walker, R. L., Hong, J. A., Zhang, M., Davis, S., Zhang, Y., Hussain, M., Xi, S., Rao, M., Meltzer, P. A., & Schrupp, D. S. (2010). Epigenomic alterations and gene expression profiles in respiratory epithelia exposed to cigarette smoke condensate. *Oncogene*, 29(25), 3650–64.
- Liu, S. F., Kuo, H. C., Tseng, C. W., Huang, H. T., Chen, Y. C., Tseng, C. C., & Lin, M. C. (2015). Leukocyte mitochondrial DNA copy number is associated with chronic obstructive pulmonary disease. *PLoS One*, 10(9), e0138716.
- Liu, T. C., Jin, X., Wang, Y., & Wang, K. (2017). Role of epidermal growth factor receptor in lung cancer and targeted therapies. *Am J Cancer Res*, 7(2), 187–202.
- Liu, S. V., Fabbri, M., Gitlitz, B. J., & Laird-Offringa, I. A. (2013). Epigenetic therapy in lung cancer. *Front Oncol*, 3, 135.
- Liu, X., & Chen, Z. (2017). The pathophysiological role of mitochondrial oxidative stress in lung diseases. *J Transl Med*, 15(1), 207.
- Liu, Z. X., Hong, L., Fang, S. Q., Tan, G. H., Huang, P. G., Zeng, Z., Xia, X., & Wang, X. X. (2016). Overexpression of pyruvate kinase M2 predicts a poor prognosis for patients with osteosarcoma. *Tumour Biol*, 37(11), 14923–8.
- Lopez, A. D., Shibuya, K., Rao, C., Mathers, C. D., Hansell, A. L., Held, L. S., Schmid, V., Buist, S. (2006). Chronic obstructive pulmonary disease: current burden and future projections. *Eur Respir J*, 27(2), 397–412.
- Loschen, G., & Flohé, L. (1971). Respiratory chain linked H₂O₂ production in pigeon heart mitochondria. *FEBS Lett*, 18(2), 261–4.
- Lou, Y., Li, R., Liu, J., Zhang, Y., Zhang, X., Jin, B., Liu, Y., Wang, Z., Zhong, H., Wen, S., & Han, B. (2015). Mitofusin-2 over-expresses and leads to dysregulation of cell cycle and cell invasion in lung adenocarcinoma. *Med Oncol*, 32(4), 132.
- Low, M., Ben-Or, S. (2018). Thoracic surgery in early-stage small cell lung cancer. *Thorac Surg Clin*, 28(1), 9–14.
- Luo, W., Hu, H., Chang, R., Zhong, J., Knabel, M., O'Meally, R., Cole, R. N., Pandey, A., & Semenza, G. L. (2011). Pyruvate kinase M2 is a PHD3-stimulated coactivator for hypoxia-inducible factor 1. *Cell*, 145(5), 732–44.
- Macheda, M. L., Rogers, S., & Best, J. D. (2005). Molecular and cellular regulation of glucose transporter (GLUT) proteins in cancer. *J Cell Physiol*, 202(3), 654–62.

- Maeno, T., Houghton, A. M., Quintero, P. A., Grumelli, S., Owen, C. A., & Shapiro, S. D. (2007). CD8⁺ T Cells are required for inflammation and destruction in cigarette smoke-induced emphysema in mice. *J Immunol*, 178(12), 8090–6.
- Mahmood, M. Q., Ward, C., Muller, H. K., Sohal, S. S., & Walters, E. H. (2017). Epithelial mesenchymal transition (EMT) and non-small cell lung cancer (NSCLC): a mutual association with airway disease. *Med Oncol*, 34(3), 45.
- Maioli, N. A., Zarpelon, A. C., Mizokami, S. S., Calixto-Campos, C., Guazelli, C. F. S., Hohmann, M. S., Pinho-Ribeiro, F. A., Carvalho, T. T., Manchope, M. F., Ferraz, C. R., Casagrande, R., Verri, W. A. (2015). The superoxide anion donor, potassium superoxide, induces pain and inflammation in mice through production of reactive oxygen species and cyclooxygenase-2. *Braz J Med Biol Res*, 48(4), 321–31.
- Majmundar, A. J., Wong, W. J., & Simon, M. C. (2010). Hypoxia-inducible factors and the response to hypoxic stress. *Mol Cell*, 40(2), 294–309.
- Makino, N., Mise, T., & Sagara, J. I. (2008). Kinetics of hydrogen peroxide elimination by astrocytes and C6 glioma cells: Analysis based on a mathematical model. *Biochim Biophys Acta*, 1780(6), 927–36.
- Mannino, D. M., Aguayo, S. M., Petty, T. L., & Redd, S. C. (2003). Low lung function and incident lung cancer in the United States: data from the first national health and nutrition examination survey follow-up. *Arch Intern Med*, 163(12), 1475–80.
- Mata, M., Morcillo, E., Gimeno, C., & Cortijo, J. (2011). N-acetyl-L-cysteine (NAC) inhibit mucin synthesis and pro-inflammatory mediators in alveolar type II epithelial cells infected with influenza virus A and B and with respiratory syncytial virus (RSV). *Biochem Pharmacol*, 82(5), 548–55.
- Matera, M. G., Calzetta, L., & Cazzola, M. (2016). Oxidation pathway and exacerbations in COPD: the role of NAC. *Expert Rev Respir Med*, 10(1), 89–97.
- Mathers, C. D., & Loncar, D. (2006). Projections of global mortality and burden of disease from 2002 to 2030. *PLoS Med*, 3(11), 2011–30.
- McCarthy, C., & Kenny, L. C. (2016). Therapeutically targeting mitochondrial redox signalling alleviates endothelial dysfunction in preeclampsia. *Sci Rep*, 6(1), 32683.
- McLean, J. R., Cohn, G. L., Brandt, I. K., & Simpson, M. V. (1958). Incorporation of labeled amino acids into the protein of muscle and liver mitochondria. *J Biol Chem*, 233(3), 657–63.
- Mehta, A., Dobersch, S., Romero-Olmedo, A. J., & Barreto, G. (2015). Epigenetics in lung cancer diagnosis and therapy. *Cancer Metastasis Rev*, 34(2), 229–41.
- Messier, E. M., Bahmed, K., Tudor, R. M., Chu, H. W., Bowler, R. P., & Kosmider, B. (2013). Trolox contributes to Nrf2-mediated protection of human and murine primary alveolar type II cells from injury by cigarette smoke. *Cell Death Dis*, 4(4), e573.

- Michaeloudes, C., Bhavsar, P. K., Mumby, S., Chung, K. F., & Adcock, I. M. (2017). Dealing with stress: defective metabolic adaptation in chronic obstructive pulmonary disease pathogenesis. *Ann Am Thorac Soc*, 14(Supplement_5), S374–82.
- Michaeloudes, C., Kuo, C. H., Haji, G., Finch, D. K., Halayko, A. J., Kirkham, P., Chung, K. F., & Adcock, I. M. (2017). Metabolic re-patterning in COPD airway smooth muscle cells. *Eur Respir J*, 50(5), 1700202.
- Michot, J. M., Bigenwald, C., Champiat, S., Collins, M., Carbonnel, F., Postel-Vinay, S., Berdelou, A., Varga, A., Bahleda, R., Hollebecque, A., Massard, C., Fuerea, A., Ribrag, V., Gazzah, A., Armand, J. P., Ammellal, N., Angevin, E., Noel, N., Boutros, C., Mateus, C., Robert, C., Soria, J. C., Marabelle, A., & Lambotte, O. (2016). Immune-related adverse events with immune checkpoint blockade: a comprehensive review. *Eur J Cancer*, 54, 139–48.
- Miglino, N., Roth, M., Lardinois, D., Sadowski, C., Tamm, M., & Borger, P. (2012). Cigarette smoke inhibits lung fibroblast proliferation by translational mechanisms. *Eur Respir J*, 39(3), 705–11.
- Mihaylova, M. M., & Shaw, R. J. (2011). The AMPK signalling pathway coordinates cell growth, autophagy and metabolism. *Nat Cell Biol*, 13(9), 1016–23.
- Mills, E. L., Kelly, B., Logan, A., Costa, A. S., Varma, M., Bryant, C. E., Tourlomousis, P., Däbritz, J. H., Gottlieb, E., Latorre, I., Corr, S. C., McManus, G., Ryan, D., Jacobs, H. T., Szibor, M., Xavier, R. J., Braun, T., Frezza, C., Murphy, M. P., & O'Neill, L. A. (2016). Succinate dehydrogenase supports metabolic repurposing of mitochondria to drive inflammatory macrophages. *Cell*, 167(2), 457–70.e13.
- Mimaki, M., Wang, X., McKenzie, M., Thorburn, D. R., & Ryan, M. T. (2012). Understanding mitochondrial complex I assembly in health and disease. *Biochim Biophys Acta*, 1817(6), 851–62.
- Min, K. A., Rosania, G. R., & Shin, M. C. (2016). Human airway primary epithelial cells show distinct architectures on membrane supports under different culture conditions. *Cell Biochem Biophys*, 74(2), 191–203.
- Minami, K. I., Saito, Y., Imamura, H., & Okamura, A. (2002). Prognostic significance of p53, Ki-67, VEGF and Glut-1 in resected stage I adenocarcinoma of the lung. *Lung Cancer*, 38(1), 51–7.
- Ming, Z., Jiang, M., Li, W., Fan, N., Deng, W., Zhong, Y., Zhang, Y., Zhang, Q., & Yang, S. (2014). Bioinformatics analysis and expression study of fumarate hydratase in lung cancer. *Thorac Cancer*, 5(6), 543–9.
- Mio, T., Romberger, D. J., Thompson, A. B., Robbins, R. A., Heires, A., & Rennard, S. I. (1997). Cigarette smoke induces interleukin-8 release from human bronchial epithelial cells. *Am J Respir Crit Care Med*, 155(5), 1770–6.
- Mizumura, K., Cloonan, S. M., Nakahira, K., Bhashyam, A. R., Cervo, M., Kitada, T., Glass, K., Owen, C. A., Mahmood, A., Washko, G. R., Hashimoto, S., Ryter, S.

- W., & Choi, A. M. (2014). Mitophagy-dependent necroptosis contributes to the pathogenesis of COPD. *J Clin Invest*, 124(9), 3987–4003.
- Morabito, A., Carillio, G., Daniele, G., Piccirillo, M. C., Montanino, A., Costanzo, R., Sandomenico, C., Giordano, P., Normanno, N., Perrone, F., Rocco, G., & Di Maio, M. (2014). Treatment of small cell lung cancer. *Crit Rev Oncol Hematol*, 91(3), 257–70.
- Moretti, M., Bottrighi, P., Dallari, R., Da Porto, R., Dolcetti, A., Grandi, P., Garuti, G., Guffanti, E., Roversi, P., De Gugliemo, M., & Potena, A. (2004). The effect of long-term treatment with erdosteine on chronic obstructive pulmonary disease: the EQUALIFE Study. *Drugs Exp Clin Res*, 30(4), 143–52.
- Mortaz, E., Henricks, P. A. J., Kraneveld, A. D., Givi, M. E., Garssen, J., & Folkerts, G. (2011). Cigarette smoke induces the release of CXCL-8 from human bronchial epithelial cells via TLRs and induction of the inflammasome. *Biochim Biophys Acta*, 1812(9), 1104–10.
- Mossman, B. T., Lounsbury, K. M., & Reddy, S. P. (2006). Oxidants and signaling by mitogen-activated protein kinases in lung epithelium. *Am J Respir Cell Mol Biol*, 34(6), 666–9.
- Motori, E., Puyal, J., Toni, N., Ghanem, A., Angeloni, C., Malaguti, M., Cantelli-Forti, G., Berninger, B., Conzelmann, K. K., Götz, M., Winklhofer, K. F., Hrelia, S., Bergami, M. (2013). Inflammation-induced alteration of astrocyte mitochondrial dynamics requires autophagy for mitochondrial network maintenance. *Cell Metab*, 18(6), 844–59.
- Müller, K. C., Welker, L., Paasch, K., Feindt, B., Erpenbeck, V. J., Hohlfeld, J. M., Krung, N., Nakashima, M., Branscheid, D., Magnussen, H., Jörres, R. A., & Holz, O. (2006). Lung fibroblasts from patients with emphysema show markers of senescence in vitro. *Respir Res*, 7(1), 32.
- Nair, S., Li, W., & Kong, A. N. (2007). Natural dietary anti-cancer chemopreventive compounds: redox-mediated differential signaling mechanisms in cytoprotection of normal cells versus cytotoxicity in tumor cells. *Acta Pharmacol Sin*, 28(4), 459–72.
- Nam, H. S., Izumchenko, E., Dasgupta, S., & Hoque, M. O. (2017). Mitochondria in chronic obstructive pulmonary disease and lung cancer: where are we now? *Biomark Med*, 11(6), 475–89.
- Nanavaty, U. B., Pawliczak, R., Doniger, J., Gladwin, M. T., Cowan, M. J., Logun, C., & Shelhamer, J. H. (2002). Oxidant-induced cell death in respiratory epithelial cells is due to DNA damage and loss of ATP. *Exp Lung Res*, 28(8), 591–607.
- Natarajan, M., Mohan, S., Martinez, B. R., Meltz, M. L., & Herman, T. S. (2000). Antioxidant compounds interfere with the 3-[4,5-dimethylthiazol-2-yl]-2,5-diphenyltetrazolium bromide cytotoxicity assay. *Cancer Detect Prev*, 24(5), 405–14.
- National Institute for Health and Care Excellence (NICE). (2017). Lung cancer |

- Guidance and guideline topic | NICE, <https://www.nice.org.uk/guidance/conditions-and-diseases/cancer/lung-cancer>.
- National Institute for Health and Care Excellence (NICE). (2011). Lung cancer: diagnosis and management, Clinical guideline [CG121], <https://www.nice.org.uk/guidance/cg121>.
- Nauseef, W. M. (2014). Detection of superoxide anion and hydrogen peroxide production by cellular NADPH oxidases. *Biochim Biophys Acta*, 1840(2), 757–67.
- Negro, R. W. (2008). Erdosteine: antitussive and anti-inflammatory effects. *Lung*, 186(S1), 70–3.
- Neill, T., Torres, A., Buraschi, S., Owens, R. T., Hoek, J. B., Baffa, R., & Iozzo, R. V. (2014). Decorin induces mitophagy in breast carcinoma cells via peroxisome proliferator-activated receptor γ coactivator-1 α (PGC-1 α) and mitostatin. *J Biol Chem*, 289(8), 4952–68.
- Nelson, D. A., Tan, T. T., Rabson, A. B., Anderson, D., Degenhardt, K., & White, E. (2004). Hypoxia and defective apoptosis drive genomic instability and tumorigenesis. *Genes Dev*, 18(17), 2095–107.
- Ng Kee Kwong, F., Nicholson, A. G., Harrison, C. L., Hansbro, P. M., Adcock, I. M., & Chung, K. F. (2017). Is mitochondrial dysfunction a driving mechanism linking COPD to nonsmall cell lung carcinoma? *Eur Respir Rev*, 26(146), 170040.
- Ng, M., Freeman, M. K., Fleming, T. D., Robinson, M., Dwyer-Lindgren, L., Thomson, B., Wollum, A., Sanman, E., Wulf, S., Lopez, A. D., Murray, C. J., & Gakidou, E. (2014). Smoking prevalence and cigarette consumption in 187 countries, 1980-2012. *JAMA*, 311(2), 183-92.
- Ngo, D. C., Ververis, K., Tortorella, S. M., & Karagiannis, T. C. (2015). Introduction to the molecular basis of cancer metabolism and the Warburg effect. *Mol Biol Rep*, 42(4), 819–23.
- Nogueira, V., & Hay, N. (2013). Molecular pathways: reactive oxygen species homeostasis in cancer cells and implications for cancer therapy. *Clin Cancer Res*, 19(16), 4309–14.
- Novak, E. A., & Mollen, K. P. (2015). Mitochondrial dysfunction in inflammatory bowel disease. *Front Cell Dev Biol*, 3, 62.
- Novellademunt, L., Antas, P., & Li, V. S. (2015). Targeting Wnt signaling in colorectal cancer. A review in the theme: cell signaling: proteins, pathways and mechanisms. *Am Journal Physiol*, 309(8), C511–21.
- Ollikainen, T. R., Linnainmaa, K. I., Raivio, K. O., & Kinnula, V. L. (1998). DNA single strand breaks and adenine nucleotide depletion as indices of oxidant effects on human lung cells. *Free Radic Biol Med*, 24(7–8), 1088–96.
- Onishi, Y., Ueha, T., Kawamoto, T., Hara, H., Toda, M., Harada, R., Minoda, M., Kurosaka, M., & Akisue, T. (2014). Regulation of mitochondrial proliferation by

- PGC-1 α induces cellular apoptosis in musculoskeletal malignancies. *Sci Rep*, 4:3916.
- Onodera, T., Takahashi, Y., Yokoi, Y., Ato, M., Kodama, Y., Hachimura, S., Kurosaki, T., & Kobayashi, K. (2012). Memory B cells in the lung participate in protective humoral immune responses to pulmonary influenza virus reinfection. *Proc Natl Acad Sci U S A*, 109(7), 2485–90.
- Orr, A. L., Vargas, L., Turk, C. N., Baaten, J. E., Matzen, J. T., Dardov, V. J., Attle, S. J., Li, J., Quackenbush, D. C., Goncalves, R. L., Perevoshchikova, I. V., Petrassi, H. M., Meeusen, S. L., Ainscow, E. K., & Brand, M. D. (2015). Suppressors of superoxide production from mitochondrial complex III. *Nat Chem Biol*, 11(11), 834–6.
- Osei, E. T., Noordhoek, J. A., Hackett, T. L., Spanjer, A. I., Postma, D. S., Timens, W., Brandsma, C. A., & Heijink, I. H. (2016). Interleukin-1 α drives the dysfunctional cross-talk of the airway epithelium and lung fibroblasts in COPD. *Eur Respir J*, 48(2), 359–69.
- Oyewole, A. O., & Birch-Machin, M. A. (2015). Mitochondria-targeted antioxidants. *FASEB J*, 29(12), 4766–71.
- Pace, E., Ferraro, M., Di Vincenzo, S., Gerbino, S., Bruno, A., Lanata, L., & Gjomarkaj, M. (2014). Oxidative stress and innate immunity responses in cigarette smoke stimulated nasal epithelial cells. *Toxicol In Vitro*, 28(2), 292–9.
- Palade, G. E. (1953). An electron microscope study of the mitochondrial structure. *J Histochem Cytochem*, 1(4), 188–211.
- Palmieri, D., Fitzgerald, D., Shreeve, S. M., Hua, E., Bronder, J. L., Weil, R. J., Davis, S., Stark, A. M., Merino, M. J., Kurek, R., Mehdorn, H. M., Davis, G., Steinberg, S. M., Meltzer, P. S., Aldape, K., & Steeg, P. S. (2009). Analyses of resected human brain metastases of breast cancer reveal the association between up-regulation of hexokinase 2 and poor prognosis. *Mol Cancer Res*, 7(9), 1438–45.
- Panduri, V., Liu, G., Surapureddi, S., Kondapalli, J., Soberanes, S., de Souza-Pinto, N. C., Bohr, V. A., Budinger, G. R., Schumaker, P. T., Weitzman, S. A., & Kamp, D. W. (2009). Role of mitochondrial hOGG1 and aconitase in oxidant-induced lung epithelial cell apoptosis. *Free Radic Biol Med*, 47(6), 750–9.
- Pao, W., & Girard, N. (2011). New driver mutations in non-small-cell lung cancer. *Lancet Oncol*, 12(2), 175–80.
- Papandreou, I., Cairns, R. A., Fontana, L., Lim, A. L., & Denko, N. C. (2006). HIF-1 mediates adaptation to hypoxia by actively downregulating mitochondrial oxygen consumption. *Cell Metab*, 3(3), 187–97.
- Papi, A., Casoni, G., Caramori, G., Guzzinati, I., Boschetto, P., Ravenna, F., Calia, N., Petruzzelli, S., Corbetta, L., Cavalleco, G., Forini, E., Saetta, M., Ciaccia, A., & Fabbri, L. M. (2004). COPD increases the risk of squamous histological subtype in smokers who develop non-small cell lung carcinoma. *Thorax*, 59(8),

679–81.

- Papi, A., Vestbo, J., Fabbri, L., Corradi, M., Prunier, H., Cohuet, G., Guasconi, A., Montagna, I., Vezzoli, S., Petruzzelli, S., Scrui, M., Roche, N., & Singh, D. (2018). Extrafine inhaled triple therapy versus dual bronchodilator therapy in chronic obstructive pulmonary disease (TRIBUTE): a double-blind, parallel group, randomised controlled trial. *Lancet*, 391(10125), 1076–84.
- Paradies, G., Paradies, V., Ruggiero, F. M., & Petrosillo, G. (2014). Oxidative stress, cardiolipin and mitochondrial dysfunction in nonalcoholic fatty liver disease. *World J Gastroenterol*, 20(39), 14205–18.
- Park, J., Min, J. S., Kim, B., Chae, U. B., Yun, J. W., Choi, M. S., Kong, I. K., Chang, K. T., & Lee, D. S. (2015). Mitochondrial ROS govern the LPS-induced pro-inflammatory response in microglia cells by regulating MAPK and NF- κ B pathways. *Neurosci Lett*, 584, 191–6.
- Patel, A. S., Song, J. W., Chu, S. G., Mizumura, K., Osorio, J. C., Shi, Y., El-Chemaly, S., Lee, C. G., Rosas, I. O., Elias, J. A., Choi, A. M., & Morse, D. (2015). Epithelial cell mitochondrial dysfunction and PINK1 are induced by transforming growth factor- β 1 in pulmonary fibrosis. *PLoS One*, 10(3), e0121246.
- Patti, M. E., & Corvera, S. (2010). The role of mitochondria in the pathogenesis of type 2 diabetes. *Endocr Rev*, 31(3), 364–95.
- Pera, T., Gosens, R., Lesterhuis, A. H., Sami, R., van der Toorn, M., Zaagsma, J., & Meurs, H. (2010). Cigarette smoke and lipopolysaccharide induce a proliferative airway smooth muscle phenotype. *Respir Res*, 11(1), 48.
- Pérez-Escuredo, J., Dadhich, R. K., Dhup, S., Cacace, A., Van Hée, V. F., De Saedeleer, C. J., Sboarina, M., Rodriguez, F., Fontenille, M.J., Brisson, L., Porporato, P. E., & Sonveaux, P. (2016). Lactate promotes glutamine uptake and metabolism in oxidative cancer cells. *Cell Cycle*, 15(1), 72–83.
- Perotin, J. M., Adam, D., Vella-Boucaud, J., Delepine, G., Sandu, S., Jonvel, A. C., Prevost, A., Berthiot, G., Pison, C., Lebargy, F., Birembaut, P., Coraux, C., & Deslee, G. (2014). Delay of airway epithelial wound repair in COPD is associated with airflow obstruction severity. *Respir Res*, 15(1), 151.
- Perry, M., Baker, J., & Chung, K. F. (2011). Airway smooth muscle cells from patients with COPD exhibit a higher degree of cellular proliferation and steroid insensitivity than that from healthy patients. *Eur Respir J*, 38, 748.
- Perry, M. M., Durham, A. L., Austin, P. J., Adcock, I. M., & Chung, K. F.. (2015). BET bromodomains regulate transforming growth factor- β -induced proliferation and cytokine release in asthmatic airway smooth muscle. *J Biol Chem*, 290(14), 9111-21.
- Petersen, I. (2011). The morphological and molecular diagnosis of lung cancer. *Dtsch Arztebl Int*, 108(31-32), 525–31.
- Picard, M., Godin, R., Sinnreich, M., Baril, J., Bourbeau, J., Perrault, H., Taivassalo,

- T., & Burelle, Y. (2008). The mitochondrial phenotype of peripheral muscle in chronic obstructive pulmonary disease. *Am J Respir Crit Care Med*, 178(10), 1040–7.
- Pini, L., Pinelli, V., Modena, D., Bezzi, M., Tiberio, L., & Tantucci, C. (2014). Central airways remodeling in COPD patients. *Int J Chron Obstruct Pulmon Dis*, 9, 927–32.
- Polverino, F., Seys, L. J., Bracke, K. R., & Owen, C. A. (2016). B cells in chronic obstructive pulmonary disease: moving to center stage. *Am J Physiol Lung Cell Mol Physiol*, 311, 687–95.
- Pore, M. M., Hiltermann, T. J., & Kruyt, F. A. (2013). Targeting apoptosis pathways in lung cancer. *Cancer Lett*, 332(2), 359–68.
- Potnis, P. A., Mitkus, R., Elnabawi, A., Squibb, K., & Powell, J. L. (2013). Role of NF- κ B in the oxidative stress-induced lung inflammatory response to iron and selenium at ambient levels. *Toxicol Res*, 2, 259–69.
- Poullis, M., Mcshane, J., Shaw, M., Shackcloth, M., Page, R., Mediratta, N., & Gosney, J. (2013). Smoking status at diagnosis and histology type as determinants of long-term outcomes of lung cancer patients. *Eur J Cardiothorac Surg*, 43(5), 919–24.
- Puente-Maestu, L., Pérez-Parra, J., Godoy, R., Moreno, N., Tejedor, A., González-Aragoneses, F., Bravo, J. L., Alvarez, F. V., Camaño, S., & Agustí, A. (2009). Abnormal mitochondrial function in locomotor and respiratory muscles of COPD patients. *Eur Respir J*, 33(5), 1045–52.
- Puente-Maestu, L., Tejedor, A., Lázaro, Al., de Miguel, J., Álvarez-Sala, L., González-Aragoneses, F., Simón, C., & Agustí, A. (2012). Site of mitochondrial reactive oxygen species production in skeletal muscle of chronic obstructive pulmonary disease and its relationship with exercise oxidative stress. *Am J Respir Cell Mol Biol*, 47(3), 358–62.
- Quinlan, C. L., Orr, A. L., Perevoshchikova, I. V., Treberg, J. R., Ackrell, B. A., & Brand, M. D. (2012). Mitochondrial complex II can generate reactive oxygen species at high rates in both the forward and reverse reactions. *Journal Biol Chem*, 287(32), 27255–64.
- Qutub, A. A., & Popel, A. S. (2008). Reactive oxygen species regulate hypoxia-inducible factor 1 α differentially in cancer and ischemia. *Mol Cell Biol*, 28(16), 5106–19.
- Radomska-Leśniewska, D. M., Sadowska, A. M., Overveld, F. J. Van, Demkow, U., Zieliński, J., & De Backer, W. A. (2006). Influence of N-acetylcysteine on ICAM-1 expression and IL-8 release from endothelial and epithelial cells. *J Physiol Pharmacol*, 57, 325–34.
- Rahman, I., & Adcock, I. M. (2006). Oxidative stress and redox regulation of lung inflammation in COPD. *Eur Respir J*, 28(1), 219–42.
- Rahman, I., & MacNee, W. (1996). Oxidant/antioxidant imbalance in smokers and

- chronic obstructive pulmonary disease. *Thorax*, 51(4), 348–50.
- Rahman, I. (2008). Antioxidant therapeutic advances in COPD. *Ther Adv Respir Dis*, 2(6), 351–74.
- Rahman, I. (2012). Pharmacological antioxidant strategies as therapeutic interventions for COPD. *Biochim Biophys Acta*, 1822(5), 714–28.
- Rahman, I., Gilmour, P. S., Jimenez, L. A., & MacNee, W. (2002). Oxidative stress and TNF- α induce histone acetylation and NF- κ B/AP-1 activation in alveolar epithelial cells: potential mechanism in gene transcription in lung inflammation. *Mol Cell Biochem*, 234-235(1-2), 239-48.
- Rahman, I., Mulier, B., Gilmour, P. S., Watchorn, T., Donaldson, K., Jeffery, P. K., & MacNee, W. (2001). Oxidant-mediated lung epithelial cell tolerance: the role of intracellular glutathione and nuclear factor-kappaB. *Biochem Pharmacol*, 62(6), 787–94.
- Rahman, I., van Schadewijk, A. A., Crowther, A. J., Hiemstra, P. S., Stolk, J., MacNee, W., & De Boer, W. I. (2002). 4-Hydroxy-2-nonenal, a specific lipid peroxidation product, is elevated in lungs of patients with chronic obstructive pulmonary disease. *Am J Respir Crit Care Med*, 166(4), 490–5.
- Rahman, S. M., Jamshedur, J., Xiangming, Z., Lisa J., Li, M., Harris, B. K., Hoeksema, M. D., Trenary, I. A., Zou, Y., Qian, J., Slebos, R. J., Beane, J., Spira, A., Shyr, Y., Eisenberg, R., Liebler, D. C., Young, J. D., & Massion, P. P. (2016). The airway epithelium undergoes metabolic reprogramming in individuals at high risk for lung cancer. *JCI Insight*, 1(19), e88814.
- Raimundo, N., Baysal, B. E., & Shadel, G. S. (2011). Revisiting the TCA cycle: signaling to tumor formation. *Trends Mol Med*, 17(11), 641–9.
- Rakoff-Nahoum, S. (2006). Why cancer and inflammation? *Yale J Biol Med*, 79(3-4), 123-30.
- Rambold, A. S., Kostecky, B., Elia, N., & Lippincott-Schwartz, J. (2011). Tubular network formation protects mitochondria from autophagosomal degradation during nutrient starvation. *Proc Natl Acad Sci U S A*, 108(25), 10190–5.
- Raviv, S., Hawkins, K. A., DeCamp, M. M., & Kalhan, R.. (2011). Lung cancer in chronic obstructive pulmonary disease: enhancing surgical options and outcomes. *Am J Respir Crit Care Med*, 183(9), 1138-46.
- Raza, H., John, A., & Shafarin, J. (2016). Potentiation of LPS-induced apoptotic cell death in human hepatoma HepG2 cells by aspirin via ROS and mitochondrial dysfunction: protection by N-acetyl cysteine. *PLoS One*, 11(7), e0159750.
- Reck, M., Bondarenko, I., Luft, A., Serwatowski, P., Barlesi, F., Chacko, R., Sebastian, M., Lu, H., Cuillerot, J. M., & Lynch, T. J. (2013). Ipilimumab in combination with paclitaxel and carboplatin as first-line therapy in extensive-disease-small-cell lung cancer: results from a randomized, double-blind, multicenter phase 2 trial. *Ann Oncol*, 24(1), 75–83.

- Reck, M., Luft, A., Szczesna, A., Havel, L., Kim, S. W., Akerley, W., Pietanza, M. C., Wu, Y. L., Zielinski, C., Thomas, M., Felip, E., Gold, K., Horn, L., Aerts, J., Nakagawa, K., Lorigan, P., Pieters, A., Kong Sanchez, T., Fairchild, J., & Spigel, D. (2016). Randomized, multicenter, double-blind, phase 3 trial comparing the efficacy of ipilimumab plus etoposide/platinum versus etoposide/platinum in subjects with newly diagnosed extensive-stage disease small cell lung cancer. *J Clin Oncol*, 34(31), 3740–8
- Reddel, R. R., Yang, K., Rhim J. S., Brash, D., Su, R. T., Kans, L., Lechner, J. F., Gerwin, B. I., Harris, C. C., & Amstad, P. (1989). U.S. Patent No. 4885238. (5 December, 1989).
- Rehman, J., Zhang, H. J., Toth, P. T., Zhang, Y., Marsboom, G., Hong, Z., Salgia, R., Husain, A. N., Wietholt, C., Archer, S.L. (2012). Inhibition of mitochondrial fission prevents cell cycle progression in lung cancer. *FASEB J*, 26(5), 2175–86.
- Remels, A. H., Schrauwen, P., Broekhuizen, R., Willems, J., Kersten, S., Gosker, H. R., & Schols, A. M. (2007). Peroxisome proliferator-activated receptor expression is reduced in skeletal muscle in COPD. *Eur Respir J*, 30(2), 245–52.
- Reynolds, S. D., Giangreco, A., Power, J. H., & Stripp, B. R. (2000). Neuroepithelial bodies of pulmonary airways serve as a reservoir of progenitor cells capable of epithelial regeneration. *Am J Pathol*, 156(1), 269–78.
- Richter, S., Peitzsch, M., Rapizzi, E., Lenders, J. W., Qin, N., de Cubas, A. A., Schiavi, F., Rao, J. U., Beuschlein, F., Quinkler, M., Timmers, H. J., Opocher, G., Mannelli, M., Pacak, K., Robledo, M., & Eisenhofer, G. (2014). Krebs cycle metabolite profiling for identification and stratification of pheochromocytomas /paragangliomas due to succinate dehydrogenase deficiency. *J Clin Endocrinol Metab*, 99(10), 3903–11.
- Ridker, P. M., MacFadyen, J. G., Thuren, T., Everett, B. M., Libby, P., & Glynn, R. J. (2017). Effect of interleukin-1 β inhibition with canakinumab on incident lung cancer in patients with atherosclerosis: exploratory results from a randomised, double-blind, placebo-controlled trial. *Lancet*, 390(10105), 1833–42.
- Roberts, D. J., & Miyamoto, S. (2015). Hexokinase II integrates energy metabolism and cellular protection: Akt-ing on mitochondria and TORC-ing to autophagy. *Cell Death Differ*, 22(2), 248–57.
- Roberts, E. R., & Thomas, K. J.. (2013). The role of mitochondria in the development and progression of lung cancer. *Comput Struct Biotechnol J*, 6, e201303019.
- Rock, J. R., Onaitis, M. W., Rawlins, E. L., Lu, Y., Clark, C. P., Xue, Y., Randell, S. H., & Hogan, B. L. (2009). Basal cells as stem cells of the mouse trachea and human airway epithelium. *Proc Natl Acad Sci U S A*, 106(31), 12771–5.
- Roger, A. J., Muñoz-Gómez, S. A., & Kamikawa, R. (2017). The origin and diversification of mitochondria. *Curr Biol*, 27(21), R1177–92.
- Rooney, C., & Sethi, T. (2011). The epithelial cell and lung cancer: the link between chronic obstructive pulmonary disease and lung cancer. *Respiration*, 81(2), 89–

104.

- Rosanna, D. P., & Salvatore, C. (2012). Reactive oxygen species, inflammation, and lung diseases. *Curr Pharm Des*, 18(26), 3889–900.
- Rowlands, D. J., Islam, M. N., Das, S. R., Huertas, A., Quadri, S. K., Horiuchi, K., Inamdar, N., Emin, M. T., Lindert, J., Ten, V. S., Bhattacharya, S., & Bhattacharya, J. (2011). Activation of TNFR1 ectodomain shedding by mitochondrial Ca²⁺ determines the severity of inflammation in mouse lung microvessels. *J Clin Invest*, 121(5), 1986–99.
- Royal College of Physicians, Clinical Effectiveness and Evaluation Unit. (2016). National Lung Cancer Audit annual report 2016 (for the audit period 2015). *National Lung Cancer Audit*.
- Ryan, D. M., Vincent, T. L., Salit, J., Walters, M. S., Agosto-Perez, F., Shaykhiev, R., Strulovici-Barel, Y., Downey, R. J., Buro-Aurion, L. J., Staudt, M. R., Hackett, N. R., Mezey, J. G., & Crystal, R. G. (2014). Smoking dysregulates the human airway basal cell transcriptome at COPD risk locus 19q13.2. *PLoS One*, 9(2), e88051.
- Sabari, J. K., & Paik, P. K. (2017). Relevance of genetic alterations in squamous and small cell lung cancer. *Ann Transl Med*, 5(18), 373.
- Saber, A., van der Wekken, A. J., Kerner, G. S., van den Berge, M., Timens, W., Schuurings, E., ter Elst, A., van den Berg, A., Hiltermann, T. J., & Groen, H. J. (2016). Chronic obstructive pulmonary disease is not associated with KRAS mutations in non-small cell lung cancer. *PLoS One*, 11(3), e0152317.
- Sabharwal, S. S., & Schumacker, P. T. (2014). Mitochondrial ROS in cancer: initiators, amplifiers or an Achilles' heel? *Nat Rev Cancer*, 14(11), 709–21.
- Saetta, M., Di Stefano, A., Turato, G., Facchini, F. M., Corbino, L., Mapp, C. E., Maestreslli, P., Ciaccia, A., & Fabbri, L. M. (1998). CD8+ T-lymphocytes in peripheral airways of smokers with chronic obstructive pulmonary disease. *Am J Respir Crit Care Med*, 157(3), 822–6.
- Safka, K. A., & McIvor, R. A. (2015). Non-pharmacological management of chronic obstructive pulmonary disease. *Ulster Med J*, 84(1), 13–21.
- Saladino, A. J., Willey, J. C., Lechner, J. F., Grafstrom, R. C., LaVeck, M., & Harris, C. C. (1985). Effects of formaldehyde, acetaldehyde, benzoyl peroxide, and hydrogen peroxide on cultured normal human bronchial epithelial cells. *Cancer Res*, 45(6), 2522–6.
- Salvi, S., Fontana, V., Boccardo, S., Merlo, D. F., Margallo, E., Laurent, S., Morabito, A., Rijavec, E., Dal Bello, M. G., Mora, M., Ratto, G. B., Grossi, F., Truini, M., & Pistillo, M. P. (2012). Evaluation of CTLA-4 expression and relevance as a novel prognostic factor in patients with non-small cell lung cancer. *Cancer Immunol Immunother*, 61(9), 1463–72.
- Samuni, A., Krishna, C. M., Mitchell, J. B., Collins, C. R., & Russo, A. (1990). Superoxide reaction with nitroxides. *Free Radic Res Commun*, 9(3–6), 241–9.

- Sanguinetti, C. M. (2015). N-acetylcysteine in COPD: why, how, and when? *Multidiscip Respir Med*, 11(1), 8.
- Santos, P. P., Oliveira, F., Ferreira, V. C., Polegato, B. F., Roscani, M. G., Fernandes, A. A., Modesto, P., Rafacho, B. P., Zanati, S. G., Di Lorenzo, A., Matsubara, L. S., Paiva, S. A., Zornoff, L. A., & Azevedo, P. S. (2014). The role of lipotoxicity in smoke cardiomyopathy. *PLoS One*, 9(12), e113739.
- Sato, M., Hirose, K., Kashiwakura, I., Aoki, M., Kawaguchi, H., Hatayama, Y., Akimoto, H., Narita, Y., & Takai, Y. (2015). LW6, a hypoxia-inducible factor 1 inhibitor, selectively induces apoptosis in hypoxic cells through depolarization of mitochondria in A549 human lung cancer cells. *Mol Med Rep*, 12(3), 3462–8.
- Sato, M., Shames, D. S., Gazdar, A. F., & Minna, J. D. (2007). A translational view of the molecular pathogenesis of lung cancer. *J Thorac Oncol*, 2(4), 327–43.
- Sato, N., Ueno, T., Kubo, K., Suzuki, T., Tsukimura, N., Att, W., Yamada, M., Hori, N., Maeda, H., & Ogawa, T. (2009). N-Acetyl cysteine (NAC) inhibits proliferation, collagen gene transcription, and redox stress in rat palatal mucosal cells. *Dent Mater*, 25(12), 1532–40.
- Scarpulla, R. C. (2011). Metabolic control of mitochondrial biogenesis through the PGC-1 family regulatory network. *Biochim Biophys Acta*, 1813(7), 1269–78.
- Scarpulla, R. C., Vega, R. B., & Kelly, D. P. (2012). Transcriptional integration of mitochondrial biogenesis. *Trends Endocrinol Metab*, 23(9), 459–66.
- Schneider, J., Neu, K., Velcovsky, H. G., Morr, H., & Eigenbrodt, E. (2003). Tumor M2-pyruvate kinase in the follow-up of inoperable lung cancer patients: a pilot study. *Cancer Lett*, 193(1), 91–8.
- Sekine, Y., Hata, A., Koh, E., & Hiroshima, K. (2014). Lung carcinogenesis from chronic obstructive pulmonary disease: characteristics of lung cancer from COPD and contribution of signal transducers and lung stem cells in the inflammatory microenvironment. *Gen Thorac Cardiovasc Surg*, 62(7), 415–21.
- Sena, L. A., & Chandel, N. S. (2012). Physiological roles of mitochondrial reactive oxygen species. *Mol Cell*, 48(2), 158–167.
- Senft, D., & Ronai, Z. A. (2016). Regulators of mitochondrial dynamics in cancer. *Curr Opin Cell Biol*, 39, 43–52.
- Shahriary, C. M., Chin, T. W., & Nussbaum, E. (2012). Respiratory epithelial cell lines exposed to anoxia produced inflammatory mediator. *Anat Cell Biol*, 45(4), 221–8.
- Shao, Z. R., Wang, Q., Xu, X. F., Zhang, Z., Lu, Y. B., Shen, G., & Wu, M. (2012). Phospholipase D participates in H₂O₂ -induced A549 alveolar epithelial cell migration. *Exp Lung Res*, 38(8), 427–33.
- Shuto, T., Kamei, S., Nohara, H., Fujikawa, H., Tasaki, Y., Sugahara, T., Ono, T., Matsumoto, C., Sakaguchi, Y., Maruta, K., Nakashima, R., Kawakami, T., Suico, M. A., Kondo, Y., Ishigami, A., Takeo, T., Tanaka, K. I., Watanabe, H.,

- Nakagata, N., Uchimura, K., Kitamura, K., Li, J. D., & Kai, H. (2016). Pharmacological and genetic reappraisals of protease and oxidative stress pathways in a mouse model of obstructive lung diseases. *Sci Rep*, 6, 39305.
- Siejka, A., Barabutis, N., & Schally, A. V. (2011). GHRH antagonist MZ-5-156 increases the expression of AMPK in A549 lung cancer cells. *Cell Cycle*, 10(21), 3714–8.
- Sigaud, S., Evelson, P., & González-Flecha, B. (2005). H₂O₂-induced proliferation of primary alveolar epithelial cells is mediated by MAP kinases. *Antioxid Redox Signal*, 7(1–2), 6–13.
- Singh, K. K., Costello, L. C. (Eds.). (2009). *Mitochondria and Cancer*. New York, USA: Springer-Verlag New York.
- Singh, S., & Chellappan, S. (2014). Lung cancer stem cells: molecular features and therapeutic targets. *Mol Aspects Med*, 39, 50–60.
- Sinthupibulyakit, C., Ittarat, W., St Clair, W. H., & St Clair, D. K. (2010). p53 protects lung cancer cells against metabolic stress. *Int J Oncol*, 37(6), 1575–81.
- Skillrud, D. M., Offord, K. P., & Miller, R. D.. (1986). Higher risk of lung cancer in chronic obstructive pulmonary disease. *Ann Intern Med*, 105(4), 503-7.
- Slaughter, D. P., Southwick, H. W., & Smejkal, W. (1953). "Field cancerization" in oral stratified squamous epithelium. Clinical implications of multicentric origin. *Cancer*, 6(5), 963–8.
- Smit-de Vries, M. P., van der Toorn, M., Bischoff, R., & Kauffman, H. F. (2007). Resistance of quiescent and proliferating airway epithelial cells to H₂O₂ challenge. *Eur Respir J*, 29(4), 633–42.
- Smith, B. D., Smith, G. L., Hurria, A., Hortobagyi, G. N., & Buchholz, T. A. (2009). Future of cancer incidence in the United States: burdens upon an aging, changing nation. *J Clin Oncol*, 27(17), 2758–65.
- Sonoda, J., Laganière, J., Mehl, I. R., Barish, G. D., Chong, L. W., Li, X., Scheffler, I. E., Mock, D. C., Bataille, A. R., Robert, F., Lee, C. H., Giguère, V., & Evans, R. M. (2007). Nuclear receptor ERR alpha and coactivator PGC-1 beta are effectors of IFN-gamma-induced host defense. *Genes Dev*, 21(15), 1909–20.
- Spinelli, J. B., & Haigis, M. C. (2018). The multifaceted contributions of mitochondria to cellular metabolism. *Nat Cell Biol*, 20(7), 745–54.
- St-Pierre, J., Lin, J., Krauss, S., Tarr, P. T., Yang, R., Newgard, C. B., & Spiegelman, B. M. (2003). Bioenergetic analysis of peroxisome proliferator-activated receptor γ coactivators 1 α and 1 β (PGC-1 α and PGC-1 β) in muscle cells. *J Biol Chem*, 278(29), 26597–603.
- Stamatiou, R., Paraskeva, E., Gourgouljanis, K., Molyvdas, P. A., & Hatziefthimiou, A. (2012). Cytokines and growth factors promote airway smooth muscle cell proliferation. *ISRN Inflamm*, 2012, 731472.

- Starkov, A. A. (2008). The role of mitochondria in reactive oxygen species metabolism and signaling. *Ann N Y Acad Sci*, 1147, 37–52.
- Stringer, K. A., Tobias, M., O'Neill, H. C., & Franklin, C. C. (2007). Cigarette smoke extract-induced suppression of caspase-3-like activity impairs human neutrophil phagocytosis. *Am J Physiol Lung Cell Mol Physiol*, 292(6), L1572–9.
- Stroud, D. A., Formosa, L. E., Wijeyeratne, X. W., Nguyen, T. N., & Ryan, M. T. (2013). Gene knockout using transcription activator-like effector nucleases (TALENs) reveals that human NDUFA9 protein is essential for stabilizing the junction between membrane and matrix arms of complex I. *J Biol Chem*, 288(3), 1685–90.
- Stupp, R., Monnerat, C., Turrisi, A. T., Perry, M. C., & Leyvraz, S. (2004). Small cell lung cancer: state of the art and future perspectives. *Lung Cancer*, 45(1), 105–17.
- Succony, L., & Janes, S. M. (2014). Airway stem cells and lung cancer. *QJM*, 107(8), 607–12.
- Suh, D. H., Kim, M. A., Kim, H., Kim, M. K., Kim, H. S., Chung, H. H., Kim, Y. B., & Song, Y. S. (2014). Association of overexpression of hexokinase II with chemoresistance in epithelial ovarian cancer. *Clin Exp Med*, 14(3), 345–53.
- Sun, H. W., Yu, X. J., Wu, W. C., Chen, J., Shi, M., Zheng, L., & Xu, J. (2016). GLUT1 and ASCT2 as predictors for prognosis of hepatocellular carcinoma. *PLoS One*, 11(12), e0168907.
- Sureshbabu, A., & Bhandari, V. (2013). Targeting mitochondrial dysfunction in lung diseases: emphasis on mitophagy. *Front Physiol*, 4, 384.
- Swinson, D. E., Jones, J. L., Cox, G., Richardson, D., Harris, A. L., & O'Byrne, K. J. (2004). Hypoxia-inducible factor-1 α in non small cell lung cancer: relation to growth factor, protease and apoptosis pathways. *Int J Cancer*, 111(1), 43–50.
- Szczesny, B., Módis, K., Yanagi, K., Coletta, C., Le Trionnaire, S., Perry, A., Wood, M. E., Whiteman, M., & Szabo, C. (2014). AP39, a novel mitochondria-targeted hydrogen sulfide donor, stimulates cellular bioenergetics, exerts cytoprotective effects and protects against the loss of mitochondrial DNA integrity in oxidatively stressed endothelial cells in vitro. *Nitric Oxide*, 41, 120–30.
- Taguchi, A., Delgado, O., Celiktaş, M., Katayama, H., Wang, H., Gazdar, A. F., & Hanash, S. M. (2014). Proteomic signatures associated with p53 mutational status in lung adenocarcinoma. *Proteomics*, 14(23–24), 2750–9.
- Takehige, K., & Minakami, S. (1979). NADH- and NADPH-dependent formation of superoxide anions by bovine heart submitochondrial particles and NADH-ubiquinone reductase preparation. *Biochem J*, 180(1), 129–35.
- Tan, F., Jiang, Y., Sun, N., Chen, Z., Lv, Y., Shao, K., Li, N., Qiu, B., Gao, Y., Tan, X., Zhou, F., Wang, Z., Ding, D., Wang, J., Sun, J., Hang, J., Shi, S., Feng, X., He, F., & He, J. (2012). Identification of isocitrate dehydrogenase 1 as a potential diagnostic and prognostic biomarker for non-small cell lung cancer by

- proteomic analysis. *Mol Cell Proteomics*, 11(2), M111.008821.
- Tan, Z., Luo, X., Xiao, L., Tang, M., Bode, A. M., Dong, Z., & Cao, Y. (2016). The role of PGC1 α in cancer metabolism and its therapeutic implications. *Mol Cancer Ther*, 15(5), 774–82.
- Tang, X., Varella-Garcia, M., Xavier, A. C., Massarelli, E., Ozburn, N., Moran, C., & Wistuba, I. I. (2008). Epidermal growth factor receptor abnormalities in the pathogenesis and progression of lung adenocarcinomas. *Cancer Prev Res (Phila)*, 1(3), 192–200.
- Tavilani, H., Nadi, E., Karimi, J., & Goodarzi, M. T. (2012). Oxidative stress in COPD patients, smokers, and non-smokers. *Respir Care*, 57(12), 2090–4.
- Tay, S. P., Yeo, C. W., Chai, C., Chua, P. J., Tan, H. M., Ang, A. X., Yip, D. L., Sung, J. X., Tan, P. H., Bay, B. H., Wong, S. H., Tang, C., Tan, J. M., & Lim, K. L. (2010). Parkin enhances the expression of cyclin-dependent kinase 6 and negatively regulates the proliferation of breast cancer cells. *J Biol Chem*, 285(38), 29231–8.
- Tello, D., Balsa, E., Acosta-Iborra, B., Fuertes-Yebra, E., Elorza, A., Ordóñez, Á., Corral-Escariz, M., Soro, I., López-Bernardo, E., Perales-Clemente, Martínez-Ruiz, A., Enríquez, J. A., Aragonés, J., Cadenas, S., & Landázuri, M. O. (2011). Induction of the mitochondrial NDUFA4L2 protein by HIF-1 α decreases oxygen consumption by inhibiting Complex I activity. *Cell Metab*, 14(6), 768–79.
- Teramoto, S., Tomita, T., Matsui, H., Ohga, E., Matsuse, T., & Ouchi, Y. (1999). Hydrogen peroxide-induced apoptosis and necrosis in human lung fibroblasts: protective roles of glutathione. *Jpn J Pharmacol*, 79(1), 33–40.
- Tetley, T. D. (2005). Inflammatory cells and chronic obstructive pulmonary disease. *Curr Drug Targets Inflamm Allergy*, 4(6), 607–18.
- Thaikootathil, J. V., Martin, R. J., Zdunek, J., Weinberger, A., Rino, J. G., & Chu, H. W. (2009). Cigarette smoke extract reduces VEGF in primary human airway epithelial cells. *Eur Respir J*, 33(4), 835–43.
- Thannickal, V. J., & Fanburg, B. L. (1995). Activation of an H₂O₂-generating NADH oxidase in human lung fibroblasts by transforming growth factor beta 1. *J Biol Chem*, 270(51), 30334–8.
- Thomas, K. J., & Jacobson, M. R. (2012). Defects in mitochondrial fission protein dynamin-related protein 1 are linked to apoptotic resistance and autophagy in a lung cancer model. *PLoS One*, 7(9), e45319.
- Thorne, D., & Adamson, J. (2013). A review of in vitro cigarette smoke exposure systems. *Exp Toxicol Pathol*, 65(7–8), 1183–93.
- Togo, S., Holz, O., Liu, X., Sugiura, H., Kamio, K., Wang, X., Kawasaki, S., Ahn, Y., Fredriksson, K., Skold, C. M., Mueller, K. C., Branscheid, D., Welker, L., Watz, H., Magnussen, H., & Rennard, S. I. (2008). Lung fibroblast repair functions in patients with chronic obstructive pulmonary disease are altered by multiple mechanisms. *Am J Respir Crit Care Med*, 178(3), 248–60.

- Tomasini, P., Barlesi, F., Mascaux, C., & Greillier, L. (2016). Pemetrexed for advanced stage nonsquamous non-small cell lung cancer: latest evidence about its extended use and outcomes. *Ther Adv Med Oncol*, 8(3), 198–208.
- Tondera, D., Grandemange, S., Jourdain, A., Karbowski, M., Mattenberger, Y., Herzig, S., Da Cruz, S., Clerc, P., Raschke, I., Merkwirth, C., Ehses, S., Krause, F., Chan, D. C., Alexander, C., Bauer, C., Youle, R., Langer, T., & Martinou, J. C. (2009). SLP-2 is required for stress-induced mitochondrial hyperfusion. *EMBO J*, 28(11), 1589–600.
- Trachootham, D., Alexandre, J., & Huang, P. (2009). Targeting cancer cells by ROS-mediated mechanisms: a radical therapeutic approach? *Nat Rev Drug Discov*, 8(7), 579–91.
- Tran, H. B., Ahern, J., Hodge, G., Holt, P., Dean, M. M., Reynolds, P. N., & Hodge, S. (2014). Oxidative stress decreases functional airway mannose binding lectin in COPD. *PLoS One*, 9(6), e98571.
- Traves, S. L., Culpitt, S. V., Russell, R. E. K., Barnes, P. J., & Donnelly, L. E. (2002). Increased levels of the chemokines GRO α and MCP-1 in sputum samples from patients with COPD. *Thorax*, 57(7), 590–5.
- Travis, W. D. (2011). Pathology of lung cancer. *Clin Chest Med*, 32(4), 669–92.
- Travis, W. D., Brambilla, E., Nicholson, A. G., Yatabe, Y., Austin, J. H., Beasley, M. B., Chirieac, L. R., Dacic, S., Duhig, E., Flieder, D. B., Geisinger, K., Hirsch, F. R., Ishikawa, Y., Kerr, K. M., Noguchi, M., Pelosi, G., Powell, C. A., Tsao, M. S., Wistuba, I. (2015). The 2015 World Health Organization classification of lung tumors: impact of genetic, clinical and radiologic advances since the 2004 classification. *J Thorac Oncol*, 10(9), 1243–60.
- Trnka, J., Blaikie, F. H., Smith, R. A., & Murphy, M. P. (2008). A mitochondria-targeted nitroxide is reduced to its hydroxylamine by ubiquinol in mitochondria. *Free Radic Biol Med*, 44(7), 1406–19.
- Turrens, J. F. (2003). Mitochondrial formation of reactive oxygen species. *J Physiol*, 552(Pt 2), 335–44.
- Turrens, J. F., Alexandre, A., & Lehninger, A. L. (1985). Ubisemiquinone is the electron donor for superoxide formation by complex III of heart mitochondria. *Arch Biochem Biophys*, 237(2), 408–14.
- van Belle, G. (2008). Sample size. In G, van Belle (Ed.). *Statistical Rules of Thumbs* (2nd ed., pp. 27–51). Hoboken, Wiley-Blackwell.
- van den Eeden, S. K., & Friedman, G. D. (1992). Forced expiratory volume (1 second) and lung cancer incidence and mortality. *Epidemiology*, 3(3), 253–7.
- van der Molen, T., & Cazzola, M. (2012). Beyond lung function in COPD management: effectiveness of LABA/LAMA combination therapy on patient-centred outcomes. *Prim Care Respir J*, 21(1), 101–8.
- van der Toorn, M., Rezayat, D., Kauffman, H. F., Bakker, S. J., Gans, R. O., Koëter,

- G. H., Choi, A. M., van Oosterhout, A. J., & Slebos, D. J. (2009). Lipid-soluble components in cigarette smoke induce mitochondrial production of reactive oxygen species in lung epithelial cells. *Am J Physiol Lung Cell Mol Physiol*, 297(1), L109-14.
- van Klaveren, R. J., Roelant, C., Boogaerts, M., Demedts, M., & Nemery, B. (1997). Involvement of an NAD(P)H oxidase-like enzyme in superoxide anion and hydrogen peroxide generation by rat type II cells. *Thorax*, 52(5), 465–71.
- van Overveld, F. J., Demkow, U., Górecka, D., de Backer, W. A., & Zielinski, J. (2005). New developments in the treatment of COPD: comparing the effects of inhaled corticosteroids and N-acetylcysteine. *J Physiol Pharmacol*, 56 Suppl 4, 135–42.
- Veeriah, S., Taylor, B. S., Meng, S., Fang, F., Yilmaz, E., Vivanco, I., Janakiraman, M., Schultz, N., Hanrahan, A. J., Pao, W., Ladanyi, M., Sander, C., Heguy, A., Holland, E. C., Paty, P. B., Mischel, P. S., Liau, L., Cloughesy, T. F., Mellinghoff, I. K., Solit, D. B., & Chan, T. A. (2010). Somatic mutations of the Parkinson's disease-associated gene PARK2 in glioblastoma and other human malignancies. *Nat Genet*, 42(1), 77–82.
- Venditti, P., Di Stefano, L., & Di Meo, S. (2013). Mitochondrial metabolism of reactive oxygen species. *Mitochondrion*, 13(2), 71-82.
- Vermaelen, K., & Brusselle, G. (2013). Exposing a deadly alliance: Novel insights into the biological links between COPD and lung cancer. *Pulmonary Pharmacology & Therapeutics*, 26(5), 544–554.
- Vignola, A. M., Chanez, P., Chiappara, G., Merendino, A., Pace, E., Rizzo, A., la Rocca, A. M., Bellia, V., Bonsignore, G., & Bousquet, J. (1997). Transforming growth factor- β expression in mucosal biopsies in asthma and chronic bronchitis. *Am J Respir Crit Care Med*, 156(2), 591–9.
- Vine, M. F., Schoembach, V. J., Hulka, B. S., Koch, G. G., & Samsa, G. (1990). Atypical metaplasia and incidence of bronchogenic carcinoma. *Am J Epidemiol*, 131(5), 781–93.
- Viotti, J., Duplan, E., Caillava, C., Condat, J., Goiran, T., Giordano, C., Marie, Y., Idbaih, A., Delattre, J. Y., Honnorat, J., Checler, F., & Alves da Costa, C. (2014). Glioma tumor grade correlates with parkin depletion in mutant p53-linked tumors and results from loss of function of p53 transcriptional activity. *Oncogene*, 33(14), 1764–75.
- Vlahos, R., & Bozinovski, S. (2014). Role of alveolar macrophages in chronic obstructive pulmonary disease. *Front Immunol*, 5, 435.
- Vyas, S., Zaganjor, E., & Haigis, M. C. (2016). Mitochondria and cancer. *Cell*, 166(3), 555-66.
- Wada, S., Cuiz, Z. G., Kondo, T., Zhao, Q. L., Ogawa, R., Shoji, M., Arai, T., Makino, K., & Furuta, I. (2005). A hydrogen peroxide-generating agent, 6-formylpterin, enhances heat-induced apoptosis. *Int J Hyperthermia*, 21(3), 231–46.

- Wakelee, H., Kelly, K., & Edelman, M. J. (2014). 50 Years of progress in the systemic therapy of non-small cell lung cancer. *Am Soc Clin Oncol Educ Book*, 177–89.
- Wang, A., Keita, A. V., Phan, V., McKay, C. M., Schoultz, I., Lee, J., Murphy, M. P., Fernando, M., Ronaghan, N., Balce, D., Yates, R., Dickey, M., Beck, P. L., MacNaughton, W. K., Söderholm, J. D., & McKay, D. M. (2014). Targeting mitochondria-derived reactive oxygen species to reduce epithelial barrier dysfunction and colitis. *Am J Pathol*, 184(9), 2516–27.
- Wang, D. F., Rong, W. T., Lu, Y., Hou, J., Qi, S. S., Xiao, Q., Zhang, J., You, J., Yu, S. Q., & Xu, Q. (2015). TPGS2k/PLGA nanoparticles for overcoming multidrug resistance by interfering mitochondria of human alveolar adenocarcinoma cells. *ACS Appl Mater Interfaces*, 7(7), 3888–901.
- Wang, H., Nicolay, B. N., Chick, J. M., Gao, X., Geng, Y., Ren, H., Gao, H., Yang, G., Williams, J. A., Suski, J. M., Keibler, M. A., Sicinska, E., Gerdemann, U., Haining, W. N., Roberts, T. M., Polyak, K., Gygi, S. P., Dyson, N. J., & Sicinski, P. (2017). The metabolic function of cyclin D3-CDK6 kinase in cancer cell survival. *Nature*, 546(7658), 426–30.
- Wang, L., Zhang, L. F., Wu, J., Xu, S. J., Xu, Y. Y., Li, D., Lou, J. T., & Liu, M. F. (2014). IL-1 β -mediated repression of microRNA-101 is crucial for inflammation-promoted lung tumorigenesis. *Cancer Res*, 74(17), 4720–30.
- Wang, M., Zhao, J., Zhang, L., Wei, F., Lian, Y., Wu, Y., Gong, Z., Zhang, S., Zhou, J., Cao, K., Li, X., Xiong, W., Li, G., Zeng, Z., & Guo, C. (2017). Role of tumor microenvironment in tumorigenesis. *J Cancer*, 8(5), 761–73.
- Wang, W., Zheng, J. P., Zhu, S. X., Guan, W. J., Chen, M., & Zhong, N. S. (2015). Carbocysteine attenuates hydrogen peroxide-induced inflammatory injury in A549 cells via NF- κ B and ERK1/2 MAPK pathways. *Int Immunopharmacol*, 24(2), 306–13.
- Wang, X., Chorley, B. N., Pittman, G. S., Kleeberger, S. R., Brothers, J., Liu, G., Spira, A., & Bell, D. A. (2010). Genetic variation and antioxidant response gene expression in the bronchial airway epithelium of smokers at risk for lung cancer. *PLoS One*, 5(8), e11934.
- Wang, Y., Pan, T., Wang, H., Li, L., Li, J., Zhang, C., & Yang, H. (2016). Silencing of TGIF attenuates the tumorigenicity of A549 cells in vitro and in vivo. *Tumor Biol*, 37(9), 12725–30.
- Wang, Z., Choi, S., Lee, J., Huang, Y. T., Chen, F., Zhao, Y., Lin, X., Neuberg, D., Kim, J., & Christiani, D. C. (2015). Mitochondrial variations in non-small cell lung cancer (NSCLC) survival. *Cancer Inform*, 14(Suppl 1), 1–9.
- Warburg, O., Wind, F., & Negelein, E. (1927). The metabolism of tumors in the body. *J Gen Physiol*, 8(6), 519–30.
- Ward, P. S., Patel, J., Wise, D. R., Abdel-Wahab, O., Bennett, B. D., Collier, H. A., Cross, J. R., Fantin, V. R., Hedvat, C. V., Perl, A. E., Rabinowitz, J. D., Carroll,

- M., Su, S. M., Sharp, K. A., Levine, R. L., & Thompson, C. B. (2010). The common feature of leukemia-associated IDH1 and IDH2 mutations is a neomorphic enzyme activity converting α -ketoglutarate to 2-hydroxyglutarate. *Cancer Cell*, 17(3), 225–34.
- Warner, S. L., Carpenter, K. J., & Bearss, D. J. (2014). Activators of PKM2 in cancer metabolism. *Future Med Chem*, 6(10), 1167–78.
- Weinberg, F., Hamanaka, R., Wheaton, W. W., Weinberg, S., Joseph, J., Lopez, M., Kalyanaraman, B., Mutlu, G. M., Budinger, G. R., & Chandel, N. S. (2010). Mitochondrial metabolism and ROS generation are essential for Kras-mediated tumorigenicity. *Proc Natl Acad Sci U S A*, 107(19), 8788–93.
- Weinberg, S. E., & Chandel, N. S. (2015). Targeting mitochondria metabolism for cancer therapy. *Nat Chem Biol*, 11(1), 9–15.
- Welte, T. (2009). Optimising treatment for COPD--new strategies for combination therapy. *Int J Clin Pract*, 63(8), 1136–49.
- Wheaton, W. W., Weinberg, S. E., Hamanaka, R. B., Soberanes, S., Sullivan, L. B., Anso, E., Glasauer, A., Dufour, E., Mutlu, G. M., Budigner, G. S., & Chandel, N. S. (2014). Metformin inhibits mitochondrial complex I of cancer cells to reduce tumorigenesis. *ELife*, 3, e02242.
- White, E. S. (2015). Lung extracellular matrix and fibroblast function. *Ann Am Thorac Soc*, 12(Suppl 1), S30-3.
- Wiegman, C. H., Michaeloudes, C., Haji, G., Narang, P., Clarke, C. J., Russell, K. E., Bao, W., Pavlidis, S., Barnes, P. J., Kanerva, J., Bittner, A., Rao, N., Murphy, M. P., Kirkham, P. A., Chung, K. F., & Adcock, I. M. (2015). Oxidative stress-induced mitochondrial dysfunction drives inflammation and airway smooth muscle remodeling in patients with chronic obstructive pulmonary disease. *J Allergy Clin Immunol*, 136(3), 769–80.
- Wilson, J. E. (2003). Isozymes of mammalian hexokinase: structure, subcellular localization and metabolic function. *J Exp Biol*, 206(Pt 12), 2049–57.
- Wu, K. I., Pollack, N., Panos, R. J., Sporn, P. H., & Kamp, D. W. (1998). Keratinocyte growth factor promotes alveolar epithelial cell DNA repair after H₂O₂ exposure. *Am J Physiol Lung Cell Mol Physiol*, 275(4), L780–7.
- Xie, Z., Zhang, J., Wu, J., Viollet, B., & Zou, M. H. (2008). Upregulation of mitochondrial uncoupling protein-2 by the AMP-activated protein kinase in endothelial cells attenuates oxidative stress in diabetes. *Diabetes*, 57(12), 3222–30.
- Xu, X. D., Shao, S. X., Jiang, H. P., Cao, Y. W., Wang, Y. H., Yang, X. C., Wang, Y. L., Wang, X. S., & Niu, H. T. (2015). Warburg effect or reverse Warburg effect? A review of cancer metabolism. *Oncol Res Treat*, 38(3), 117–22.
- Yaffe, M. P. (1999). Dynamic mitochondria. *Nat Cell Biol*, 1(6), E149–50.
- Yamada, T., Amann, J. M., Tanimoto, A., Taniguchi, H., Shukuya, T., Timmers, C.,

- Yano, S., Shilo, K., & Carbone, D. P. (2017). Histone deacetylase inhibition enhances the antitumor activity of a MEK inhibitor in lung cancer cells harboring RAS mutations. *Mol Cancer Ther*.
- Yamadori, T., Ishii, Y., Homma, S., Morishima, Y., Kurishima, K., Itoh, K., Yamamoto, M., Minami, Y., Noguchi, M., & Hizawa, N. (2012). Molecular mechanisms for the regulation of Nrf2-mediated cell proliferation in non-small-cell lung cancers. *Oncogene*, 31(45), 4768–77.
- Yan, H., Parsons, D. W., Jin, G., McLendon, R., Rasheed, B. A., Yuan, W., Kos, I., Batinic-Habele, I., Jones, S., Riggins, G. J., Friedman, H., Friedman, A., Reardon, D., Herndon, J., Kinzler, K. W., Velculescu, V. E., Vogelstein, B., & Bigner, D. D. (2009). IDH1 and IDH2 mutations in gliomas. *New Engl J Med*, 360(8), 765–73.
- Yan, Z., Wang, J., Li, J., Jiang, N., Zhang, R., Yang, W., Yao, W., Wu, W. (2016). Oxidative stress and endocytosis are involved in upregulation of interleukin-8 expression in airway cells exposed to PM2.5. *Environ Toxicol*, 31(12), 1869–78.
- Yang, D., Elner, S. G., Bian, Z. M., Till, G. O., Petty, H. R., & Elner, V. M. (2007). Pro-inflammatory cytokines increase reactive oxygen species through mitochondria and NADPH oxidase in cultured RPE cells. *Exp Eye Res*, 85(4), 462–72.
- Yasuda, H., Yamaya, M., Sasaki, T., Inoue, D., Nakayama, K., Tomita, N., Yoshida, M., & Sasaki, H. (2006). Carbocysteine reduces frequency of common colds and exacerbations in patients with chronic obstructive pulmonary disease. *J Am Geriatr Soc*, 54(2), 378–80.
- Yasuo, M., Mizuno, S., Kraskauskas, D., Bogaard, H. J., Natarajan, R., Cool, C. D., Zamora, M., & Voelkel, N. F. (2011). Hypoxia inducible factor-1 α in human emphysema lung tissue. *Eur Respir J*, 37(4), 775–83.
- Ye, S. F., Wu, Y. H., Hou, Z. Q., & Zhang, Q. Q. (2009). ROS and NF- κ B are involved in upregulation of IL-8 in A549 cells exposed to multi-walled carbon nanotubes. *Biochem Biophys Res Commun*, 379(2), 643–8.
- Yohena, T., Yoshino, I., Takenaka, T., Kameyama, T., Ohba, T., Kuniyoshi, Y., & Maehara, Y. (2009). Upregulation of hypoxia-inducible factor-1 α mRNA and its clinical significance in non-small cell lung cancer. *J Thorac Oncol*, 4(3), 284–90.
- Yokohori, N., Aoshiba, K., & Nagai, A. (2004). Increased levels of cell death and proliferation in alveolar wall cells in patients with pulmonary emphysema. *Chest*, 125(2), 626–32.
- Yoshikawa, T., Dent, G., Ward, J., Angco, G., Nong, G., Nomura, N., Hirata, K., & Djukanovic, R. (2007). Impaired neutrophil chemotaxis in chronic obstructive pulmonary disease. *Am J Respir Crit Care Med*, 175(5), 473–9.
- Younes, M., Lechago, L. V., Somoano, J. R., Mosharaf, M., & Lechago, J. (1996). Wide expression of the human erythrocyte glucose transporter Glut1 in human cancers. *Cancer Res*, 56(5), 1164–7.

- Young, R. P., Hopkins, R. J., Christmas, T., Black, P. N., Metcalf, P., & Gamble, G. D. (2009). COPD prevalence is increased in lung cancer, independent of age, sex and smoking history. *Eur Respir J*, 34(2), 380–6.
- Zhang, B. B., Wang, D. G., Guo, F. F., & Xuan, C. (2015). Mitochondrial membrane potential and reactive oxygen species in cancer stem cells. *Fam Cancer*, 14(1), 19–23.
- Zhang, F., Lau, S. S., & Monks, T. J. (2011). The cytoprotective effect of N-acetyl-L-cysteine against ROS-induced cytotoxicity is independent of its ability to enhance glutathione synthesis. *Toxicol Sci*, 120(1), 87–97.
- Zhang, S., Yang, C., Yang, Z., Zhang, D., Ma, X., Mills, G., & Liu, Z. (2015). Homeostasis of redox status derived from glucose metabolic pathway could be the key to understanding the Warburg effect. *Am J Cancer Res*, 5(3), 928–44.
- Zhang, W., Jiang, W., Luan, L., Wang, L., Zheng, X., & Wang, G. (2014). Prophylactic cranial irradiation for patients with small-cell lung cancer: a systematic review of the literature with meta-analysis. *BMC Cancer*, 14, 793.
- Zhang, X., Zheng, H., Zhang, H., Ma, W., Wang, F., Liu, C., & He, S. (2011). Increased interleukin (IL)-8 and decreased IL-17 production in chronic obstructive pulmonary disease (COPD) provoked by cigarette smoke. *Cytokine*, 56(3), 717–25.
- Zhang, Y., Huang, S., Gong, D., Qin, Y., & Shen, Q. (2010). Programmed death-1 upregulation is correlated with dysfunction of tumor-infiltrating CD8+ T lymphocytes in human non-small cell lung cancer. *Cell Mol Immunol*, 7(5), 389–95.
- Zhao, F., & Klimecki, W. T. (2015). Culture conditions profoundly impact phenotype in BEAS-2B, a human pulmonary epithelial model. *J Appl Toxicol*, 35(8), 945–51.
- Zhao, F., Severson, P., Pacheco, S., Futscher, B. W., & Klimecki, W. T. (2013). Arsenic exposure induces the Warburg effect in cultured human cells. *Toxicol Appl Pharmacol*, 271(1), 72–7.
- Zhao, F. L., Fang, F., Qiao, P. F., Yan, N., Gao, D., & Yan, Y. (2016). AP39, a mitochondria-targeted hydrogen sulfide donor, supports cellular bioenergetics and protects against Alzheimer's disease by preserving mitochondrial function in APP/PS1 mice and neurons. *Oxid Med Cell Longev*, 2016, 8360738.
- Zhao, J. G., Ren, K. M., & Tang, J. (2014). Overcoming 5-Fu resistance in human non-small cell lung cancer cells by the combination of 5-Fu and cisplatin through the inhibition of glucose metabolism. *Tumor Biol*, 35(12), 12305–15.
- Zhao, K., Luo, G., Giannelli, S., & Szeto, H. H. (2005). Mitochondria-targeted peptide prevents mitochondrial depolarization and apoptosis induced by tert-butyl hydroperoxide in neuronal cell lines. *Biochem Pharmacol*, 70(12), 1796–806.
- Zhao, K., Zhao, G. M., Wu, D., Soong, Y., Birk, A. V., Schiller, P. W., & Szeto, H. H. (2004). Cell-permeable peptide antioxidants targeted to inner mitochondrial

- membrane inhibit mitochondrial swelling, oxidative cell death, and reperfusion injury. *J Biol Chem*, 279(33), 34682–90.
- Zhao, W. Y., Han, S., Zhang, L., Zhu, Y. H., Wang, L. M., & Zeng, L. (2013). Mitochondria-targeted antioxidant peptide SS31 prevents hypoxia / reoxygenation-induced apoptosis by down-regulating p66Shc in renal tubular epithelial cells. *Cell Physiol Biochem*, 32(3), 591–600.
- Zhao, Y., Biggs, T. D., & Xian, M. (2014). Hydrogen sulfide (H₂S) releasing agents: chemistry and biological applications. *Chem Commun (Camb)*, 50(80), 11788–805.
- Zheng, J. P., Wen, F. Q., Bai, C. X., Wan, H. Y., Kang, J., Chen, P., Yao, W. Z., Ma, L. J., Li, X., Raiteri, L., Sardina, M., Gao, Y., Wang, B. S., & Zhong, N. S. (2014). Twice daily N-acetylcysteine 600 mg for exacerbations of chronic obstructive pulmonary disease (PANTHEON): a randomised, double-blind placebo-controlled trial. *Lancet Respir Med*, 2(3), 187–94.
- Zhong, Z., Liang, S., Sanchez-Lopez, E., He, F., Shalapour, S., Lin, X. J., Wong, J., Ding, S., Seki, E., Schnabi, B., Hevener, A. L., Greenberg, H. B., Kisseleva, T., & Karin, M. (2018). New mitochondrial DNA synthesis enables NLRP3 inflammasome activation. *Nature*, 560(7717), 198–203.
- Zhou, R., Yazdi, A. S., Menu, P., & Tschopp, J. (2011). A role for mitochondria in NLRP3 inflammasome activation. *Nature*, 469(7329), 221–5.
- Zhu, Y., Zhang, B., Gong, A., Fu, H., Zhang, X., Shi, H., Sun, Y., Wu, L., Pan, Z., Mao, F., Zhu, W., Qian, H., & Xu, W. (2016). Anti-cancer drug 3,3'-diindolylmethane activates Wnt4 signaling to enhance gastric cancer cell stemness and tumorigenesis. *Oncotarget*, 7(13), 16311–24.